AF JFW

PATENT
ATTORNEY DOCKET NO. 07891/009004

Certificate of Mailing: Date of Deposit: December 13, 2005

I hereby certify under 37 C.F.R. § 1.8(a) that this correspondence is being deposited with the United States Postal Service as **first class mail** with sufficient postage on the date indicated above and is addressed to Mail Stop Appeal Brief - Patents, Commissioner for Patents, P.O. Box 1450, Alexandria, VA 22313-1450.

Heidi Wright
Printed name of person mailing correspondence

Signature of person mailing

IN THE UNITED STATES PATENT AND TRADEMARK OFFICE

Applicant:	Robert G. Korneluk et al.	Art Unit:	1635
Serial No.:	09/974,592	Examiner:	Amy J. Hudson
Filed:	October 9, 2001	Customer No.:	21559
Title:	DETECTION AND MODULATION OF IAPS AND NAIP FOR THE DIAGNOSIS AND TREATMENT OF PROLIFERATIVE DISEASE		

Mail Stop Appeal Brief—Patents
Commissioner for Patents
P.O. Box 1450
Alexandria, VA 22313-1450

APPEAL BRIEF ON APPEAL PURSUANT TO 37 C.F.R. § 41.37

In support of appellant's Notice of Appeal that was filed in connection with the above-captioned case, and with reference to the Office action that was mailed in this case on September 14, 2004, submitted herewith is appellant's Appeal Brief.

Real Party in Interest

The Real Party in Interest in this case is Aegera Therapeutics Inc., to whom all interest in the present application has been assigned.

Related Appeals and Interferences

There are currently no pending appeals or interferences related to this case.

Status of Claims

Claims 5 and 9-15 are pending in this application. Claims 5 and 9-15 are rejected. Claims 5 and 9-15 are on appeal.

Status of Amendments

All amendments have been entered and are reflected in the appended claims.

Summary of Claimed Subject Matter

Appellant's invention features a method of inducing apoptosis in a cell in a mammal diagnosed as having a proliferative disease by administering a modified antisense oligonucleotide of length sufficient to inhibit an inhibitor of apoptosis (IAP) biological activity, wherein the antisense oligonucleotide is complementary to a portion of human X-linked IAP (XIAP) (SEQ ID NO:3). Appellant's invention also features a method of treating a patient diagnosed as having a proliferative disease by administering to the patient a modified antisense oligonucleotide of length sufficient to inhibit an IAP

biological activity, wherein the antisense oligonucleotide is complementary to a portion of human XIAP. See, e.g., page 8, line 23, to page 9, line 8; page 27, line 21, to page 28, line 3, and page 55, line 19, to page 56, line 14, of the specification.

Ground of Rejection to be Reviewed on Appeal

Claims 5 and 9-15 stand rejected under 35 U.S.C. § 112 for lack of enablement.

Argument

Rejection of claims 5 and 9-15 under 35 U.S.C. § 112, first paragraph

Claims 5 and 13-15, which feature a method for inducing apoptosis in a cell in a mammal diagnosed as having a proliferative disease, and claims 9-12, which feature methods for treating a patient diagnosed as having a proliferative disease, stand rejected as lacking enablement based on the assertion that undue experimentation would be required to practice the full scope of the invention. While the Examiner acknowledges that appellant has enabled the *in vivo* use of a particular antisense oligonucleotide (i.e., a 19-mer phosphorothioate modified antisense XIAP oligonucleotide), the Examiner argues that the use of an antisense oligonucleotide of any other length is unpredictable.

This rejection is in error and should be reversed.

The proper test of enablement is "whether one reasonably skilled in the art could make or use the invention from the disclosures in the patent coupled with the information known in the art without undue experimentation." *Hybritech, Inc. v. Monoclonal*

Antibodies, Inc. 802 F.2d. 1318 (Fed. Cir. 1985). The M.P.E.P. § 2164.04 provides guidance regarding how this test is to be applied. The M.P.E.P. states:

> (I)t is incumbent upon the Patent Office, whenever a rejection on this basis is made, to explain why it doubts the truth or accuracy of any statement in a supporting disclosure and *to back up assertions of its own with acceptable evidence or reasoning which is inconsistent with the contested statement.* Otherwise there would be no need for the Appellant to go to the trouble and expense of supporting his presumptively accurate disclosure. (Emphasis added.)

In short, the Examiner must provide specific technical reasons showing why appellant's disclosure fails to satisfy the enablement requirement.

In the present case, there is no reason to expect that a XIAP antisense oligonucleotide that is nineteen nucleotides in length is unique in its ability to induce apoptosis. In fact, appellant discloses that antisense XIAP oligonucleotides may be used to induce apoptosis in a cell *regardless of the length of the antisense oligonucleotide.* The Examiner has acknowledged that appellant's disclosure enables the *in vivo* use of an antisense oligonucleotide of one particular length (see page 3, first paragraph, of the Office action mailed September 14, 2004), and appellant's specification discloses that other antisense molecules are also expected to have the desired activity, in a manner that is independent of their length. At this juncture it is incumbent upon the Examiner to provide evidence showing why undue experimentation would be required to identify antisense oligonucleotides of other lengths that also induce apoptosis if this rejection is to be maintained.

To support the enablement rejection, the Examiner cites Chirila et al., (Biomaterials 23:321-342, 2002, hereafter "Chirila"), Jen et al. (Stem Cells 18:307-319, 2000, hereafter "Jen"), and Stein (Pharmacology & Therapeutics 85:231-236, hereafter "Stein"). For the reasons discussed in detail below, none of these references supports the Examiner's position of lack of enablement.

Chirila

Chirila provides a review of the use of synthetic polymers for delivery of therapeutic antisense oligonucleotides. The Examiner cites passages from Chirila to support the assertion that methods for the *in vivo* delivery of oligonucleotides were inadequate at the time of filing. For example, the Examiner asserts that antisense oligonucleotide delivery must be maintained for a sufficient period of time to achieve therapeutic efficacy and that at the time of filing methods for such delivery were inadequate. A thorough reading of the entire passage suggests that this challenge can be overcome by repeated administration, a method known to the skilled artisan at the time of filing. At page 327, right column, last paragraph, Chirila states (emphasis added), "Many studies indicate that although ODNs can gain access to the target tissue *in vivo*, they are eliminated rapidly and repeated administration is required to achieve therapeutic effects."

In another passage cited by the Examiner, Chirila appears to support the assertion that methods of antisense delivery at the time of filing were insufficient. But a careful reading of the entire passage suggests that it may be *the use of polymers* as a delivery system that holds future promise. Polymer delivery strategies are discussed as a potential

replacement for existing oligonucleotide delivery methods. At page 337, left column, lines 26-48, Chirila states:

> In spite of profuse research, none of the polymer carriers developed so far were able to replace convincingly as a delivery system the infusion (or injection) of free or liposome-encapsulated AS ODNs [antisense oligonuclotides], although some of the proposed carriers (cationic polymers, biodegradable polymers) showed promising results...However, the fact that the outcome so far is not of decisive help in establishing which polymers shall be the carriers of choice is rather a moot point. This review clearly demonstrates a consistent and ever increasing interest in the polymer-aided delivery of therapeutic AS ODNs, which brings hopes that this biomaterials application will be successful in the forthcoming future. As a new generation of drug therapy in an advanced stage of development, the antisense strategy only awaits a suitable delivery system in order to live up to its promise.

With respect to existing methods for antisense oligonucleotide delivery, Chirila states:

> There is, however, some skepticism about the need for delivery systems for AS ODNs [15]...Since the AS ODNs can be delivered without any carrier and they still can display AS activity, is there any need to bother with developing delivery systems? In reply, there are many reports indicating enhanced therapeutic effect of AS ODNs when they are delivered in association with an adjuvant (page 327, right column, first paragraph). (Emphasis added.)

Thus, Chirila accepts that antisense nucleic acids delivered by infusion or injection display antisense activity, but advocates the development of alternate delivery systems to enhance the therapeutic efficacy of these antisense oligonucleotides.

In fact, Chirila provides numerous examples demonstrating the successful use of antisense oligonucleotides *in vivo*. For example, at page 322, right column, first paragraph, Chirila observes that a commercial antisense therapeutic, Fomivirsen, was approved by the FDA as a treatment for cytomegalovirus retinitis; at page 326, left

column, lines 6-11, Chirila notes that antisense effects were obtained *in vivo* with naked oligonucleotides in animal and clinical trials; at page 330, right column, second paragraph, Chirila reveals that antisense oligonucleotides, covalently coupled to poly(L-lysine), were effectively delivered to hepatoma cells *in vitro* and *in vivo,* citing three references by Wu and colleagues (Wu et al., J. Biol. Chem. 263:14621-4; 1988; Wu, J. Biol. Chem. 262:4429-32; 1987; Wu, J. Biol. Chem. 267:12436-9, 1992); at page 330, right column, last paragraph, Chirila notes that the poly(L-lysine) oligonucleotide complexes were used to efficiently deliver antisense oligonucleotides to animal organs where they targeted a retroviral mRNA; at page 332, right column, lines 12-16, Chirila notes that polyspermine poly(ethylene oxide) copolymers were used to deliver antisense oligonucleotides into the vitreous cavity of rat eyes where they successfully downregulated expression of their target, fibronectin, citing Roy et al., (Nature Biotech. 17:476-9, 1999); at page 333, left column, lines 15-22, Chirila relates that antisense oligonucleotides were used to inhibit tumour growth in mice injected with oncogene-carrying cells; at page 335, right column, second paragraph, Chirila, citing Edelman et al., (Circ. Res. 76:176-82, 1995), observes that antisense oligonucleotides in poly(ethylene-co-vinyl acetate) produced a 99.6% inhibition of hyperplasia when surgically implanted around denuded rat carotid artery. Finally, Chirila notes, at page 336, right column, lines 6-11, that antisense oligonucleotides in hydrogels inhibited cell proliferation in pig arteries after angioplasty, citing Azrin et al. (Cath. Cardiovasc. Diag. 41:232-40, 1997).

In sum, Chirila fails to support the Examiner's assertion that at the time of filing methods for the *in vivo* delivery of therapeutic oligonucleotides were unpredictable. In fact, contrary to this assertion, Chirila provides numerous examples demonstrating the successful therapeutic use of antisense oligonucleotides. Thus, this basis for the enablement rejection should be withdrawn.

Jen

Jen provides a review of strategies and options for suppressing gene expression by targeting mRNA. The Examiner cites Jen in support of the assertion that antisense therapy methods are not routine. In a passage cited by the Examiner, Jen opines, "the effective and efficient clinical translation of the antisense strategy has remained elusive." Jen supports this opinion by citing Waters et al. (J. Clin. Oncol. 18:1812-1823, 2000). In particular Jen states:

> While a number of phaseI/II trials employing ONs [oligonucleotides] have been reported, virtually all have been characterized by a lack of toxicity but only modest clinical effects. A recent paper by Waters et al. describing the use of a bcl-2-targeted ON in patients with non-Hodgkin's lymphoma is typical in this regard (page 315, lines 9-15).

While Jen characterizes Water's results as showing only "modest clinical effects," Waters's *in vivo* administration of antisense oligonucleotides downregulated the target protein in many of the patients that received treatment (Waters et al., J. Clin. Oncol. 18:1812-1823, 2000). This is particularly impressive given that Waters et al. describe a

phase I trial, designed primarily to assess toxicity, rather than efficacy. On this point, Waters et al. state:

> Bcl-2 protein was reduced in seven of 16 assessable patients. This reduction occurred in tumor cells derived from lymph nodes in two patients and from peripheral blood or bone marrow mononuclear cell populations in the remaining five patients.
>
> CONCLUSION: Bcl-2 antisense therapy is feasible and shows potential for antitumor activity in NHL [Non-Hodgkin's Lymphoma]. Downregulation of Bcl-2 protein suggests a specific antisense mechanism (emphasis added) (page 1812, right column, abstract).

Thus, Waters et al. successfully used antisense oliognucleotides *in vivo* to inhibit the biological activity of a target protein. Thus, Waters et al. fail to support Jen's opinions regarding the difficulties associated with the therapeutic use of antisense oligonucleotides *in vivo*.

Stein

The Examiner also cites Stein to support the assertion that the use of antisense oligonucleotide therapeutics is unpredictable because such use lacks sequence specificity. In fact, a thorough reading of Stein fails to support this assertion. While Stein believes that nonsequence specific effects are a problem for researchers interested in determining the function of particular genes, Stein does not believe that such effects are a problem for medical providers interested in the therapeutic use of antisense oligonucleotides. On this point, Stein states:

> These nonsequence-specific effects of phosphorothioate oligonucleotides themselves may be therapeutic. Sorting out specific and nonspecific

> mechanisms of action may often be extremely difficult, if not well nigh impossible. Fortunately, this matters neither to the physical health of a patient being treated with an antisense oligonucleotide nor to the financial health of the treating entity (page 232, left column, paragraph spanning pages 231 and 232).

In fact, Stein provides examples of the successful therapeutic use of the non-sequence specific antisense therapeutic Fomivirsen.

> In this particular case, however, while Fomivirsen is undeniably active clinically, some doubts remain as to its mechanism of action. These doubts relate to the nonspecificity of phosphorothioates, engendered by their ability to nonsequence-specifically bind heparin-binding proteins (page 231, right column, paragraph spanning pages 231 and 232).

In fact, regarding the use of antisense oligonucleotides, Stein states, "Over the past decade, the antisense biotechnology has been employed many times to reproducibly demonstrate truly stunning down-regulation in a variety of systems (page 231, left column, first paragraph). While Stein acknowledges that conflicts exist regarding some data, Stein regards the antisense data as widely reproducible.

> ...[T]argets, such as protein kinase C (PKC)-α, c-raf kinase, intercellular adhesion molecule-1, and bcl-2 have been examined by several laboratories, producing a consensus that in these examples down-regulation of translation is indeed due to a Watson-Crick hybridization mechanism. Indeed, evidence exists that such a mechanism may have clinical applicability (page 231, left column, first paragraph, continued in the right column).

Stein goes on to cite examples of the successful therapeutic use of antisense oligonucleotides *in vivo*, in particular, the use of phosphorothioate antisense oligonucleotides to target intercellular adhesion molecule-1 mRNA for the treatment of Crohn's disease (page 231, left column, first paragraph, continued in the right column)

and the use of Fomivirsen, a phosphorothioate oligodeoxynucleotide, to target cytomegalovirus immediate early mRNA as a treatment for cytomegalovirus retinitis (page 231, right column, first paragraph, continued on page 232).

In sum, Chirila, Stein, and Jen fail to support the Examiner's assertion that methods for delivering antisense oligonucleotides provided an obstacle to their therapeutic use at the time of filing. In fact, Chirila and Stein tend to support appellant's position that at the time of filing antisense oligonucleotides could predictably target specific mRNA sequences for inhibition.

Routine screening identifies antisense oligonucleotides

The skilled artisan, provided with appellant's disclosure and using methods known in the art, could easily screen any antisense oligonucleotide, regardless of its length, for its ability to induce apoptosis in a cell. As disclosed in appellant's specification, antisense oligonucleotides may be designed using computer algorithms and screened *in vitro* to identify those that effectively inhibit protein expression (pages 54-55). Antisense oligonucleotides that are selected for efficacy *in vitro* are typically effective *in vivo*, as well, as stated in the Declaration of Dr. Eric Lacasse (the "Lacasse Declaration") ¶3 (submitted June 14, 2004; considered September 14, 2004). *In vivo* screening is used to identify those antisense oligonucleotides having the greatest efficacy (pages 55 and 56 of the specification). Such screening is merely routine and thus cannot constitute undue experimentation.

Antisense oligonucleotide length is not a determinant of efficacy

Antisense oligonucleotides are potent and specific therapeutic molecules that share a common mechanism of action: they interfere with protein production by binding to a complementary target mRNA. This binding inhibits protein production by interfering with the ribosome's ability to translate the mRNA, by interfering with splicing, and/or by inducing the degradation of the mRNA by RNAse H, an enzyme that recognizes and degrades mRNA/DNA hybrids. Regardless of the length of the antisense oligonucleotide, if it binds an accessible site on the target RNA in the cell, the antisense oligonucleotide will successfully inhibit protein production. (Lacasse Declaration ¶4)

As stated in the Lacasse Declaration ¶5, the results shown in Shankar et al., J. Neurochem. 79:426-436, 2001 (hereafter "Shankar"), Kallio et al. FASEB J. express article, 10.1096/fj.01-0280fj3, 2001 (hereafter "Kallio"), and Fukuda et al. Blood 100:2463-2471, 2002 (hereafter "Fukuda") were carried out using methods available at the time appellant's priority document was filed. These references describe the use of antisense oligonucleotides of varying lengths to decrease the expression of the inhibitor of apoptosis protein survivin. The results of these studies are summarized below.

Shankar: 20-mer antisense oligonucleotide

Shankar describes the use of phosphorothioate modified antisense oligonucleotides, 20 nucleotides in length, to downregulate expression of human survivin expression and to induce apoptosis in neural tumor cells in culture. (Lacasse Declaration ¶6)

Kallio: 18-mer antisense oligonucleotide

Kallio describes the use of phosphorothioate modified antisense oligonucleotides, 18 nucleotides in length, to downregulate human survivin expression in HeLa and PtK1 cells in culture. The antisense oligonucleotides were conjugated to fluorescein isothiocyanate, which allowed them to be visualized by fluorescence microscopy. (Lacasse Declaration ¶7)

Fukuda: full length antisense oligonucleotide

Fukuda describes the use of a full-length antisense survivin expression construct to modulate survivin expression in CD34 cells. (Lacasse Declaration ¶8)

As further evidence that one skilled in the art could have practiced the claimed invention as of the filing date of the application, the Lacasse Declaration discusses U.S. Patent Nos. 5,958,771 ("the '771 patent") and 5,958,772 ("the '772 patent"), which were each filed on December 3, 1998, and 6,087,173 ("the '173 patent"), which was filed on September 9, 1999. As detailed below, each of these patents relates to the use of phosphorothioate modified antisense oligonucleotides to inhibit the expression of an IAP. This work was carried out using methods available at the time appellant's priority document was filed (Lacasse Declaration, ¶9).

The '771 patent describes the identification of twelve phosphorothioate modified 18-mer oligodeoxynucleotides that inhibited Cellular Inhibitor of Apoptosis-2 (cIAP-2) expression in cells *in vitro* (Table 1 and column 41, first paragraph) (Lacasse Declaration, ¶10).

The '772 patent describes the identification of six 18-mer phosphorothioate oligodeoxynucleotides that inhibited cIAP-1 expression in cells *in vitro* (Table 1 and column 39, first paragraph) (Lacasse Declaration, ¶11).

The '173 patent describes the identification of twenty-four 20-mer antisense oligodeoxynucleotides that inhibited XIAP expression in cells in vitro (Table 1, and column 41, first paragraph) (Lacasse Declaration, ¶12).

The examples cited above demonstrate that a full range of antisense oligonucleotide lengths work to inhibit the biological activity of an IAP target gene.

Clinical applications for antisense oligonucleotides

In addition, with respect to Jansen et al., The Lancet Oncology 3:672-683, 2002 (hereafter "Jansen"), which provides a review of the *in vivo* use of antisense oligonucleotides of varying lengths, the Lacasse Declaration states that the examples cited below, which relate to the use of phosphorothioate modified antisense oligonucleotides to inhibit protein production, were also carried out using methods available at the time applicants' priority document was filed. (Lacasse Declaration ¶13)

18-mer phosphorothioate antisense oligonucleotide

Jansen describes 1997 phase I clinical trials that used an 18-mer phosphorothioate Bcl-2 antisense oligonucleotide to treat patients diagnosed with non-Hodgkin lymphoma. Treatment with the 18-mer antisense oligonucleotide decreased BCL-2 protein levels in

half of all patients that received it (page 676, right column, first paragraph). (Lacasse Declaration ¶14)

20-mer phosphorothioate antisense oligonucleotide

In a 1996 study by Yazaki et al. (Mol Pharmacol 50:236-42, 1996), which is also reviewed by Jansen, a 20-mer phosphorothioate modified antisense oligonucleotide was used to inhibit Protein Kinase C expression in glioblastoma xenografts in mice (paragraph spanning page 677, right column, to page 678, left column). (Lacasse Declaration ¶15)

24-mer antisense oligonucleotide

A clinical pilot study, carried out by Ratjczak and colleagues in 1992, is also reviewed in Jansen. In this study, a 24-mer phosphorothioate modified antisense oligonucleotide was used *ex vivo* to successfully target and decrease the expression of the c-MYB proto-oncogene in bone-marrow cells harvested from patients with chronic myelogenous leukemia (page 679, right column, first paragraph). (Lacasse Declaration ¶16)

As further evidence of enablement, the Lacasse Declaration referred to Sugano et al., J. Biol. Chem. 271:19080-19083, 1996 (hereafter "Sugano"), Galvin-Parton et al., J. Biol. Chem. 272: 4335-4341, 1997 (hereafter "Galvin-Parton"), MacLeod et al., J. Biol. Chem. 270:8037-8043, 1995 (hereafter "MacLeod"), and Ramchandani et al., Proc. Natl. Acad. Sci. USA 94:684-689, 1997 (hereafter "Ramchandani"), all of which were received

for publication prior to the date on which appellant's priority document was filed, and all of which relate to methods of using antisense oligonucleotides to inhibit protein production. (Lacasse Declaration ¶17)

21-mer antisense oligonucleotide

Sugano, published in 1996, used a 21-mer antisense oligonucleotide to inhibit expression of cholesteryl ester transfer protein (CETP), the enzyme that facilitates the transfer of cholesterylester from high density lipoprotein to apoB-containing lipoprotein. The asialoglycoprotein-coupled 21-mer antisense oligonucleotide, which was administered to rabbits intravenously, decreased CETP biological activity and also decreased total cholesterol levels. (Lacasse Declaration ¶18)

39-mer antisense oligonucleotide

As published in February 1997, Galvin-Parton expressed a 39-mer antisense oligonucleotide in transgenic mice. This 39-mer antisense oligonucleotide, which targeted the nucleic acid encoding G-protein, $G\alpha_q$, decreased $G\alpha_q$ polypeptide levels, and caused an increase in body mass and hyperadiposity. (Lacasse Declaration ¶19)

600-mer and 20-mer antisense oligonucleotides

MacLeod, in 1995, expressed a 600-mer antisense oligonucleotide, which was complementary to DNA methyltransferase mRNA, in Y1 cells, a tumorigenic adrenocortical cell line. This antisense oligonucleotide decreased DNA

methyltransferase gene expression, protein activity, and also decreased the ability of the Y1 cells to form tumors when injected into mice. (Lacasse Declaration ¶20)

In a related study published in January 1997, Ramchandani designed a phosphorothioate modified 20-mer antisense oligonucleotide that targeted the same region of DNA methyltransferase mRNA that was targeted by the 600-mer described by MacLeod. Ramchandani injected tumorigenic Y1 cells into the flanks of mice, allowed tumors to form, then administered the 20-mer antisense oligonucleotide to the tumor. The 20-mer and the 600-mer antisense oligonucleotides, though of widely differingly lengths, both decreased DNA methyltransferase levels and inhibited tumor growth. (Lacasse Declaration ¶21)

In sum, Shankar, Kallio, Fukuda, the '771 patent, the '772 patent, the '173 patent, Jansen, Sugano, Galvin-Parton, and MacLeod describe the use of antisense oligonucleotides that range in length between 18 and 600 nucleotides to inhibit the expression of a target gene and achieve a desired biological effect. These antisense oligonucleotides, regardless of length, bind to a complementary target mRNA and inhibit protein production, just as appellant's antisense oligonucleotides do. One skilled in the field of antisense, being familiar with the art available at the time of filing (of which the above is but a sample) would know that antisense molecules complementary to a portion of XIAP could be a variety of different lengths. (Lacasse Declaration ¶22)

The Examiner has acknowledged that appellant has enabled the *in vivo* use of certain 19-mer antisense oligonucleotides to inhibit the biological activity of XIAP. No evidence has been made of record to show that a 19-mer antisense oligonucleotide is

unique in its ability to inhibit XIAP biological activity. Indeed, appellant has provided abundant evidence showing that virtually any antisense oligonucleotide that binds to its complementary target mRNA will inhibit protein production. On this basis alone, the enablement rejection should be withdrawn.

In vivo efficacy of antisense XIAP therapy reduced to practice

The sufficiency of appellant's disclosure is evidenced in the Declaration of Dr. Robert Korneluk (submitted May 20, 2003; considered August 8, 2003) and accompanying exhibits, showing that appellant has successfully reduced to practice the present invention using techniques known to those skilled in the art of antisense oligonucleotide technology at the time of filing. Specifically, appellant i) identified antisense oligonucleotides; ii) rapidly screened IAP antisense therapies in cell lines; iii) tested the efficacy of identified antisense oligonucleotides in animal models; and iv) tested the efficacy of antisense oligonucleotides in combination with traditional therapies. These experiments, as detailed below, plainly demonstrate that the *in vivo* administration of antisense oligonucleotides complementary to XIAP SEQ ID NO:3 was enabled as a cancer therapy at the time appellant's priority document was filed.

Identification of antisense oligonucleotides

In the Korneluk Declaration, appellant discloses that antisense oligonucleotides were identified using methods outlined in the specification (Korneluk Declaration ¶4). Specifically, appellant identified ninety-six oligonucleotide sequences complementary to

a portion of XIAP (each sequence having nineteen nucleotides) (SEQ ID NOs: 1 through 96) from a region approximately 1 kb upstream of the start codon to approximately 1 kb downstream of the stop codon of the XIAP cDNA sequence.

In vitro screening of oligonucleotides

In the Korneluk Declaration, appellant discloses that the XIAP synthetic library of 96 antisense oligonucleotides was rapidly screened in cell lines (Korneluk Declaration ¶5). Specifically, T24 cells (1.5×10^4 cells/well) were seeded in wells of a 96-well plate on day 1, and were cultured in antibiotic-free McCoy's medium for 24 hours. On day 2, the cells were transfected with XIAP antisense oligonucleotides. On day 3, XIAP RNA levels were measured using quantitative real-time PCR techniques. At day 4, XIAP protein levels were measured by ELISA and total cellular protein was measured biochemically. These results were compared to a mock transfection sample (treated with the transfection agent without oligonucleotide DNA, and then processed as for the other samples).

These methods identified 16 antisense oligonucleotides that decreased XIAP protein levels relative to control cells that were mock transfected. As expected, the ability of an antisense oligonucleotide to decrease XIAP protein levels correlated with its ability to decrease XIAP mRNA levels. Sixteen of these oligonucleotides decreased by at least 50% levels of XIAP protein or mRNA levels. The G4 antisense oligonucleotides (G4AS) exhibited the strongest down-regulating effect on XIAP protein, reducing XIAP protein levels by 62% within twenty-four hours after the end of transfection when

compared with control, lipofectin alone, other antisense oligonucleotides (F3AS, C5AS), and oligonucleotide controls (F3RP, G4SC, C5RP). Cells treated with G4 antisense oligonucleotides had higher levels of apoptotic DNA content than control cells or cells treated with a G4 control oligonucleotide, and underwent morphological changes characteristic of apoptosis. Few control cells showed these morphological changes. Forty-eight hours after transfection, G4 antisense oligonucleotides reduced H460 cell growth 55% relative to untreated controls. *In vivo* studies with lung carcinoma and breast carcinoma cells were then carried out, as is described below.

Efficacy testing in animal models

In the Korneluk Declaration, appellant discloses that the efficacy of identified antisense oligonucleotides was tested in animal models (Korneluk Declaration ¶6, ¶7). In particular, appellant teaches that SCID-RAG2 mice were inoculated with H460 human lung carcinoma cells (subcutaneous shoulder injection of 10^6 cells) and treatments with G4 and F3 AS PS-ODNs, as well as a scrambled control, were initiated three days after tumor inoculation. Oligonucleotide injections were administered intraperitoneally at 12.5 mg/kg three times a week for three weeks. At the end of the treatment period, mean tumor sizes in the groups treated with either G4 or F3 antisense oligonucleotides were ~ 50 % smaller relative to tumor size in a control group treated with a scrambled control oligonucleotide or vehicle alone.

The treatment protocol described above was also tested on female SCID-RAG2 mice in groups 1-4 inoculated orthotopically with MDA-MB-435/LCC6 human breast

carcinoma cells. Two weeks after the last treatment (day 35) tumor volumes of mice treated with F3, C5 or G4 antisense oligonucleotides were 70%, 60% and 45% smaller than vehicle controls, respectively.

Appellant further discloses that G4 antisense oligonucleotides in SCID-RAG2 mice bearing xenografts of H460 human non-small-cell lung tumors were implanted subcutaneously (Korneluk Declaration ¶8). Saline-treated control tumors grew reproducibly to a size of 0.75 cm^3 within approximately 24 days. Oligonucleotide treatments were initiated three days after tumor cell inoculation. G4 antisense oligonucleotides (5 to 15 mg/kg) or a control oligonucleotide were administered using a treatment schedule of intraperitoneal injections given on days 3-7, 10-14, and 17-21 (once a day). The treatment with 5 or 15 mg/kg G4 antisense oligonucleotides greatly delayed tumor growth: on day 24 mean tumor sizes were 0.75, 0.45 and 0.29 cm^3 in control, 5 and 15 mg/kg treated groups, respectively. There was a dose-dependent inhibition of tumor growth. Tumor size in mice treated with 15 mg/kg G4 antisense oligonucleotides was significantly smaller than in control groups, and represented 39% of control mean tumor size. In contrast, administration of G4 scrambled oligonucleotides at 15 mg/kg provided no therapeutic activity. None of the mice treated with oligonucleotides displayed any signs of toxicities, and both doses of oligonucleotides were well tolerated. A dose of 15 mg/kg was selected for the future combination treatment regimens with anticancer drugs.

Appellant further discloses that to correlate G4 antisense oligonucleotide tumor growth inhibitory effects with XIAP protein expression, the changes in XIAP expression

at the end of the *in vivo* treatment with 15 mg/kg of G4, F3, and C5 antisense and scrambled oligonucleotides were examined (Korneluk Declaration ¶9). At day 21 or 24 post-tumor inoculation when tumors reached 1 cm^3 in size, tumors were harvested and lysates from tumor homogenates were used for western blot analysis. XIAP and β-actin antibodies against the human protein were used, allowing for determination of human XIAP levels obtained from tumor cells specimens without contamination from XIAP derived from mouse cells. XIAP protein levels in tumors treated with G4 antisense oligonucleotides were quantitated by densitometry. Appellant found that XIAP protein levels were significantly reduced to approximately 85% of control tumors (P <0.005). XIAP protein in tumors treated with G4 scrambled oligonucleotides were reduced in size by 24% of control tumors. These results indicated that inhibition of H460 tumor growth by G4 antisense oligonucleotides correlated with the down-regulation of XIAP protein expression.

To evaluate whether XIAP antisense oligonucleotide administration results in direct tumor cell kill, the histology of tumors after treatment was examined both for morphology and ubiquitin immunostaining (Korneluk Declaration ¶10). At day 21 or 24 post-tumor inoculation, tumors treated with 15 mg/kg of G4 antisense, scrambled oligonucleotides, or saline control were excised, sectioned, and stained with hematoxylin and eosin. The results demonstrated that tumors in animals administered given XIAP antisense oligonucleotides treatment contained an increased number of dead cells, identified morphologically by their amorphous shape and condensed nuclear material.

Efficacy testing of combination therapy

The Korneluk Declaration ¶12 discloses the *in vivo* efficacy of combination therapy. Appellant combined treatments of G4 antisense oligonucleotides with a known chemotherapeutic agent. The therapeutic efficacy of vinorelbine, an agent used for lung cancer treatment, was assayed in the presence and absence of G4 antisense oligonucleotides or scrambled oligonucleotides. Treatment was initiated on day 3 after tumor inoculation. Each of the two regimens induced significant tumor growth suppression in a dose-dependent manner without showing significant signs of undesirable toxicity (i.e., body weight loss). When administration of G4 antisense oligonucleotides (15 mg/kg) was combined with vinorelbine (5 mg/kg) for the treatment of H460 tumors, a more pronounced delay of H460 tumor growth was observed compared to either treatment administrated alone. Again, the mice did not show any significant signs of toxicity (i.e., body weight loss). Mean tumor size in mice treated with 5 mg/kg vinorelbine in the presence or absence of G4 AS or scrambled oligonucleotides was compared on day 29. The tumor sizes in the group receiving combination therapy was 0.22 ± 0.03 cm^3, significantly smaller than the tumor sizes of groups receiving any other treatment (tumor size in control mice receiving 5 mg/kg vinorelbine alone or a combination of vinorelbine and G4 scrambled oligonucleotide was 0.59 ± 0.04 and 0.48 ± 0.05 cm^3, respectively).

In sum, using routine methods described in the specification, appellant has demonstrated the *in vivo* therapeutic efficacy of antisense XIAP oligonucleotides for enhancing apoptosis in a cell of a mammal and for the treatment of a patient diagnosed as

having a proliferative disease. Clearly, appellant has enabled a method for inducing apoptosis in a cell in a mammal and a method for treating a patient having a proliferative disease by administering antisense nucleic acids complementary to XIAP (SEQ ID NO:3) to inhibit XIAP biological activity. Reconsideration and withdrawal of the rejection for lack of enablement is respectfully requested.

CONCLUSION

Appellant respectfully requests that the rejection of claims 5 and 9-15 be reversed.

This Appeal Brief is in reply to a Notification of Non-Compliant Appeal Brief mailed on December 7, 2005, and replaces the Appeal Brief filed October 14, 2005. Appellant previously enclosed a check for $250.00 in payment of the fee required by 37 C.F.R. § 41.20(b)(2), a petition to extend the period for replying for five months, to and including October 14, 2005, and a check for the fee required by 37 C.F.R. § 1.17(a). If there are any charges, or any credits, please apply them to Deposit Account No. 03-2095.

Respectfully submitted,

Date: 12/13

Kristina Bieker-Brady, Ph.D.
Reg. No. 39,109

Michael J. Bellivera Ph.D.
Reg. No. 52,608

Clark & Elbing LLP
101 Federal Street
Boston, MA 02110
Telephone: 617-428-0200
Facsimile: 617-428-7045

Claims Appendix

5. A method of inducing apoptosis in a cell in a mammal diagnosed as having a proliferative disease, said method comprising administering to said mammal a modified antisense oligonucleotide of length sufficient to inhibit an inhibitor of apoptosis (IAP) biological activity, wherein said antisense oligonucleotide is complementary to a portion of human X-linked IAP (XIAP) (SEQ ID NO:3).

9. A method of treating a patient diagnosed as having a proliferative disease, said method comprising administering to said patient a modified antisense oligonucleotide of length sufficient to inhibit an inhibitor of apoptosis (IAP) biological activity, wherein said antisense oligonucleotide is complementary to a portion of human X-linked IAP (XIAP) (SEQ ID NO:3).

10. The method of claim 9, wherein said mammal is a human.

11. The method of claim 9, wherein said proliferative disease is cancer.

12. The method of claim 11, wherein said cancer is ovarian cancer, adenocarcinoma, lymphoma, or pancreatic cancer.

13. The method of claim 5, wherein said mammal is a human.

14. The method of claim 5, wherein said proliferative disease is cancer.

15. The method of claim 14, wherein said cancer is ovarian cancer, adenocarcinoma, lymphoma, or pancreatic cancer.

Evidence Appendix

Exhibit	Evidence	Where in file history evidence is made of record
A	Chirila et al., Biomaterials 23:321-342, 2002	Cited by Examiner November 20, 2002
B	Declaration of Dr. Eric Lacasse	Submitted June 14, 2004; considered September 14, 2004
C	Declaration of Dr. Robert G. Korneluk and related exhibits	Submitted May 20, 2003; considered August 8, 2003
D	Fukuda et al. Blood 100:2463-2471, 2002	Submitted June 14, 2004; considered September 14, 2004
E	Galvin-Parton et al., J. Biol. Chem. 272: 4335-4341, 1997	Submitted June 14, 2004; considered September 14, 2004
F	Jansen et al., The Lancet Oncology 3:672-683, 2002	Submitted June 14, 2004; considered September 14, 2004
G	Jen et al., Stem Cells 18:307-319, 2000	Cited by Examiner November 20, 2002
H	Kallio et al. FASEB J. express article, 10.1096/fj.01-0280fj3, 2001	Submitted June 14, 2004; considered September 14, 2004
I	MacLeod et al., J. Biol. Chem. 270:8037-8043, 1995	Submitted June 14, 2004; considered September 14, 2004
J	Ramchandani et al., Proc. Natl. Acad. Sci. USA 94:684-689, 1997	Submitted June 14, 2004; considered September 14, 2004
K	Shankar et al., J. Neurochem. 79:426-436, 2001	Submitted June 14, 2004; considered September 14, 2004
L	Stein, Pharmacology & Therapeutics 85:231-236	Cited by Examiner November 20, 2002
M	Sugano et al., J. Biol. Chem. 271:19080-19083, 1996	Submitted June 14, 2004; considered September 14, 2004
N	U.S. Patent No. 5,958,772	Submitted June 14, 2004; considered September 14, 2004
O	U.S. Patent No. 6,087,173	Submitted June 14, 2004; considered September 14, 2004
P	U.S. Patent Nos. 5,958,771	Submitted June 14, 2004; considered September 14, 2004

Related Proceedings Appendix

There are no related proceedings.

ELSEVIER

Biomaterials 23 (2002) 321–342

Biomaterials

www.elsevier.com/locate/biomaterials

Review

The use of synthetic polymers for delivery of therapeutic antisense oligodeoxynucleotides

Traian V. Chirila*, Piroska E. Rakoczy, Kerryn L. Garrett, Xia Lou, Ian J. Constable

Centre for Ophthalmology & Visual Science and Lions Eye Institute, University of Western Australia, 2 Verdun Street, Nedlands, WA 6009, Australia

Received 15 August 2000; accepted 26 March 2001

Abstract

Developed over the past two decades, the antisense strategy has become a technology of recognised therapeutic potential, and many of the problems raised earlier in its application have been solved to varying extents. However, the adequate delivery of antisense oligodeoxynucleotides to individual cells remains an important and inordinately difficult challenge. Synthetic polymers appeared on this scene in the middle 1980s, and there is a surprisingly large variety used or proposed so far as agents for delivery of oligodeoxynucleotides. After discussing the principles of antisense strategy, certain aspects of the ingestion of macromolecules by cells, and the present situation of delivery procedures, this article analyses in detail the attempts to use synthetic polymers as carrier matrices and/or cell membrane permeabilisation agents for delivery of antisense oligodeoxynucleotides. Structural aspects of various polymers, as well as the results, promises and limitations of their use are critically evaluated.

Keywords: Antisense strategy; Antisense oligodeoxynucleotides; Endocytosis: Drug delivery; Charged polymers; Neutral polymers

Contents

Abbreviations: A, adenine; AS, antisense; C, cytosine; CD, cyclodextrin; DNA, deoxyribonucleic acid; EVAc, poly(ethylene-*co*-vinyl acetate); G, guanine; HART, hybrid-arrested translation; HELP, high-efficiency liquid phase; HEMA, 2-hydroxyethyl methacrylate; HPMA, *N*-(2-hydroxypropyl)methacrylamide; IPEC, interpolyelectrolyte complex; ODN, oligodeoxyribonucleotide, oligodeoxynucleotide; PAMAM, polyamidoamines; PCA, polycyanoacrylates; PDTEMA, *N*-[2-(2-pyridyldithio)]ethylmethacrylamide; PEDOT, poly(3,4-ethylenedioxythiophene); PEG, poly(ethylene glycol); PEI, polyethyleneimine; PEO, poly(ethylene oxide); PGA, poly(glycolic acid); PL, polylysine; PLA, poly(lactic acid); PLL, poly(L-lysine); POR, polyornithine; PS, polyspermine; RME, receptor-mediated endocytosis; RNA, ribonucleic acid; mRNA, messenger ribonucleic acid; RNase, ribonuclease; SNAIGE, synthetic or small nucleic acids interfering with gene expression; T, thymine; VP, 1-vinyl-2-pyrrolidinone

*Corresponding author. Tel.: +61-8-9381-0856; fax: +61-8-9382-1171.

E-mail address: tchirila@cyllene.uwa.edu.au (T.V. Chirila).

0142-9612/02/$ - see front matter
PII: S0142-9612(01)00125-9

1. Introduction

Treatment with traditional drugs is based on molecular substitution, which involves the chemical modification of various compounds that are then subjected to screening programmes. An increasing array of inherited and acquired diseases is now understood by an 'inside out' approach involving the identification and targeting of the underlying genetic cause. As a result, therapeutic strategies based on the addition of genes to compensate for faulty genes, addition of genes with new functions, or disruption of gene expression have been developed and they are rapidly growing in diversity and scope. Gene therapy treats diseases caused by the malfunction of a gene by transferring genetic material into cells either to correct a genetic error (gene targeting) or to introduce a new function with therapeutic benefit (gene augmentation) [1–7].

Recent years have witnessed the development of gene disruption technologies. One of such approaches is the antigene strategy [8,9], which aims either at the inactivation of genes by homologous recombination with DNA constructs or at disturbing gene function by combination with short fragments of DNA, i.e. oligodeoxynucleotides (ODNs), able to form triple helix structures. Differing in its approach from both traditional drug therapy and gene therapy, and—to a certain extent—from antigene strategy, is the *antisense* (AS) strategy (sometimes called 'anti-mRNA' or 'antimessenger'). The ODNs used in AS strategy target the molecule acting as an intermediary in genetic expression, i.e. the messenger ribonucleic acid (mRNA), with the aim to inhibit the production of the proteins. This technology makes use of very short fragments of nucleic acid molecules, most commonly ODNs (typically 15–30 nucleotides long) (Fig. 1) that display a complementary base sequence to the target mRNA. They are able to interact in a rational way with the mRNA transcripts of a mutant or overexpressed gene, preventing their translation into disease-related proteins. In an ideal situation, the mRNA molecule is vulnerable to selective attack, resulting in the arrest of its processing and the suppression of protein biosynthesis. In AS strategy, the target is not the gene, and there is no transfer of genetic material involved. Compared to the traditional drug strategies that are usually nonspecific, the use of AS ODNs provides high specificity and selectivity. Ideally, an AS ODN of a precise length has only one target (the mRNA), and the binding to target is sequence specific. Considering that every single mRNA molecule would be able to generate a large multitude of protein copies unless its processing is arrested, the inhibition of gene expression has to be more efficient and specific than the inhibition of resulting proteins.

Zamecnik and Stephenson were first to propose in 1978 the use of synthetic AS ODNs for therapeutic purpose [10,11], but the term 'antisense' came into use in 1984 when it was coined by Izant and Weintraub [12,13]. Over the last two decades, the AS strategy has received special attention due to the rationality of its foundation and the apparent ease in synthesising and using ODNs as potential drugs. Recent reports [14,15] suggest that at least a dozen human clinical trials with AS ODNs have been initiated since 1992, directed at targets with roles in cancers, AIDS, inflammatory disorders, psoriasis, cytomegalovirus retinitis, and renal transplant rejections. A commercial antisense therapeutic product (Fomivirsen®) was approved by the FDA in 1998 for the treatment of cytomegalovirus retinitis. Although AS technology is becoming an established strategy of undisputed potential therapeutic power, controversies regarding the mechanism of action and experimental reproducibility, as well as some issues that are presently not well understood, are slowing down the progress in this field. The difficulty in finding an adequate delivery method for AS ODNs in relation to their cellular (or nuclear) uptake is currently perceived as one of the major drawbacks. A number of ingenious stratagems have been developed to deal with this problem, and the use of synthetic polymers as carriers for AS ODNs is one of them. This article attempts to provide a detailed account of the structure, suitability, limitations, and outcomes of the polymers proposed so far for the delivery of AS ODNs.

One expects that the problems underlying the delivery of ODNs in AS strategy should not be significantly different from those underlying the nonviral delivery of DNA in gene therapy. The latter topic has been extensively reviewed [16–18]. Indeed, many polymer carriers presented here have been also tried for delivery of DNA. However, the size of DNA (commonly a plasmid) is considerably larger than that of an

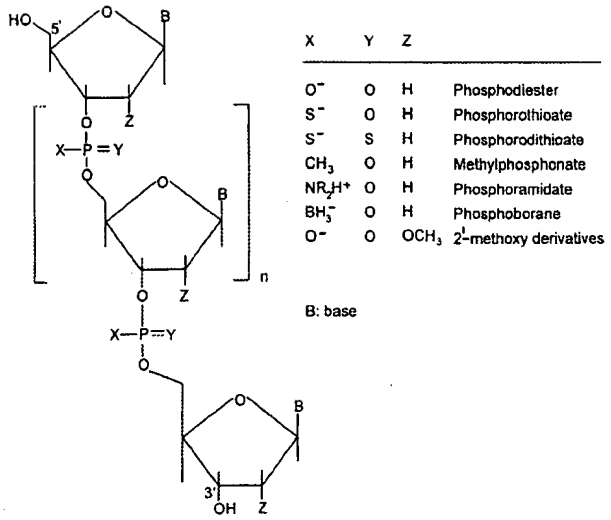

X	Y	Z	
O^-	O	H	Phosphodiester
S^-	O	H	Phosphorothioate
S^-	S	H	Phosphorodithioate
CH_3	O	H	Methylphosphonate
NR_2H^+	O	H	Phosphoramidate
BH_3^-	O	H	Phosphoborane
O^-	O	OCH_3	2'-methoxy derivatives

Fig. 1. Structure of oligodeoxynucleotides used in antisense strategy.

oligonucleotide, which makes cellular and nuclear uptake of plasmids more difficult and creates an additional technical challenge that may limit the range of potential carriers. The nonviral delivery methods employed in gene therapy appear to be less efficient than the virus-mediated delivery [17,19].

2. Antisense strategy: principles and mechanism

The principle of AS therapeutic action follows the central dogma of molecular biology in eukaryotic cells, and was comprehensively discussed in some major reviews [20–26]. The basic assumption is simple: if a single-stranded nucleic acid could hybridise to a nucleic acid, the result should be blockage of the normal utilisation in cells of the latter.

Every gene (a double-stranded DNA), carrying the genetic information for a particular protein, is *transcribed* in the cell nucleus to copies of single-stranded mRNA, the intermediary carrier of information. The primary transcript, the so-called pre-mRNA, undergoes a number of maturation processes to become mature mRNA, which is then translocated into the cytoplasm. Each copy of mRNA then serves as a template for the biosynthesis of a large number of molecules of the particular protein by *translation* on ribosomes (the protein biosynthesis apparatus in cell), leading to the appearance of the phenotype determined by the original gene. A description of an ideal AS mechanism would be that an AS ODN enters the cell and interacts specifically and directly with molecules of its complementary mRNA. These ODNs are called 'antisense' because they constitute a complementary strand to a portion of a coding sequence, generally designated the 'sense' strand. Single-stranded mRNA binds to the AS ODN by hydrogen bonds, usually by Watson–Crick base pairing (Fig. 2), and forms a double-helix hybrid (duplex). Regarding AS ODNs as drugs, their affinity for receptors (the mRNA sequences) is the result of two processes, the hybridisation by base pairing and the base stacking in the double helix that is formed. The specificity of AS ODNs as drugs results from the highly selective nature of the base pairing itself.

The hybridised mRNA species become obsolete for translation from several possible causes. For instance, binding of an AS ODN to the mRNA at the site where translation starts prevents the binding of factors that initiate or modulate the translation. Also, the hybrid formation may block the movement of the ribosomes along the mRNA molecule; their progress is held up for a while until they finally drop off. Translation being suppressed, the biosynthesis of the protein for which the target mRNA served as a template is no longer possible (Fig. 3). Paterson et al. [27] demonstrated this mechanism for the first time in a cell-free system, and coined for it the term of 'hybrid-arrested translation' (HART). Its therapeutic consequence is obvious when the aim is the cancellation of a disease-related protein.

Translational arrest is indeed the inhibitory mechanism for which the majority of AS ODNs have been initially designed. However, there is compelling experimental evidence that more than one mechanism can be operative besides HART. The mechanisms by which AS ODNs induce effects appear to be complex, many, and might even be more numerous than thought. In fact, only in a limited number of cases a true antisense inhibitory action has been rigorously demonstrated. Since rather little is presently understood about the contributions of various mechanisms to the events that happen after the ODNs were delivered and exposed to their nucleic acid receptors, a treatment of the operative inhibitory mechanisms involved in the so-called 'antisense' activity would remain largely theoretical and beyond the aim of this review. The specialists in the field have extensively discussed these mechanisms [4,9,20,21,23,24,26,28–34]. Attempts to rationalise both proven and putative mechanisms led to classifications which take into account that any of the events occurring in the processing of mRNA may be inhibited by intervening ODNs [21,23,26,34]. For instance, AS ODNs can interfere with any of the events preceding translation and taking place in the nucleus, i.e. transcription (in which case the target is DNA), splicing, or maturation. These inhibitory pathways are sometimes classified as 'occupancy-mediated mechanisms' [23], a category that also includes HART. Other mechanisms, classified as 'occupancy-mediated destabilisation' [23,26], refer to the inhibition of early post-transcriptional key steps in the processing of pre-mRNA. In order to assure a stable mature mRNA, the pre-mRNA must undergo both capping with a specific protein at

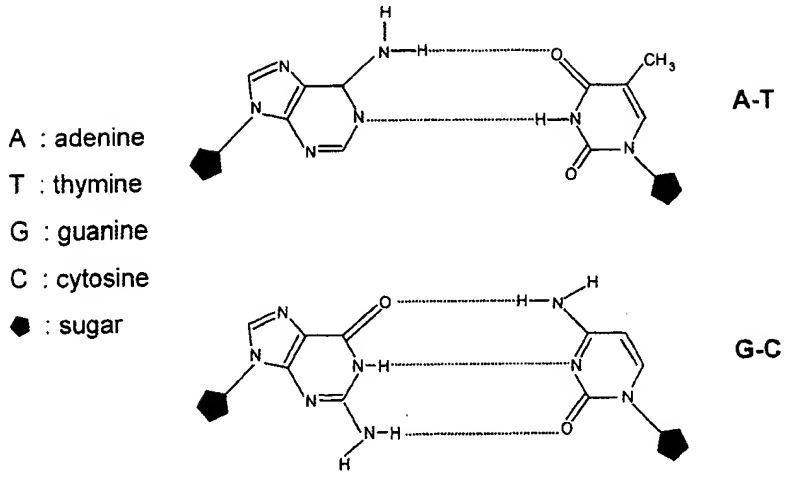

Fig. 2. Watson–Crick base pairing.

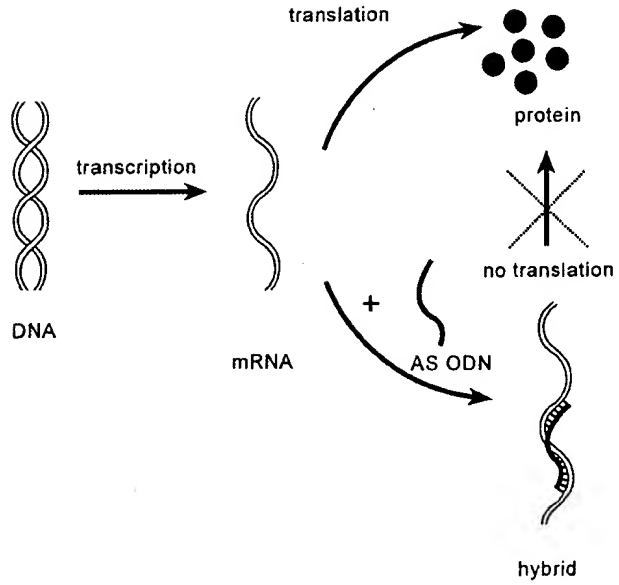

Fig. 3. Inhibition of translation by an AS ODN.

the 5′-end and addition of polyadenylate chains at the 3′-end. By interacting with 5′- and 3′-regions of the pre-mRNA, the ODNs can inhibit these steps and thus destabilise the RNA species. Another important mechanism relies on the activation of ribonuclease H (RNase H), a group of ubiquitous enzymes that specifically cleave the RNA strand of an RNA–DNA duplex. The RNase H-mediated cleavage is very effective and appears to be the most commonly accepted mechanism for the activity of AS ODNs, although the recognition of the ODN substrates by RNase H is restricted due to its high sensitivity to the structural changes in ODNs.

Another mechanism is based on the chemical alteration of the target nucleic acid by oligonucleotides bearing reactive species that can induce alkylation or crosslinking. When the oligonucleotides are conjugated to complexes of redox-active metals able to generate activated oxygen species, they can specifically bind to, and then cleave, the target nucleic acid (hence the term 'artificial endonucleases' [21]). Related to the latter method, the use of ribozymes has attracted much attention [20,34,35]. Ribozymes are RNA species able to catalyse the cleavage of the RNA species within RNA–ribozyme duplexes. The therapeutic exploitation involves their attachment to oligonucleotides in order to be delivered as synthetic entities consisting of antisense domains and catalytic domains. Other single- or double-stranded nucleic acid species, known as 'aptamers' [15,32], bind to proteins that have regulatory functions in the expression of genes. Finally, nonspecific effects of certain sense or homopolymeric ODNs have been observed in many instances [21], suggesting more intricate inhibitory mechanisms.

Strictly speaking, most of these mechanisms are not antisense processes. While, by definition, an AS mechanism is sequence specific and has the mRNA as the target of its action, many of the above mechanisms are sequence independent and/or are targeting DNA or proteins. In an attempt to reconcile this discrepancy and envelop more adequately the large variety of mechanisms and approaches commonly covered by the antisense umbrella term, Leonetti et al. [29] proposed the generic concept of 'synthetic or small nucleic acids interfering with gene expression' (SNAIGE). Apart from HART and the mechanisms mentioned above, SNAIGE also includes the disruption of gene expression by triple-helix formation through the hybridisation of oligonucleotides with double-stranded DNA, which is clearly an antigene strategy aimed at transcriptional arrest.

Regardless of the precise mechanism of action, which is still a matter of conjecture from case to case, the

advances in AS strategy are afflicted by major problems. While significant progress has been lately recorded toward solving some of these problems, such as stability of ODNs and their hybrids to nuclease activity, target selection and specificity, sequence accessibility, biological activity in vivo, and technical feasibility, there remains a predominant challenge: the ability to suitably deliver the ODNs in order to assure maximum cellular permeability, effective internalisation, and improved efficiency in reaching the target.

3. Cellular internalisation of oligodeoxynucleotides and intracellular events

It is perhaps beneficial to briefly recapitulate what is known about the processes by which eukaryotic cells are able to ingest or eject macromolecules, a topic routinely treated in cell biology textbooks. The import and export of macromolecules (mainly proteins), other particulate matter, and low molecular weight solutes across the plasma membrane is a way by which the cells continuously communicate with the environment. Plasma membrane is the key factor in accumulation or elimination of various components, and it performs these tasks through transport (passive diffusion) and *endocytosis*. In the transport process, the membrane is stationary, and the solutes (mainly those with low molecular weight) diffuse through it. Endocytosis is the process of ingesting macromolecules or other particulate matter and involves formation of membrane-bounded vesicles. We will not discuss here the release of substances from cell (exocytosis), as it is not yet clear what role this process has in the intracellular trafficking of ODNs.

Endocytosis consists sequentially of inward folding of the plasma membrane (invagination), enveloping a droplet of extracellular medium, pinching off the membrane, and formation of an intracellular vesicle containing the ingested material. The vesicles fuse to form *endosomes*, which increase their size (to maximum 500 nm) by further fusing with each other or with other intracellular vesicles. This process is known as *pinocytosis*, and is different from phagocytosis, an endocytic process involving ingestion of bacteria or very large particles of food or foreign material by specialised cells. Most endosomes fuse with membrane-bounded organelles, known as *lysosomes*, which contain large amounts of hydrolytic enzymes. Endosomes fuse with primary lysosomes to form secondary lysosomes, which are the final destination of the internalised macromolecules targeted for degradation. While the ingested material is rapidly broken down by the lysosomal enzymes, the endocytic membranes are returned to the plasma membrane. Some endosomes bypass the lysosomes, traverse the cytoplasm (transcytosis), and either are incorporated into the plasma membrane or they release their contents by exocytosis. Macromolecules that do not have features recognisable by the membrane are ingested by nonspecific endocytosis, and some cells (e.g. those of the reticuloendothelial system) perform this process at a much higher rate than other cells (e.g. fibroblasts). The main idea to be retained is that the endosomal compartment of a cell performs the important task of sorting the internalised material for (a) degradation in lysosomes, (b) recycling to the plasma membrane, and (c) transcytosis.

Usually, the endocytic cycle begins with endosomes generated by small invaginations occurring in regions of the plasma membrane that are coated with electron-dense structures and are known as coated pits. The pits pinch off the membrane and form coated vesicles, which eventually shed their coats and fuse with early endosomes. The main protein of the coat is clathrin. As the clathrin-coated pits invaginate to become vesicles, the entrapped extracellular fluid (with its components) is internalised by a process called *fluid-phase endocytosis*. In most animal cells, clathrin-coated pits and vesicles provide a specialised pathway for ingestion of certain macromolecules by cells, termed *receptor-mediated endocytosis* (RME) or *specific adsorptive endocytosis*. This process takes place when a receptor at the plasma membrane binds to an extracellular macromolecule (ligand), and the receptor–ligand complex is internalised at a much higher rate than the macromolecules ingested through other pathways. The receptors are present in coated pits even in the absence of ligands but additional receptors accumulate after the binding of ligands. Models have been developed to explain the role of clathrin in the accumulation of receptors in coated pits [36]. While the clathrin-mediated pathways appear to be responsible for the majority of RME and for some pinocytic processes, clathrin-independent pathways for endocytosis have been demonstrated in several situations. Such pathways may proceed via small (50–100 nm) invaginations (caveolae) that contain a specific protein (caveolin) and certain receptors, or through smooth uncoated invaginations (150–300 nm). This process, which is termed 'potocytosis' [32], appears to deposit the macromolecules directly into cytosol, avoiding the lysosomal compartments, and some authors regard it as a nonendocytic process.

In order to perform their inhibitory tasks, the AS ODNs must pass through the plasma membrane, escape from cytoplasmic vesicles, and then reach the target in cytoplasm. (When nuclear events are targeted, the ODNs must also enter the nucleus.) There is, however, a serious difficulty: plasma membrane is a potent natural barrier both to large molecules and to negatively charged molecules. Surprisingly, although ODN molecules have at least one of these characteristics, implying little or no proficiency in diffusing across membranes,

their ingestion takes place better than would have been expected. For instance, it was demonstrated [37] that about 7.5% of a radiolabeled AS ODN added as a solution in serum-free medium to human cultured cells was internalised by cells within 15 min. The uptake of 'naked' AS ODNs is generally too low for a telling biological effect in an in vitro setting. On the contrary, AS effects have been attained in the in vivo setting with naked ODNs, not only in animal experiments but also in some clinical trials, and tentative explanations have been advanced for this apparent dichotomy [15].

Although many aspects of the ingestion of ODNs by cells have yet to be clarified, there is compelling evidence that they enter the cells by an endocytic process [15,29,32,36,38–46], not through passive diffusion as earlier thought. Pinocytosis, RME, nonspecific adsorptive endocytosis, and endocytosis mediated by membrane destabilisation were amongst the pathways suggested or demonstrated in different experimental conditions. Non-endocytic processes (e.g. potocytosis) have been also proposed [32,45–47]. The identification of receptors for ODNs and their role in RME remain to be elucidated. A number of cell surface 'receptor-like' proteins, yet to be characterised, have been associated with the internalisation of AS ODNs [39,40,45]; the results are sometimes conflicting and seem to be affected by the type of cells and experimental conditions. It was also shown [46] that the cellular uptake, intracellular trafficking, and activity of AS ODNs were related to the phases of the cell cycle, while the ingestion mechanism was apparently not influenced. According to some authors, two aspects of the internalisation of ODNs should be distinguished [48]: cellular uptake as such and release into the cytoplasm (or nucleus). Cellular uptake refers to binding of ODNs to the plasma membrane and their general ingestion by the cell. Release into the cytoplasm refers to the amount of ODNs that actually reach a compartment where they can be pharmacologically active.

After entering the cell, ODNs accumulate in endosomes and lysosomes. In lysosomes, their predictable fate is degradation. However, a fraction of ODNs escapes from endosomes into cytoplasm by mechanisms not completely understood. This efflux may take place through simple diffusion (unlikely), by transient destabilisation of endosomal membrane mediated by certain membrane proteins, or by leakage during a fusion event between two vesicles [39]. Regardless, it is to be assumed that the observed biological activity is due to those small amounts of AS ODNs that managed to escape from endosomes. Some of the released ODNs may be then transported to the nucleus and eventually enter the nucleus where they may interact with nuclear DNA and RNA species. This scenario is probably more complex than it appears and certainly raises additional problems. Pharmacologically, the endosomal sequestration of ODNs is a nonproductive detour, while lysosomal degradation is a dead end. Facilitation of endosomal escape was consequently an important aim of various stratagems to improve the efficacy of AS ODNs. The endosomal compartmentalisation can be completely bypassed by injecting ODNs directly into cytosol (microinjection), which leads to their rapid accumulation in the nucleus [29,45]. (For this reason, microinjection experiments are of little significance for the study of compartmentalisation of the ODNs internalised by endocytosis.) The penetration into the nucleus can take place through passive diffusion through nuclear pores or through active signal-mediated diffusion [29,32]. The former pathway is not possible for macromolecules exceeding 60 kDa in molecular weight, in which case the contribution of nuclear localisation signal molecules is necessary. As the AS ODNs seldom exceed 9 kDa, their nuclear uptake through the pores is unlikely to be obstructed. Although the intracellular fate of ODNs seems to favour a nuclear localisation, there is evidence that they are distributed both in the nucleus and in the cytosol [39,40]. The conflicting results regarding the preferential distribution may rather come from the large variation of the experimental conditions and from the notoriously poor reproducibility of antisense experiments.

4. Delivery of AS ODNs: the current status

There have been many strategies developed for the enhancement of rate and/or selectivity of cellular internalisation of AS ODNs. In an attempt to make more intelligible the vast literature currently available on this topic, a recent review [48] classifies the delivery strategies into two groups. The first group concerns the cellular uptake process and includes systems able to promote the binding of ODNs to the plasma membrane by either protecting them from degradation or by enhancing their interaction with the membrane. Such systems include conjugation of various compounds (e.g. cholesterol) to ODNs, complexation of ODNs with cationic compounds (e.g. cationic polymers), encapsulation of ODNs (e.g. within liposomes, cyclodextrins), and labeling targets (e.g. intercalating agents, ligands for cell-surface receptors) to ODNs. The second group concerns the entry into the cytoplasm (or nucleus) and includes systems able to facilitate the escape from endosomes, such as cytoplasmic transfer techniques (e.g. microinjection, electroporation) or endosomal membrane destabilising agents (e.g. viral peptides, fusogenic agents). The strategies are used alone or in combination, and every system has its own advantages and drawbacks. Only a brief overview of strategies that do not involve synthetic polymers is presented below.

Administration of naked AS ODNs by infusion or injection in various parts of the body is still the preferred method in vivo, however it requires multiple doses. Experiments in animals showed that nondamaging administration routes (nasally, orally, dermal patches, eye drops) are much less efficient [44]. The AS ODNs can be delivered as naked molecules by microinjection into the cytoplasm or nucleus [49–53]. Technically, this is a very complex procedure, mainly achievable in cell cultures, and is associated with poor reproducibility and unsatisfactory error range. Electroporation, an electrophoresis-mediated technique, was thought to be feasible only for cell lines in culture and also may induce damage to cells. Although the use of electroporation has been recently re-advocated in gene therapy, there are only a few reports on its application to delivery of ODNs [52,54]. Viral delivery systems have been used to a little extent in AS strategy [55–58].

Encapsulation or incorporation in liposomes is currently the preferred method for the delivery of AS ODNs [21,29,32,41,45,59–69] and, besides the intravenous infusion and subcutaneous, intramuscular or intraocular injection of naked ODNs, probably the only other method used in human clinical trials. (Ultimately, the suspensions of liposomes are also administered by infusion or injection.) Liposomes are microscopic closed vesicles varying between 20 nm and 4 μm in diameter and consisting of unilamellar or multilamellar phospholipid membranes that surround aqueous spaces where ODNs can be entrapped. Enhancement of cellular uptake of AS ODNs and, in some cases, of antisense effects has been reported with a large variety of liposomal carrier systems including anionic liposomes, pH-sensitive liposomes, immunoliposomes (i.e. containing antibodies directed at specific cell-surface receptors), fusogenic liposomes (i.e. able to merge with the cellular or endosomal membranes), and cationic liposomes. By far, the cationic lipids are the most frequently used in AS strategies, to the extent that some preparations are now available commercially (e.g. Cytofectin® and Lipofectin® products), as they appear to be active permeabilisation agents and destabilisers of the endosomal membrane. When using cationic lipids, the encapsulation is not a necessary step, as they easily form complexes with ODNs. In spite of their popularity, it is perceived that the liposomes have not been investigated sufficiently as carriers for AS ODNs. Also, there are some limitations on their use. For instance, the basic tendency of cationic liposomes is to accumulate in the reticuloendothelial system [70], leading to a short life in the serum and reduced access to other tissues. Generally, the size of the liposomes of practical importance is too large and their surface charge density is too high. Finally, some types of liposomes display poor encapsulation efficiency. There is no wonder that the search for other carriers has ever continued, one of the results being the association of AS ODNs with synthetic polymer carriers, the topic of our present article.

There is, however, some skepticism about the need for delivery systems for AS ODNs [15]. Most permeabilisation adjuvants employed in delivery systems interact with the plasma membrane, which is the very reason why they are used in this capacity. Consequently, the receptors, signaling processes, and then other functions of the cell may be seriously affected. This aspect has not been properly investigated. Other important questions also arise. Since the AS ODNs can be delivered without any carrier and they still can display AS activity, is there any need to bother with developing delivery systems? In reply, there are many reports indicating enhanced therapeutic effects of AS ODNs when they are delivered in association with an adjuvant. Another issue is that the association of AS ODNs with carriers will increase the size and complexity of the particles to be delivered, thus limiting their access to certain targets or even contributing to their degradation. In reply, we can cite some of the reasons why delivery systems are employed in the first place, i.e. increased cellular uptake, protection against degradation, and improved specificity. Nevertheless, debate is still open about the large size of ODN/carrier pharmacophores and toxicity of carriers.

The improvement of delivery systems for AS ODNs must be therefore an ongoing challenge for those involved in AS strategy research. One reason is the recognition of the fact that the way in which AS ODNs are delivered has dramatic consequences on their fate, as demonstrated in vitro by Wagner et al. [71–73] in a series of elegant experiments. They found that naked AS ODNs incubated with cells in culture were accumulated in cytoplasmic vesicles (likely endosomes and lysosomes), but not in the nucleus. When the ODNs were microinjected directly into the cytoplasm, all cells showed nuclear localisation of ODNs. When delivery to the cell cultures took place via cationic liposomes, 90% of cells showed nuclear localisation of ODNs. Another reason, probably the most important albeit seldom acknowledged, is the need for a sustained delivery in vivo. Many studies indicate that although ODNs can gain access to the target tissue in vivo, they are eliminated rapidly and repeated administration is required to achieve therapeutic effects [9]. It should be also considered that biological activity of an AS ODN needs to be maintained for additional periods of time to allow for the decay of the preexisting levels of the disease-related protein. The in vivo delivery techniques chiefly used at the present, i.e. infusion or injection of naked molecules and liposomal systems, do not assure adequately long-term maintenance of ODNs in tissues.

5. Synthetic polymers as carriers for delivery of AS ODNs

A detailed overview of the polymer carriers used in AS strategy is attempted in this section. In most of the experiments to be discussed here, phosphorothioate and phosphodiester ODNs were employed as antisense agents, with a preference for the former due to their enhanced resistance to enzymatic attack. The nature of AS ODNs plays, however, a less significant role in the choice and performance of the carrier. Unless relevant to other issues, the phosphorothioate or phosphodiester nature of the AS ODNs was not specified in our exposition.

5.1. Cationic polymers

Since the cellular membrane is negatively charged, it was the cationic polymers that have received the most attention as potential carriers for AS ODNs. The coulombic forces governing the interaction between plasma membrane and polycations are so strong that the influence of other properties of the polymers (e.g. hydrophilicity) is drastically diminished. Indeed, a variety of cationic polymers were able to promote the internalisation of AS ODNs in some cell types, as will be described further. However, the cationic polymers do not constitute the ideal solution. Some cell lines do not take up the ODN–polymer conjugates for reasons yet to be elucidated. There are also serious concerns about the cytotoxicity of positively charged polymers. Cationic carriers must contain enough charge to neutralise the ODNs and also to provide sufficient residual charge for interaction with the membrane of cells. It is, nevertheless, difficult to ascertain how much residual charge is enough, and even more difficult to adjust it to levels that will not render the carrier–ODN conjugate cytotoxic. On the other hand, in conditions of contact with serum, the positive charge of the carrier might be never enough to counterbalance the negatively charged serum components. The internalisation of conjugates can be prohibited in such cases, as firstly demonstrated with a cationic liposome–plasmid DNA conjugate [74].

5.1.1. Synthetic peptides

The interaction of nucleic acids with basic polyelectrolytes is a process that has been known for a long time. In 1946, Kleczkowski showed [75] that the conjugation of proteins with nucleic acids is a general phenomenon that takes place whenever the pH allows them to be of opposite charges, and also suggested that the interaction of proteins with viral nucleoproteins may be responsible for reducing the infectivity of some viruses. At about the same time, other investigators found that the growth of *Bacillus anthracis* was inhibited by a fraction of the calf thymus [76], as well as by a detergent (a benzylalkylammonium chloride) and by a protein, histone [77]. Both histone and thymus fractions are polypeptides with a high content in the amino acid L-lysine. In further studies, polylysine (PL, Fig. 4) and, to a lesser extent, copolymers lysine–valine were shown to induce the agglutination of avian erythrocytes [78], to reduce the infectivity of type A influenza virus [79] and of tobacco mosaic virus [80,81], and to induce the agglutination of bacterial cells [82]. Electrostatic binding of the cationic polypeptides to the surface of cells or viruses was suggested as the responsible mechanism. These findings were later confirmed [83] for a greater range of polypeptides and bacteria. As the neutral or anionic peptides did not show any effect, it was also suggested [83] that the effect of cationic peptides may be due to a more complex mechanism that includes the destabilisation of cellular membrane and penetration of polymers into the cell, the interaction between nucleic acids and polymers, or the blockage of some enzymatic processes. The effects of variously charged peptides on the agglutination of human erythrocytes were attributed to the same mechanism [84,85].

An early application of polycations was the development of a standard procedure for assaying infectious viral nucleic acids, based on the observation that cationic polyelectrolytes such as PL, polyornithine (POR, Fig. 4), or diethylaminoethyl dextran, enhance substantially the infectivity of poliovirus single- and multi-stranded RNAs by promoting their adsorption by cells [86–89]. Peptide-induced enhancement of viral activity, noticed in other viruses too [90], was regarded as a result of the polycations acting as permeabilisation agents. The enhancement by cationic polyelectrolytes of polynucleotide-induced interferon production was explained by the same mechanism [91–93]. Another application of cationic polypeptides (PL, POR, polyarginine) included their use as model compounds in the investigation of interaction between nucleic acids and histone species, which plays an important role in the regulation of genetic process. These studies [94–99] suggested that the binding reaction is more than a simple electrostatic neutralisation, involving steric selectivity and inducing stabilisation of DNA.

As expected, these findings eventually triggered the use of cationic polypeptides as carriers for transportation of bioactive agents. In 1965, Ryser's group at the Harvard Medical School found that the uptake of radiolabeled serum albumin by sarcoma-180 cell cultures is significantly enhanced by the presence of proteins rich in lysine or of synthetic peptides obtained from lysine (L, D or LD), L-ornithine, or L-histidine [100]. They concluded that the process must be more than a simple result of electrostatic interaction and suggested polycation-induced changes in the structure of cellular membrane, as surmised previously by others [85]. Subsequent investigations [101,102] indicated that

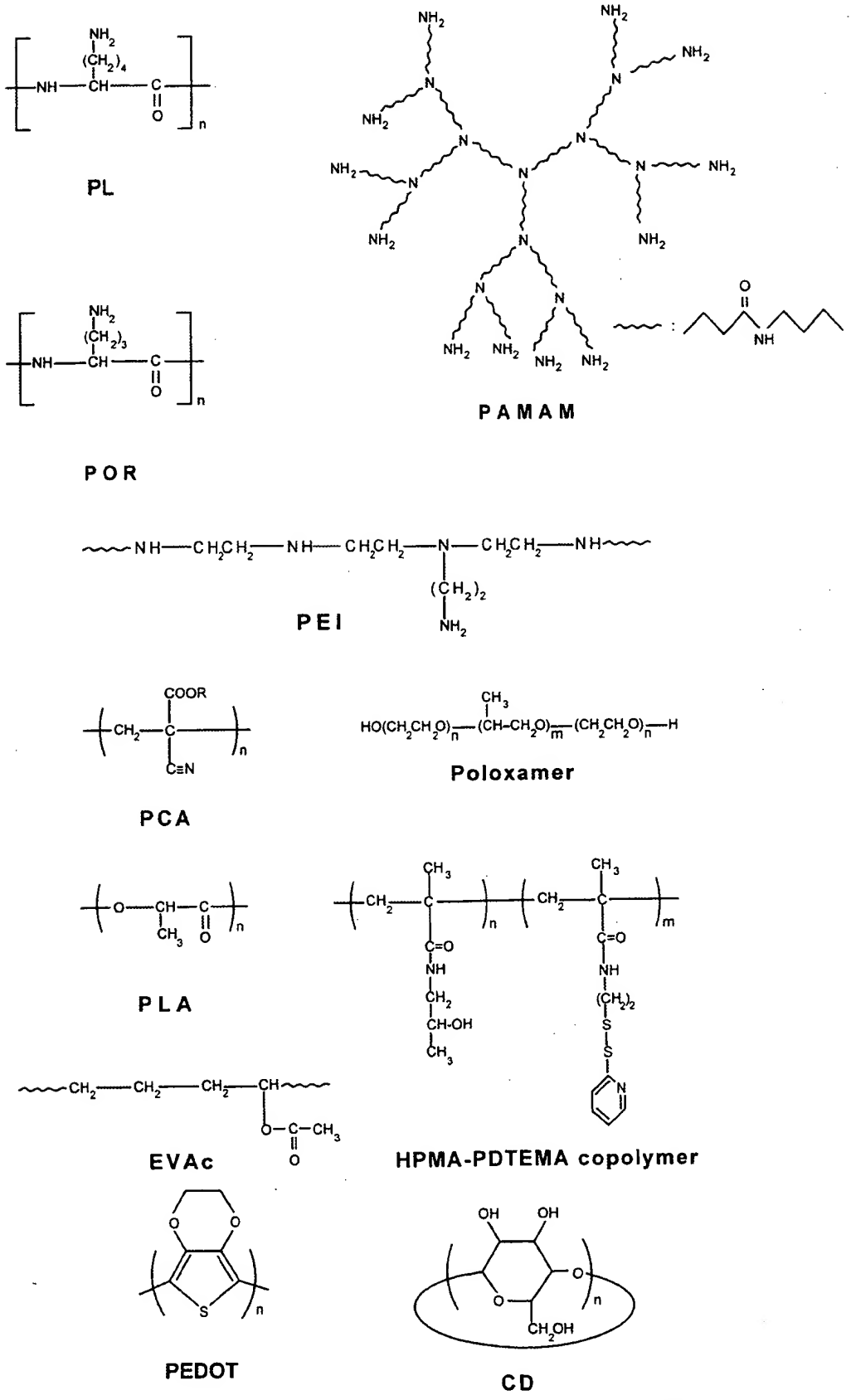

Fig. 4. Structure of some of the polymers used as carriers for AS ODNs.

individual amino acids or diamines do not have promoting effects, and that the effect of polypeptides is related to their molecular weight and to the distance between amino groups in their molecule, from which it was concluded that their attachment to the cellular membrane must take place through multiple centres. In later studies [103–105], Ryser's group advocated the covalent binding of carrier polypeptides to the bioactive agent. The cellular uptake of a drug (methotrexate) was considerably enhanced by binding it to poly(L-lysine) (PLL), and the drug was released into the cell in a pharmacologically active form [104]. Its potency was further increased by complexation of the drug–PLL conjugate with heparin, which was believed to facilitate the endosomal escape [105].

Although seldom acknowledged, the first study of the effect of PLL on the cellular uptake of polynucleotides has to be credited to Schell [106], who demonstrated that both pretreatment of cells with PLL and complexation of the polynucleotides with PLL enhanced the uptake of radiolabeled synthetic polyhomoribonucleotides by Ehrlich ascites tumour cells. The mechanisms suggested were based on the interaction between PLL and cellular membrane or on the formation of polynucleotide–PLL complexes with a high affinity for the cellular membrane. It was, however, more than a decade later that PLL was eventually considered as a potential carrier for AS ODNs delivery, mainly due to the pioneering work of Lebleu's group at the University of Montpellier (France), who demonstrated the efficiency of PLL–ODN covalent conjugates in several in vitro biological models. Initially, a dose-dependent inhibition of virus growth was observed when conjugates of PLL and 2′–5′ oligoadenylates (mediators of antiviral activity of interferons) were administered to L1210 or L929 cell cultures infected with various viruses (vesicular stomatitis, vaccinia, etc.) [107,108]. As cells do not take free oligoadenylates, this was a clear demonstration of PLL efficiency as a permeabilisation agent. Subsequently, the same group showed that AS ODNs complementary to certain regions of the vesicular stomatitis virus nucleocapsid protein mRNA were much more active in cell cultures when conjugated to PLL (10–50 times relative to free ODNs) [109–112], providing a sequence-specific and dose-dependent antiviral activity. However, it was also noticed that PLL is cytotoxic in high doses or ineffective in some cell lines. By using fluorescein-labeled ODNs, these investigators demonstrated that the uptake of conjugates is both accelerated and enhanced as compared to the unconjugated ODNs. As a mechanism, it was suggested that the conjugates are taken up by cells by nonspecific adsorptive endocytosis, and the AS ODNs are then released through the enzymatic degradation of the lysine moiety after the conjugates were sequestered within acidic cytoplasmic compartments. In summarising their results [29,41], the authors recommended the use of PLL in order to assure an efficient delivery of AS ODNs. PLL–ODN conjugates were also used to protect infected human MT4 cell lines from the pathologic effects of human immunodeficiency virus type 1 (HIV-1), by significantly reducing the production of viral proteins [113]. In other studies, the effect of PLL–ODN conjugates was further enhanced by complexation with a polyanion (heparin) [29,114], and some tentative explanations were advanced (reduction of PLL cytotoxicity, modification of the ODN release from conjugate, and/or interference of heparin with virus multiplication). The use of PLL in AS strategy, partially reviewed in a number of articles [9,29,32,41,48,115], is still advocated, and a large range of synthetic PLL products (3–60 kDa) are available commercially.

Other synthetic peptides were also investigated as carriers. Covalent conjugates of POR with AS ODNs were evaluated in a cell-free in vitro system by estimating their capacity to stimulate RNase H activity and the effect on the translation of complementary radiolabeled mRNA [116]. Both tests showed enhancement of the activity of POR–ODN conjugates as compared to unconjugated ODNs. Recently, a copolymer of lysine with serine, modified with poly(ethylene glycol), was used as a carrier for AS ODNs targeted against c-*raf* protein mRNA in pancreatic cancer cells in vitro [117]. The antiproliferative effect of the noncovalent complexes was evident, while the free AS ODNs had no such effect.

Target-labeling strategies using PLL were developed independently at the same time when PLL was proposed as a carrier. Targeting agents are tissue-specific ligands that are linked to PLL and are able to interact specifically with receptors on the target cells. Wu's group at the University of Connecticut was the first to develop a glycoprotein ligand (asialoglycoprotein) covalently coupled to PLL, resulting in conjugates able to function as carriers for delivery of DNA [118,119] or AS ODNs [120] to hepatoma cells in vitro and in vivo. Not only were the soluble ODN (or DNA)–PLL–asialoglycoprotein conjugates effective in delivering the ODNs or DNA specifically to target cells, but their resistance to nuclease degradation was also enhanced substantially [121]. Although other investigators [122–124] confirmed the efficacy of PLL–glycoprotein conjugates, more recent research suggested that the direct covalent binding of asialoglycoprotein to ODNs, which excludes the use of PLL, might provide a more efficient delivery system [125]. Other PLL–ligand systems are currently investigated for delivery of AS ODNs [32,48].

In another approach, noncovalent PLL–ODN complexes were incorporated by diffusion into alginate nanoparticles [126]. This system provided protection against nuclease degradation and also delivered efficiently into animal organs an AS ODN targeted to the mRNA of a retrovirus protein. PLL is also an essential

component of the so-called 'terplex system' developed for the delivery of DNA and AS ODNs [127,128]. The system is based on a balanced hydrophobicity and net surface charge between *N*-stearyl PLL, a lipoprotein and DNA (or ODN). When delivered in vitro by this system, a c-*myb* AS ODN (18 mer) showed distinctive antiproliferative effects in cultured smooth muscle cells and human lung fibroblasts.

Unlike PLL and other homopoly(amino acids), which are mainly employed because of their electropositive charge, the design and use of some heteropeptides was prompted by their translocation properties, i.e. the ability to destabilise the endosomal membrane and thus facilitate the release of ODN molecules into the cytoplasm before their degradation prevails [48]. These 'fusogenic' peptides perform the task through conformational changes induced by the increase of acidity that follows the cytoplasmic compartmentalisation. Most of such peptides were designed and synthesised using as a model the hemagglutinin envelop protein of the influenza virus [48,129,130], and the biological activity of their covalent conjugates with AS ODNs has been demonstrated in vitro in various cell lines. Another peptide that proved to be an effective permeabilisation agent was designed to contain a hydrophobic domain like in the fusion sequence of an HIV protein and a hydrophilic domain like in the nuclear localisation sequence of a T-antigen [131]. While the fusogenic peptides have the advantage of following a natural pathway for entering the cytoplasm, they are too expensive to produce and can also cause immunogenic reaction. The results of a recent study [132] provide an even more pessimistic prospect. Eighteen fusogenic peptides containing membrane translocation and nuclear localisation structural motifs were covalently bound to AS ODNs complementary to the initiation codon region of firefly luciferase mRNA and administered to a stable cell line in culture (CHO-AA8-Luc) expressing luciferase activity. None of the conjugates were able to inhibit significantly the luciferase expression, while a formulation based on liposomes (Cytofectin®) induced the expected inhibition. Studies by confocal fluorescein microscopy showed that the conjugates were entrapped in endosomes, and the authors concluded that additional structural motives in the fusogenic peptides are necessary to enable them to escape from endosomes.

In an attempt to rationalise the use of polycations as carriers for nucleic acids, Kabanov et al. [133,134] extended the use of the term 'interpolyelectrolyte complex' (IPEC) to define the water-soluble product of the spontaneous assembling of DNA and a polycation upon mixing. In IPECs, the DNA molecules change their conformation becoming more compact, hence more resistant to nuclease attack. The polycationic component can release some DNA chains during competitive interaction with elements of the cellular membrane. A considerable range of polycations were tentatively used for delivery of DNA in gene therapy, including PLL and derivatives, poly(4-vinylpyridinium) salts, polyamidoamine dendrimers, polyethyleneimine, polymers of 2-alkylaminoethyl methacrylates, diethylaminoethyl dextran, and 'oligocations' such as spermidine derivatives. As shown in this article, only some of these polymers have been used so far in the AS strategy.

5.1.2. *Dendritic polyamidoamines*

The dendrimers are highly branched polymers with a globular architecture. Polyamidoamine (PAMAM) dendrimers (Fig. 4) can be synthesised with a well-defined diameter and a precise number of terminal amino groups at each branching level ('generation'). Haensler and Szoka Jr [135] were the first to investigate their use as carriers for DNA in gene therapy. Subsequent studies [136–138] demonstrated that PAMAM–DNA complexes were able to mediate an efficient transfer of plasmid DNA into various cell types in vitro. So far, PAMAM dendrimers have been applied to a little extent as carriers for AS ODNs. In such a study [139], a 27-mer AS ODN complementary to the ATG region of pCMV luciferase plasmid inhibited luciferase expression when delivered as a complex with a PAMAM dendrimer to D5 mouse melanoma cells and Rat2 embryonic fibroblasts, while the AS ODN alone had a negligible effect. A generation 7 ethylenediamine-core dendrimer (512 surface amino groups, MW 90 kDa) was the most efficient carrier when complexed at 1 : 10 charge ratio (ODN to dendrimer). In another study [140], the uptake of a fluorescein-labeled phosphorothioate ODN by human astrocytoma cells was enhanced 50-fold by complexation with a generation 3 dendrimer at 1 : 20 charge ratio. The ODN was distributed both in cytoplasm and in nuclei.

5.1.3. *Polyethyleneimine*

Polyethyleneimine (PEI, Fig. 4) is produced by the acid-catalysed polymerisation of aziridine, involving propagation through cyclic immonium cations. Due to end-group reactions and to the high reactivity of the intermediate immonium species, the resulting polymer is usually branched. PEI is very soluble in water and has a high capacity to charge electropositively, as every third atom is ionisable nitrogen. PEI was proposed as a carrier for both AS ODNs and plasmid DNA in the same study [141]. A rhodamine-labeled AS ODN targeted at the translation region of the chicken α-thyroid hormone receptor was successfully delivered to embryonic chicken hypothalamic neurons as a complex with PEI, while the uptake of the free ODN could not be detected. Interestingly, the ingested ODN was almost entirely localised into cell nuclei. Since then, PEI has been episodically evaluated as a carrier for plasmid DNA into various cell types and experimental

animals, but there was little reported on its use for the delivery of AS ODNs. It was shown [142] that complexation with PEI improved both the uptake and the biological activity of phosphodiester AS ODNs targeted to different regions of Ha-*ras* mRNA and to the 3′-untranslated region of C-*raf* kinase, when evaluated in cultures of human bladder carcinoma T24 cells. On the contrary, their liposomal delivery (Lipofectin®) did not elicit antisense activity probably because of nuclease degradation. However, the complexes of PEI with phosphorothioate AS ODNs were so stable that they were taken up by the cells without releasing the ODNs, which therefore were not able to hybridise and show antisense activity.

A recent report on the fate of PEI/DNA complexes in cells is of a general relevance to the use as carriers not only of PEI but, perhaps, of all cationic polymers. In carefully conducted experiments, Mikos et al. [143] followed the path of fluorescein-labeled PEI and PEI/DNA complexes when delivered to cultured EA.hy 926 cells, a line of mixed human immortalised cells. Using confocal microscopy, they found that both complexes and polymer particles attach to cells and are ingested by endocytosis as 'clumps'. The cytoplasmic vesicles grew in number and size and some of them underwent disruption and released their contents. But the most significant finding was that PEI particles, either delivered as part of complexes with DNA or alone, were eventually localised into nuclei as ordered structures. This suggests the possibility that PEI or other cationic polymers may interfere adversely with host genes, raising serious concerns about their use in human therapies.

5.1.4. Cationic block copolymers

Cationic block copolymers have been developed as carriers for DNA or AS ODNs by Kabanov et al. [144,145] from polyspermine (PS) and poly(ethylene oxide) (PEO), and by Kataoka et al. [146] from PLL and PEO. Conceptually, these amphiphilic polymers (consisting of a hydrophilic PEO shield surrounding a hydrophobic polycationic core) are able to form micellar structures with DNA or ODNs, which were termed 'block ionomer complexes' [145] or 'polyion complex micelles' [146]. The synthesis of such block copolymers is quite difficult and, as it is usually accompanied by a high polydispersion of the molecular weights, their purification is extremely laborious. In addition, their complexation with AS ODNs is a difficult problem because of the large difference between the size of the two macromolecules [145]. These drawbacks likely prevented a more extended use of the cationic block copolymers as carriers for AS ODNs. Nevertheless, some studies clearly indicated their efficiency. For instance, a PS–PEO block copolymer was used to deliver an AS ODN complementary to the splice junction of herpes virus type 1 early pre-mRNAs 4 and 5, to infected Vero cells in culture [144]. The inhibition of virus reproduction was markedly increased as compared to that induced by the free AS ODN. It was demonstrated [147] that both PS–PEO and PEI–PEO block copolymers form easily water-soluble complexes with a 24-mer AS ODN and increase its resistance to nuclease degradation. In another study [148], the delivery of AS ODNs, targeted at the suppression of amphiphysin I, as complexes with PS–PEO block copolymers was significantly successful in cultures of hippocampal neurons. In a recent study [149], PS–PEO block copolymers were used to deliver an AS ODN targeted to the fibronectin mRNA into the vitreous cavity of rat eyes, where downregulation of fibronectin expression was achieved successfully.

5.1.5. Polymers with induced surface charge

In some neutral polymers positive surface charges were induced deliberately in order to render them carriers for AS ODNs, based on the principle that cationic polymers will perform better due to the negative charge of the cell membrane. Positive charges were generated in polystyrene nanoparticles by performing the emulsion polymerisation in the presence of cationic initiators, such as 2,2′-azo-bis-(2-amidinopropane) dihydrochloride or 2,2′-azo-bis-[2-(2-imidazoline-2-yl)propane] dihydrochloride [150]. These nanoparticles were thoroughly characterised (size distribution, surface charge, colloidal stability, cytotoxicity, adsorption/desorption of ODNs) and complexed with four different ODNs. It was observed that the resistance to nuclease degradation of the complexed ODNs increased significantly when compared to that of free ODNs. Although a total desorption of ODNs from the particles was achieved only by adding an ionic surfactant, the authors concluded that the cationic polystyrene nanoparticles could function as a suitable delivery system for ODNs. However, no in vitro or in vivo experiments were reported to date.

Polycyanoacrylates (PCA, Fig. 4) are neutral polymers that, in the form of nanoparticles, have been made suitable to function as carriers for AS ODNs by generating positively charged entities on their surface which are able to mediate the electrostatic adsorption of AS ODNs by formation of ion pairs. Unlike the cationic polystyrene described above, the charges on the surface of PCAs are not part of the chemical structure of the polymer, as they are introduced in the system at the time of complexation with ODNs. These investigations were commenced by a group at the Centre National de la Recherche Scientifique in Paris, which provided most of the results currently available [151–156]. As mediators for ion-pair formation, hydrophobic cations such as quaternary ammonium salts or tetraphenylphosphomium chloride were proposed; in the majority of

experiments, cetyltrimethylammonium bromide was added to ODN prior to complexation to the polymer nanoparticles. It was also demonstrated that in the absence of such cations, only negligible amounts of ODNs are complexed to PCAs. It was suggested that the ion-paring cationic agents bind to the polymer through hydrophobic interactions, while their ionic moieties bind electrostatically to ODN. The experiments showed that both the resistance to nuclease degradation and the intracellular concentration of AS ODNs were considerably enhanced by complexation via ion-pairing agents to PCAs. Systems employed so far include poly(isobutyl cyanoacrylate) [151,156] and poly(isohexyl cyanoacrylate) [151,152,154,155], and this group has achieved significant success in delivery of certain AS ODNs. For instance [152], complexes of AS ODNs targeted to a point mutation in codon 12 of the Ha-*ras* mRNA inhibited the proliferation of cells expressing the mutated gene at concentrations 100 times lower than free ODNs, and inhibited tumour growth in mice after injection of oncogene-carrying cells. In another experiment [154], AS ODNs complementary to vesicular stomatitis virus nucleocapsid protein mRNA were ingested efficiently by human macrophage-like U937 cells, and their stability was greatly improved by complexation. Since at high concentrations the ion-pairing agents can elicit cytotoxic reactions, an attempt has been made to remove them from the system by covalently modifying the ODNs with hydrophobic moieties, such as cholesterol [155]. Up to 60% of the covalent conjugates were adsorbed onto PCA nanoparticles in the absence of ion-pairing cations, however the modification of ODNs reduced their AS activity. In a recent study [157], transient positive charges were generated on the surface of poly(n-hexyl cyanoacrylate) nanoparticles by using diethylaminoethyl dextran as an emulsion stabiliser during polymerisation. A fluorescein-labeled AS ODN complementary to the splice junction of herpes virus type 1 pre-mRNA 4 was complexed to these nanoparticles and delivered to cultured Vero cells. While the free AS ODN was almost completely degraded in the culture medium, the adsorbed AS ODN remained intact, and its effective ingestion by the cells was demonstrated by laser scanning confocal microscopy and flow cytometry.

5.2. *Neutral polymers*

The use of neutral polymers came into existence likely because the cationic polymers did not prove to be the ideal carriers for AS ODNs delivery, due especially to their intrinsic cytotoxicity. There are no interactions between the electronegative cellular membrane and a neutral polymer that may facilitate some internalisation process of polymer–ODN conjugates. The neutral polymers are used for their ability to act as carrier systems which assure a sustained release in the long term of the ODN molecules, rather than for a role they may play in the process of cellular uptake, the latter being essentially reduced in this case to the problem of ingestion of free ODN molecules. However, neutral polymers and their conjugates with ODNs can be, in principle, ingested by cells through a pinocytic process. Whether the physical or chemical bond between ODN and polymer is cleaved before or after ingestion of conjugates is an issue little investigated.

5.2.1. *Synthetic hydrogels*

The synthetic hydrogels are the epitome of soft polymeric biomaterials, which cause insignificant damage to the soft tissue. However, there are very few applications in the delivery of AS ODNs. A class of gels, known by the trade names of Pluronic® or Poloxamer®, has attracted the attention of some investigators due to their reversible thermal gelation properties. These water-soluble materials are uncrosslinked block copolymers of poly(ethylene oxide) and poly(propylene oxide) (Fig. 4), which for particular compositions and block sequences acquire the unusual property of being liquid at ambient or low temperatures while becoming gels at the physiological temperature of the living tissues. Such a block copolymer, supplied as F-127 by BASF Corporation, was the subject of two reports regarding its use as a carrier for AS ODNs. In a study of AS treatment of vasculoproliferative disease [158], AS ODNs targeted to c-*myc* and c-*myb* mRNAs were incorporated in a solution of Pluronic® F-127 and then administered to cultured vascular smooth muscle cells or surgically inserted around denuded carotid artery of rats. While the delivery system assured an efficient in vitro cellular uptake of the ODNs and reduced cellular proliferation, the inhibition in vivo of hyperplasia was not effective. Since another system offering prolonged delivery of the ODNs was efficient in vivo (see Section 5.2.5), it was concluded that the release duration from the gel was too short. In an attempt to improve the liposomal delivery of AS ODNs to the vitreous body of the eye, Couvreur et al. [159] dispersed liposomes in a mixture of ODN and aqueous solutions of copolymer F-127, the latter being chosen on the presumption that it will form a gel at the temperature in the eye. Only the influence of the copolymer concentration on the release profile of a radiolabeled model ODN (oligothymidylate, pdT16) in a cell-free in vitro setting was investigated in this study. It was found that the release of liposomes content could be controlled by varying the concentration of Pluronic® in the medium. However, this concentration eventually dropped, as the copolymer is soluble in water. Indeed, the solubility in water seems to be the major drawback of this class of polymers as carriers for ODNs. Ultimately, the carrier will be dispersed into the surrounding physiological medium at a rate that is too

high for a proper sustained release, while it is unlikely that its presence affects the mechanism of ODN ingestion.

The crosslinked hydrogels, able to absorb large amounts of water while not dissolving, also attracted attention as possible carriers for ODNs. Aiming at producing artificial vitreous substitutes, a group at Lions Eye Institute (Western Australia) has developed crosslinked hydrogels by homopolymerisation of 1-vinyl-2-pyrrolidinone (VP) or its copolymerisation with 2-hydroxyethyl methacrylate (HEMA) [160–165]. These materials, which displayed viscoelastic behaviour and could be injected through needles of common sizes, proved not only to lack cytotoxicity [166] but they also showed serum-like growth promoting effect on an anchorage-dependent cell line (3T3 mouse fibroblasts) in static cultures [167]. It was hypothesised that the latter is due to the physical protection of cells by hydrogels and to the ability of hydrogels to mimic the extracellular matrix. As physical protection may involve the interaction between polymer and cell membrane in a way that is not harmful to the cell, it is conceivable that the hydrogel particles can come very close to cells and even contact their membrane without destabilising it or affecting the cell functions. On this background, the group designed a crosslinked copolymer of VP with HEMA (5%), which was covalently bound to an AS ODN targeted to the human rhodopsin gene coding for a mutation at amino acid 351 of the protein [168]. The conjugate was subjected to cell-free in vitro release experiments over 46 days in the presence of natural bovine vitreous humour. Compared to the control (no enzyme present), a significant amount of ODN was released from the hydrogel–ODN conjugate. A possible explanation is that the presence of the enzymes contained in the natural vitreous humour may cleave the covalent bond and induce the release of the ODN. Being a directly injectable gel, this system is attractive for intravitreal delivery of AS ODNs, and further investigations are in progress.

5.2.2. Biodegradable lactone-based polymers

The polyesters produced from cyclic monomers containing lactone structural moieties have a long history of use as biodegradable biomaterials. This class mainly includes polyesters made by polycondensation of L-lactide, glycolide, caprolactone, dioxanone, cyclic carbonates and their derivatives. Polylactide and polyglycolide, respectively known also as poly(lactic acid) (PLA) and poly(glycolic acid) (PGA), are the most investigated biodegradable polymers, which also found applications as carriers for AS ODNs. Akhtar's group at the Aston University in Birmingham (UK) were the first to propose PLA (Fig. 4) for this purpose [169]. Radiolabeled AS ODNs, targeted to the splicing region of *tat* gene in HIV mRNA or to the AUG initiation codon of human c-*myc* oncogene exon 2, were incorporated within chloroform-cast films of PLA, and the release profile was monitored over 28 days in cell-free serum or buffer media. The release data corresponded kinetically to the case of diffusion from monolithic devices, and included an initial burst release. The PLA-entrapped ODNs were resistant to degradation by serum nucleases, while the free ODNs were rapidly degraded in serum. The same group developed P(LA-*co*-GA) microspheres (1–2 or 10–20 μm in size) and evaluated them in vitro [170]. The AS ODNs employed in the preceding study were incorporated in microspheres by a double-emulsion solvent evaporation method and their release profile was studied in buffer media. Microspheres containing radiolabeled AS ODNs were also administered to cultures of mouse macrophage cells (RAW 264.7 line). It was found that the cellular uptake was enhanced and a diffuse intracellular and intranuclear distribution of ODNs occurred when delivered through microspheres. The release duration from larger microspheres was much longer than that from the smaller ones. Further investigations in vitro [171] with a series of AS ODNs showed great advantages of the P(LA-*co*-GA) microspheres regarding the release characteristics and the enhancement of resistance to nuclease attack. The efficiency of this system was independently confirmed [172] when used to deliver an AS ODN complementary to the translation initiation start region of the rat tenascin mRNA, which led to the inhibition of proliferation and migration of vascular muscle cells in culture. Other investigators used cylindrical implants of P(LA-*co*-GA) in an attempt to improve the delivery of AS ODNs into the vitreous humour of the eye [173]. An AS ODN complementary to the translation initiation codon region of herpes simplex virus mRNA was incorporated into cylinders of P(LA-*co*-GA) by heating in an appropriate mould. Each implant contained about 0.5 mg of ODN. The release was studied both in buffer media and by incubation in bovine vitreous fluid (double-filtered natural humour). It was determined that the molecular weight of the polymer did not affect the duration of release. The amount of ODN released in the vitreous fluid was lower than in the buffer solutions, presumably due to the enzymatic degradation of the ODN.

5.2.3. Poly(ethylene glycol)

Poly(ethylene glycol) (PEG) is the term used for the polyoxyethylene polymers with low molecular weight, while the term poly(ethylene oxide) is preferred to designate polyoxyethylenes with high molecular weight. As this convention is rather obscure and generally overlooked, the acronym PEG will be used throughout this section regardless of molecular weight.

PEGs constitute a class of water-soluble polymers with many applications. When crosslinked, PEGs behave like typical hydrogels, a form in which they

Exhibit B

PATENT
ATTORNEY DOCKET NO. 07891/009004

Certificate of Mailing: Date of Deposit: June 14, 2004

I hereby certify under 37 C.F.R. § 1.8(a) that this correspondence is being deposited with the United States Postal Service as first class mail with sufficient postage on the date indicated above and is addressed to Commissioner for Patents, P.O. Box 1450, Alexandria, VA 22313-1450.

Caryn Scafati
Printed name of person mailing correspondence

Caryn Scafati
Signature of person mailing correspondence

IN THE UNITED STATES PATENT AND TRADEMARK OFFICE

Applicant:	Robert G. Korneluk et al.	Art Unit:	1635
Serial No.:	09/974,592	Examiner:	Janet L. Epps
Filed:	October 9, 2001	Customer No.:	21559
Title:	DETECTION AND MODULATION OF IAPS AND NAIP FOR THE DIAGNOSIS AND TREATMENT OF PROLIFERATIVE DISEASE		

Commissioner for Patents
P.O. Box 1450
Alexandria, VA 22313-1450

DECLARATION OF DR. ERIC LACASSE UNDER 37 C.F.R. § 1.132 TRAVERSING GROUNDS OF REJECTION

Under 37 C.F.R.§ 1.132, I declare:

1. I am Senior Scientist and Head of the Department of Oncology at Aegera Therapeutics, Inc, and have published 16 papers relating to IAPs, cancer biology, and antisense therapeutics.

2. I have read the Office Action mailed on August 8, 2003.

3. As disclosed in our specification, antisense oligonucleotides are designed using computer algorithms and screened *in vitro* to identify those that

effectively inhibit protein expression (pages 54-55). Antisense oligonucleotides that are selected for efficacy *in vitro* are typically effective *in vivo*, as well. *In vivo* screening is used to identify those antisense oligonucleotides having the greatest efficacy (pages 55 and 56). Such screening is merely routine.

4. Antisense oligonucleotides are potent and specific therapeutic molecules that share a common mechanism of action: they interfere with protein production by binding to a complementary target mRNA. This binding inhibits protein production by interfering with the ribosome's ability to translate the mRNA, by interfering with splicing, and/or by inducing the degradation of the mRNA by RNAse H, an enzyme that recognizes and degrades mRNA/DNA hybrids. Regardless of the length of the antisense oligonucleotide, if it binds an accessible site on the target RNA in the cell, the antisense oligonucleotide will successfully inhibit protein production.

5. The results shown in Exhibits A (Shankar et al., J. of Neurochem. 79:426-436, 2001, hereafter "Shankar"), B (Kallio et al. FASEB J. express article, 10.1096/fj.01-0280fj3, 2001, hereafter "Kallio"), and C (Fukuda et al. Blood 100:2463-2471, 2002, hereafter "Fukuda"), previously of record, were carried out using methods available at the time applicants' priority document was filed. These references describe the use of antisense oligonucleotides of varying lengths to decrease the expression of an inhibitor of apoptosis protein, i.e., human survivin.

6. Shankar describes the use of phosphorothioate modified antisense oligonucleotides, 20 nucleotides in length, to downregulate expression of human survivin expression and to induce apoptosis in neural tumor cells in culture.

7. Kallio describes the use of phosphorothioate modified antisense oligonucleotides, 18 nucleotides in length, to downregulate human survivin expression in HeLa and PtK1 cells in culture. The antisense oligonucleotides were conjugated to fluorescein isothiocyanate, which allowed them to be visualized by fluorescence microscopy.

8. Fukuda describes the use of a full-length antisense survivin expression construct to modulate survivin expression in CD34 cells.

9. In further support of the enablement of the claimed methods, provided herewith are U.S. Patent Nos. 5,958,771 ("the '771 patent") and 5,958,772 ("the '772 patent"), which were filed on December 3, 1998, and 6,087,173 ("the '173 patent"), which was filed on September 9, 1999, (Exhibits E, F, and G, respectively). As detailed below, each of these patents relates to the use of phosphorothioate modified antisense oligonucleotides to inhibit the expression of an IAP, and each of the cited examples was carried out using methods available at the time applicants' priority document was filed.

10. The '771 patent describes the identification of twelve phosphorothioate modified 18-mer oligodeoxynucleotides that inhibited Cellular Inhibitor of Apoptosis-2 (cIAP-2) expression in cells *in vitro* (Table 1 and column 41, first paragraph).

11. The '772 patent describes the identification of six 18-mer phosphorothioate oligodeoxynucleotides that inhibited cIAP-1 expression in cells *in vitro* (Table 1 and column 39, first paragraph).

12. The '173 patent describes the identification of twenty-four phosphorothioate modified 20-mer antisense oligodeoxynucleotides that inhibited XIAP expression in cells in vitro (Table 1, and column 41, first paragraph).

13. The examples cited below, and reviewed by Jansen, Exhibit D, which relate to the use of phosphorothioate modified antisense oligonucleotides to inhibit protein production, were also carried out using methods available at the time applicants' priority document was filed.

14. Jansen describes phase I trials, which were carried out in 1997, using an 18-mer phosphorothioate Bcl-2 antisense oligonucleotide (page 676, right column, first paragraph) to treat non-Hodgkin lymphoma. The 18-mer antisense oligonucleotide decreased BCL-2 protein levels in half of all patients that received it.

15. In a 1996 study by Yazaki et al. (Mol Pharmacol 50:236-42, 1996), which is also reviewed by Jansen, a 20-mer phosphorothioate Protein Kinase C antisense oligonucleotide was used to inhibit glioblastoma xenografts in mice (paragraph spanning page 677, right column, to page 678, left column).

16. A clinical pilot study, carried out by Ratjczak and colleagues in 1992 is also reviewed in Jensen. In this study, a 24-mer phosphorothioate antisense oligonucleotide was used *ex vivo* to target the c-MYB proto-oncogene in bone-

marrow cells harvested from patients with chronic myelogenous leukemia (page 679, right column, first paragraph).

17. As further evidence of enablement, provided herewith are Exhibits H (Sugano et al., J. Biol. Chem. 271:19080-19083, 1996, hereafter "Sugano"), I (Galvin-Parton et al., J. Biol. Chem. 272: 4335-4341, 1997, hereafter "Galvin-Parton"), J (MacLeod et al., J. Biol. Chem. 270:8037-8043, 1995, hereafter "MacLeod"), and K (Ramchandani et al., P.N.A.S. 94:684-689, 1997, "Ramchandani"), all of which were received for publication prior to the date on which applicants' priority document was filed, and all of which relate to methods of using antisense oligonucleotides to inhibit protein production.

18. Sugano, published in 1996, used a 21-mer antisense oligonucleotide to inhibit expression of cholesteryl ester transfer protein (CETP), the enzyme that facilitates the transfer of cholesterylester from high density lipoprotein to apoB-containing lipoprotein. The asialoglycoprotein-coupled 21-mer antisense oligonucleotide, which was administered to rabbits intravenously, decreased CETP biological activity and also decreased total cholesterol levels.

19. As published in February 1997, Galvin-Parton expressed a 39-mer antisense oligonucleotide in transgenic mice. This 39-mer antisense oligonucleotide, which targeted the nucleic acid encoding G-protein, $G\alpha_q$, decreased $G\alpha_q$ polypeptide levels, and caused an increase in body mass and hyperadiposity.

20. MacLeod, in 1995, expressed a 600-mer antisense oligonucleotide, which was complementary to DNA methyltransferase mRNA, in Y1 cells, a tumorigenic adrenocortical cell line. This antisense oligonucleotide decreased DNA methyltransferase gene expression, protein activity, and also decreased the ability of the Y1 cells to form tumors when injected into mice.

21. In a related study published in January 1997, Ramchandani designed a phosphorothioate modified 20-mer antisense oligonucleotide that targeted the same region of DNA methyltransferase mRNA that was targeted by the 600-mer described by MacLeod. Ramchandani injected tumorigenic Y1 cells into the flanks of mice, allowed tumors to form, then administered the 20-mer antisense oligonucleotide to the tumor. The 20-mer and the 600-mer antisense oligonucleotides, though of widely differingly lengths, both decreased DNA methyltransferase levels and inhibited tumor growth.

22. In sum, Shankar, Kallio, Fukuda, the '771 patent, the '772 patent, the '173 patent, Jansen, Sugano, Galvin-Parton, and MacLeod describe the use of antisense oligonucleotides that range in length between 18 and 600 nucleotides to inhibit the expression of a target gene and achieve a desired biological effect. These antisense oligonucleotides, regardless of length, bind to a complementary target mRNA and inhibit protein production, just as applicants' antisense oligonucleotides do. One skilled in the field of antisense, being familiar with the art available at the time of filing (of which the above is but a sample) would know

that antisense molecules complementary to a portion of XIAP could be a variety of different lengths.

23. I hereby declare that all statements made herein of my own knowledge are true and that all statements made on information and belief are believed to be true; and further that these statements were made with the knowledge that willful false statements and the like so made are punishable by fine or imprisonment, or both, under Section 1001 of Title 18 of the United States Code and that such willful false statements may jeopardize the validity of the application or any patents issued thereon.

Date: June 11, 2004

Dr. Eric Lacasse

Exhibit C

PATENT
ATTORNEY DOCKET NO. 07891/009004

Certificate of Mailing: Date of Deposit: 5-20, 2003

I hereby certify under 37 C.F.R. § 1.8(a) that this correspondence is being deposited with the United States Postal Service as first class mail with sufficient postage on the date indicated above and is addressed to the Commissioner for Patents, Washington, D.C. 20231.

Tracey Simmons
Printed name of person mailing correspondence

Tracey Simmons
Signature of person mailing correspondence

IN THE UNITED STATES PATENT AND TRADEMARK OFFICE

Applicant:	Robert G. Korneluk et al.	Art Unit:	1635
Serial No.:	09/974,952	Examiner:	Janet L. Epps
Filed:	October 9, 2001	Customer No.:	21559
Title:	DETECTION AND MODULATION OF IAPS AND NAIP FOR THE DIAGNOSIS AND TREATMENT OF PROLIFERATIVE DISEASE		

Commissioner For Patents
Washington, D.C. 20231

DECLARATION UNDER 37 C.F.R. § 1.132 OF ROBERT G. KORNELUK, PH.D.

1. I am an inventor on the above-captioned patent application.

2. I have read the Office Action mailed November 20, 2002.

3. We have successfully reduced to practice the present invention using techniques known to those skilled in the art of antisense oligonucleotide technology at the time the priority application for the presently claimed invention was filed. Specifically, we showed the effect of XIAP down-regulation by antisense oligonucleotides on human non-small cell lung cancer (NIH-H460) growth *in vivo*. In animal models, we demonstrated that the G4 antisense oligonucleotide at 15 mg/kg had significant sequence-specific

RCQ

growth inhibitory effects on human H460 tumors in xenograft models of SCID/RAG2-immunodeficient mice by systemic intraperitoneal administration. Systemic antisense oligonucleotide administration was associated with an 85% down-regulation of XIAP protein in tumor xenografts. The combination of 15 mg/kg G4 AS ODN with 5 mg/kg vinorelbine significantly inhibited tumor growth, more than either agent alone. These studies indicated that down-regulation of XIAP is a potent death signal in lung carcinoma cells and is able to inhibit tumor growth *in vivo*. These studies support the contention that the *in vivo* administration of antisense oligonucleotides complementary to XIAP SEQ ID NO:3 was enabled as a cancer therapy at the time applicants' priority document was filed.

4. The antisense oligonucleotides were selected using methods outlined in our disclosure. Specifically, we selected ninety-six oligonucleotide sequences complementary to a portion of XIAP (each sequence having nineteen nucleotides) (SEQ ID NOs: 1 through 96; Table 1), from a region approximately 1 kb upstream of the start codon to approximately 1 kb downstream of the stop codon of the XIAP cDNA sequence.

5. As described in our specification, the XIAP synthetic library of 96 antisense oligonucleotides was first screened *in vitro* to identify antisense oligonucleotides that decreased XIAP protein levels. Specifically, T24 cells (1.5×10^4 cells/well) were seeded in wells of a 96-well plate on day 1, and were cultured in antibiotic-free McCoy's medium for 24 hours. On day 2, the cells were transfected with XIAP antisense oligonucleotides. On day 3, XIAP RNA levels were measured using quantitative real-time PCR techniques. At day 4, XIAP protein levels were measured by ELISA (Exhibit B-A, C, E, G, I, and K) and total cellular protein was measured biochemically (Exhibit B-B, D, F, H, J, and L); and used to normalize the XIAP protein levels). These results were

RC

compared to a mock transfection sample (treated with the transfection agent without oligonucleotide DNA, and then processed as for the other samples).

These methods identified 16 antisense oligonucleotides that decreased XIAP protein levels relative to control cells that were mock transfected. As expected, the ability of an antisense oligonucleotide to decrease XIAP protein levels correlated with its ability to decrease XIAP mRNA levels (Exhibit C-A and B). Sixteen of these oligonucleotides decreased by at least 50% levels of XIAP protein or mRNA levels. The G4 AS ODNs exhibited the strongest down-regulating effect on XIAP protein, reducing XIAP protein levels by 62% within twenty-four hours after the end of transfection (Exhibit D-A and D-B). As shown in Exhibit E, cells treated with G4 AS ODNs underwent morphological changes characteristic of apoptosis, including chromatin condensation and nuclear DNA fragmentation. Few control cells showed these morphological changes. Forty-eight hours after transfection, G4 AS ODNs reduced H460 cell growth 55% relative to untreated controls (Exhibit F). *In vivo* studies with lung carcinoma and breast carcinoma cells were then carried out.

6. SCID-RAG2 mice were inoculated with H460 human lung carcinoma cells (subcutaneous shoulder injection of 10^6 cells) and treatments with G4 and F3 AS PS-ODNs, as well as a scrambled control, were initiated three days after tumor inoculation. ODN injections were administered intraperitoneally at 12.5 mg/kg three times a week for three weeks. At the end of the treatment period, mean tumor sizes in the groups treated with either G4 or F3 antisense oligonucleotides were ~ 50 % smaller relative to tumor size in a control group treated with a scrambled control oligonucleotide (Exhibit G).

7. The treatment protocol described above was also tested on female SCID-RAG2 mice inoculated orthotopically with MDA-MB-435/LCC6 human breast carcinoma

E O

cells. Two weeks after the last treatment (day 35) tumor volumes of mice treated with F3, C5 or G4 AS ODNs were 70 %, 60 % and 45 % smaller than vehicle controls (Exhibit H).

8. G4 AS ODNs in SCID-RAG2 mice bearing xenografts of H460 human non-small-cell lung tumors implanted subcutaneously. Saline-treated control tumors grew reproducibly to a size of 0.75 cm^3 within approximately 24 days (Exhibit I). ODN treatments were initiated three days after tumor cell inoculation. G4 AS ODNs (5 to 15 mg/kg) were administered using a treatment schedule of intraperitoneal injections given on days 3-7, 10-14, and 17-21 (once a day). The treatment with 5 or 15 mg/kg G4 AS ODNs greatly delayed tumor growth: on day 24 mean tumor sizes were 0.75, 0.45 and 0.29 cm^3 in control, 5 and 15 mg/kg treated groups, respectively (Exhibit I). There was a dose-dependent inhibition of tumor growth. Tumor size in mice treated with 15 mg/kg G4 AS ODNs was significantly smaller than in control groups, and represented 39% of control mean tumor size. In contrast, administration of G4 scrambled oligonucleotides at 15 mg/kg provided no therapeutic activity. None of the mice treated with ODNs displayed any signs of toxicities, and both doses of ODNs were well tolerated. A dose of 15 mg/kg was selected for the future combination treatment regimens with anticancer drugs.

9. To correlate G4 AS ODN tumor growth inhibitory effects with XIAP protein expression, we examined the changes in XIAP expression at the end of the *in vivo* treatment with 15 mg/kg of G4 AS and scrambled oligonucleotides. At day 21 or 24 post-tumor inoculation when tumors reached 1 cm^3 in size, tumors were harvested and lysates from tumor homogenates were used for western blot analysis. XIAP and β-actin antibodies against the human protein were used, allowing for determination of human

XIAP levels obtained from tumor cells specimens without contamination from XIAP derived from mouse cells. XIAP protein levels in tumors treated with G4 AS ODNS were significantly reduced to approximately 85% of control tumors (P <0.005) (Exhibit J). XIAP protein in tumors treated with G4 Scrambled oligonucleotides were reduced in size by 24% of control tumors. These results indicated that inhibition of H460 tumor growth by G4 AS ODNS correlated with the down-regulation of XIAP protein expression.

10. To evaluate whether XIAP AS ODN administration results in direct tumor cell kill, we examined the histology of tumors after treatment both for morphology and ubiquitin immunostaining (Exhibit K-A and B). At day 21 or 24 post-tumor inoculation, tumors treated with 15 mg/kg of G4 AS, scrambled oligonucleotides, or saline control were excised, sectioned, and stained with hematoxylin and eosin. The results demonstrated that tumors in animals administered given XIAP AS ODNs treatment contained an increased number of dead cells, identified morphologically by their amorphous shape and condensed nuclear material.

12. As described in our specification, we also combined treatments of G4 AS ODNs with known a chemotherapeutic agent used for lung cancer treatment. The therapeutic efficacy of vinorelbine in the presence and absence of G4 AS ODNs or scrambled oligonucleotides. Treatment was initiated on day 3 after tumor inoculation. Exhibit L presents the *in vivo* efficacy results for 5 mg/kg and 10 mg/kg doses of vinorelbine given to H460 tumor-bearing mice and compared with saline controls. Each of the two regimens induced significant tumor growth suppression in a dose-dependent manner without showing significant signs of undesirable toxicity (i.e., body weight loss). When administration of G4 AS ODNs (15 mg/kg) was combined with vinorelbine (5 mg/kg) for the treatment of H460 tumors, a more pronounced delay of H460 tumor

growth was observed compared to either treatment administrated alone (Exhibit L). Again, the mice did not show any significant signs of toxicity (i.e., body weight loss). Mean tumor size in mice treated with 5 mg/kg vinorelbine in the presence or absence of G4 AS or Scrambled oligonucleotides was compared on day 29 (Exhibit L A and B). The tumor sizes in the group receiving combination therapy was 0.22 ± 0.03 cm^3, significantly smaller than the tumor sizes of groups receiving any other treatment (tumor size in control mice receiving 5 mg/kg vinorelbine alone or a combination of vinorelbine and G4 scrambled oligonucleotides was 0.59 ± 0.04 and 0.48 ± 0.05 cm^3, respectively).

13. In sum, using routine methods described in our specification at the time of filing, we have now demonstrated the *in vivo* therapeutic efficacy of antisense oligonucleotides for enhancing apoptosis in a cell of a mammal and for the treatment of a patient diagnosed as having a proliferative disease.

14. I hereby declare that all statements made herein of my own knowledge are true and that all statements made on information and belief are believed to be true; and further that these statements were made with the knowledge that willful false statements and the like so made are punishable by fine or imprisonment, or both, under Section 1001 of Title 18 of the United States Code and that such willful false statements may jeopardize the validity of the application or any patents issued thereon.

Date: May 5/03

Robert G. Korneluk, Ph.D.

The antiapoptosis protein survivin is associated with cell cycle entry of normal cord blood CD34+ cells and modulates cell cycle and proliferation of mouse hematopoietic progenitor cells

Seiji Fukuda, Richard G. Foster, Scott B. Porter, and Louis M. Pelus

The inhibitor of the apoptosis protein (IAP) survivin is expressed in proliferating cells such as fetal tissues and cancers. We previously reported that survivin is expressed and growth factor regulated in normal adult CD34+ cells. Herein, we examined survivin expression in CD34+ cells before and after cell cycle entry and demonstrate a role for survivin in cell cycle regulation and proliferation. Analysis of known human IAPs revealed that only survivin is cytokine regulated in CD34+ cells. Survivin expression is coincident with cell cycle progression. Up-regulation of survivin by thrombopoietin (Tpo), Flt3 ligand (FL), and stem cell factor (SCF) occurred in underphosphorylated-retinoblastoma protein (Rb)^{positive}, Ki-67^{negative}, and cyclin D^{negative} CD34+ cells. Quantitative real-time reverse transcription–polymerase chain reaction (RT-PCR) and multivariate flow cytometry demonstrated that Tpo, SCF, and FL increase survivin mRNA and protein in quiescent G_0 CD34+ cells without increasing Ki-67 expression, indicating that cytokine-stimulated up-regulation of survivin in CD34+ cells occurs during G_0, before cells enter G_1. Selective inhibition of the PI3-kinase/AKT and mitogen-activated protein kinase (MAPK$^{p42/44}$) pathways blocked survivin up-regulation by growth factors before arresting cell cycle. Retrovirus transduction of survivin-internal ribosome entry site–enhanced green fluorescent protein (survivin-IRES-EGFP) in primary mouse marrow cells increased granulocyte macrophage–colony-forming units (CFU-GM) by 1.7- to 6.2-fold and the proportion of CFU-GM in S phase, compared to vector control. An antisense survivin construct decreased total and S-phase CFU-GM. These studies provide further evidence that survivin up-regulation by growth factors is not a consequence of cell cycle progression and strongly suggest that survivin is an important early event for cell cycle entry by CD34+ cells. (Blood. 2002;100:2463-2471)

Introduction

Apoptosis and cell cycle regulation are tightly orchestrated processes involving multiple effector molecules.[1-3] Pathways that regulate cell cycle and cell survival overlap, but distinct mechanisms are involved.[4,5] The inhibitor of apoptosis protein (IAP) family proteins inhibit apoptosis by inactivating several caspases. There are 7 known IAP family proteins: NAIP,[6,7] XIAP,[7] c-IAP1,[7-9] c-IAP2,[7,8] survivin,[10,11] livin,[12] and murine Bruce[13] and its human homolog, Apollon.[14] Survivin and livin are frequently overexpressed in cancer cells and fetal tissues but are barely detectable in adult quiescent tissues.[10-12,15] While most IAPs block apoptosis,[3,8,12,16,17] their roles in cell cycle regulation are unclear.

We recently reported that survivin is expressed and cytokine regulated in normal adult marrow CD34+ cells, umbilical cord blood (UCB) CD34+ cells, and adult peripheral blood T cells.[18] Survivin blocks caspase-3 activity and inhibits apoptosis in cancer cells,[11,15,16,19-21] and an inverse correlation between survivin and active caspase-3 expression was observed in CD34+ cells.[18] Survivin expression in cytokine-stimulated CD34+ cells was associated with cell cycle progression, being highest in G_2/M. However, in contrast to expression occurring only during G_2/M in cancer cells,[15] survivin is expressed in all phases of the cell cycle in cytokine-stimulated CD34+ cells.[18] These studies indicate that survivin is not a cancer-specific protein and suggest that survivin plays a role in the proliferation and survival of normal hematopoietic cells.

Since most proliferating cells express survivin, including cancer cells,[10,11,15] normal T cells,[18] and normal CD34+ cells,[18] it is unclear whether survivin is expressed simply because cells are dividing or whether survivin expression directly affects cell cycle progression and proliferation. Since survivin interacts with the cdk4/cyclin D complex and enhances Rb phosphorylation[4,22,23] and overexpression of survivin enhances cell cycle progression in hepatoma cells, survivin may be involved in cell cycle regulation, at least in cancer cells.[24] Our previous findings that survivin is found in G_0 CD34+ cells after growth factor stimulation for 48 hours[18] raised the question of whether up-regulation of survivin by growth factors occurs in quiescent G_0 CD34+ cells before they enter G_1.

In this study, we examined whether IAPs in general, and survivin in particular, are expressed and growth factor regulated in normal CD34+ cells. Using real-time reverse transcription–polymerase chain reaction (RT-PCR) and multivariate flow cytometry, we now demonstrate that up-regulation of survivin expression by growth factors occurs in quiescent (G_0) CD34+ cells before entering G_1 and that survivin expression is not a consequence of cell cycle progression. Overexpression of survivin in normal

From the Department of Microbiology and Immunology and the Walther Oncology Center, Indiana University School of Medicine; and the Walther Cancer Institute, Indianapolis, IN.

Submitted October 22, 2001; accepted May 22, 2002.

Reprints: Louis M. Pelus, Walther Oncology Center, Indiana University School of Medicine, 1044 W Walnut St, Indianapolis, IN 46202; e-mail: lpelus@iupui.edu.

The publication costs of this article were defrayed in part by page charge payment. Therefore, and solely to indicate this fact, this article is hereby marked "advertisement" in accordance with 18 U.S.C. section 1734.

primary mouse bone marrow cells enhanced granulocyte macrophage–colony-forming unit (CFU-GM) production and cell cycle, suggesting that survivin plays a regulatory role in cell cycle entry and proliferation of normal hematopoietic cells.

Materials and methods

Animals

Specific pathogen-free female C57Bl/6 mice, 8 to 12 weeks of age, were purchased from Harlan Sprague-Dawley, Indianapolis, IN. Mice were provided continuous access to rodent chow and acidified water. The Institutional Animal Care and Use Committee of Indiana University School of Medicine approved all experimental procedures.

Growth factors, antibodies, and reagents

Recombinant human granulocyte-macrophage colony-stimulating factor (GM-CSF), Flt3 ligand (FL), and thrombopoietin (Tpo) were provided by Immunex, Seattle, WA. Recombinant human and mouse stem cell factor (SCF) were a gift from Dr Karl Nocka, UCB Research (Cambridge, MA). Recombinant murine GM-CSF was purchased from BioVision (Palo Alto, CA). Affinity purified antihuman survivin polyclonal antibody (AF886) and mouse IgG_1 were purchased from R&D Systems (Minneapolis, MN). We previously described the specificity of the AF886 survivin antibody for intracellular staining in $CD34^+$ cells.[18] Monoclonal antihuman survivin antibody (6E4) was purchased from Cell Signaling (Beverly, MA). Antihuman retinoblastoma protein (Rb) monoclonal antibody (mAb) (G3-245), fluorescein isothiocyanate (FITC)–conjugated anti–underphosphorylated-Rb mAb (clone G99-549), FITC–antihuman cyclin D1/D2/D3 mAb (clone G124-259), FITC–anti-Ki-67 mAb (clone B56), FITC–antimouse Ig, FITC-mouse IgG1 and 7-AAD (Via Probe) were obtained from BD Pharmingen (San Diego, CA). Normal rabbit IgG was purchased from Santa Cruz Biotechnology (Santa Cruz, CA). FITC- and phycoerythrin (PE)-goat anti–rabbit IgG was from Caltag Laboratories (Burlingame, CA). FITC- and Cy-chrome anti-CD34 antibodies (BIRMA-K3) were from Dako (Carpinteria, CA). Affinity purified polyclonal antihuman phosphorylated-Rb (Ser780, Ser795, and Ser807/811) antibodies were obtained from Cell Signaling. LY294002 and PD98059 were from BioMol (Plymouth Meeting, PA) and Calbiochem (San Diego, CA), respectively.

Isolation of cord blood $CD34^+$ cells and cell culture

Normal UCB was obtained with institutional review board approval. Low-density mononuclear cells were separated on Ficoll-Paque (1.077 g/mL) (Amersham Pharmacia Biotech, Piscataway, NJ) and $CD34^+$ cells isolated with antihuman CD34 mAb (QBEND/10) and 2 sequential positive selections with immunomagnetic beads (Miltenyi Biotech, Auburn, CA) as previously described.[18] The purity of $CD34^+$ cells routinely exceeded 95%. Fresh $CD34^+$ cells or cells incubated with 100 ng/mL each of thrombopoietin (Tpo), Flt3 ligand (FL), and stem cell factor (SCF) in 10% heat-inactivated fetal bovine serum (HI-FBS) (Hyclone Laboratories, Logan, UT), 2 mM glutamine, and Iscove modified Dulbecco medium (IMDM) for up to 48 hours were fixed in 4% paraformaldehyde and frozen. For cell cycle fractionation, fresh or cultured $CD34^+$ cells were stained with Hoechst 33342 (Hst) (Molecular Probes, Eugene, OR) and pyronin Y (PY) (Polysciences, Warrington, PA) as described.[18,25,26] G_0 and G_1 cells were defined as Hst^{low}/PY^{low} and Hst^{low}/PY^{high}, respectively. The 20% dimmest cells in the pyronin Y gate having 2N DNA were collected as G_0 cells in all experiments.[27] In some experiments, fresh G_0 $CD34^+$ cells were sorted based on Hst/PY staining and then stained with 1 μM of 5- (and 6-) carboxyfluorescein diacetate succinimidyl ester (CFSE) (Molecular Probes) in Hanks balanced salt solution (HBSS) (Gibco-BRL/Invitrogen, Carlsbad, CA) for 10 minutes at 37°C. The reaction was stopped with 500 μL of ice-cold HBSS with 10% FBS, then cells were washed 3 times and resuspended at 1-2 × 10^5 cells/mL in IMDM with 10% HI-FBS, 2 mM glutamine, plus 100 ng/mL each of Tpo, FL, and SCF.[28,29] After culture, $CD34^+$ cells were sorted and reanalyzed for cell cycle and cell division based on CFSE and Hst/PY staining.

RNA isolation and RT-PCR

Total RNA isolation and RT-PCR were performed as previously described.[18] PCR primers for amplification of IAPs were: survivin: 5′-GAGCTGCAGGTTCCTTATC-3′ and 5′-ACAGCATCGAGCCAAGTCAT-3′[18]; livin: 5′-TGAGGTGCTTCTTCTGCTAT -3′ and 5′-TTTCAGACTG-GACCTCTCTC-3′; XIAP: 5′-GAAGACCCTTGGGAACAACA-3′ and 5′-GTCCTTGAAACTGAACCCCA-3′; c-IAP1: 5′-GCCTTTCTCCAAA-CCCTCTT-3′ and 5′-CATTCGAGCTGCATGTGTCT-3′; c-IAP2: 5′-CAG-TGGATATTTCCGTGGCT-3′ and 5′-ATTTTCCACCACAGGCAAAG-3′; NAIP: 5′-CCGAACAGGAACTGCTTCTC-3′ and 5′-AAATTTG-GCAAACTGGCAAC-3′; Apollon: 5′-AAGTGGCACCCGTAAATCTG-3′ and 5′-CCTGCCTCAAAGAAGCAAAC-3′. Amplification of all IAPs was carried out for 30 to 40 cycles of denaturation at 95°C for 1 minute, annealing at 55°C for 1 minute, and elongation for 1 minute at 72°C, followed by final extension for 7 minutes at 72°C. For NAIP, annealing was carried out at 60°C. PCR products were visualized in 2% agarose gels stained with ethidium bromide.

Quantitative real-time RT-PCR

Primers and probes for human survivin, Ki-67, and glyceraldehyde-3-phosphate dehydrogenase (GAPDH) were designed using Primer Express Software (Applied Biosystems, Foster City, CA) and purchased from Applied Biosystems. For survivin, the forward and reverse primers were 5′-TGAACTTCAGGTGGATGAGGAGA-3′ and 5′-GTCTAATCACA-CAGCAGTGGCAA-3′, and the TaqMan probe was 6 FAM-AATAGAGT-GATAGGAAGCGTCTGGCAGATACTC-TAMRA. For Ki-67, the forward and the reverse primers were 5′-CCACACTGTGTCGTCGTTTG-3′ and 5′-CCGTGCGCTTATCCATTCA-3′, and the TaqMan probe was 6 FAM-CCTATGTTCTCCAGGGCACGGTGG-TAMRA. Total RNA was treated with DNase (Promega, Madison, WI) for 30 minutes at 37°C, followed by real-time RT-PCR. The RT-PCR cycle parameters were 48°C for 30 minutes and 95°C for 10 minutes, followed by 50 cycles at 95°C for 15 seconds and 60°C for 1 minute. Survivin, Ki-67, and GAPDH PCR reactions were performed in separate tubes in triplicate, and the average threshold cycle (CT), representing the cycle at which a significant increase in fluorescence occurs, was used in subsequent calculations. The relative differences for survivin and Ki-67, before and after cytokine stimulation, were determined using the CT method as outlined in the Applied Biosystems protocol for RT-PCR. Briefly, a CT value for GAPDH was subtracted from the CT values for survivin and Ki-67 for each sample. The CT values were then converted to fold differences compared to unstimulated cells by raising 2 to the −CT power.

Intracellular staining and flow cytometry

Multivariate intracellular staining of $CD34^+$ cells with anti–total-Rb, phosphorylated-Rb, underphosphorylated-Rb, cyclin-D, Ki-67, and survivin antibodies in combination with DNA staining were performed as previously described[18] with minor modifications. $CD34^+$ cells were fixed with 4% paraformaldehyde, washed with 0.1% bovine serum albumin/phosphate-buffered saline (BSA/PBS), resuspended in ice-cold 80% ethanol, and incubated for 24 hours at −20°C. Cells were washed with PBS containing 0.25% Triton X-100 and 1% BSA and stained with either FITC–anti-underphosphorylated-Rb, FITC–anti-Ki-67, or FITC–anti-cyclin D mAbs and antihuman survivin antibody. DNA staining was performed using 7-AAD. Stained cells were analyzed using a FACScan and ModFIT (for cell cycle) and CellQuest software (Becton Dickinson, San Jose, CA).

Retrovirus production and infection of mouse bone marrow progenitor cells

Human survivin cDNA was obtained from Dr Hari Nakshatri (Indiana University School of Medicine, Indianapolis, IN). Mouse survivin cDNA was amplified by RT-PCR from total RNA harvested from NIH3T3 cells

using random hexamers and the primers 5′-GTTTGAGTCGTCTTGGCG-GAGGTTGTGGTGACGCCATC-3′ and 5′-CTCAGGTCCAAGTTATCT-CAGCAAAGGCTCAGCA-3′. The bicistronic retrovirus plasmid MIEG3 containing internal ribosome entry site–enhanced green fluorescent protein (IRES-EGFP)[30] was obtained from Dr David Williams (Indiana University). Full-length human and mouse survivin cDNAs were cloned into the MIEG3 plasmid. The orientation and sequence of every construct were confirmed before transfection. A clone showing a reverse direction was used as an antisense construct. Ecotropic retrovirus containing human, mouse, and antisense-mouse survivin and MIEG3 backbone were produced using Phoenix eco cells (ATTC, Manassas, VA) as described.[30] Briefly, 5×10^6 Phoenix eco cells were seeded onto 100-mm dishes and transfected with 8 μg plasmid using Lipofectamine and Plus Reagent (Gibco BRL/Invitrogen) 16 hours later. Transfected cells were incubated in serum-free media for 3 hours, followed by readdition of serum. After 24 hours, cells were exposed to 50 mM sodium butyrate for 8 hours, followed by sequential washing with PBS. Cells were fed with IMDM containing 10% HI-FBS and 2 mM glutamine, incubated at 32°C for 24 hours, and the supernatant was collected, filtered, and stored at −70°C. Virus titer was usually $1\text{-}2 \times 10^5$ plaque-forming units (pfu)/mL. Mouse bone marrow cells were harvested, and mononuclear cells were isolated on Lympholyte-M (Cedarlane Laboratories, ON, Canada) and stimulated with 100 ng/mL each human Tpo, murine SCF, and human G-CSF for 48 hours.[30] Media were replaced with freshly thawed retrovirus supernatant containing the identical cytokine cocktail, and the cells were cultured on wells precoated with recombinant fibronectin fragment CH296 (Takara Shuzo, Otsu, Japan) for 48 hours.

CFU-GM and thymidine suicide assay

Mouse bone marrow cells cultured with retrovirus supernatant were collected and FACS sorted based on green fluorescence protein (GFP) expression. Ten thousand GFP+ cells were plated in 0.3% agar (Difco Laboratories, Detroit, MI) containing supplemented McCoy 5a medium with 15% HI-FBS, 10 ng/mL rmGM-CSF, and 50 ng/mL rmSCF.[31] CFU-GMs were scored after 7 days' incubation at 37°C in a humidified 5% CO_2, 5% O_2 air atmosphere. S-phase CFU-GMs were quantitated by thymidine suicide as previously described.[32] Briefly, GFP+ cells were incubated with either 5 mg/mL thymidine (Sigma Chemical, St Louis, MO) or 50 μCi (1.85 MBq) [methyl-^{3}H]thymidine (20 Ci/mmol [740 GBq/mmol], New England Nuclear, Boston, MA) at 37°C for 30 minutes. Reactions were terminated by adding 100-fold excessive thymidine (300 μg/mL). Cells were washed twice with IMDM and CFU-GM/1 $\times 10^4$ cells quantitated as described above. In some experiments, growth factor addition was delayed for up to 48 hours and colonies scored after 10 days.

Western blot analyses

Western blot analyses were performed on lysates from 5×10^5 GFP+ cells from each transduced group using the rabbit polyclonal antihuman survivin (AF886) antibody. Preliminary flow cytometry and Western blot analyses experiments demonstrated the cross-reactivity of this antibody for murine survivin.

Results

Expression of mRNA for inhibitor of apoptosis proteins in cord blood CD34+ cells

Since we previously demonstrated that survivin is expressed and cytokine regulated in normal CD34+ cells, we examined expression and growth factor regulation of all other human IAPs. Comparison of mRNA before and after culture with Tpo, SCF, and FL by RT-PCR for 48 hours demonstrated that in addition to survivin, XIAP, c-IAP1, c-IAP2, and Apollon are expressed in fresh CD34+ cells (Figure 1). Livin and NAIP were not detectable. Only survivin mRNA expression was up-regulated after cytokine

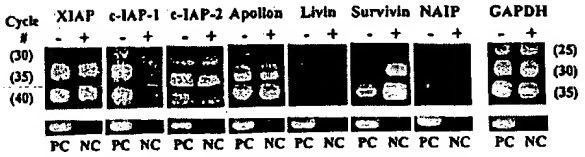

Figure 1. Semiquantitative RT-PCR for IAPs in UCB CD34+ cells before and after growth factor stimulation. Total RNA from CD34+ cells before (−) and after (+) Tpo, SCF, and FL stimulation was subjected to 30, 35, and 40 cycles of RT-PCR for all 7 known human IAPs and 25, 30, and 35 cycles for GAPDH. The number of PCR cycles is shown in parentheses. Total RNA derived from human melanoma G361 cells was used as positive control (PC). NC represents reactions without RNA template. Reaction products were visualized in 2% agarose gels stained with ethidium bromide.

stimulation, whereas expression of c-IAP1 and c-IAP2 decreased. Identical results were observed in CD34+ cells from 5 UCB samples, although in 2 of 5 samples, c-IAP1 remained unchanged after culture with Tpo, SCF, and FL, while decreasing in 3 of 5 samples.

Survivin, Rb protein, cyclin D, and Ki-67 expression in CD34+ cells

A number of proteins have been linked to cell cycle entry. D cyclins are induced upon mitogenic stimulation in quiescent cells,[33-35] and Ki-67 is a nuclear antigen found exclusively in proliferating cells.[33,34,36,37] Upon mitogenic stimulation, Rb becomes phosphorylated, allowing cells to transit from G_1 to S phase.[5,35,38-40] In unstimulated lymphocytes, underphosphorylated Rb predominates, and the proportion of cells with underphosphorylated Rb decreases within 3 to 8 hours of mitogenic stimulation.[39] To address whether survivin up-regulation by growth factors in CD34+ cells occurs before or after cell cycle entry, survivin, total Rb, underphosphorylated Rb, phosphorylated Rb (Ser780, Ser795, and Ser807/811), D cyclins, Ki-67, and cell cycle status were measured by multivariate intracellular flow cytometry following cytokine stimulation. Survivin mRNA was also quantitated by real-time RT-PCR. Within 2 hours, cytokine-stimulated up-regulation of survivin mRNA and protein was observed coincident with up-regulation of D cyclins and Ki-67 (Table 1). Total Rb protein gradually increased, whereas phosphorylated Rb increased dramatically. Underphosphorylated-Rb protein remained constant or marginally decreased (not shown). The ratio of phosphorylated Rb to total Rb protein was dramatically elevated following growth factor addition, whereas the ratio of underphosphorylated Rb to total Rb gradually declined (Table 1). The increase in the percentage of S + G_2M phase cells correlated with up-regulation of survivin, Ki-67, D cyclins, and phosphorylated Rb. Because cells that express underphosphorylated Rb and are negative for Ki-67 and D cyclins are believed to be quiescent, expression of survivin in underphosphorylated-Rb^{positive}, Ki-67^{negative}, and cyclin D^{negative} CD34+ cells was examined before and after growth factor stimulation (Table 2). Survivin protein was up-regulated by growth factors in underphosphorylated-Rb^{positive}, Ki-67^{negative}, and cyclin D^{negative} CD34+ cells as well as in underphosphorylated-Rb^{negative}, Ki-67^{positive}, and cyclin D^{positive} CD34+ cells, suggesting that survivin expression is up-regulated in quiescent cells before cell cycle entry.

Survivin expression in G_0 CD34+ cells before and after growth factor stimulation

We previously demonstrated that survivin expression is elevated in G_0 cells after incubation of unseparated CD34+ cells with cytokines.[18] However, these studies did not address the issue of whether

Table 1. Survivin, Ki-67, cyclin D, phosphorylated-Rb, underphosphorylated-Rb, and % S + G_2/M cells in Tpo-, SCF-, and FL-stimulated CD34$^+$ cells

Cell population	No. of experiments	Fold increase			
		2 hours after growth factor addition*	4 hours after growth factor addition*	6 hours after growth factor addition*	18 hours after growth factor addition*
Survivin protein	4	1.4 ± 0.2	1.8 ± 0.2‡	2.4 ± 0.5†	6.2 ± 2.4†
Survivin mRNA	3	1.1 ± 0.1	1.2 ± 0.1†	2.1 ± 0.5†	10.3 ± 3.8†
%S + G_2M phase	4	7.5 ± 1.2	6.9 ± 1.0	8.5 ± 1.2†	19.9 ± 3.1†
Ki-67	2	1.3 ± 0.01§	1.3 ± 0.02§	1.2 ± 0.01§	1.5 ± 0.2§
Cyclin D	5	1.1 ± 0.1†	1.2 ± 0.1†	1.2 ± 0.1‡	1.5 ± 0.2†
Phosphorylated Rb/Total Rb	2	1.7 ± 0.6†	1.5 ± 0.5†	1.8 ± 0.7†	2.3 ± 0.6†
Underphosphorylated Rb/Total Rb	3	0.8 ± 0.1†	0.7 ± 0.1‡	0.7 ± 0.1†	0.5 ± 0.1§

Survivin, cyclin D, Ki-67, phosphorylated-Rb (Ser 807/811), underphosphorylated-Rb, and total-Rb protein levels were determined by intracellular flow cytometry in the CD34$^+$ cell population from UCB. The fold increases in mean channel fluorescence for each protein and the ratio of fold changes of phosphorylated Rb/total Rb and underphosphorylated Rb/total Rb are shown as means ± SEM of the number of experiments indicated. Survivin mRNA was determined by real-time RT-PCR. The percentage of CD34$^+$ cells in S + G_2/M phase was measured by DNA staining with 7-AAD and analyzed using ModFit software. Data are presented as means ± SEM of 4 experiments.

*100 ng/mL each rhTpo, rhFL, rhSCF.

†$P < .05$.

‡$P < .01$.

§$P < .005$ compared with time 0.

these cells had yet to enter cell cycle or had already completed mitosis and returned to G_0. We therefore investigated whether survivin up-regulation by growth factors observed in G_0 cells is specifically regulated before cells enter cell cycle. Fresh G_0 CD34$^+$ cells were isolated based upon Hoechst 33342/pyronin Y (Hst/PY) staining (Figure 2A, gate R1) and incubated for 12 hours with 100 ng/mL each of Tpo, SCF, and FL. After culture, cells were restained with Hst/PY, and Hst^{low}, PY^{low} cells (gate R2), representing cells in G_0, were collected by FACS sorting. Replicate freshly isolated G_0 cells were stained with CFSE before culture to monitor cell division. No cell division occurred during the 12-hour culture period as defined by CFSE analysis before sorting (Figure 2A). The purity of the G_0 population (Figure 2A, gate R2) assessed by Hst/PY resorting was 98% (Figure 2B, gate R2) and was 97% ± 2% in 5 experiments. No cell division in the G_0 CD34$^+$ population (gate R2) was observed based on CFSE analysis. Because Ki-67 is undetectable in G_0 cells[41] but expressed in cells entering G_1, Ki-67, and 7-AAD, staining was used to validate the Hst/PY sort for cell cycle status of CD34$^+$ cells. Approximately 99% of cells in the R2 gate, that is, G_0 CD34$^+$ cells, did not express Ki-67 after culture with cytokines (Figure 2C). In 3 experiments, 89.9% ± 9.1% of fresh G_0 cells (R1) and 95.2% ± 4.3% of cultured G_0 cells (R2) were Ki-67^{negative}, whereas only 65.9% ± 18.3% of fresh G_1 cells were Ki-67^{negative} (not shown). Survivin protein increased 2.1 ± 0.3 fold in G_0 CD34$^+$ cells (R2 gate) following culture with growth factors, and the percentage of survivin-positive cells increased from 4.7% ± 1.4% (R1) to 32.5% ± 9.3% (R2) (Figure 2D; Table 3). Because the G_0 cells isolated based on Hst/PY staining were not 100% negative for Ki-67 expression (98.9%, Figure 2C, gate R2), survivin protein expression was examined in Ki-67^{negative} cells in the R1 and R2 gates (Figure 2E; Table 3). Survivin protein increased 1.9 ± 0.1-fold in G_0 CD34$^+$ cells (R2 gate) after culture, and the percentage of survivin-positive cells increased from 1.6% ± 0.7% to 40.0% ± 18.5%. Up-regulation of survivin in G_0 cells after growth factor incubation was verified at the mRNA level using quantitative real-time RT-PCR (Figure 2F; Table 3). Cells in the R1 and R2 gates were harvested and total RNA analyzed for survivin and Ki-67 expression. Ki-67 expression was essentially negative both before and after growth factor stimulation, confirming the quiescent nature of these cells. The threshold CT values for survivin were 34.7 and 37.8 in R2 and R1 cells, respectively, representing a 2.4 ± 0.7-fold increase in survivin mRNA in R2 cells compared to R1 cells (2 experiments). No increase in Ki-67 mRNA was observed in R2 cells compared with cells in R1 (0.8 ± 0.3-fold, 2 experiments), indicating that survivin is up-regulated in quiescent G_0 cells after cytokine stimulation. Real-time RT-PCR analysis of freshly isolated G_0 cells and CFSE^{bright} G_0 cells cultured for 48 hours with growth factors produced similar results (not shown).

PI3-kinase/AKT and MAP kinase pathway inhibitors block survivin up-regulation by growth factors before cell cycle arrest

Activation of the PI3-kinase and MAPK$^{p42/44}$ pathways correlates with survival of CD34$^+$ cells stimulated by hematopoietic

Table 2. Survivin expression in CD34$^+$ cell populations following growth factor addition

Cell population	Fold increase in survivin protein		
	2 hours after growth factor addition*	4 hours after growth factor addition*	6 hours after growth factor addition*
CD34$^+$, cyclin D^{negative}	1.8 ± 0.3†	2.2 ± 0.4‡	2.4 ± 0.4‡
CD34$^+$, cyclin D^{positive}	1.7 ± 0.2‡	2.3 ± 0.5‡	2.7 ± 0.5‡
CD34$^+$, Ki-67^{negative}	2.4 ± 0.2§	3.2 ± 0.2§	4.2 ± 0.5§
CD34$^+$, Ki-67^{positive}	3.9 ± 1.0‡	5.4 ± 1.8†	6.5 ± 2.0‡
CD34$^+$, underphosphorylated Rb^{positive}	2.2 ± 0.2§	3.2 ± 0.3§	3.7 ± 0.6§
CD34$^+$, underphosphorylated Rb^{negative}	1.9 ± 0.3‡	3.2 ± 0.5§	3.5 ± 0.6§

Survivin, cyclin D, Ki-67, and underphosphorylated-Rb protein levels were determined by intracellular flow cytometry in the CD34$^+$ cell population from UCB. Data are expressed as means ± SEM from 3 experiments.

*100 ng/mL each rhTpo, rhFL, rhSCF.

†$P < .05$.

‡$P < .01$.

§$P < .005$ compared with time 0.

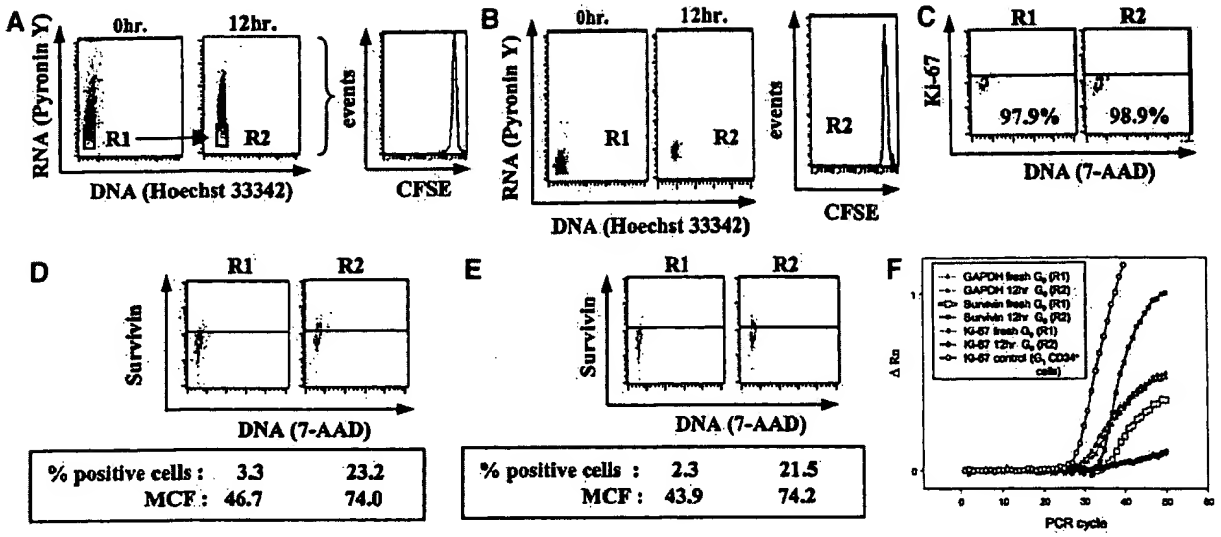

Figure 2. Expression of survivin protein and mRNA in G_0 CD34+ cells isolated by Hoechst 33342/pyronin Y staining before and after 12 hours' growth factor stimulation. (A) Hoechst 33342/pyronin Y staining of UCB CD34+ cells before and after incubation for 12 hours with 100 ng/mL each Tpo, SCF, and FL. The left panel represents the gate for fresh G_0 CD34+ cells (R1). Fresh G_0 cells (R1) were incubated with Tpo, SCF, and FL for 12 hours, restained with Hoechst 33342/pyronin Y, and G_0 cells isolated by FACS sorting (middle panel; gate R2). In replicate cultures, R1 cells were prestained with CFSE before incubation, and cell division in the unseparated cell population was analyzed after 12 hours' culture (right panel). Data represent 1 of 5 identical experiments. (B) Postsort analysis of Hoechst 33342/pyronin Y and CFSE staining on cells from the R1 and R2 gates in Figure 2A. Data represent 1 of 5 identical experiments. The R1 and R2 gates were set so that the 20% dimmest pyronin Y cells were collected for fresh and cultured CD34+ cells. The gates for the postsort analysis were adjusted for the characteristic progressive loss of pyronin Y fluorescence with time.[27,33] (C) Intracellular Ki-67 protein expression and DNA staining of fresh G_0 cells (R1) and G_0 cells isolated after culture for 12 hours with growth factors (R2) from Figure 2A. The percentage of cells negative for Ki-67 expression, that is, below isotype staining (horizontal bar), is shown. Data represent 1 of 3 independent experiments. (D) Intracellular survivin protein expression in fresh G_0 CD34+ cells (R1) and in G_0 cells (R2) from Figure 2A, harvested after 12 hours' incubation with growth factors. Mean channel fluorescence (MCF) of survivin and the percentage of cells staining positive (above isotype control [horizontal bar]) for survivin are shown below each blot. Data represent 1 of 3 identical experiments. (E) Survivin expression was quantitated in the Ki-67–negative fraction of fresh or cultured G_0 cells from Figure 2C. The MCF for survivin and the percentage of survivin-positive cells (above isotype control [horizontal bar]) are shown beneath the blot. Data represent 1 of 3 identical experiments. (F) Total RNA from G_0 cells before (R1) and after (R2) growth factor incubation was subjected to real-time RT-PCR to quantify survivin and Ki-67 mRNA expression. GAPDH was used as the internal control. Because Ki-67 expression of both samples was extremely low, G_1 CD34+ cells were used to verify the PCR reaction of Ki-67. The y-axis represents ΔRn, which indicates the magnitude of the signal generated at each cycle. The x-axis shows the reaction cycle. Data represent 1 of 2 identical experiments.

cytokines,[42,43] and inhibition of these pathways results in reduction of cytokine action[44] and decreased proliferation of normal CD34+ cells.[45] Because inhibition of PI3-kinase/AKT and MAPK$^{p42/44}$ pathways by LY294002 and PD98059, respectively, resulted in down-regulation of survivin accompanied by cell cycle arrest in cytokine-stimulated AML cells,[46] we used these selective inhibitors to determine whether changes in survivin expression preceded cell cycle arrest induced by these inhibitors. CD34+ cells were treated with 1 and 5 μM LY294002, 20 and 40 μM PD98059 or dimethyl sulfoxide (DMSO) for 1 hour, followed by incubation with 100 ng/mL each Tpo, SCF, and FL.

Table 3. Fold increase in survivin and Ki-67 in G_0 CD34+ cells after growth factor addition

	0 hours after growth factor addition*	12 hours after growth factor addition*
Fold increase survivin protein	–	2.1 ± 0.3† (1.9 ± 0.1)†
% survivin-positive cells	4.7 ± 1.4 (1.6 ± 0.7)	32.5 ± 9.3† (40.0 ± 18.5)†
Fold increase survivin mRNA	–	2.4 ± 0.7‡
Fold increase Ki-67 protein	–	0.9 ± 0.1
% Ki-67^{negative} cells	89.9 ± 9.1	95.2 ± 4.3
Fold increase Ki-67 mRNA	–	0.8 ± 0.3

Survivin and Ki-67 protein expression (means ± SEM from 3 experiments) was determined by intracellular flow cytometry; mRNA levels were determined by real-time RT-PCR (means ± SD from 2 experiments). Data are expressed as the fold increase in survivin and Ki-67 protein or percentage survivin-positive or Ki-67^{negative} cells in G_0 CD34+ cells or in the G_0 CD34+ Ki-67^{negative} cell population (shown in parentheses).

*100 ng/mL each rhTpo, rhFL, and rhSCF.

†$P < .005$.

‡Range, 1.42-3.27-fold; n = 2 experiments.

Survivin expression and cell cycle status were analyzed over time by flow cytometry. In control cultures, multivariate staining of survivin and DNA in CD34+ cells demonstrated that survivin expression was up-regulated in a time-dependent manner coincident with cell cycle progression (not shown). The PI3-kinase/AKT pathway inhibitor LY294002 (5 μM) reduced survivin expression by 15.2% ± 5.9% and 35.7% ± 11.7% (means ± SEM, 3 experiments) at 4 and 8 hours after cytokine stimulation, respectively, with no effect on cell cycle progression. At 18 hours, survivin expression was reduced by 44.7% ± 10.3% with a concomitant 57.3% ± 15.5% increase in the number of CD34+ cells in G_0/G_1 phase (Figure 3A). Similar results were observed with 1 μM LY294002. CD34+ cell viability was greater than 90% in all groups up to 8 hours after cytokine addition, but was ~85% in cells treated with 1 or 5 μM LY294002 at 18 hours. Inhibition of survivin was observed in both G_0/G_1 and S + G_2/M cells (data not shown). The MAPK$^{p42/44}$ inhibitor PD98059 at 20 μM reduced survivin expression in CD34+ cells by 19.1% ± 8.0% at 8 hours, without any effect on the ability of CD34+ cells to progress through cell cycle. However, at 18 hours, survivin expression was reduced by 37.0% ± 9.5%, concomitant with an 18.6% ± 11% increase in G_0/G_1 cells (Figure 3B). Similar results were obtained using 40 μM PD98059. Forward and side scatter analysis indicated that greater than 90% of cells in all groups remained viable. Incubation of CD34+ cells with 20 and 40 μM PD98059 for longer than 24 hours or at concentrations greater than or equal to 60 μM for up to 20 hours inhibited survivin up-regulation and reduced cell cycle (not shown). Similar to LY294002, inhibition

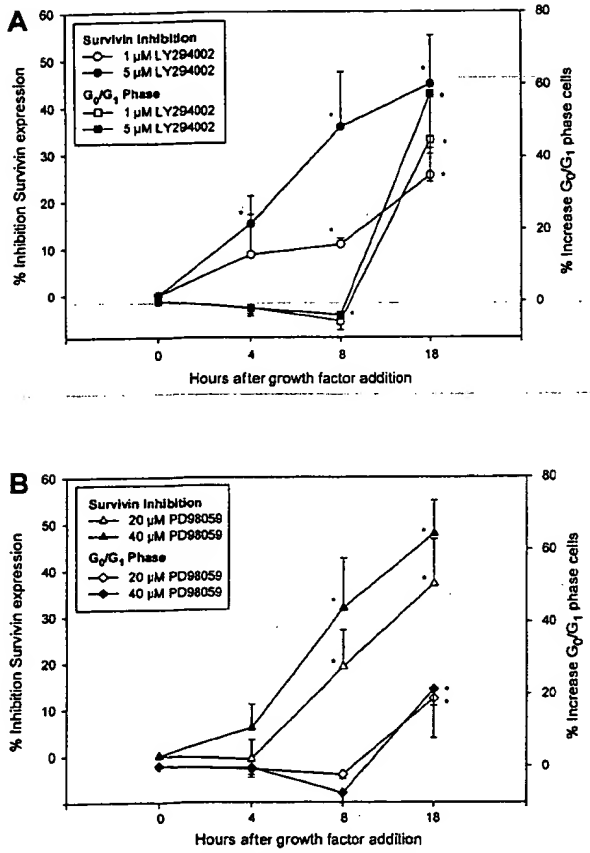

Figure 3. Effects of PI3-kinase and MAPK$^{p42/44}$ inhibitors on survivin expression and cell cycle in CD34$^+$ cells. CD34$^+$ cells were pretreated with either DMSO, 1 and 5 μM LY294002 (A), or 20 and 40 μM PD98059 (B), followed by incubation with 100 ng/mL each Tpo, SCF, and FL. Cells were fixed at 4, 8, and 18 hours after growth factor stimulation and analyzed for survivin protein and cell cycle. Percent inhibition of survivin expression was calculated as percent reduction of mean channel fluorescence of survivin compared to DMSO control at each time point. Percent increase in G_0/G_1 phase cells was calculated based on the increase in G_0/G_1 population over DMSO control at each time. Data are shown as means ± SEM of 3 independent experiments. *$P < .05$.

of survivin up-regulation by PD98059 was observed in S + G_2/M and G_0/G_1 cells (not shown).

Overexpression of wild-type and antisense survivin cDNA in primary mouse bone marrow cells

Mouse bone marrow mononuclear cells were infected with the retrovirus MIEG3 vector, human, mouse, or antisense-mouse survivin. GFP$^+$ cells were sorted, collected, and assayed for CFU-GM. Approximately 13% of GFP$^+$ cells from each group were c-kit$^+$, and 0.5% were c-kit$^+$, Sca-1$^+$. Intracellular staining of GFP$^+$ cells for survivin indicated that 72.3% ± 3.0% and 54.9% ± 16.3% of human and mouse transduced cells, respectively, were survivin positive compared with 33.9% ± 1.3% of vector control cells, whereas 14.5% ± 1.2% of antisense-mouse survivin–transduced cells were positive for survivin (Figure 4A). Western analysis of human or mouse survivin-transduced marrow cells confirmed elevated expression of survivin, while reduced survivin was observed in cells transduced with an antisense-mouse survivin (Figure 4A, insert). The number of proliferating CFU-GM was increased 1.7 to 6.2-fold in marrow cells transduced with human (301% ± 66% increase, $P < .005$, 4 experiments) or mouse (285% ± 79% increase, $P < .01$, 4 experiments) survivin, compared with cells transduced with vector (Figure 4B). Transduction of mouse marrow cells with an antisense-mouse survivin construct decreased total CFU-GM by 69% ± 5% ($P < .05$, 4 experiments). Analysis of the proportion of CFU-GM in S phase indicated that 78.9% ± 1.8% ($P < .05$; 3 experiments) and 77.6% ± 3.0% ($P < .01$, 3 experiments) of CFU-GM transduced with human or mouse survivin, respectively, were in S phase, compared with vector control (55.0% ± 5.0%) (Figure 4C). Transduction of marrow cells with antisense-mouse survivin reduced the proportion of S-phase CFU-GM to 42.1% ± 4.7% ($P < .05$, 3 experiments). Delayed addition of growth factors for 24 and 48 hours to vector or human (h)-survivin–transduced marrow cells resulted in progressive apoptosis of CFU-GM. However, after normalization for CFU-GM enhancement at time 0, 16% to 77% and 61% to 244% more CFU-GM (2 experiments) were observed in h-survivin–transduced cells after 24 and 48 hours of delayed growth factor addition, respectively, than in vector control cultures, suggesting that survivin overexpression blocked CFU-GM apoptosis caused by cytokine starvation.

Discussion

The IAP proteins are the only known endogenous caspase inhibitors that suppress apoptosis.[47] The IAPs XIAP, c-IAP1, and c-IAP2 directly bind to and inhibit caspases 3, 7, and 9 via their BIR domains.[48] In this report, we demonstrate that in addition to survivin, XIAP, c-IAP1, and c-IAP2 are expressed in CD34$^+$ cells; however, survivin is the only cytokine-regulated IAP in these cells and therefore is the only likely IAP mediating suppression of apoptosis by hematopoietic cytokines. Similarly, survivin is the only IAP up-regulated by CD40 ligation in B-CLL cells.[49] The relationship between survivin and other antiapoptotic molecules that play a role in hematopoietic cells, such as Bcl2,[50,51] is not known. Both proteins are up-regulated in breast cancer cells,[52] and their expression can be regulated by the tumor suppressor gene p53.[52,53] Whether there is a direct link between the Bcl2 family members and survivin or, given the importance of apoptosis, that their effects are independent, remains to be determined.

Since the original reports that cancer cells and embryonic tissues, but not normal adult tissues, express survivin,[10,15,54] others and we have described survivin expression in normal adult cells. Survivin expression is not observed in resting endothelial cells but is up-regulated in a cell cycle–dependent manner[55] by vascular endothelial growth factor[55,56] or angiopoietin-1.[57] The murine homolog of survivin, *Tiap*, is induced in T lymphocytes activated by mitogens.[11] We previously reported that survivin is expressed and growth factor regulated in normal adult CD34$^+$ cells and T lymphocytes in all phases of cell cycle.[18] Because it is apparent that survivin is expressed in proliferating cells, the questions of whether survivin expression in CD34$^+$ cells is cytokine regulated or simply reflects cell division and cell cycle progression and whether survivin expression affects proliferation and cell cycle of normal hematopoietic cells are raised. To address these questions, we examined survivin expression in CD34$^+$ cells relative to the cell cycle markers Ki-67, cyclin D, and underphosphorylated-Rb and in Hst^{low}, PY^{low}, CFSE^{bright} G_0 CD34$^+$ cells relative to Ki-67 expression. We also investigated the effects of PI3-kinase/AKT and MAPK$^{p42/p44}$ pathway inhibitors on survivin expression and cell cycle in CD34$^+$ cells. Finally, we introduced survivin cDNA into primary mouse bone marrow cells and examined the effects of modulating survivin expression on cell cycle and proliferation of

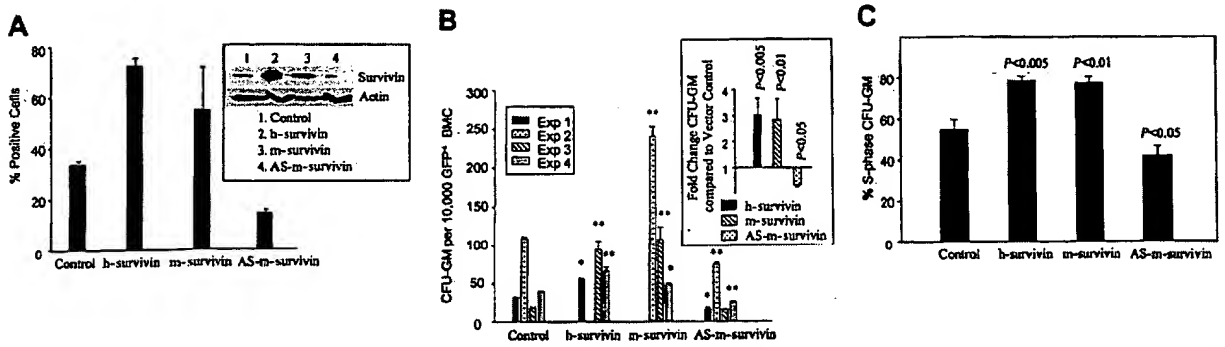

Figure 4. Retrovirus transduction of IRES-EGFP control (control), human survivin IRES-EGFP (h-survivin), mouse survivin IRES-EGFP (m-survivin), and antisense survivin-IRES-EGFP (AS-m-survivin) into primary mouse bone marrow cells. (A) GFP-positive bone marrow mononuclear cells in each transduced group were FACS sorted and the percentage of survivin-positive cells was determined by flow cytometry after staining with PE-antisurvivin antibody. Data are expressed as means ± SEM from 2 experiments. Western analysis for survivin in GFP+ mononuclear cells from each transduced group is shown in the insert. The same filter was stripped and reprobed with antihuman actin antibody as a loading control. Cross-reactivity of this antibody to mouse has been validated by the manufacturer. (B) CFU-GM production in transduced mouse bone marrow cells. Ten thousand GFP-positive marrow mononuclear cells were cultured in soft agar with 10 ng/mL rmGM-CSF and 50 ng/mL rmSCF and CFU-GM quantitated after 7 to 10 days at 37°C, 5% CO_2, 5% O_2 in air. The average number and SEM of CFU-GM from triplicate plates of 4 individual experiments are shown. Combined data from all 4 experiments are shown in the insert. Retrovirus harboring human survivin was used in experiments 1, 3, and 4. Mouse survivin was used in experiments 2, 3, and 4. Vector backbone and antisense-mouse survivin were used in all 4 experiments. *$P < .005$; **$P < .001$. (C) The proportion of CFU-GM in S phase of the cell cycle was determined by thymidine suicide with high specific activity [^{3}H]thymidine. Data are the averages ± SEM of 3 independent experiments.

myeloid progenitor cells. Up-regulation of survivin expression in CD34+ cells by hematopoietic growth factors was coincident with up-regulation of phosphorylated Rb, D cyclins, and Ki-67, indicating that survivin expression parallels cell cycle progression. Multivariate intracellular staining of survivin, Rb, Ki-67, cyclin D, and DNA in CD34+ cells upon growth factor stimulation demonstrated that survivin is up-regulated not only in underphosphorylated-$Rb^{negative}$, cyclin $D^{positive}$, and $KI\text{-}67^{positive}$ cells, but also in the underphosphorylated-$Rb^{positive}$,[5,38-40,58-60] cyclin $D^{negative}$,[33-35] and $Ki\text{-}67^{negative}$ [33,34,36,37] cells. Isolation of G_0 CD34+ cells sorted based on Hoechst 33342/Pyronin Y and staining with CFSE before incubation with growth factors indicated that survivin mRNA and protein are up-regulated in cytokine-stimulated G_0 CD34+ cells that had not yet up-regulated Ki-67 and had not yet divided. These data demonstrate that survivin is up-regulated in CD34+ cells by growth factors during G_0 before cells enter G_1 and that survivin expression is specifically regulated by growth factors in CD34+ cells and not merely a consequence of cell cycle progression.

We have previously shown that like cancer cells, survivin expression in CD34+ cells is highest during G_2/M.[18] Our present study clearly demonstrates that unlike cancer cells, survivin expression is up-regulated in quiescent CD34+ cells following growth factor stimulation before cell cycle entry. This raises the question of whether survivin expression in quiescent CD34+ cells is unique to normal hematopoietic cells. Murine survivin (TIAP) mRNA has been demonstrated in quiescent T cells, though its expression was low.[11] In addition, survivin up-regulation in synchronized NIH3T3 cells following 12 hours' serum stimulation was observed, where greater than 90% of the cells still remained in G_0/G_1 without any increase in S + G_2/M cells.[11] These studies indicate that survivin expression is observed before cell cycle entry in nonhematopoietic cells. Li et al, who reported the specific expression of survivin during G_2/M in HeLa cells, used cell cycle synchronization and Northern and Western analyses[15] to demonstrate that treatment of HeLa cells with mimosine reduced survivin expression coincident with G_1 arrest. Failure to detect survivin expression in G_1-arrested cells might be due to the methodology employed. We used real-time RT-PCR and intracellular flow cytometry to demonstrate G_0 expression of survivin mRNA and protein, which are more sensitive. Furthermore, survivin inhibition by mimosine could be due to a direct effect on survivin expression rather than an effect on cell cycle arrest.

The selective PI3-kinase/AKT pathway inhibitor LY294002 and $MAPK^{p42/p44}$ pathway inhibitor PD98059 significantly blocked up-regulation of survivin expression by growth factors in CD34+ cells. Survivin protein expression decreased in the absence of any effect on cell cycle progression or cell viability, at least during the initial 8 hours, although there was reduction of cell cycle progression after longer exposure. Most importantly, these compounds inhibited up-regulation of survivin expression before an arresting effect on cell cycle was observed. If survivin expression were a result of cell cycle progression, reduction of survivin would be accompanied by cell cycle arrest. Although we did not analyze changes in the proportion of G_0 and G_1 cells, these data strongly suggest that survivin expression in CD34+ cells is regulated by growth factors and is not merely a consequence of cell cycle progression. These findings also indicate that both the PI3-kinase/AKT and $MAPK^{p42/p44}$ pathways are involved in cytokine regulation of survivin expression in normal CD34+ cells, which is consistent with the involvement of these pathways in regulating survivin expression in AML cells.[46]

Overexpression of human or mouse survivin cDNA in primary mouse bone marrow cells dramatically enhanced CFU-GM proliferation and the proportion of CFU-GM in S phase of the cell cycle. An antisense-mouse survivin construct had the opposite effect. These findings indicate that modulating survivin expression modulates proliferation and cell cycle of primary hematopoietic progenitor cells. Although we did not quantitate survivin protein levels in survivin or antisense survivin-transduced CFU-GM due to technical limitations, an increase in survivin-positive marrow cells could be quantitated by flow cytometry following transduction with human or mouse survivin. A decrease in survivin-positive cells was observed following transduction with antisense mouse survivin. A similar trend in survivin protein expression in transduced primary marrow cells was observed by Western analysis. In addition, following transduction of these same MIEG3 constructs into BaF/3 cells, elevated protein levels of h-survivin (237%-466% increase, 3 experiments), mouse (m)-survivin (118%-287% increase, 3 experiments), and antisense-m–survivin (9%-25% decrease in survivin protein levels, 3 experiments) were observed.

Survivin has been shown to interact with cdk4, and overexpression of survivin enhances Rb phosphorylation in hepatoma cells by releasing $p16^{INK4a}$ and $p21^{WAF1/CIP1}$ from the cdk4/$p16^{INK4a}$ and cdk4/$p21^{WAF1/CIP1}$ complexes, respectively.[4,22-24] This suggests that survivin promotes cell cycle progression by inactivating the $p16^{INK4a}$/Rb pathway, a finding consistent with our observation that overexpression of survivin enhances the cell cycle rate of primary mouse CFU-GM. Because survivin is an antiapoptotic protein, it is possible that the enhanced CFU-GM proliferation observed following survivin transduction results from increased CFU-GM survival. This is consistent with reduced apoptosis of survivin-transduced CFU-GM observed in cultures in which growth factor addition was delayed. However, this does not adequately explain the increase in the proportion of S-phase CFU-GMs observed following survivin transduction. There is no reason to assume that enhanced CFU-GM survival means that the additional surviving cells are in S phase.

In conclusion, we have provided evidence demonstrating that survivin expression in $CD34^+$ cells is growth factor regulated and not a consequence of cell cycle progression. First, survivin is up-regulated in $CD34^+$ cells that are underphosphorylated $Rb^{positive}$, $Ki\text{-}67^{negative}$, and $cyclin\text{-}D^{negative}$, that is, quiescent cells. Second, survivin up-regulation by growth factors occurs in G_0 $CD34^+$ cells before these cells enter G_1. Third, inhibition of survivin by selective PI3-kinase/AKT and $MAPK^{p42/44}$ pathway inhibitors occurs before cell cycle arrest. Finally, survivin overexpression enhances and antisense survivin reduces cell cycle rate and proliferation of CFU-GM. Taken together, these data demonstrate that survivin expression is specifically regulated by growth factors in quiescent $CD34^+$ cells and strongly suggest that up-regulation of survivin is an early and important event for cell cycle entry and proliferation of normal hematopoietic stem and progenitor cells.

Acknowledgments

The authors thank Suzan Rice for sorting cells by flow cytometry, Charlie Mantel for helpful suggestions, and Hui-min Bian, Jonathan Pelus, and Jessie Mindel for technical assistance.

References

1. Smith DM, Gao G, Zhang X, Wang G, Dou QP. Regulation of tumor cell apoptotic sensitivity during the cell cycle. Int J Mol Med. 2000;6:503-507.
2. Guo M, Hay BA. Cell proliferation and apoptosis. Curr Opin Cell Biol. 1999;11:745-752.
3. Deveraux QL, Reed JC. IAP family proteins-suppressors of apoptosis. Genes Dev. 1999;13: 239-252.
4. Suzuki A, Shiraki K. Tumor cell "dead or alive": caspase and survivin regulate cell death, cell cycle and cell survival. Histol Histopathol. 2001; 16:583-593.
5. Harbour JW, Dean DC. Rb function in cell-cycle regulation and apoptosis. Nat Cell Biol. 2000;2: 65-67.
6. Roy N, Mahadevan MS, McLean M, et al. The gene for neuronal apoptosis inhibitory protein is partially deleted in individuals with spinal muscular atrophy. Cell. 1995;80:167-178.
7. Liston P, Roy N, Tamai K, et al. Suppression of apoptosis in mammalian cells by NAIP and a related family of IAP genes. Nature. 1996;379:349-353.
8. Roy N, Deveraux QL, Takahashi R, Salvesen GS, Reed JC. The c-IAP-1 and c-IAP-2 proteins are direct inhibitors of specific caspases. EMBO J. 1997;16:6914-6925.
9. Rothe M, Pan MG, Henzel WJ, Ayres TM, Goeddel DV. The TNFR2-TRAF signaling complex contains two novel proteins related to baculoviral inhibitor of apoptosis proteins. Cell. 1995;83: 1243-1252.
10. Ambrosini G, Adida C, Altieri DC. A novel anti-apoptosis gene, survivin, expressed in cancer and lymphoma. Nat Med. 1997;3:917-921.
11. Kobayashi K, Hatano M, Otaki M, Ogasawara T, Tokuhisa T. Expression of a murine homologue of the inhibitor of apoptosis protein is related to cell proliferation. Proc Natl Acad Sci U S A. 1999;96: 1457-1462.
12. Kasof GM, Gomes BC. Livin, a novel inhibitor of apoptosis family member. J Biol Chem. 2001;276: 3238-3246.
13. Hauser H-P, Bardroff M, Pyrowolakis G, Jentsch S. A giant ubiquitin-conjugating enzyme related to IAP apoptosis inhibitors. J Cell Biol. 1998;141: 1415-1422.
14. Chen Z, Naito M, Hori S, Mashima T, Yamori T, Tsuruo T. A human IAP-family gene, apollon, expressed in human brain cancer cells. Biochem Biophys Res Commun. 1999;264:847-854.
15. Li F, Ambrosini G, Chu EY, Plescia J, Tognin S, Marchisio PC, Altieri DC. Control of apoptosis and mitotic spindle checkpoint by survivin. Nature. 1998;396:580-584.
16. Tamm I, Wang Y, Sausville E, et al. IAP-family protein survivin inhibits caspase activity and apoptosis induced by Fas (CD95), Bax, caspases, and anticancer drugs. Cancer Res. 1998;58: 5315-5320.
17. Deveraux QL, Takahashi R, Salvesen GS, Reed JC. X-linked IAP is a direct inhibitor of cell-death proteases. Nature. 1997;388:300-304.
18. Fukuda S, Pelus LM. Regulation of the inhibitor-of-apoptosis family member survivin in normal cord blood and bone marrow $CD34^+$ cells by hematopoietic growth factors: implication of survivin expression in normal hematopoiesis. Blood. 2001;98:2091-2100.
19. Olie RA, Simoes-Wust AP, Baumann B, et al. A novel antisense oligonucleotide targeting survivin expression induces apoptosis and sensitizes lung cancer cells to chemotherapy. Cancer Res. 2000; 60:2805-2809.
20. Conway EM, Pollefeyt S, Cornelissen J, et al. Three differentially expressed survivin cDNA variants encode proteins with distinct antiapoptotic functions. Blood. 2000;95:1435-1442.
21. Li F, Ackermann EJ, Bennett CF, et al. Pleiotropic cell-division defects and apoptosis induced by interference with survivin function. Nat Cell Biol. 1999;1:461-466.
22. Suzuki A, Hayashida M, Ito T, et al. Survivin initiates cell cycle entry by the competitive interaction with Cdk4/p16 (INK4a) and Cdk2/cyclin E complex activation. Oncogene. 2000;19:3225-3234.
23. Suzuki A, Ito T, Kawano H, et al. Survivin initiates procaspase 3/p21 complex formation as a result of interaction with Cdk4 to resist Fas-mediated cell death. Oncogene. 2000;19:1346-1353.
24. Ito T, Shiraki K, Sugimoto K, et al. Survivin promotes cell proliferation in human hepatocellular carcinoma. Hepatology. 2000;31:1080-1085.
25. Uchida N, He D, Friera AM, et al. The unexpected G0/G1 cell cycle status of mobilized hematopoietic stem cells from peripheral blood. Blood. 1997;89:465-472.
26. Gothot A, Pyatt R, McMahel J, Rice S, Srour EF. Functional heterogeneity of human CD34(+) cells isolated in subcompartments of the G0 /G1 phase of the cell cycle. Blood. 1997;90:4384-4393.
27. Wilpshaar J, Falkenburg JHF, Tong X, et al. Similar repopulating capacity of mitotically active and resting umbilical cord blood $CD34^+$ cells in NOD/SCID mice. Blood. 2000;96:2100-2107.
28. Murray LJ, Young JC, Osborne LJ, Luens KM, Scollay R, Hill BL. Thrombopoietin, flt3, and kit ligands together suppress apoptosis of human mobilized $CD34^+$ cells and recruit primitive $CD34^+$ $THy\text{-}1^+$ cells into rapid division. Exp Hematol. 1999;27:1019-1028.
29. Nordon RE, Ginsberg SS, Eaves CJ. High-resolution cell division tracking demonstrates theFlt-3 ligand-dependence of human marrow $CD34^+CD38^-$ cell production in vitro. Br J Haematol. 1997;98:528-539.
30. Williams DA, Tao W, Yang F, et al. Dominant negative mutation of the hematopoietic-specific Rho GTPase, Rac2, is associated with human phagocyte immunodeficiency. Blood. 2000;96: 1646-1654.
31. King AG, Horowitz D, Dillon SB, et al. Rapid mobilization of murine hematopoietic stem cells with enhanced engraftment properties and evaluation of hematopoietic progenitor cell mobilization in rhesus monkeys by a single injection of SB-251353, a specific truncated form of the human CXC chemokine GROβ. Blood. 2000;97:1534-1542.
32. Pelus LM. Association between colony forming units-granulocyte macrophage expression of Ia-like (HLA-DR) antigen and control of granulocyte and macrophage production: a role for prostaglandin E. J Clin Invest. 1981;70:568-578.
33. Glimm H, Oh I-H, Eaves CJ. Human hematopoietic stem cells stimulated to proliferate in vitro lose engraftment potential during their $S/G_2/M$ transit and do not reenter G_0. Blood. 2000;96: 4185-4193.
34. Holyoake T, Jiang X, Eaves C, Eaves A. Isolation of a highly quiescent subpopulation of primitive leukemic cells in chronic myeloid leukemia. Blood. 1999;94:2056-2064.
35. Sherr CJ. Mammalian G1 cyclins. Cell. 1993;73: 1059-1065.
36. Jordan CT, Yamasaki G, Minamoto D. High-resolution cell cycle analysis of defined phenotypic subsets within primitive human hematopoietic cell populations. Exp Hematol. 1996;24:1347-1355.
37. Schluter C, Duchrow M, Wohlenberg C, et al. The cell proliferation-associated antigen of antibody Ki-67: a very large, ubiquitous nuclear protein with numerous repeated elements representing a new kind of cell cycle-maintaining protein. J Cell Biol. 1993;123:513-522.

38. Zarkowska T, Mittnacht S. Differential phosphorylation of the retinoblastoma protein by G_1/S cyclin-dependent kinases. J Biol Chem. 1997;272: 12738-12746.
39. Juan G, Gruenwald S, Darzynkiewicz Z. Phosphorylation of retinoblastoma susceptibility gene protein assayed in individual lymphocytes during their mitogenic stimulation. Exp Cell Res. 1998; 239:104-110.
40. Weinberg RA. The retinoblastoma protein and cell cycle control. Cell. 1995;81:323-330.
41. Gore SD, Amin S, Weng LJ, Civin CI. Steel factor supports the cycling of isolated human CD34+ cells in the absence of other growth factors. Exp Hematol. 1995;23:413-421.
42. Ratajczak J, Majka M, Kijowski J, et al. Biological significance of MAPK, AKT and JAK-STAT protein activation by various erythropoietic factors in normal human early erythroid cells. Br J Haematol. 2001;115:195-204.
43. Lataillade J-J, Clay D, Bourin P, et al. Stromal cell-derived factor 1 regulates primitive hematopoiesis by suppressing apoptosis and by promoting G_0/G_1 transition in CD34+ cells: evidence for an autocrine/paracrine mechanism. Blood. 2002; 99:1117-1129.
44. Minamiguchi H, Kimura T, Urata Y, et al. Simultaneous signaling through c-mpl, c-kit and CXCR4 enhances the proliferation and differentiation of human megakaryocyte progenitors: possible roles of the PI3-K, PKC and MAPK pathways. Br J Haematol. 2001;115:175-185.
45. Birkenkamp KU, Esselink MT, Kruijer W, Vellenga E. An inhibitor of PI3-K differentially affects proliferation and IL-6 protein secretion in normal and leukemic myeloid cells depending on the stage of differentiation. Exp Hematol. 2000;28:1239-1249.
46. Carter BZ, Milella M, Altieri DC, Andreeff M. Cytokine-regulated expression of survivin in myeloid leukemia. Blood. 2001;97:2784-2790.
47. Huang Y, Park YC, Rich RL, Segal D, Myszka DG, Wu H. Structural basis of caspase inhibition by XIAP: differential roles of the linker versus the BIR domain. Cell. 2001;104:781-790.
48. Goyal L. Cell death inhibition: keeping caspases in check. Cell. 2001;104:805-808.
49. Granziero L, Ghia P, Circosta P, et al. Survivin is expressed on CD40 stimulation and interfaces proliferation and apoptosis in B-cell chronic lymphocytic leukemia. Blood. 2001;97:2777-2783.
50. Veis DJ, Sorenson CM, Shutter JR, Korsmeyer SJ. Bcl-2-deficient mice demonstrate fulminant lymphoid apoptosis, polycystic kidneys and hypopigmented hair. Cell. 1993;75:229-240.
51. Bonati A, Albertini R, Garau D, et al. BCL2 oncogene protein expression in human hematopoietic precursors during fetal life. Exp Hematol. 1996; 24:459-465.
52. Formby B, Wiley TS. Bcl-2, survivin and variant CD44 v7–v10 are downregulated and p53 is upregulated in breast cancer cells by progesterone: inhibition of cell growth and induction of apoptosis. Mol Cell Biochem. 1999;202:53-61.
53. Hoffman WH, Biade S, Zilfou JT, Chen J, Murphy M. Transcriptional repression of the anti-apoptotic survivin gene by wild type p53. J Biol Chem. 2002;277:3247-3257.
54. Adida C, Crotty PL, McGrath J, Berrebi D, Diebold J, Altieri DC. Developmentally regulated expression of the novel cancer anti-apoptosis gene survivin in human and mouse differentiation. Am J Pathol. 1998;152:43-49.
55. O'Connor DS, Schechner JS, Adida C, et al. Control of apoptosis during angiogenesis by survivin expression in endothelial cells. Am J Pathol. 2000;156:393-398.
56. Tran J, Rak J, Sheehan C, et al. Marked induction of the IAP family antiapoptotic proteins survivin and XIAP by VEGF in vascular endothelial cells. Biochem Biophys Res Commun. 1999;264:781-788.
57. Papapetropoulos A, Fulton D, Mahboubi K, et al. Angiopoietin-1 inhibits endothelial cell apoptosis via the Akt/survivin pathway. J Biol Chem. 2000; 275:9102-9105.
58. Buchkovich K, Duffy LA, Harlow E. The retinoblastoma protein is phosphorylated during specific phases of the cell cycle. Cell. 1989;58:1097-1105.
59. DeCaprio JA, Ludlow JW, Lynch D, et al. The product of the retinoblastoma susceptibility gene has properties of a cell cycle regulatory element. Cell. 1989;58:1085-1095.
60. Ludlow JW, Shon J, Pipas JM, Livingston DM, DeCaprio JA. The retinoblastoma susceptibility gene product undergoes cell cycle-dependent dephosphorylation and binding to and release from SV40 large T. Cell. 1990;60:387-396.

THE JOURNAL OF BIOLOGICAL CHEMISTRY
Vol. 272, No. 7, Issue of February 14, pp. 4335–4341, 1997
Printed in U.S.A.

Induction of $G\alpha_q$-specific Antisense RNA *in Vivo* Causes Increased Body Mass and Hyperadiposity*

(Received for publication, August 26, 1996, and in revised form, November 29, 1996)

Patricia A. Galvin-Parton‡, Xiaohui Chen‡, Christopher M. Moxham§, and Craig C. Malbon§¶

From the Departments of ‡Pediatrics and §Molecular Pharmacology, Diabetes and Metabolic Diseases Research Program, University Medical Center, SUNY/Stony Brook, Stony Brook, New York 11794-8651

Transgenic BDF-1 mice harboring an inducible, tissue-specific transgene for RNA antisense to $G\alpha_q$ provide a model in which to study a loss-of-function mutant of $G\alpha_q$ *in vivo*. $G\alpha_q$ deficiency induced in liver and white adipose tissue at birth produced increased body mass and hyperadiposity within 5 weeks of birth that persisted throughout adult life. $G\alpha_q$-deficient adipocytes display reduced lipolytic responses, shown to reflect a newly discovered, α_1-adrenergic regulation of lipolysis. This α_1-adrenergic response via phosphoinositide hydrolysis and activation of protein kinase C is lacking in the $G\alpha_q$ loss-of-function mutants *in vivo* and provides a basis for the increased fat accumulation.

Heterotrimeric G-proteins (G-proteins)[1] mediate transmembrane signaling from a populous group of cell-surface receptors to a lesser group of effector molecules that includes adenylyl cyclase, phospholipase C, and various ion channels (1). G-proteins have been shown to regulate complex biological processes, including cellular differentiation (2, 3), neonatal development (4–6), and oncogenesis (7). The expression of $G\alpha_o$, for example, is highly localized to the growth cones of developing neurites (2). Suppression of $G\alpha_o$ expression provokes the collapse of developing growth cones (8), whereas expression of constitutively active mutants of $G\alpha_o$ promote increased expression of neurites (9). In adipogenesis of 3T3 L1 embryonic fibroblasts, $G\alpha_s$ acts as a suppressor (2). Inducers of differentiation stimulate a sharp decline in $G\alpha_s$ levels, and constitutive expression of $G\alpha_s$ blocks induction of differentiation (2). $G\alpha_{i2}$ has been shown to regulate the progression of embryonic stem cells to primitive endoderm (4), acting via phospholipase C (PLC) and protein kinase C to suppress progression (10). The morphogen retinoic acid induces primitive endoderm by stimulating a sharp decline in $G\alpha_{i2}$ (4). Mimicking the decline with oligodeoxynucleotides antisense to $G\alpha_{i2}$ provokes progression in the *absence* of retinoic acid (4, 10). Study of G-proteins *in vivo* is a formidable task. The role of $G\alpha_{i2}$ *in vivo* has been studied through inducible, tissue-specific ablation by antisense RNA (5, 6) and gene inactivation by homologous recombination (11). Deficiency in $G\alpha_{i2}$ leads to a runted phenotype (5, 6, 11), insulin resistance (12), and for the transgenic mice with the inactivated $G\alpha_{i2}$ gene, ulcerative colitis and adenocarcinoma of the colon (11).

Little is known about the role of G-proteins of the G_q family *in vivo*. Two highly homologous members of the G_q subfamily of G-proteins, $G\alpha_q$ and $G\alpha_{11}$, can stimulate PLC and are insensitive to pertussis toxin (13–17). $G\alpha_{11}$ have been shown to mediate growth in fibroblasts in response to bradykinin and thrombin (18), hypertrophy in cultured neonatal ventricular myocytes (19), and transformation in NIH 3T3 cells (20). In the current work, we employ conditional, tissue-specific expression of RNA antisense to $G\alpha_q$ in transgenic mice to explore the role of this G-protein *in vivo* and more specifically in white adipocytes made deficient of $G\alpha_q$.

EXPERIMENTAL PROCEDURES

Reagents and Supplies—[^{3}H]cyclic AMP, [^{32}P]dCTP, [γ-^{32}P]ATP, [^{3}H]inositol 1,4,5-trisphosphate (IP_3), Gene Screen Plus, and anti-$G\alpha_{i3}$ antibodies (EC2) were purchased from Dupont NEN. All other reagents were purchased from Sigma or standard suppliers (5).

Mice—The B6D2F1 (BDF1) strain of mice was purchased from Taconic Farms Inc. and handled in accordance with the guidelines established by the Institutional Animal Care and Use Committee at the State University of New York at Stony Brook.

Experimental Design of the Antisense RNA Strategy—The pPCK-ASGα_q expression vector was constructed as described below using standard techniques. In order to insert the antisense sequence at the *Bgl*II site within the first exon of the phosphoenolpyruvate carboxykinase (PEPCK) gene, the 7.0-kb PEPCK gene was subcloned as a 1.0-kb *Eco*RI/*Hin*dIII and a 5.8-kb *Hin*dIII/*Bam*HI fragment into the vector pGEM7Zf(+) (Promega). The vector harboring the 1.0-kb gene fragment was digested with *Bgl*II, and the restriction ends were made flush using the Klenow fragment. The 39-bp antisense sequence was obtained within a 235-bp *Nhe*I/*Sst*I fragment excised from the vector pLNC-ASGα_{i2} (4). The restriction ends of this fragment were filled-in, ligated with the *Bgl*II-digested gene fragment, and used to transform XL-1 Blue strain of *Escherichia coli* (Stratagene) under selection with ampicillin. Plasmids with the 1.2-kb fragment and an insert oriented to produce antisense RNA were identified by direct DNA sequencing. The 1.2-kb fragment containing the antisense sequence was digested with *Sac*II and *Cla*I (sites present in the 235-bp sequence harboring the antisense sequence), and a 59-bp oligomer containing the sense sequence to $G\alpha_q$ (−33 to +3) flanked by restriction enzyme sites for *Bcl*I (5′) and *Sal*I (3′) was ligated via force cloning into the *Sac*II and *Cla*I sites. Insertion of the oligomer was confirmed by restriction digest analysis with *Bcl*I and *Sal*I. The presence of unique restriction sites within the 235-bp fragment facilitates the removal and insertion of different antisense sequences in a cassette-like fashion. The 1.2-kb fragment containing the antisense sequence was excised and ligated into the plasmid harboring the 5.8-kb gene fragment to produce the 7.0-kb pPCK-ASGα_q construct. In addition, the synthesis of primers complimentary to the flanking ends of the 235-bp insert allows for discrimination between the pPCK-ASGα_q RNA and the endogenous PEPCK RNA in subsequent reverse transcription-PCR amplification reactions (see below).

In choosing the antisense RNA target sequence, we had to consider

* This work was supported in part by American Cancer Society Award 9400504-DB (to C. C. M.) and a National Institutes of Health, NIDDK Fellowship T32 DK50721 (to C. M. M.). The costs of publication of this article were defrayed in part by the payment of page charges. This article must therefore be hereby marked "*advertisement*" in accordance with 18 U.S.C. Section 1734 solely to indicate this fact.

All authors contributed equally to work reported herein.

¶ To whom all correspondence should be addressed: Dept. of Molecular Pharmacology, DMDRP, University Medical Center, SUNY/Stony Brook, Stony Brook, NY 11794-8651; Tel.: 516-444-7873; Fax: 516-444-7696; E-mail: craig@pharm.som.sunysb.edu.

[1] The abbreviations used are: G-proteins, heterotrimeric G-proteins; PLC, phospholipase C; KRP buffer, Krebs-Ringer phosphate buffer; BSA, bovine serum albumin; PEPCK, phosphoenolpyruvate carboxykinase; IP_3, inositol 1,4,5-trisphosphate; DAG, 1,2-*sn*-diacylglycerol; PCR, polymerase chain reaction; CPT, chlorophenylthio; bp, base pair(s); kb, kilobase pair(s).

Exhibit E

the large degree of nucleotide identity among the G-protein α-subunits within their respective open reading frame regions. This prompted us to look for unique target sequences within the 5'- and 3'-untranslated regions of the $G\alpha_q$ mRNA. The 36 nucleotides immediately upstream of and including the translation initiation codon were chosen to serve as the antisense target sequence. This 39-base pair sequence (5'-CGCGC-CGGCGGGGCTGCAGCGAGGCACTTCGGAAGAATG-3') did not show any significant homology with sequences present in the GenBank™ data base, including $G\alpha_{11}$ (33% homology) and $G\alpha_{14}$ (27% homology).

Cell Culture and Transfection—FTO-2B cells were cultured in a 5% CO_2, 95% O_2 chamber and maintained in Ham's F-12/Dulbecco's modified Eagle's medium (1:1) supplemented with 10% fetal bovine serum. Cells were cotransfected with a plasmid that would allow for neomycin selection of positive transfectant clones. The control vector or pPCK-ASGα_q construct was added in 5-fold excess relative to the plasmid containing the selectable marker. Transfection was carried out using the Lipofectin reagent (Life Technologies, Inc.) according to the manufacturer's protocol.

Detection of Antisense RNA Expression—Total RNA was extracted as described previously (4). One microgram of total RNA was reverse transcribed using a pPCK-ASGa_q-specific downstream primer and then PCR-amplified in the presence of both the upstream and downstream primer set according to the manufacturer's protocol (Perkin-Elmer). The sequences for the upstream and downstream primers were dCGTTTAGTGAACCGTCAGA and dAGGTGGGGTCTTTCATTCCC, respectively.

Production of Transgenic Mice—Transgenic lines of mice were produced at the Transgenic Mouse Facility at SUNY Stony Brook using standard techniques (5, 6). Briefly the pPCK-ASGα_q construct was excised free of vector sequences and purified prior to microinjection into single-cell preimplantation embryos. Microinjected embryos were then transferred to pseudopregnant females. Offspring carrying the transgene were identified by PCR amplification and subsequent Southern analysis using a pPCK-ASGα_q-specific probe uniformly labeled with [^{32}P]dCTP (5). Five separate founder lines were identified by Southern analysis and bred over 10 generations (5).

White Adipocyte Isolation—White adipocytes were isolated from epididymal and parametrial fat pads by collagenase digestion, as described previously (5). Briefly, 0.5–1.0 g of adipose tissue was excised from male and female mice, weighed, and added to an equal volume of Krebs-Ringer phosphate buffer (KRP) containing 3% bovine serum albumin (KRP/BSA), prewarmed to 37 °C. The tissue was digested for 1 h using collagenase (1 mg/ml) at 37 °C in an orbital, shaking water bath. The isolated adipocytes were washed twice with the KRP/BSA buffer and then resuspended to a final volume to achieve 62.5 mg of wet weight of packed adipocytes/ml in the same buffer. The KRP/BSA buffer was supplemented with adenosine deaminase at a concentration of 0.5 unit/ml.

Cyclic AMP Accumulation and Lipolysis—Briefly, collagenase-digested white fat cells from epididymal and epoophoronal pads were incubated at 37 °C in KRP buffer supplemented with 3% bovine serum albumin and adenosine deaminase (0.5 unit/ml) for 30 min in the absence or presence of the drugs indicated. For lipolysis determinations, the assays were terminated with 0.65 N $HClO_4$. Samples were deproteinized and neutralized with KOH/KCl/imidazole (2.6/0.52/0.52 M, respectively) and the glycerol content determined by measuring the reduction of NAD^+ to NADH in a coupled assay. NADH production was assayed using a microplate fluorometer set to an excitation wavelength of 360 nm and an emission wavelength detection of 460 nm. The mass of glycerol per sample was extrapolated from a standard curve of stock glycerol. Cyclic AMP accumulation was measured using a competitive binding assay. Briefly, 80 μl of fat cells (~5 mg/tube) were treated with various agents for 6 min at 37 °C. The reaction was stopped by the addition of HCl (0.1 N final) and boiling for 1 min. The samples were neutralized with NaOH and assayed for cyclic AMP content. Cyclic AMP accumulation was measured in adipocytes stimulated with either phenylephrine, epinephrine, norepinephrine, or isoproterenol The data are expressed as the mean values in picomoles of cyclic AMP (±S.E.) per million cells from three independent trials, each performed in triplicate.

IP_3 and 1,2-sn-Diacyglycerol (DAG) Accumulation—Cells were incubated with the indicated agents and the IP_3 measured as described previously (21). DAG was determined using the DAG kinase assay (10). The data are expressed as the mean values in nanomoles (±S.E.) per million cells from three independent trials, each performed in triplicate.

G-protein Immunoblot Analysis—Membrane fractions were prepared from rat hepatoma FTO-2B cells, as described previously (5). Cell membranes were prepared from adipose tissue of transgenic mice and their control littermates (5). Aliquots of cell membrane were subjected to SDS-polyacrylamide (10% acrylamide) gel electrophoresis, and the separated proteins were transferred to nitrocellulose blots. The blots of the membrane proteins were probed with anti-peptide antibodies specific for $G\alpha_q$ (antibodies E973 and E976), $G\alpha_{i2}$ (antibody CM112), $G\alpha_s$ (antibody CM129), $G\beta_2$ (antibody CM162), $G\alpha_{11}$ (antibody E976), or $G\alpha_{i3}$ (antibody EC2), and the immune complexes were made visible by staining with a calf alkaline phosphatase-conjugated, goat anti-rabbit IgG second antibody (4, 5). The "CM" antibodies were prepared by our laboratory (4, 5).

RESULTS AND DISCUSSION

Defining the role of a specific G-protein subunit, like $G\alpha_q$, *in vivo* is a formidable task. We adopted the strategy of conditional, antisense RNA to ablate $G\alpha_q$ *in vivo* in a tissue-specific manner, creating loss-of-function mutants in adipose and liver, prominent sites of $G\alpha_q$ expression. The degree of nucleotide identity among the G-protein α-subunits within the open reading frames dictated selection of the 5'-untranslated region immediately upstream and including the ATG initiator codon (−33 to +3) as the antisense RNA sequence targeting Ga_q (Fig. 1). This region is unique with respect to sequences with the GenBank™ data base and does not share significant homology with other G-protein α-subunits (Fig. 1*A*), including other members of the G_q family, $G\alpha_{11}$ (33% homology with respect to $G\alpha_q$) and $G\alpha_{14}$ (27% homology with respect to $G\alpha_q$). A double-stranded oligodeoxynucleotide fragment antisense to $G\alpha_q$ was inserted into *Bcl*I and *Sal*I sites of the pPCK-AS vector (Fig. 1*B*), an inducible expression vector driven by the promoter of the PEPCK gene (5, 6). Screening of FTO-2B hepatoma cells stably transfected with pPCK-ASGα_q was performed from day 0 to day 12 following induction of the promoter with the chlorophenylthio analogue of cyclic AMP (CPT-cyclic AMP, 25 μM). Immunoblots reveal that levels of $G\alpha_{i2}$, $G\alpha_s$, and $G\beta_2$ were unaffected by induction of pPCK-ASGα_q, while staining with an antibody to $G\alpha_q$ displayed a 54% loss by day 6, and 86% loss of $G\alpha_q$ by day 9 following induction (Fig. 1*C*). By day 12 of the induction with CPT-cyclic AMP, $G\alpha_q$ was not detectable in the immunoblots of FTO-2B cell membranes. Induction of the pPCK-SGα_q vector, harboring the sense as compared to antisense sequence for $G\alpha_q$, resulted in a null phenotype, *i.e.* $G\alpha_q$ expression was normal. $G\alpha_q$ activates PLC-β in the liver (12–16) and suppression of $G\alpha_q$ in FTO-2B hepatoma cells reduced basal PLC activity from 2.7 ± 0.6 to 1.0 ± 0.3 ($p \leq 0.05$ for difference) and abolished PLC stimulation in response to either 10 nM angiotensin II (0.9 ± 0.3) or 10 μM norepinephrine (0.95 ± 0.2), as determined by mass assay of intracellular IP_3 accumulation at 30 s following hormonal stimulation ($n = 5$, pmol of IP_3 accumulation/μg of cellular protein).

The pPCK-ASGα_q construct was excised as a 7.0-kb *Eco*RI-*Bam*HI fragment, microinjected into single cell, preimplantation embryos, and the microinjected embryos were transferred into pseudopregnant recipients. BDF1 mice harboring the transgene were identified by PCR of tail DNA. Five independent founders were identified from two rounds of microinjection and implantation. Five separate founder lines have been propagated for more than 10 generations. Immunoblots of crude membranes from fat, liver, brain, and lung subjected to SDS-PAGE and stained with a $G\alpha_q$-specific antiserum reveal the near absence of $G\alpha_q$ in the tissues, fat and liver, targeted by the transgene (Fig. 1*D*). Immunoblots of brain and lung, tissues not targeted by the PEPCK vector, displayed normal levels of $G\alpha_q$ (Fig. 1*E*). Expression of $G\alpha_{i2}$, $G\beta_2$, and $G\alpha_{11}$ (not shown) were not significantly altered in the transgenic mice.

Necropsy and histology of the transgenic mice were performed. Prominent was the increase in body weight observed in the mice harboring the pPCK-ASGα_q transgene (Fig. 2*A*). By 5 weeks of age, the transgenic mice were >135% of the body weight of their control littermates, for both male and female

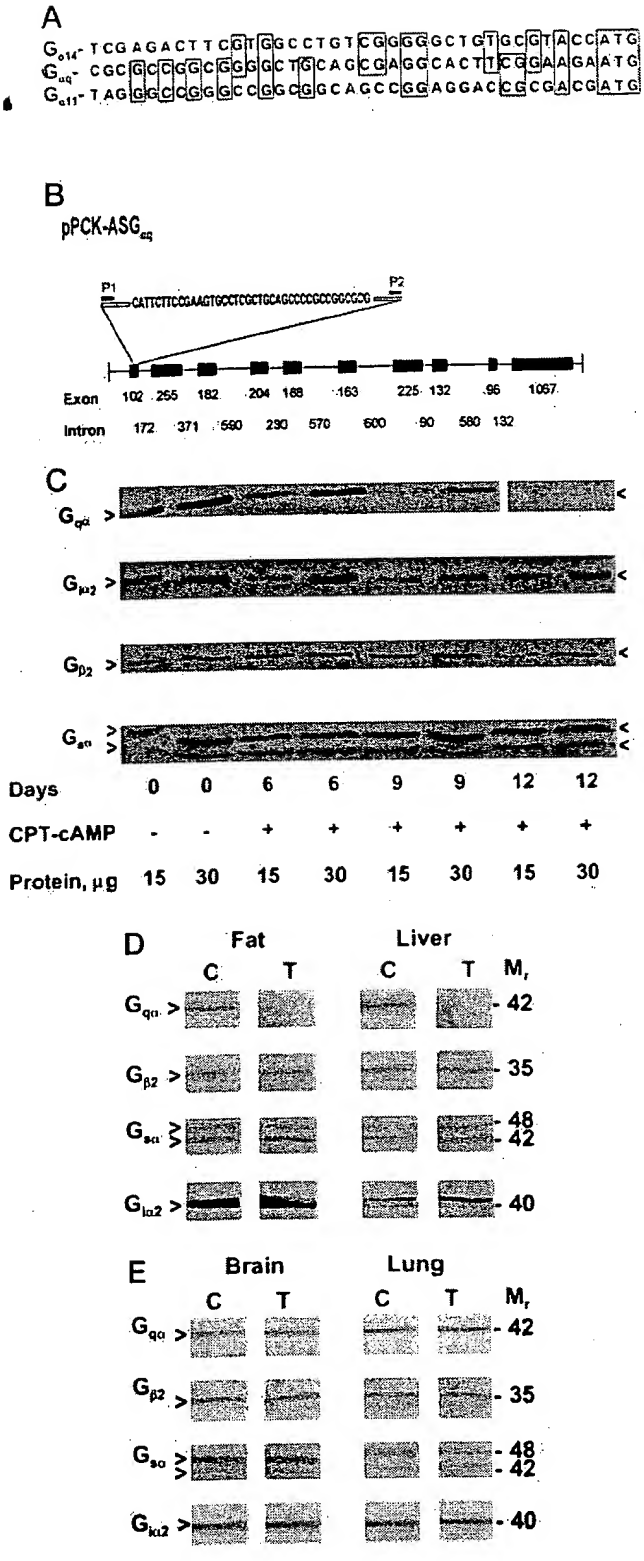

FIG. 1. $G\alpha_q$ expression is suppressed in hepatoma cell stably transfected with pPCK-ASGα_q and in mice harboring the pPCK-ASGα_q transgene. Comparison of the 5′-untranslated region from $G\alpha_q$ (nucleotides −33 to +3) with $G\alpha_{14}$ and $G\alpha_{11}$, additional members of the G_q family (*panel A*). The pPCK-ASGα_q construct for inducible expression of RNA antisense to $G\alpha_q$ (*panel B*). The 36-nucleotide sequence upstream of and including the translation initiation codon was inserted into the first exon of the rat phosphoenolpyruvate carboxykinase gene (*PCK*) to provide a 2.8-kb hybrid pPCK-ASGα_q antisense RNA, driven by a promoter which is silent *in utero* and activated at birth. Crude membranes (0.2 mg of protein/SDS-polyacrylamide gel electrophoresis lane) were prepared from rat hepatoma FTO-2B cells that were stably transfected with the pPCK-ASGα_q construct and induced with CPT-cyclic AMP for 0, 6, 9, and 12 days, subjected to SDS-polyacrylamide gel electrophoresis, transferred to nitrocellulose blots, and probed with rabbit polyclonal antisera specific for the G-protein subunits indicated (5, 6). Immunecomplexes were made visible with goat anti-rabbit IgG coupled to calf alkaline phosphatase and colorimetric development (*panel C*). Crude membranes were prepared from epididymal and epoophoronal white fat and liver (*panel D*) and brain and lung (*panel E*) tissues obtained from 24-week-old control (*C*) and transgenic (*T*) mice. Samples (15 µg of protein/lane) were subjected to SDS-polyacrylamide gel electrophoresis on a mini-gel apparatus and transferred to nitrocellulose for immunoblot analysis of various G-protein subunits, as described earlier (5, 6). For immunoblotting, the sample loading was limited to 15 µg/lane, within the range established for linearity between sample loading and quantification of immunostaining (not shown). Quantification of the blots revealed no significant change in the G-protein subunits tested between control and transgenic mouse tissues, with the exception of the loss of $G\alpha_q$ in liver and fat tissues. Expression of $G\alpha_s$ was normal in liver and fat, although reduced (<15%) occasionally in fat, but not liver, of some transgenic mice (not shown). Scanning densitometry values for immunoblots of fat tissue from control and transgenic mice, respectively, were as follows: $G\alpha_q$, 0.26, 0.01; $G\alpha_s$, 0.92, 0.88; $G\beta$, 0.31, 0.33; and $G\alpha_{i2}$, 0.72, 0.75 arbitrary OD units. Scanning densitometry values for immunoblots of liver tissue from control and transgenic mice, respectively, were as follows: $G\alpha_q$, 0.51; 0.02; $G\alpha_s$, 0.68, 0.64; $G\beta$, 0.27, 0.25; and $G\alpha_{i2}$, 0.22, 0.25 arbitrary OD units. Scanning densitometry of immunoblots from brain and lung revealed no significant differences in the values obtained with tissues from transgenic as compared to control mice (not shown). The antibodies employed for staining of immunoblots for specific G-proteins subunits were as follows: E973 for $G\alpha_q$; CM112 for $G\alpha_{i2}$; CM129 for $G\alpha_s$; E976 for $G\alpha_{11}$; and CM162 for $G\beta_2$.

mice alike (Fig. 2*B*). Progeny of the five founder lines harboring the transgene all display the increased body weight (not shown). The fat mass at 4 weeks after birth increased by 50% in the transgenic mice (Fig. 2*C*). At 8 weeks of age, the white epididymal and epoophoronal fat mass of the transgenic mice was 1.75-fold greater than that of the control mice. Segregated by gender for males, white fat mass (mg) was 215 ± 5 and 333 ± 8 ($n = 5, p \leq 0.05$) for 12-week-old control and transgenic mice, respectively. For females, white fat mass was 160 ± 10 mg and 303 ± 8 mg ($n = 6, p \leq 0.05$) for 12-week-old control and transgenic mice, respectively. By 24 weeks, the transgenic mice displayed a 1.4-fold increase in fat mass, and the percentage of whole body weight as fat mass was 2.3 ± 0.2 as compared to 1.1 ± 0.3 ($n = 6$) for control mice (Fig. 2*C*). Total body protein and nasal-anal length were unaffected by the presence of the transgene over this same range in age (not shown). Equally notable was the dramatic increase in adiposity, *i.e.* fat cell number, that occurred in the transgenic mice lacking $G\alpha_q$ expression in adipose tissue (Fig. 2*D*).

To assess the effects of $G\alpha_q$ deficiency on cell signaling, we investigated the adipocytes isolated from transgenic mice and their control littermates. PLC-β signaling by loss-of-function $G\alpha_q$-deficient white adipocytes was virtually abolished, *i.e.* IP_3 and DAG accumulation in response to norepinephrine, vasopressin, phenylephrine, or bradykinin (all hormones that activate PLC) was markedly attenuated (Fig. 3, *A* and *B*, respectively). Suppression of $G\alpha_q$ in adipocytes of the pPCK-ASGα_q mice and the stably transfected hepatoma cells abolished PLC activation by a variety of hormones (Figs. 1 and 3). This loss of signaling in $G\alpha_q$ deficiency occurs, although expression of the $G\alpha_{11}$ subunit was found to be normal (not shown). Both $G\alpha_q$ and $G\alpha_{11}$ are expressed in a number of tissues (12–14), including fat and liver. The observations from the present study suggest that $G\alpha_q$ and $G\alpha_{11}$ may not be redundant with respect to PLC activation *in vivo*.

Since PLC activation and accumulation of either IP_3 or DAG have not been implicated in controlling lipolysis, the pharmacology of the lipolytic response observed in the $G\alpha_q$-deficient adipocytes came as a great surprise (Fig. 3*C*). The lipolytic response to a mixed α- and β-adrenergic agonist norepineph-

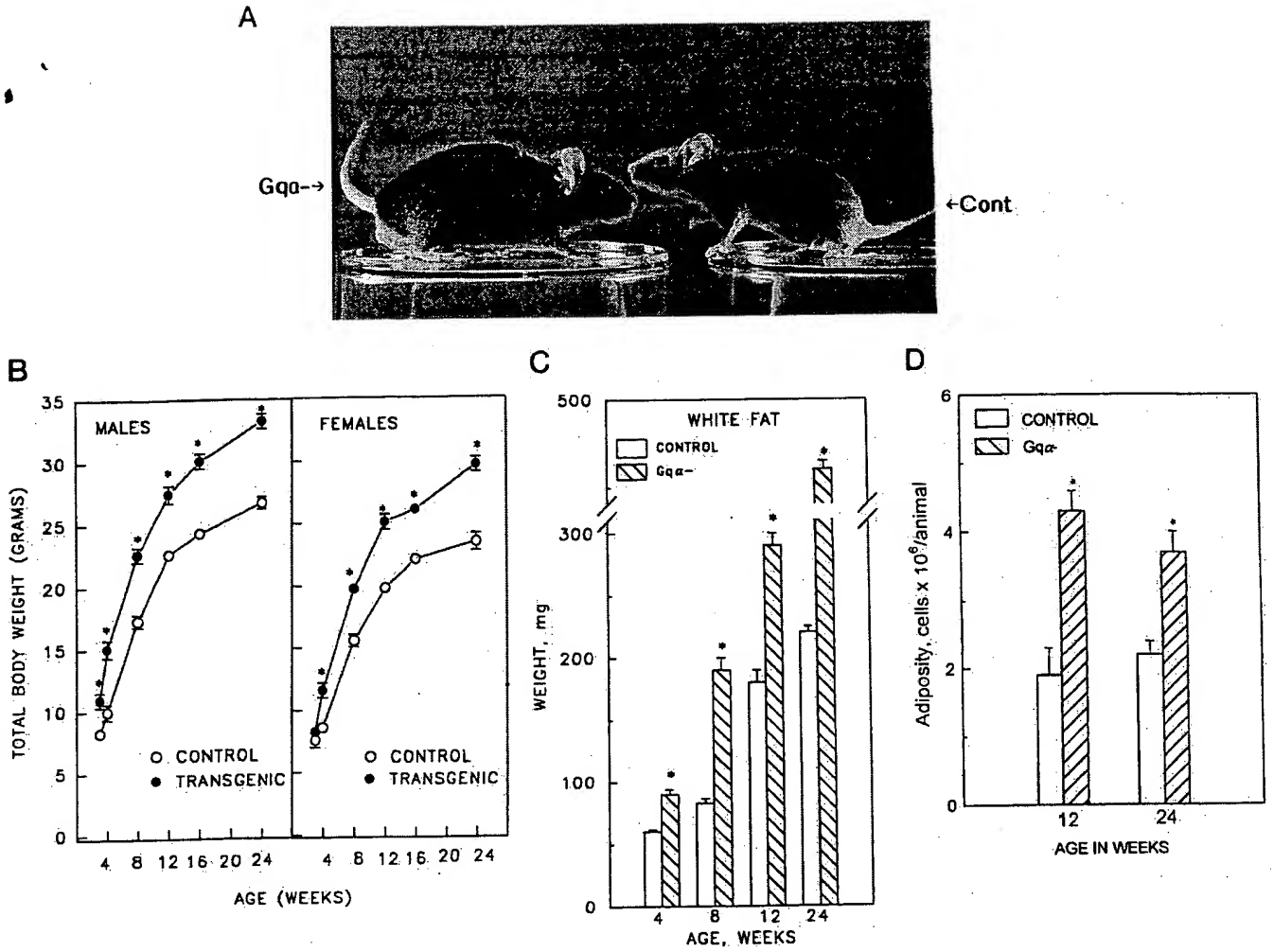

FIG. 2. **Suppression of $G\alpha_q$ expression by RNA antisense to $G\alpha_q$ causes increased body weight and fat mass.** The pPCK-ASGα_q transgenic mice have increased body weight (*panels A* and *B*), increased white fat mass (*panel C*), and increased adiposity (*panel D*). Five founders and the progeny of each of the founder lines for 10 generations were maintained and propagated by independent outbreeding to BDF1 control mice. The five founders and all members of their lineages at each generation display this phenotype (see Table I). In all cases, the data displayed were obtained from members of at least three of the five founder lines. Transgenic mice and their littermate controls were analyzed at ages spanning 3–24 weeks. The data are expressed as the mean values ± S.E. from at least six animals for each age group, transgenic and control alike. Fecundity and litter size were no different in the transgenic as compared to control mice. Mice shown in *panel A* were 12-week-old males, *left-hand panel*, transgenic mouse and *right-hand panel*, control mouse. *Panel B*, the body weight of pPCK-ASGα_q transgenic mice and their control littermates, segregated by sex. *Panel C*, the fat pad mass of pPCK-ASGα_q transgenic mice and their control littermates, pooled from male and female mice at the ages indicated for the sake of simplicity. Pair-feeding of the animals did not diminish the obese character of the transgenic mice. Nose-to-anus dimensions were not altered in the transgenic as compared to control mice. Adiposity was measured by determining the total white fat cell number from collagenase-digested, isolated epididymal and epoophoronal fat pads of single transgenic mice and paired, littermate controls, by cell counting using a hemocytometer. Throughout this work, statistical analysis was performed using the Student's *t* test. An *asterisk* denotes statistical significance with $p \leq 0.05$ for the difference between the mean values for transgenic ($G\alpha_q$-deficient) as compared to control mice.

rine was blunted in the $G\alpha_q$-deficient adipocytes. Lipolysis in response to the β-adrenergic agonist isoprenaline was impaired, whereas the response to the α_1-adrenergic agonist phenylephrine was abolished in the loss-of-function mutant cells. These results were unexpected, since neither a direct role of $G\alpha_q$ in activating adenylyl cyclase nor the existence of a prominent α_1-adrenergic stimulation of lipolysis have been reported. Analysis of cyclic AMP accumulation provided direct proof linking loss of $G\alpha_q$ to impaired lipolysis in response to β-adrenergic stimulation (acting via adenylyl cyclase) as well as to α_1-adrenergic stimulation (acting via PLC). Forskolin (10 μM)-stimulated cyclic AMP accumulation, in contrast, was actually elevated in the $G\alpha_q$-deficient as compared to control adipocytes (125 ± 15 and 160 ± 5 pmol/10^6 cells, respectively). Forskolin (10 μM)-stimulated lipolysis was equivalent in transgenic and control mice (14.1 ± 2.9 and 13.9 ± 0.8 μmol of glycerol release/10^6 cells, respectively), as were the abundance of β-adrenergic receptors (140 ± 4 and 133 ± 9 fmol/mg of protein, respectively) in crude adipocyte membranes and the amounts of cyclic AMP phosphodiesterase activity (1.33 ± 0.02 and 1.32 ± 0.09 pmol/min/mg of protein, respectively) in extracts of whole fat pads.

In the $G\alpha_q$-deficient cells, the impaired lipolytic response stimulated by norepinephrine was sensitive to the strict β-adrenergic antagonist propranolol, reflecting a residual β-adrenergic, cyclic AMP-mediated response (Fig. 4*A*). Adipocytes from control mice display sensitivity to both propranolol and the α_1-adrenergic antagonist prazosin. The former reflects the β-adrenergic response acting via cyclic AMP, while the latter reflects this newly discovered α_1-adrenergic response first detected through its loss in the $G\alpha_q$-deficient cells. Vasopressin (1 μM), which activates PLC, also stimulated lipolysis in adipocytes from control mice 1.8-fold over basal. The α_1-adrenergic stimulation of lipolysis was abolished by prazosin, but not by

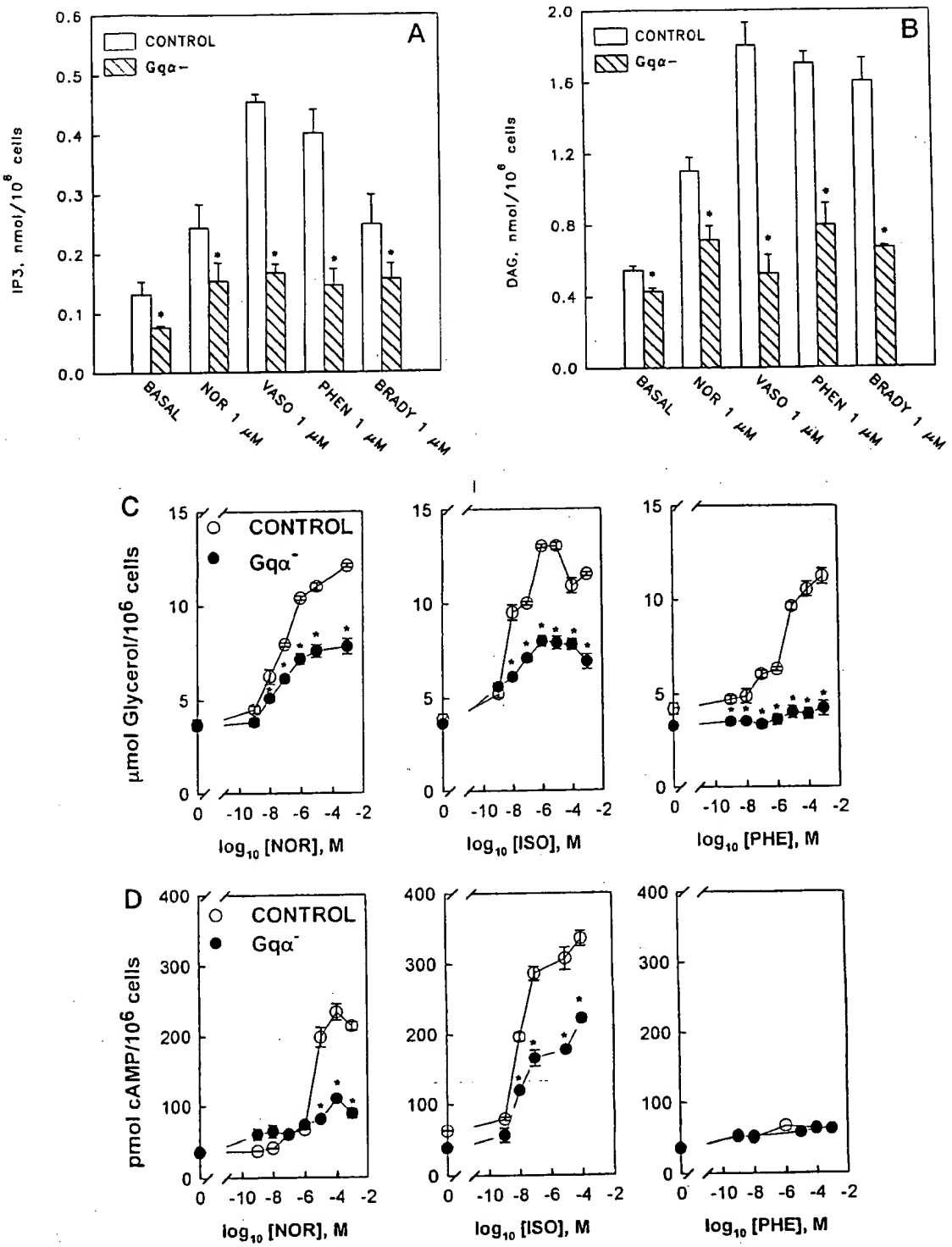

FIG. 3. **Adipocytes from pPCK-ASGα_q transgenic mice display loss-of-function with respect to activation of PLC and α_1-adrenergic regulation of lipolysis.** White adipocytes were isolated from epididymal and epoophoronal fat of transgenic mice and control littermates by collagenase digestion. Accumulation of IP_3 (*panel A*) and DAG (*panel B*) at 30 s following stimulation by 1 μM agonist (*NOR*, norepinephrine; *VASO*, vasopressin; *PHEN*, phenylephrine; *BRADY*, bradykinin) were measured in cells from mice 18–24 weeks of age. Intracellular IP_3 accumulation was measured by the mass assay employing the rabbit cerebellar IP_3-binding protein. DAG was assayed using a DAG kinase assay followed by thin-layer chromatographic separation of radiolabeled phosphate generated by the reaction. The DAG mass was calculated from a standard curve using authentic DAG. Lipolysis (*panel C*) and cyclic AMP accumulation (*panel D*) were measured in cells isolated from transgenic and control mice. The cells were challenged with varying concentrations of the mixed α- and β-adrenergic agonist norepinephrine (*NOR*), the β-adrenergic agonist isoprenaline (*ISO*), or the α-adrenergic agonist phenylephrine (*PHEN*) for 15 min (cyclic AMP accumulation) or 60 min (lipolysis via glycerol release). For cyclic AMP determinations, the assays were terminated at 15 min, and the accumulation of intracellular cyclic AMP measured using a competitive binding assay with bovine adrenal cyclic AMP binding protein. The data presented are mean values ± S.E. from at least three separate experiments, each performed on separate occasions. An *asterisk* denotes statistical significance with $p \leq 0.05$ for the difference between the mean values for transgenic ($G\alpha_q$-deficient) as compared to control mice.

propranolol (Fig. 4*B*). The loss-of-function $G\alpha_q$-deficient cells, in contrast, have essentially lost the lipolytic response to phenylephrine stimulation.

Although $G\alpha_q$ is not known to regulate adenylyl cyclase directly, the loss-of-function $G\alpha_q$ mutants displayed impaired β-adrenergic stimulation of cyclic AMP accumulation and lipol-

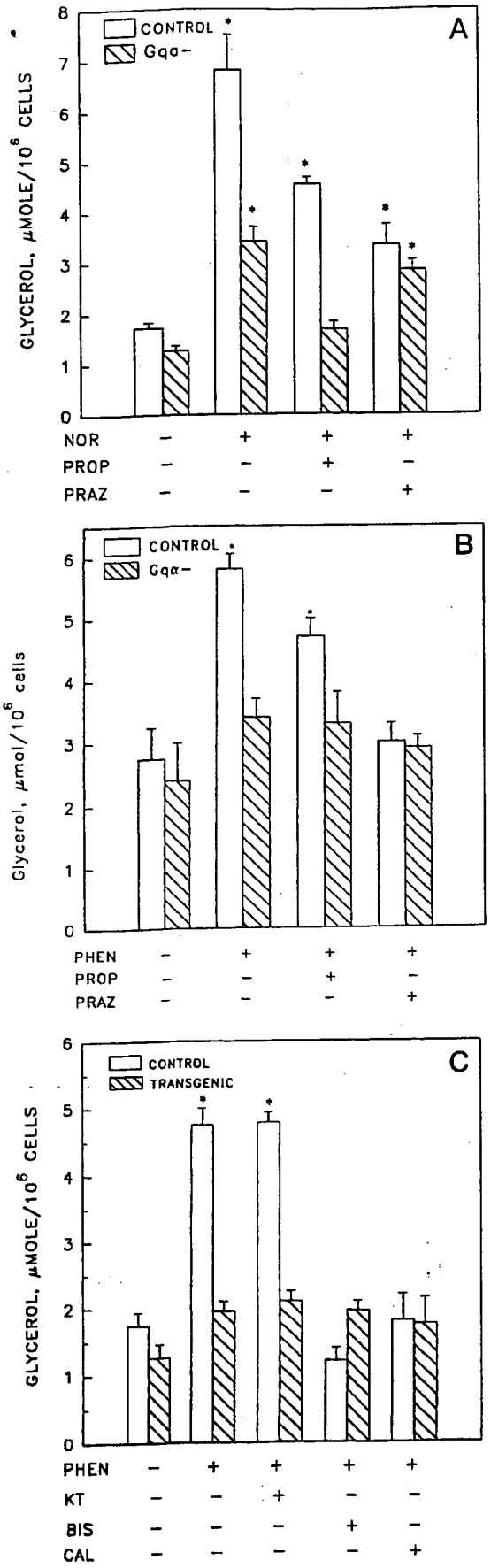

FIG. 4. **The pharmacology of the adrenergic lipolytic response reveals the existence of an α_1-adrenergic stimulatory pathway, absent in the $G\alpha_q$-deficient loss-of-function mutants.** White adipocytes were isolated from transgenic mice and their control littermates for study of the lipolytic response to adrenergic agonists. The lipolytic response was measured as described in the legend to Fig. 3. Stimulation of lipolysis by either 10 μM norepinephrine (*NOR, panel A*) or 10 μM phenylephrine (*PHEN, panels B* and *C*) was analyzed in the absence and presence of either the β-adrenergic antagonist propranolol (*PROP*, 10 μM) or the α_1-adrenergic antagonist prazosin (*PRAZ*, 1 μM). Inhibitors of protein kinase A (*KT*, KT5702, 1 μM) and protein kinase C (*BIS*, bis-indolylmaleimide, 1 μM; *CAL*, calphostin C, 100 nM) were examined for their ability to block the α_1-adrenergic stimulation of lipolysis in adipocytes from transgenic mice and their control littermates (*panel C*). The results are mean values ± S.E. from three to five separate experiments for each. An *asterisk* denotes statistical significance with $p \leq 0.05$ for the differences from mean basal values obtained with adipocytes isolated from both transgenic ($G\alpha_q$-deficient) and control mice.

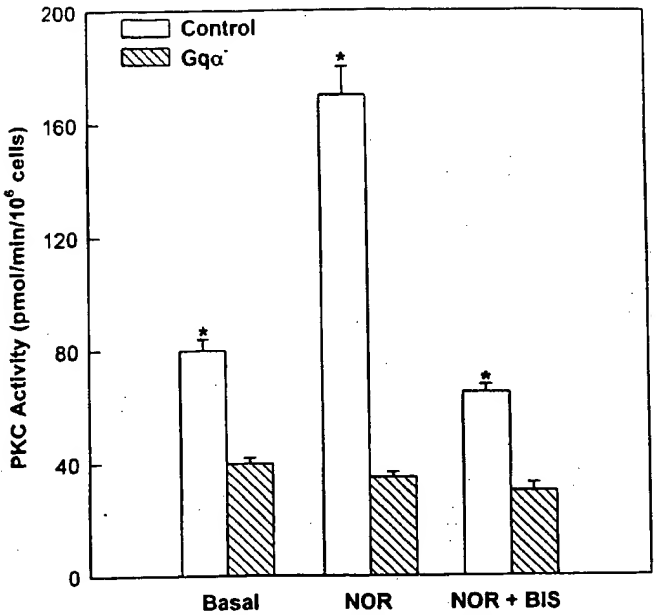

FIG. 5. **Adipocytes from pPCK-ASGα_q transgenic mice display loss of function with respect to activation of protein kinase C following challenge with norepinephrine.** White adipocytes were isolated from epididymal and epoophoronal fat of transgenic mice and control littermates by collagenase digestion. The activity of protein kinase C was measured in cells from mice 18–24 weeks of age. The cells were challenged for 5 min without (*Basal*) and with 10 μM of the mixed α- and β-adrenergic agonist norepinephrine (*NOR*), in the absence or presence of 0.1 mM bis-indolylmaleimide (*NOR + BIS*), a potent protein kinase inhibitor. Protein kinase C activity was measured in DEAE-cellulose-purified cell homogenates, as described elsewhere (30). The data presented are mean values ± S.E. from at least three separate experiments, each performed on separate occasions. An *asterisk* denotes statistical significance with $p \leq 0.05$ for the difference between the mean values for transgenic ($G\alpha_q$-deficient) as compared to control mice.

ysis. $G\alpha_q$, acting via PLC to promote IP_3 and DAG accumulation, may augment the cyclic AMP response indirectly, perhaps via effects on calcium- or protein kinase C-sensitive forms of adenylyl cyclase (22–25). We tested the role of protein kinase C using bis-indolylmaleimide and calphostin C, selective inhibitors of protein kinase C (Fig. 4*C*). Both calphostin C (100 nM) and bis-indolylmaleimide (1 μM) abolished the α_1-adrenergic stimulation of lipolysis, whereas the protein kinase A inhibitor KT-5720 (1 μM) was without effect. At 100 nM, bis-indolylmaleimide effectively blocked phenylephrine (10 μM)-stimulated lipolysis in adipocytes from control mice; glycerol release (μmol/10^6 cells), in response to this α_1-adrenergic agonist, declined from 4.7 to 1.2 in the absence *versus* presence of this protein kinase C inhibitor. The K_I for nonselective inhibition of protein kinase A by bis-indolylmaleimide is >2 μM (26). Since the protein kinase A inhibitor KT-5720 itself was without effect, nonselective effects of protein kinase C inhibitors, if they indeed occurred at these lower concentrations, would be irrelevant.

Measurement of protein kinase C activity in DEAE-cellulose-purified homogenates of cells challenged with and without norepinephrine was performed using adipocytes from the control and transgenic mice (Fig. 5). In adipocytes from control mice, norepinephrine stimulates protein kinase C activity, an action blocked by the addition of bis-indolylmaleimide. Suppression of $G\alpha_q$ in adipocytes of the pPCK-ASGα_q mice results in a frank reduction in protein kinase C activity in the basal state and a loss of norepinephrine-induced activation of protein kinase C. Total protein kinase activities for adipocytes from control and transgenic mice are equivalent, 310 ± 20 and 315 ± 18 pmol/min/million cells, respectively. Thus, α_1-adrenergic control of lipolysis is shown to be mediated via protein kinase C, a pathway revealed by its absence in the $G\alpha_q$-deficient state.

The absence of $G\alpha_q$ resulted in increased fat accumulation and hyperadiposity, observed within 5 weeks of age and sustained through adult life. Obesity has been reported in transgenic mice after genetic ablation of brown adipose tissue (27), supporting the role of this specialized tissue in preventing obesity (28). The pPCK-ASGα_q transgene was not expressed in brown adipose tissue (not shown). Expression of $G\alpha_q$, the uncoupling protein UCP, and the mRNAs for both were equivalent in brown adipose tissue from transgenic and control mice (not shown), suggesting no involvement of brown adipose tissue in enhanced fat accumulation by the pPCK-ASGα_q-expressing mice.

The absence of $G\alpha_q$ abolished an important stimulatory control of lipolysis, apparently predisposing the mice to accumulation of fat. Recently, G-proteins have been shown to play prominent roles in differentiation (2, 3) and neonatal growth (4–6). For progression of F9 teratocarcinoma cells to primitive endoderm (4) and for development of nerve growth cones (3), G-proteins appear to be acting directly or indirectly via protein kinase C (10, 29). In the present study we demonstrate the key role of PLC and protein kinase C in adipocyte signaling in the mature cells. The basis for the hyperadiposity in the cells deficient in $G\alpha_q$, however, remains to be established, but may reflect a critical role of $G\alpha_q$ in controlling adipogenic conversion *in vivo*.

Acknowledgments—We thank Dr. John H. Exton (HHMI, Vanderbilt University, Nashville, TN) for the generous gift of antibodies E973 and E976. We thank Dr. Jean Himms-Hagen (University of Ottawa, Ontario, Canada) for the generous gift of antibodies to UCP.

REFERENCES

1. Gilman, A. G. (1987) *Annu. Rev. Biochem.* **56**, 615–649
2. Wang, H.-y, Watkins, D. C., and Malbon, C. C. (1992) *Nature* **358**, 334–337
3. Strittmatter, S. M., Valenzuela, D., Kennedy, T. E., Neer, E. J., and Fishman, M. C. (1993) *Science* **259**, 77–79
4. Watkins, D. C., Johnson, G. L., and Malbon, C. C. (1992) *Science* **258**, 1373–1375
5. Moxham, C. M., Hod, Y., and Malbon, C. C. (1993) *Science* **260**, 991–995
6. Moxham, C. M., Hod, Y., and Malbon, C. C. (1993) *Dev. Genet.* **14**, 266–273
7. Bourne, H. R., Sanders, D. A., and McCormick, F. (1990) *Nature* **348**, 125–132
8. Igarashi, M., Strittmatter, S. M., Vartanian, T., and Fishman, M. C. (1993) *Science* **259**, 77–79
9. Strittmatter, S. M., Fishman, M. C., and Zhu, X. P. (1994) *J. Neurosci.* **14**, 2327–2338
10. Gao, P., and Malbon, C. C. (1996) *J. Biol. Chem.* **271**, 9002–9008
11. Rudolph, U., Finegold, M. J., Rich, S. S., Harriman, G. R., Srinivasan, Y., Brabet, P., Boulay, G., Bradley, A., and Birnbaumer, L. (1995) *Nat. Genet.* **10**, 143–150
12. Moxham, C. M., and Malbon, C. C. (1996) *Nature* **379**, 840–845
13. Taylor, S. J., Smith, J. A., and Exton, J. H. (1990) *J. Biol. Chem.* **265**, 17150–17156
14. Taylor, S. J. Choe, H. Z., Rhee, S. G., and Exton, J. H. (1991) *Nature* **350**, 516–518
15. Smrcka, A. V., Hepler, J. R., Brown, K. O., and Sternweis, P. C. (1991) *Science* **251**, 804–807
16. Waldo, G. L., Boyer, J. L., Morris, A. J., and Harden, T. K. (1991) *J. Biol. Chem.* **266**, 14217–14225
17. Hepler, J. R., Kozasa, T., Smrcka, A. V., Simon, M. I., Rhee, S. G., Sternweis, P. C., and Gilman, A. G. (1993) *J. Biol. Chem.* **268**, 14367–14375
18. LaMorte, V. J., Harootunian, A. T., Spiegel, A. M., Tsien, R. Y., and Feramisco, J. R. (1993) *J. Cell. Biol.* **121**, 91–99
19. Chien, K. R., Knowlton, K. U., Zhu, H., and Chien, S. (1991) *FASEB J.* **5**, 3037–3046
20. Kalinec, G., Nazarali, A. J., Hermouet, S., Xu, N., and Gutkind, J. S. (1992) *Mol. Cell. Biol.* **12**, 4687–4693
21. Watkins, D. C., Moxham, C. M., Morris, A. J., and Malbon, C. C. (1994) *Biochem. J.* **299**, 593–596
22. De Vivo, M., Chen, J., Codina, J., and Iyengar, R. (1992) *J. Biol. Chem.* **267**, 18263–18266
23. Kawabe, J., Iwami, G., Ebina, T., Ohno, S., Katada, T., Ueda, Y., Homcy, C. J., and Ishikawa, Y. (1994) *J. Biol. Chem.* **269**, 16554–16558
24. Jacobowitz, O., and Iyengar, R. (1994) *Proc. Natl. Acad. Sci. U. S. A.* **91**, 10630–10634
25. Taussig, R., and Gilman, A. G. (1995) *J. Biol. Chem.* **270**, 1–4
26. Toullec, D. Pianetti, P., Coste, H., Bellevergue, P., Grand-Perret, T., Ajakane, M., Baudet, V., Boisson, P., Boursier, E., Loriolle, F., Duhamel, L., Charon, D., and Kirilovsky, J. (1991) *J. Biol. Chem.* **266**, 15771–15781
27. Lowell, B. B., Susulic, V. S., Hamann, A., Lawitts, J. A., Himms-Hagen, J., Boyer, B. B., Kozak, L. P., and Flier, J. S. (1993) *Nature* **366**, 740–742
28. Himms-Hagen, J. (1989) *Proc. Lipid Res.* **28**, 67–115
29. Xie, R., Li, L., Goshima, Y., and Strittmatter, S. M. (1995) *Brain Res.* **87**, 77–86
30. Gao, P., and Malbon, C. C. (1996) *J. Biol. Chem.* **271**, 9002–9008

Antisense therapy for cancer—the time of truth

Burkhard Jansen and Uwe Zangemeister-Wittke

The recent acceleration in the identification and characterisation of new molecular targets for cancer and the limited effectiveness of conventional treatment strategies has focused considerable interest on the development of new types of anticancer agents. These new drugs are hoped to be highly specific for malignant cells with a favorable side-effect profile due to well-defined mechanisms of action. Antisense oligonucleotides are one such class of new agent—they are short, synthetic stretches of DNA which hybridise with specific mRNA strands that correspond to target genes. By binding to the mRNA, the antisense oligonucleotides prevent the sequence of the target gene being converted into a protein, thereby blocking the action of the gene. Several genes known to be important in the regulation of apoptosis, cell growth, metastasis, and angiogenesis, have been validated as molecular targets for antisense therapy. Furthermore, new targets are rapidly being uncovered through coordinated functional genomics and proteomics initiatives. Phosphorothioate oligonucleotides are the current gold standard for antisense therapy; they have acceptable physical and chemical properties and show reasonable resistance to nucleases. Recently, new generations of these phosphorothioate oligonucleotides that contain 2'-modified nucleoside building blocks to enhance RNA binding affinity and decrease indirect toxic effects have been developed. Antisense therapeutics are, after decades of difficulties, finally close to fulfilling their promise in the clinic.

Lancet Oncol 2002; **3**: 672–83

Recent technological developments that allow for robust data acquisition along with large-scale data-generating programmes, have paved the way for the identification of target genes involved in neoplastic transformation and tumour growth. Identification of the nucleotide sequences of cancer-relevant genes will lead to tailored anticancer agents that lack many of the toxic side-effects displayed by conventional therapeutics.

In this review we discuss the development of exogeneously delivered oligonucleotides for the treatment of cancer and recent progress in clinical application of these treatments. In contrast to the use of plasmid-derived endogenous expression of antisense RNA—which has failed to show activity in vivo because of inefficient plasmid delivery—the antisense oligonucleotide approach (figure 1) has overcome many of barriers to clincial success. Double-stranded, 21-nucleotide, small, interfering RNAs have recently been used to specifically suppress the expression of homologous genes.[1] Available data, however, are too preliminary to conclude that the power of RNA interference

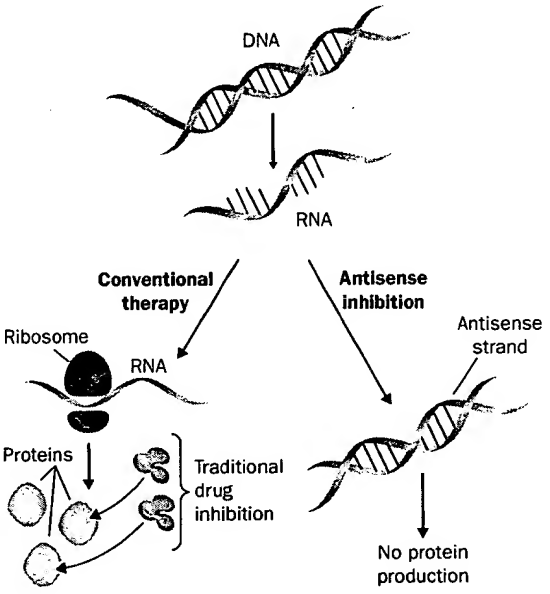

Figure 1. The antisense approach—the basic principle.

can be harnessed for the development of safe and gene-specific therapeutics.

Oligonucleotides have sequences that are complementary to specific strands of RNA. Once delivered into a target cell, the oligonucleotide hybridises with its RNA complement and inhibits expression of the corresponding disease-relevant protein. The idea of oligonucleotide-based antisense therapy is appealling and dates back to the 1960s when Belikova and colleagues[2] proposed that RNA sequences serve as endogeneous inhibitors of gene expression in prokaryotes. In the 1970s, Paterson and colleagues reported that exogeneous, single-stranded nucleic acids inhibit translation of RNA in a cell-free system.[3] 1 year later, Zamecnik and Stephenson did a cell-culture

BJ is a member of The Prostate Centre and the Division of Dermatology Vancouver General Hospital, University of British Columbia, Vancouver, BC, Canada. He is also part of the Departments of Clinical Pharmacology and Dermatology, in the Division of General Dermatology, University of Vienna, Austria. UZW is at the Department of Internal Medicine, Division of Medical Oncology, University of Zurich, Switzerland.

Correspondence: Dr Burkhard Jansen, The Prostate Centre, Vancouver General Hospital, University of British Columbia, D9, 2733 Heather Street, Vancouver, V6H 3Z3 BC, Canada. Tel: +1 604 736 3678. Fax: +1 604 736 3687.
Email: bjansen@interchange.ubc.ca

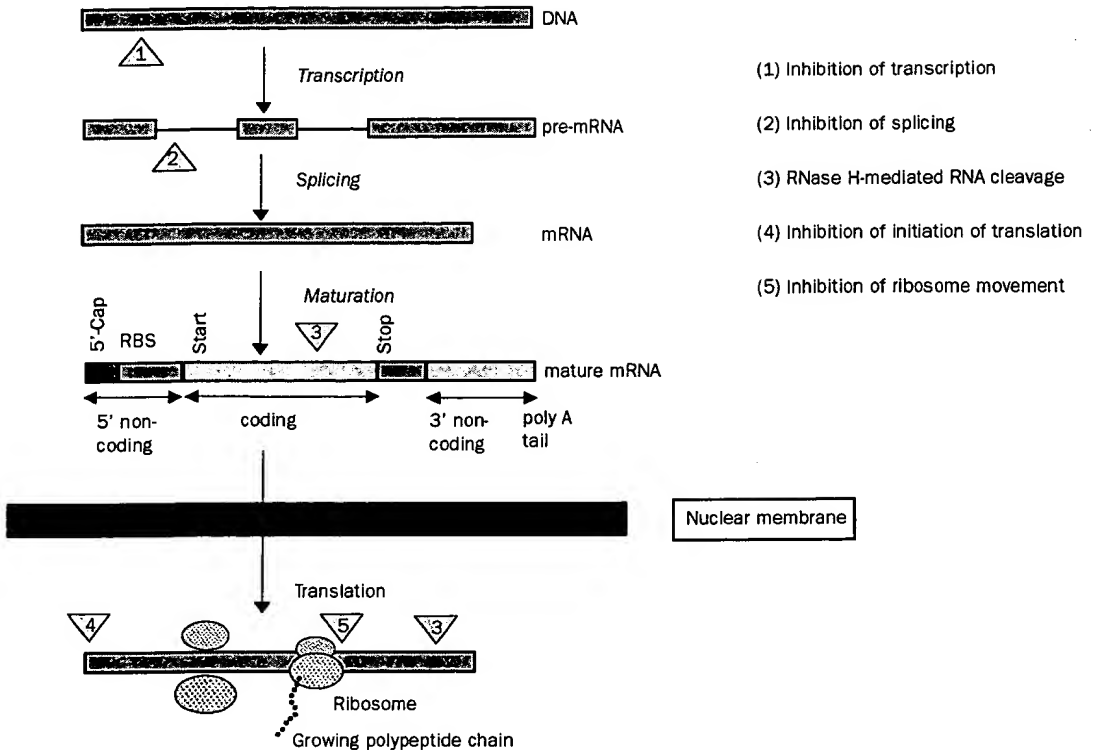

Figure 2. How antisense oligonucleotides work.

experiment which showed that an oligonucleotide complementary to the 3' end of the Rous sarcoma virus could block viral replication in chicken fibroblasts.[4] With the advent of automated DNA synthesis and advances in the field of nucleic-acid chemistry, progress in the use of this technology for target validation and therapy has accelerated considerably.

How antisense oligonucleotides work

Antisense oligonucleotides bind to selected target mRNA molecules by Watson–Crick base pairing, which results in the inhibition of mRNA processing or translation. This inhibition occurs through various mechanisms including prevention of mRNA transport, splicing, and translational arrest (figure 2). The specificity of this approach is based on the estimate that any sequence larger than a minimum number of bases—13 in RNA and 17 in DNA—occurs only once within the human genome. Thus, whereas small-molecule drugs interact with molecular targets through structural recognition, antisense oligonucleotides bind to strands of mRNA on the basis of their sequence. However, effective intracellular delivery remains an important issue for clinical application of antisense oligonucleotides; they have to reach the cytoplasm and finally the nucleus to efficiently access their mRNA target.

Intracellular penetration may occur via energy-dependent endocytosis, which has to be followed by an endosomal or lysosomal escape mechanism, or through a direct cell-membrane permeation process, which is more efficient. Unfortunately, because most oligonucleotides are hydrophilic with an anionic backbone, membrane permeation is low, and simple elimination of anionic charges does not increase this crucial step enough for delivery to be effective. Use of lipophilic transfection reagents such as cationic lipids to form conjugates or complexes, has been widely investigated for delivery of antisense molecules into cells in tissue culture. There have also been several attempts to achieve direct permeation into target cells in vivo. Interestingly, however, in animal models and in patients, all therapeutically active antisense oligonucleotides have been administered in the form of naked compounds, indicating that in intact tissues other mechanisms exist that can act in the same way as cationic carrier lipids.

Inhibition of gene expression is mainly accomplished by sterical hindrance of the target mRNA at the site of ribosomal entry and by recruitment of endogeneous RNase H. Cleavage of target mRNA by RNase H is probably the most important mechanism of antisense action and underlies the activity of all the oligonucleotides successfully tested in clinical trials so far. RNase H is a ubiquitous endonuclease involved in DNA replication, but it may also have other roles in cells. It is found both in the cytoplasm and the nucleus, although the concentration in the nucleus is thought to be greater. RNase H cleaves the RNA strand of a

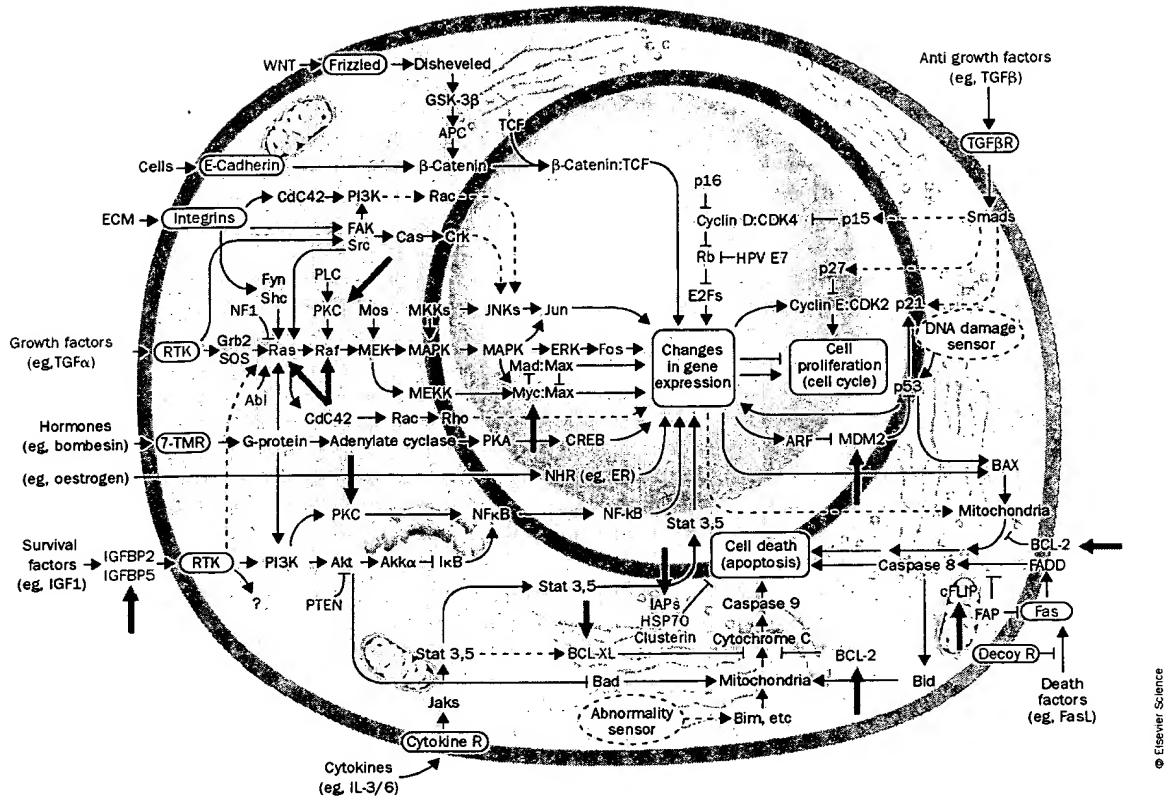

*Figure 3. The emergent integrated circuit of the cell. The blue arrows point at key proteins in pathways that contribute to malignant disease and thus represent promising targets for antisense therapy. Reproduced with modifications from Cell 2000; **100:** 57–70 with permission.*

DNA–RNA heteroduplex. The precise recognition element for the enzyme is unknown, but oligonucleotides with DNA-like properties as short as tetramers seem capable of activating this endonucleolytic process.[5] To what extent these low stringency requirements affect the expression of nonspecific genes (due to irrelevant cleavage) is unclear. In the case of high-affinity oligonucleotides it is likely that a 5 to 7 base homology provides sufficient overlap for RNase H competency.[6] Despite our increasing understanding of how specific hybridisation of antisense oligonucleotides translates into biological effects, it is important to not forget that nucleotide therapeutics are large charged molecules also capable of triggering nonantisense effects which can be both sequence specific and nonsequence specific. Sequence-specific effects include potential immune stimulation by sequences such as CpG motifs or G quartets. Charge-related phenomena include thrombocytopenia, which can also be caused by other charged macromolecules such as heparin. Although antisense inhibition seems to be the predominant mechanism responsible for antitumour activity of olignucleotides, as confirmed in several ongoing clinical trials, it is important to note that additional modes of action may also contribute to the overall responses observed.

How to find an optimal antisense sequence

The first step in validating genes as targets for antisense therapy is to identify those sites on the mRNA which are accessible and do not show sequence homologies with other genes of importance. The rationale behind the design of effective antisense oligonucleotides is based on the notion that mRNA is single-stranded at the AUG site—to allow ribosomal entry—and thus this site should also be accessible for oligonucleotide hybridisation. Oligonucleotides targeting the start codon have been used successfully for several genes, although other sites could prove to be even more effective.[7–9] Various in vitro techniques have been used in order to facilitate selection of target sites for antisense action; many of these techniques are combinatorial approaches based on annealing reactions with arrays of antisense species[10] or assessment of target accessibility by use of RNase H mapping.[11] In addition, computational attempts to predict the secondary structure and folding pattern of mRNAs have been described, and target screening with computer programs such as "mfold" or "RNAstructure" could prove to be a valid strategy for selecting effective antisense sequences.[12] This approach does not take account of other factors that could contribute to antisense efficacy, such as the three dimensional structure in vivo or accessibility of the target site for RNase H, but it substantially reduces the number of

oligonucleotides which have to be tested by high throughput screening. By comparison of the sequences of antisense oligonucleotides of varying effectiveness, the tetranucleotide motif TCCC was identified in 20 of the 42 most effective antisense sequences.[13] Thus, in addition to the techniques described above, the prediction of target sites on the basis of this motif may further assist in the design of antisense therapeutics.

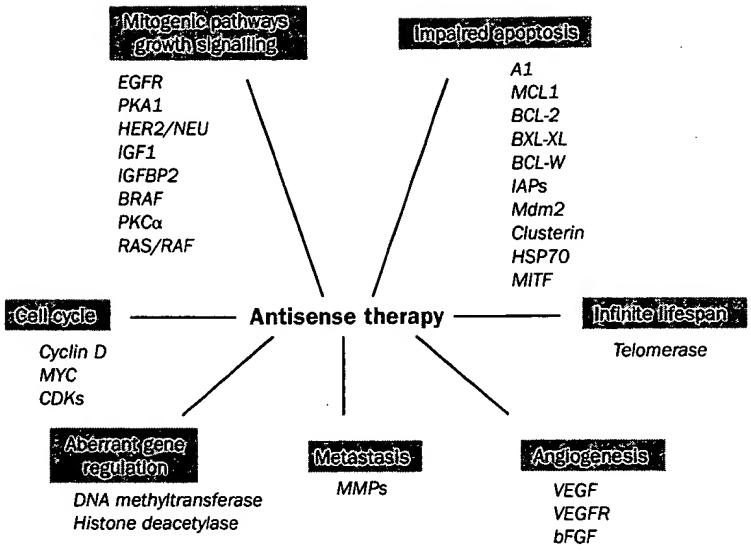

Figure 4. An overview of families of antisense targets.

Use of antisense oligonucleotides in vivo

In initial experiments, the activity of antisense oligonucleotides was limited by the susceptibility of the natural phosphodiester backbone to degradation by cellular nucleases. Several sugar, base, and backbone modifications have been investigated to make these molecules stable enough for clinical use. Significant improvements have been achieved with modifications of the backbone such as replacement of the oxygen atom of the PO moiety by sulphur (phosphorothioates, PS), a methyl group (methylphosphonates), or amines (phosphoramidates). However, although these analogues overcome the stability problem, only the phosphorothioate modification results in antisense compounds that combine serum stability, reasonably high RNA binding affinity, and the ability to elicit RNase H cleavage of the target RNA.[14] Now, after more than a decade of intensive research, phosphorothioate oligonucleotides still represent the most widely used class of antisense compounds, and several of these analogs are currently being tested in clinical trials. Investigations into their biological properties have identified several potentially toxic nonantisense effects, which become apparent at higher concentrations and include complement activation, thrombocytopenia, inhibition of cell-matrix interaction, and reduction of cell proliferation. In safety studies, repeated administration of these compounds to mice revealed several side-effects, especially with phosphorothioate oligonucleotides containing CpG motifs. When surrounded by particular bases, these unmethylated CpG dinucleotides induce immune stimulation, which leads to cytokine release, decreased platelet count, and hepatotoxicity.[15,16] Despite the current belief that phosphorothioate oligonucleotides do not yet represent the optimum antisense strategy, some have shown encouraging results in the clinic.

To improve the safety and effectiveness of phosphorothioate oligonucleotides, modifications have been aimed at increasing their metabolic stability and enhancing affinity for complementary mRNA. With these modifications, the oligonucleotides have a 0·4 °C lower melting temperature per phosphorothioate linkage than native phosphodiester counterparts.[17] As with antibody–antigen interactions, the affinity of antisense oligonucleotides for their target mRNA is a measure of the stability of the nucleic acid hybrid; high affinity represents high gene-repression activity.[6] The activity of phosphorothioate antisense oligonucleotides can be improved by modification of the ribose. Among the different sites in a nucleoside building block, the 2'-position could prove to be the most valuable.[18] 2' modification with an electronegative substituents such as 2'-O-methyl or 2'-O-(2-ethoxy)ethyl (MOE) groups,[6,19] or a 2'-O,4'-C-methylene bridge (locked nucleic acid) [20] confer an RNA-like C3'-endo conformation to the oligonucleotide, which greatly enhances affinity. However, the RNA-like conformation also abrogates the oligonucleotide's ability to activate RNase H. This problem has been addressed by generating mixed-backbone oligonucleotides that only contain the modified nucleotides at the ends, thus leaving a nonmodified DNA gap in the centre, which remains compatible with RNase H activation. Such "second generation" or "advanced chemistry" antisense compounds have favourable physicochemical, biochemical, and pharmacokinetic properties,[6] and therefore may be appropriate for oral or transdermal formulations.[21]

Targets for antisense therapy

With the completion of the first phase of the Human Genome Project, about 30 000 gene sequences and 100 000 mRNAs are now available as tools to validate candidate genes for antisense therapeutic purposes. To find suitable sequences for treating a given disease, genes which are differentially expressed in diseased and normal tissue first need to be identified. Elucidation of the roles of several cancer-related genes in tumour development is a rapidly progressing area of cancer research and has provided a steadily growing list of candidate genes. The multitude of molecular entities and signalling pathways that regulate the life/death decision in cells, and thus represent potential

Table 1. Antisense therapies in phase I–III clinical trials

mRNA target	Drug	Company or investigator	Size/ chemistry	Tumours evaluated	Development phase	Combination treatment?	Website
BCL-2	G3139 (Genasense)	Genta/Aventis	18-mer/PS	Melanoma, MM, CLL, NSCLC	III*	Y	www.genta.com
PKCα	ISIS 3521 (Affinitac)	ISIS/Eli Lilly	20-mer/PS	NSCLC, solid tumours	I–III*	Y/N	www.isispharma.com
c-RAF	ISIS 5132	ISIS	20-mer/PS	Solid tumours	I–II*	Y/N	www.isispharma.com
Ha-RAS	ISIS 2503	ISIS	20-mer/PS	Solid tumours	I–II	N	www.isispharma.com
Clusterin	OGX-011	OncoGeneX	21-mer/AC	Prostate cancer, NSCLC	I–II*	Y	www.oncogenex.ca
PKA-R1-α	GEM 231	Hybridon	18-mer/AC	Solid tumours	I–II*	N	www.hybridon.com
c-MYB	LR/INX-3001	Gewirtz et al	24-mer/PS	CML	I–II*	N	www.uphs.upenn.edu/ hematol/faculty/gewirtz.htm
Ribonucleotide reductase	GTI-2040	Lorus Therapeutics	21-mer/PS	Solid tumours	I–II*	N	www.lorusthera.com
DNA methyltransferase	MG-98	MethylGene	20-mer/AC	Solid tumours	I–II*	Y/N	www.methylgene.com
p53	OL(1)p53	Bishop et al	20-mer/PS	AML, MDS	I	N	
BCR-ABL	BCR-ABL AS	de Fabritiis et al	26-mer/PS	CML	I	N	

MM, multiple myeloma; CLL, chronic lymphatic leukaemia; NSCLC, non-small-cell lung cancer; CML, chronic myelogenous leukaemia; AML, acute myelogenous leukaemia; MDS, myelodysplastic syndrome; PS, phosphorothioate oligonucleotide; AC, advanced chemistry oligonucleotide; Y, yes; N, no. *Initiation of trial, or additional trials expected, in 2002.

targets for molecular intervention strategies including antisense therapy, are shown in figure 3. The most promising targets are those involved in cell proliferation,[22] apoptosis,[23] angiogenesis,[24] and metastasis[25] (figure 4). A comprehensive overview of the antisense oligonucleotides currently under investigation in clinical trials is provided in table 1.

Target sequences are carefully chosen to avoid hybridisation of full-length oligonucleotides to unrelated targets and to ensure they are long enough that uniqueness within the cellular mRNA pool is preserved. Despite these efforts, antisense oligonucleotides were expected to have side-effects resulting from irrelevant cleavage of non-targeted mRNA by low stringency RNase H[5,26] and from silencing of target genes which are not tumour specific. Interestingly, however, preclinical studies and initial clinical tests did not substantiate these concerns. Thus, normal healthy cells seem to tolerate the transient loss of function of genes involved in growth regulation and cytoprotection better than cancer cells, which carry the proapoptotic burden of multiple genetic alterations and genomic instability. Antisense therapeutics that tackle the apoptotic rheostat, interfere with growth signalling pathways, or target tumour microvasculature to inhibit tissue invasion and metastasis, are particularly promising when complemented by conventional anticancer treatments, because their toxicity profiles do not overlap.

BCL-2 family

BCL-2 and BCL-XL are inhibitors of apoptosis with cytoprotective function. Both proteins reside within the mitochondrial membrane where they act by inhibiting adapter molecules needed for the activation of caspases. Recent evidence also suggests a role for BCL-2 in protecting cells from APAF1-independent death. More distant relatives of the family include BAX and the BH3-only proteins, which promote apoptosis by inducing the release of cytochrome C from mitochondria and counteract the protective activity of BCL-2 and BCL-XL by heterodimerisation.[23] Alterations in this balance that favour cell survival may cause proliferative disorders such as cancer. Overexpression of BCL-2 or BCL-XL is indeed common in many types of cancer and believed to contribute to increased resistance to chemotherapy. But although the prognostic value of BCL-2 and BCL-XL overexpression seems to depend on the tumour type, preclinical and clinical data indicate that both proteins may be good targets for antisense therapy. BCL-XL is a survival factor for undifferentiated endothelium cells. So, given the recent finding that BCL-2 overexpression in endothelial and tumour cells results in the upregulation of VEGF expression and increased microvessel density in tumour xenografts, antisense strands targeted to BCL-2 and/or BCL-XL could provide a therapeutic approach that combines proapoptotic and antiangiogenic activity.

In 1997, the first results of a clinical study investigating G3139 (Genasense, table 1)—an 18-mer phosphorothioate oligonucleotide targeted to the BCL-2 translation initiation site—for treatment of non-Hodgkin lymphoma were reported.[27] This phase I, dose-escalation trial included 21 patients[28] and focused on the safety and pharmacokinetics of the drug when administered by subcutaneous infusion. Local inflammation at the infusion site was the most common side-effect; the maximum-tolerated dose was 147·2 mg/m²/day; and the dose-limiting toxic effect was thrombocytopenia. Of the 21 patients, 9 achieved stable disease, 9 had disease progression, two showed partial responses, and one patient had a complete response. However, a reduction in BCL-2 protein by antisense treatment was observed in only about half of the patients.

Drug resistance has been linked to overexpression of BCL-2 in a number of cancer types including melanoma, which is a classic example of a treatment-resistant tumour. In preclinical studies, G3139 decreased the production of BCL-2 protein, enhanced tumour-cell apoptosis, and, in combination with systemically administered dacarbazine (DTIC), led to major tumour responses in mice with human melanoma xenografts.[29] Other BCL-2 antisense oligonucleotides have also shown promise in preclinical studies.[9,30]

In the clinical setting, it was established that G3139 can be safely administered by continuous intravenous infusion in combination with full-dose DTIC in a phase I/II trial in patients with advanced melanoma. This trial also showed that G3139 causes down-regulation of BCL-2 protein in serial biopsy samples from patients with melanoma, and that this biological activity was associated with major clinical responses (figure 5). The entire group of patients, who all had advanced-stage disease, were still alive more than 1 year later.[31] Transient thrombocytopenia limited the antisense dose to 12 mg/kg each day in patients who also received full-dose DTIC treatment. An international, phase III, randomised trial has been initiated in patients with advanced melanoma by use of a 5-day pretreatment regimen of G3139 administered by continuous infusion at a dose of 7 mg/kg each day, followed by DTIC at 1000 mg/m². Additional controlled multicentre trials are ongoing in other tumours including multiple myeloma, CLL, and lung cancer (table 1), and have the goal of increasing the effectiveness of experimental treatment strategies.

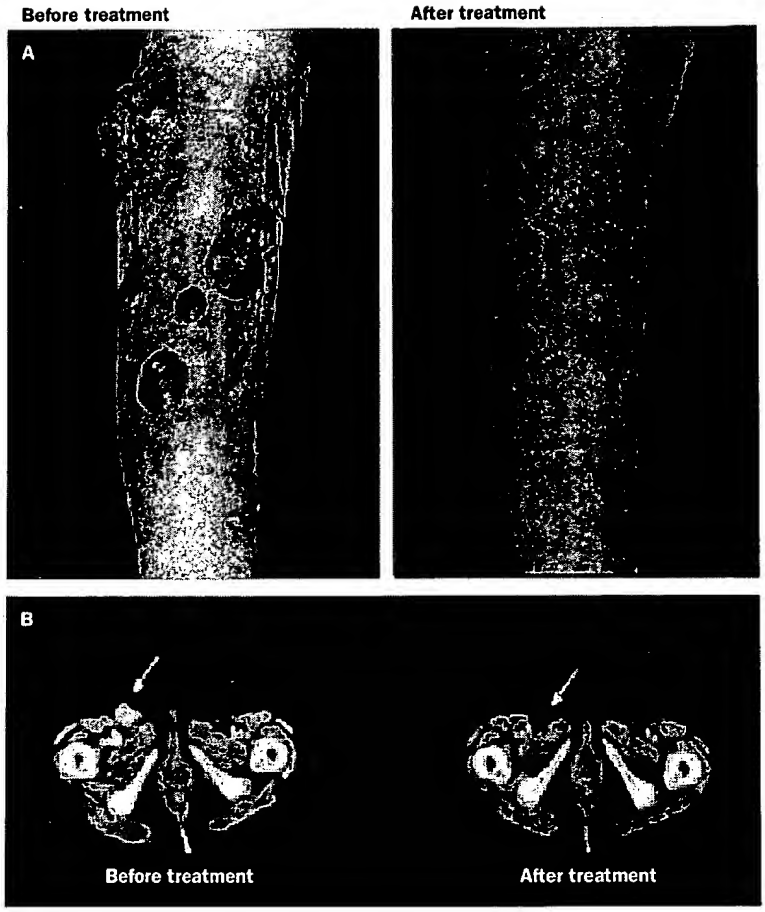

Figure 5. An example of a complete remission of advanced malignant melanoma after chemosensitisation by BCL-2 antisense (Genasense) treatment. Lower right leg (a) and a computed tomography of the pelvis (b) before and after treatment are shown (reference 31).

Alternative splicing of BCL-X pre-mRNA results in two distinct mRNAs: BCL-XL, which codes for the antiapoptotic protein, and BCL-XS, which codes for the proapoptotic variant.[32] Antisense oligonucleotides targeting the BCL-X mRNA or the BCL-XL mRNA specifically have been reported; all these oligonucleotides induce apoptosis in various tumour cells and sensitise tumour cells to chemotherapy.[33–35] Similarly, BCL-X antisense oligonucleotides designed to shift pre-mRNA splicing away from producing the BCL-XL protein to proapoptotic BCL-XS, could also prove effective in sensitising cells to apoptosis.[36] Despite these findings, clinical studies with BCL-XL antisense oligonucleotides have not yet been done. BCL-XL is also expressed in several types of normal tissue including neurons in the brain and certain cells in the bone marrow, which suggests there may be side effects with this approach. Whether BCL-XL antisense therapy can nevertheless prove clinically useful remains to be explored.

Many tumour cells coexpress BCL-2 and BCL-XL and there is uncertainty as to which target is the more important survival factor in a heterogeneous tumour cell population. Although BCL-2 and BCL-XL are functionally similar, there is evidence that they have distinct biological roles in protecting from apoptosis induced by different stimuli. Coupled with the finding that mRNA for BCL-2 and BCL-XL share homology regions with high sequence identity, this information has led to the idea of generating an antisense oligonucleotide which targets both proteins, instead of just one. The design and preclinical testing of a BCL-2/BCL-XL bispecific antisense oligonucleotide was reported recently. This 20-mer, MOE gap-mer oligonucleotide efficiently downreguated BCL-2 expression simultaneously with BCL-XL, and induced apoptosis in tumour cells of diverse histological origins in vitro and in vivo.[30,37]

Protein kinase C

Several studies have examined the role of closely related protein kinase C (PKC) isozymes in various biological

processes. PKC belongs to a class of serine–theronine kinases involved in a myriad of intracellular responses, which are stimulated by activation of G-protein-coupled tyrosine kinases; these kinases are found in both growth-factor-receptor-linked and non-receptor linked forms. Altered expression of PKC has been implicated in the deregulation of cell growth and tumour development.[38] Various inhibitors and modulators of PKC activity have been tested. The clinical limitation of these compounds is their inability to discriminate between the various isozymes of PKC, which may result in unacceptable toxic effects in normal tissues. Several antisense oligonucleotides that specifically target individual members of the PKC family have been studied. On the basis of the activity and safety profile of a murine PKCα-specific antisense inhibitor in mice, a 20-mer phosphorothioate oligonucleotide targeting human PKCα (ISIS 3521) was developed. ISIS 3521 was found to inhibit the growth of glioblastoma xenografts and extended survival in tumour-bearing mice.[39] The biological evidence implicating PKC in the pathogenesis of solid tumours and the activity of ISIS 3521 against human tumour xenografts in mice,[40] led to the initiation of clinical studies with this drug.

The phase I trials of ISIS 3521 were dose-escalation studies in patients with treatment-resistant solid tumours. The oligonucleotide therapy was well tolerated and therapeutic benefit was noted in some cases. In further trials, responses were seen at several different doses of ISIS 3521. Two patients with lymphoma experienced complete responses (after 18 and 9 months of treatment) and neither had recurrant disease after 21 and 14 months, respectively.[41] In one of the phase I trials, ISIS 3521 was administered to 21 patients with end-stage malignant disease for 3 weeks via continuous intravenous infusion, followed by a 1-week treatment-free period. Dose-limiting thrombocytopenia and fatigue were encountered at doses of 3·0 mg/kg per day. The maximum tolerated dose was found to be 2·0 mg/kg/day, which corresponded with doses showing antitumour activity in xenograft models. There was evidence of tumour responses lasting up to 11 months in 3 of 4 patients with ovarian cancer. Continuous intravenous infusion of ISIS 3521 over 3 weeks has so far not shown objective clinical benefit in patients with recurrent high-grade astrocytomas.[42] Median time to progression was 35 days and median survival was 93 days; any toxic effects were mild and reversible.

On the basis of extensive data on ISIS 3521 as a single-agent, a phase I/II study combining the PKC antisense oligonucleotide with carboplatin and paclitaxel in patients with stage IIIB or IV non-small-cell lung cancer (NSCLC) was initiated.[43,44] A recent update of 24 evaluable patients with NSCLC showed that 1 year survival was 78 %, with a median survival of 18 months. Survival in comparable patient cohorts receiving chemotherapy alone was reported to be 8 months. The combination of ISIS 3521, carboplatin, and paclitaxel was well tolerated with manageable thrombocytopenia and neutropenia as the main side-effects. These promising results led to a 600-patient randomised phase III clinical trial of ISIS 3521 in combination with chemotherapy for NSCLC, which is now underway.[45]

RAF kinase

The *RAF* proto-oncogene encodes a serine–threonine kinase that is activated by the RAS protein as part of the mitogen-activated protein kinase (MAPK) signalling cascade.[46] c-RAF kinase binds to BCL-2 and thus may also play an indirect role in the regulation of apoptosis. Mutations of the *RAS* or *RAF* gene resulting in their constitutive activation have been identified and their aberrant expression reported in many tumours where it may serve as a negative prognostic factor. Because 75–90% of all pancreatic adenocarcinomas harbour activating mutations in the *k-RAS* oncogene it has been expected for a long time that inhibitors of the RAF-1-MEK-MAPK pathway may be useful to control diseases associated with abnormal cell proliferation. A series of 34 phosphorothioate antisense oligonucleotides were designed and screened for reducing c-RAF mRNA concentrations in vitro.[8,47] ISIS 5132, a 20-mer targeting a site at the 3' untranslated region, was identified as the most potent in inhibiting c-RAF expression, and showed antiproliferative and antitumour activity against various tumour-cell lines in vitro and in xenograft models in mice.[8]

2 h intravenous infusions of ISIS 5132 were administered 3 times a week for 3 consecutive weeks with doses ranging from 0·5 to 6·0 mg/kg; the infusions were well tolerated without dose-limiting toxic effects.[48] Furthermore, an additional phase I dose-escalation trial (continuous intravenous infusion of ISIS 5132 for 21 days every 4 weeks) in 34 patients suffering from different refractory solid tumours was done.[49] Continuous administration of ISIS 5132 up to 4·0 mg/kg led to no dose-limiting toxic effects. At 5·0 mg/kg, fever and thrombocytopenia were dose-limiting. One patient who had treatment-refractory ovarian cancer experienced a reduction in CA125 concentration of more than 90%; 2 other patients achieved stable disease for 9 and 10 months. Statistically significant downregulation of c-RAF1 mRNA by ISIS 5132 in peripheral blood mononuclear cells of patients with advanced malignant disease was observed in most cases.

Accumulation of evidence for proof of principle and the confirmation of an acceptable safety profile, led to the initiation of several phase II trials of ISIS 5132. However, in one study investigating the antitumour activity of ISIS 5132 (4 mg/kg per day, 21-day continuous intravenous infusion every 4 weeks) in 22 pretreated patients with recurrent ovarian cancer, the drug did not seem to have therapeutic activity as a single agent.[50] Results of other phase II clinical studies targeting c-RAF kinase in prostate and colon cancer are pending.

Protein kinase A

The cAMP-dependent protein kinase A (PKA) is involved in various biological functions including cell proliferation, induction of gene expression, and ion-channel regulation. PKA is composed of two catalytic and two regulatory subunits and has type-I and type-II isozymes containing different R subunits, termed RI and RII. Of the 4 isoforms of R increased expression of RIα is associated with cell proliferation and neoplastic transformation. Accordingly, overexpression of the RIα subunit of PKA is found in many

tumours in which it is a negative prognostic factor.[51] The catalytic subunit of PKA also phosphorylates the EGF receptor, which is accompanied by decreased auto-phosphorylation and diminished tyrosine kinase activity. The finding that decreased expression of RIα and thus release of the catalytic subunit correlates with growth inhibition induced by cAMP analogues in transformed cell lines, has prompted studies to investigate the potential of antisense inhibitors of RIα as anticancer agents that interfere with the mitogen-activated signalling pathway. Oligonucleotides targeted to various sites within the coding region of the RIα mRNA that showed antiproliferative activity in different tumour cells and cooperatively acted with EGF-receptor inhibitors were identified.[52]

The 18-mer mixed-backbone antisense oligonucleotide GEM231 (table 1), designed to interfere with the production of the RIα regulatory subunit of PKA, inhibited the growth of tumour cell lines in vitro and displayed antitumour activity against human tumour xenografts when given orally to mice.[21,53] Phase I preliminary data show that escalating doses of GEM231 were also well tolerated in repeat cycles when administered twice weekly by intravenous injections at doses of up to 360 mg/m² (equivalent to about 7–9 mg/kg). Additional studies designed to evaluate the safety and efficacy of GEM231 in combination with taxotere or taxol in patients with advanced cancers have been initiated. Early results suggest that side-effects caused by GEM231 were mild and reversible and do not overlap with the side-effects caused by taxanes.

p53/MDM2

The tumour suppressor p53 is a master-switch for cell cycle regulation and apoptosis. Terms like "guardian of the genome" have been coined for p53 and mutations resulting in its inactivation or deletion have been found in a number of hematological and non-hematological malignant diseases. OL(1)p53 (table 1) is a phosphorothioate antisense oligonucleotide complementary to 20 bases within exon 10 of the p53 mRNA. A total of 21 patients with either refractory acute myelogenous leukemia (AML) or advanced myelodysplastic syndrome received OL(1)p53 at doses up to 0·25 mg/kg/h for 10 days by continuous infusion during two initial phase I trials. Neither specific toxic effects nor complete hematological responses were observed. More recently, 9 patients participated in a phase I study evaluating OL(1)p53 as a bone-marrow purging agent [54]. Harvested marrow was incubated with OL(1)p53 at 10 μM of the oligonucleotide for 36 h before transplantation. However, clear clinical benefits were not observed.

MDM2 is a negative feedback regulator of p53 which interferes with the control of cell proliferation and apoptosis. It interacts not only with p53, but also with p14ARF, which antagonises its function as a suppressor of p53. MDM2 is amplified/overexpressed in various tumours. A mixed-backbone antisense oligonucleotide targeting MDM2 released p53, which resulted in increased p21/WAF1 expression. This effect was synergystic with different classes of anticancer agents and significantly increased apoptosis in tumour cells in vitro. In mice, MDM2 antisense drugs have shown antitumour activity against human tumour xenografts and seem to potentiate the effect of anticancer agents.[55]

c-MYB

The *c-MYB* proto-oncogene encodes a DNA-binding transcription factor involved in the control of the G1/S transition of the cell cycle.[56] c-MYB is located on chromosome 6q22–24, on which abnormalities have been observed in cells from leukaemias, lymphomas, colon carcinomas, and malignant melanoma.[57] Ratajczak and colleagues[58] used 18-mer and 24-mer phosphorothioate antisense oligonucleotides targeted to codons 2–7 and 2–9, respectively, of the c-myb gene to inhibit the proliferation in AML, CML, and T-cell leukaemia cultures by induction of apoptosis. In a clinical pilot study, the 24-mer antisense oligonucleotide LR-3001 showed promise in purging ex vivo bone-marrow harvests from patients with CML before autologous transplantation. The patients (seven in chronic phase CML and one in accelerated phase) received chemotherapy with busulfan and cytoxan, followed by re-infusion of previously cryopreserved mononuclear cells purged for 24 hours with LR-3001. Seven of eight patients were reconstituted successfully. In 4 of 6 evaluable patients, 85–100% normal metaphases were found 3 months after engraftment, supporting the notion that significant ex vivo purging of the marrow graft was achieved. A phase II study has been initiated to validate these promising findings.

DNA methyltransferase

Aberrant expression of the DNA methyltransferase enzyme is implicated in multiple tumorigenic pathways and there are several lines of evidence suggesting that this alteration plays a causal role in neoplastic transformation and tumour development. The possible mechanism by which overexpression of DNA methyltransferase may induce tumorigenesis is promoter hypermethylation, which inactivates a large number of genes that induce apoptosis, and suppress tumorigenesis, tumour invasion, and angiogenesis, or that control DNA replication and cell-cycle progression. Inhibition of DNA methyltransferase by antisense treatment was shown to revert the malignant phenotype of tumour cells in vitro and in mice.[59,60] The mixed-backbone antisense oligonucleotide MG-98, originally developed by Hybridon Inc and further evaluated by MethylGene Inc (table 1) was shown to effectively downmodulate the methylation of candidate genes involved in tumorigenesis and has found its way to early clinical testing. MG-98 was given to 9 patients with advanced solid tumours as a continuous 21-day intravenous infusion, with cycles to be repeated at 4-week intervals. Dose-limiting, drug-related increases in the production of transaminases were found in 2 of 2 patients receiving a dose of 240 mg/m² per day. Reductions of DNA methyltransferase mRNA considered to be biologically relevant were seen at the lowest dose (40 mg/m² per day). However, changes in DNA methyltransferase mRNA did not translate into clinical benefit.[61]

BCR-ABL

The Philadelphia chromosome is the result of a translocation found in chronic myelogenous leukemia (CML) cells resulting in the juxtaposition of the *ABL* gene (normally found on chromosome 9) and the *BCR* gene of chromosome 22. The resultant p210 fusion protein functions as a tyrosine kinase and is believed to cause the neoplastic phenotype of CML. A 26-mer oligonucleotide targeted against the BCR-ABL transcript has shown selective inhibition of in vitro cell growth. This strategy also proved successful in an SCID mouse model. Mice with CML survived 18 to 23 weeks, whereas controls died within 8–13 weeks after tumour cell inoculation.[62] On the basis of these encouraging preclinical findings, clinical studies investigating ex vivo bone-marrow purging by BCR-ABL antisense oligonucleotides in patients with CML were initiated.[63] The bone-marrow sections from eight patients were incubated for 24 or 72 hours with 150 μg/ml BCR-ABL antisense oligonucleotides. Two complete karyotypic responses were noted; the karyotypes of the remaining 6 patients showed no or only minimal responses. These results translated into a persistent second chronic phase lasting 14–26 months after transplantation in three patients.

Clusterin

Clusterin, also known as testosterone-repressed message 2 (TRPM2) or sulfated glycoprotein 2, has been implicated in a variety of physiological and pathological processes. An increasing body of evidence supports a role for this protein in apoptotic cell death. More recent studies also suggest that clusterin acts in a chaperone-like way—similar to that of small heat shock proteins—potentially inhibiting stress-induced protein misfolding in vitro; it also improves cell survival in vivo.[64] In prostate cancer, experimental and clinical studies provided evidence that clusterin concentrations increase in response to therapeutic cell death signals, such as androgen ablation or chemotherapy, and protect against apoptosis.[65] When overexpressed, clusterin confers a hormone-resistant or chemotherapy-resistant phenotype in a number of malignant diseases including prostate cancer, indicating that it is an attractive target for antisense therapy. Phase I/II clinical trials evaluating the therapeutic potential of OGX-011, a 21-mer MOE gap-mer oligonucleotide targeting the translation initiation site of clusterin, in combination with androgen ablation or chemotherapy have been initiated in patients with prostate cancer and will be initiated in the near future in patients with other types of solid tumour including NSCLC (table 1).

Inhibitors of apoptosis proteins

The inhibitors of apoptosis proteins (IAPs) act as roadblocks in the apoptosis signalling pathway by directly binding to caspases, thereby blocking their processing and activity. Evolutionarily conserved from viruses to mammalian cells, these proteins are characterised by a 70 aminoacid domain called baculoviral inhibitory repeat (BIR). The IAPs XIAP, c-IAP1, c-IAP2 can interact with the effector caspases 3 and 7, but also with the initiator caspase 9. The IAP survivin seems to associate with caspase 3 in the vicinity of centrosomes during mitosis and is required for suppression of caspase-mediated cleavage of centrosome-associated p21waf1.[66] Recent evidence suggests that survivin also interacts with pro-caspase 9 and that phosphorylation of survivin by $p34^{cdc2}$–cyclin B1 is required for its cytoprotective function. Survivin is expressed in the G2/M phase and its overexpression in cells may overcome the G2/M checkpoint to enforce progression of cells through mitosis. In colorectal, gastric, breast, bladder, and lung cancers, and in certain leukaemias and lymphomas, survivin expression is associated with shorter survival and correlates with a higher stage of disease. Together with the finding that survivin lacks expression in terminally differentiated tissues, but becomes re-expressed during neoplastic transformation, this IAP deserves attention as a truly tumour-specific target for antisense therapy. Antisense oligonucleotides targeting different sites within the survivin mRNA have been tested in different cell systems and shown to induce apoptosis directly or sensitise cells to additional apoptotic stimuli.[67]

Other potential targets for antisense therapy

As a consequence of the encouraging preclinical findings with evidence of selective inhibition of Ha-RAS expression by ISIS 2503, a 20-mer phosphorothioate antisense oligonucleotide targeting the translation initiation site of the Ha-RAS mRNA, ISIS 2503 (table 1) has been evaluated alone and in combination with chemotherapy in phase I and II trials in a number of solid tumours.[68] There is clear evidence that ISIS 2503 is well tolerated. However, ISIS 2503 has not shown antitumour activity as a single agent in the cancer types so far tested and antisense strategies targeting other RAS isoforms seem more attractive, since 75–90% of pancreatic adenocarcinomas and 50% of colon cancers harbor activating mutations in K-RAS but not Ha-RAS.[69] Antisense oligonucleotides targeting the ribonuclease reductase (table 1), an enzyme of importance in DNA synthesis and cell proliferation, have recently reached the stage of early clinical evaluation. Insulin-like growth factor 1 (IGF1) has mitogenic and antiapoptotic effects modulated by insulin-like growth-factor binding proteins (IGFBPs) in various tissues. Downregulation of IGFBP5 expression by antisense oligonucleotides inhibited the growth of Shionogi cancer cells in vitro and inhibited the growth of androgen-independent tumours after castration.[70] This finding suggests that the increase of IGFBP5 concentrations observed after castration in models of prostate cancer is an adaptive cell-survival mechanism that helps potentiate the antiapoptotic and mitogenic effects of IGF1, thereby accelerating androgen-independent progression towards a treatment resistant phenotype.[71] Clinical studies with antisense oligonucleotide (OGX-133) designed to attenuate IGFBP5 function in patients with advanced prostate cancer are being planned.

The cellular Fas-associated death domain (FADD)-like interleukin-1β-converting enzyme-like (FLICE) inhibitory protein (cFLIP) resembles caspase 8 in structure, but lacks protease activity. It interacts with both FADD and caspase 8 to inhibit the apoptotic signal of death receptors and, at the same time, can stimulate survival signalling through

Search strategy and selection criteria

Published data for this review were identified by searches of MEDLINE, EMBASE, CancerLit, METACRAWLER, the websites of companies that produce antisense compounds (table 1), and references from relevant articles up to August 2002. The terms "cancer therapy", "antisense", "oligonucleotides", "RNA", "gene expression/regulation", "oncogenes", "apoptosis", "angiogenesis", "metastasis". Only articles published in English were used. In addition, we contacted researchers, clinicians and companies working on antisense strategies.

activation of NFκB. Inhibition of FLIP may also be useful in the treatment of carcinomas with acquired resistance to death-receptor-induced apoptosis and chemoresistance.[72] The stress-inducible heat-shock protein Hsp70 is a chaperone selectively expressed in tumours and tumour cell lines, which seem to depend on its constitutive high expression to suppress a transformation-associated death programme. Depletion of Hsp70 by antisense constructs was shown to induce cell death; the mechanism of action was possibly disruption of Hsp70-BCL-2 interaction, but Hsp70 has recently also been shown to bind and inhibit Apaf-1 and apoptosis-inducing factor. Interestingly, cell death was induced in various tumour cell lines and in cells from primary tumours, but not in normal epithelial cells and fibroblasts.[73] Whether Hsp70 indeed confers a survival advantage selectively to tumour cells and whether targeted disruption of *Hsp70* gene expression can provide a reasonable therapeutic index remains to be determined. Further preclinical data are clearly needed to convincingly demonstrate that chaperoning by Hsp70 is more dispensable for the function of normal tissues than for the survival of tumours. Other genes currently validated as targets for antisense therapy in preclinical studies include growth-factor-receptor tyrosine kinases such as HER2/neu, the epidermal and vascular endothelial growth-factor receptors, transcription factors involved in cell survival like NFκB, the myriad of protein kinases involved in cell cycle regulation, and thymidylate synthase. Additional attractive targets of great potential and importance for antisense strategies highlighted by most recent reports include BRAF, mutated in about 60% of melanomas and at somewhat lower frequencies in a variety of other malignant diseases,[74] and MITF, a transcription factor shown to regulate BCL-2 in cells of the melanocytic lineage as well as in certain bone cells.[75] Although the available data are still preliminary, there is hope that some of these cancer-related targets will maintain their allure beyond clinical scrutinisation.

The future of antisense

There is increasing evidence that antisense oligonucleotides can work in a sequence-specific manner in patients and will finally live up to their promise. Although a number of challenges remain, these are probably easier to overcome in oncology than in any other field since there are large unmet medical needs. Furthermore, several antisense oligonucleotides have displayed acceptable toxicity profiles. Antisense strategies which aim at restoration of apoptosis signalling, alter signalling pathways involved in cell proliferation, or target the tumour's micro-vasculature, may prove particularly useful in combination with conventional anticancer agents. Lowering the apoptotic threshold of cancer cells could prove to be the single most attractive strategy to overcome chemo- and radiation resistance. But studies focusing on other possible mechanisms of action for antisense oligonucleotides, beyond anticipated clinical successes, will be instrumental to progress in the field. These studies are mandatory to highlight antisense oligonucleotides as rationally designed molecules with predictable properties; the potential for rapid development and improvement places them apart from conventional drugs.

Conflict of Interest

BJ and his Vienna Laboratory received limited financial support or antisense compounds free of charge from ISIS Pharmaceuticals, Genta Inc, OncoGeneX Technologies Inc, and Hybridon Inc. BJ is currently on sabbatical from all academic positions at the University of Vienna and serves at OncoGenex Technologies, Inc as Vice President, Clinical Development. The group of UZW received limited financial support and antisense compounds free of charge from Novartis Pharma AG.

Acknowledgements

Work in the authors' laboratories is supported by the Swiss National Science Foundation (Grant No. 31-40473.94 to UZW), Oncosuisse (Grant No. 549-0-1997 to UZW), the Foundation for Applied Cancer Research Zürich, the Austrian Science Fund, the Austrian National Bank, the Niarchos Foundation, the Kamillo Eisner Foundation, and the University of Vienna Hygiene Fund.

References

1 Elbashir SM, Harborth J, Lendeckel W, et al. Duplexes of 21-nucleotide RNAs mediate RNA interference in cultured mammalian cells. *Nature* 2001; 411: 494–98.
2 Belikova AM, Zarytova VF, Grineva NI. Synthesis of ribonucleosides and diribonucleosides phosphates containing 2-chloroethylamine and nitrogen mustard residues. *Tetrahedron Lett* 1967; 37: 3557–62.
3 Paterson BM, Roberts BE, Kuff EL. Structural gene identification and mapping by DNA-mRNA hybrid-arrested cell-free translation. *Proc Natl Acad Sci USA* 1977; 74: 4370–74.
4 Zamecnik PC, Stephenson ML. Inhibition of Rous sarcoma virus replication and cell transformation by a specific oligodeoxynucleotide. *Proc Natl Acad Sci USA* 1978; 75: 280–84.
5 Donis-Keller H. Site specific enzymatic cleavage of RNA. *Nucleic Acids Res* 1979; 7: 179–92.
6 Monia BP, Lesnik EA, Gonzalez C, et al. Evaluation of 2'-modified oligonucleotides containing 2'-deoxy gaps as antisense inhibitors of gene expression. *J Biol Chem* 1993; 268: 14514–22.
7 Bacon TA, Wickstrom E. Walking along human c-MYC mRNA with antisense oligodeoxynucleotides: maximum efficacy at the 5' cap region. *Oncogene Res* 1991; 6: 13–19.
8 Monia BP, Johnston JF, Geiger T, et al. Antitumor activity of a phosphorothioate antisense oligodeoxynucleotide targeted against C-raf kinase. *Nat Med* 1996; 2: 668–75.
9 Ziegler A, Luedke GH, Fabbro D, et al. Induction of apoptosis in small-cell lung cancer cells by an antisense oligodeoxynucleotide targeting the Bcl-2 coding sequence. *J Nat Cancer Inst* 1997; 89: 1027–36.
10 Milner N, Mir KU, Southern EM. Selecting effective antisense reagents on combinatorial oligonucleotide arrays. *Nat Biotechnol* 1997; 15: 537–41.
11 Ho SP, Bao Y, Lesher T, et al. Mapping of RNA accessible sites for antisense experiments with oligonucleotide libraries. *Nat Biotechnol* 1998; 16: 59–63.
12 Mathews DH, Sabina J, Zuker M, Turner DH. Expanded sequence dependence of thermodynamic parameters improves prediction of RNA secondary structure. *J Mol Biol* 1999; 288: 911–40.
13 Tu GC, Cao QN, Zhou F, Israel Y. Tetranucleotide GGGA motif in primary RNA transcripts. Novel target site for antisense design. *J Biol Chem* 1998; 273: 25125–31.

14 Crooke ST. Molecular mechanisms of antisense drugs: RNase H. *Antisense Nucleic Acid Drug Dev* 1998; 8: 133–34.

15 Agrawal S. Importance of nucleotide sequence and chemical modifications of antisense oligonucleotides. *Biochim Biophys Acta* 1999; 1489: 53–68.

16 Krieg AM, Yi AK, Hartmann G. Mechanisms and therapeutic applications of immune stimulatory cpG DNA. *Pharmacol Ther* 1999; 84: 113–20.

17 Hoke GD, Draper K, Freier SM, et al. Effects of phosphorothioate capping on antisense oligonucleotide stability, hybridization and antiviral efficacy versus herpes simplex virus infection. *Nucleic Acid Res* 1991; 19: 5743–38.

18 Martin P. A new access to 2'-O-alkylated ribonucleosides and properties of 2'-O-alkylated oligoribonucleotides. *Helvetica Chimica Acta* 1995; 78: 486–504.

19 Kandimalla ER, Manning A, Zhao Q, et al. Mixed backbone antisense oligonucleotides: design, biochemical and biological properties of oligonucleotides containing 2'-5'-ribo- and 3'- 5'-deoxyribonucleotide segments. *Nucleic Acid Res* 1997; 25: 370–78.

20 Wahlestedt C, Salmi P, Good L, et al. Potent and nontoxic antisense oligonucleotides containing locked nucleic acids *Proc Natl Acad Sci USA* 2000; 97: 5633–38.

21 Wang H, Cai Q, Zeng X, et al. Antitumor activity and pharmacokinetics of a mixed-backbone antisense oligonucleotide targeted to the Rlalpha subunit of protein kinase A after oral administration. *Proc Natl Acad Sci USA* 1999; 96: 13989–94.

22 Hanahan D, Weinberg RA. The hallmarks of cancer. *Cell* 2000; 100: 57–70.

23 Adams JM, Cory S. The BCL-2 protein family: arbiters of cell survival. *Science* 1998; 281: 1322–26.

24 Folkman J. The role of angiogenesis in tumor growth. *Semin Cancer Biol* 1992; 3: 65–71.

25 John A, Tuszynski G. The role of matrix metalloproteinases in tumor angiogenesis and tumor metastasis. *Pathol Oncol Res* 2001; 7: 14–23.

26 Stein CA. Is irrelevant clevage the price of antisense efficacy? *Pharmacol Ther* 2000; 85: 231–36.

27 Webb A, Cunningham D, Cotter F, et al. BCL-2 antisense therapy in patients with non-Hodgkin lymphoma. *Lancet* 1997; 349: 1137–41.

28 Waters JS, Webb A, Cunningham D, et al. Phase I clinical and pharmacokinetic study of BCL-2 antisense oligonucleotide therapy in patients with non-Hodgkin's lymphoma. *J Clin Oncol* 2000; 18: 1812–23.

29 Jansen B, Schlagbauer-Wadl H, Brown BD, et al. BCL-2 antisense therapy chemosensitizes human melanoma in SCID mice. *Nature Med* 1998; 4: 232–34.

30 Zangemeister-Wittke U, Leech SH, Olie RA, et al. A novel bispecific antisense oligonucleotide inhibiting both BCL-2 and BCL-XL expression efficiently induces apoptosis in tumor cells. *Clin Cancer Res* 2000; 6: 2547–55.

31 Jansen B, Wacheck V, Heere-Ress E, et al. Chemosensitisation of malignant melanoma by BCL-2 antisense therapy. *Lancet* 2000; 356: 1728–33.

32 Boise LH, González-Garcia M, Postema CE, et al. BCL-X, a BCL-2-related gene that functions as a dominant regulator of apoptotic cell death. *Cell* 1993; 74: 597–608.

33 Leech SH, Olie RA, Gautschi O, et al. Induction of apoptosis in lung-cancer cells following BCL-XL antisense treatment. *Int J Cancer* 2000; 86: 570–76.

34 Simoes-Wust AP, Olie RA, Gautschi O, et al. BCL-XL antisense treatment induces apoptosis in breast carcinoma cells. *Int J Cancer* 2000; 87: 582–90.

35 Lebedeva I, Rando R, Ojwang J, et al. BCL-XL in prostate cancer cells: effects of overexpression and down-regulation on chemosensitivity. *Cancer Res* 2000; 60: 6052–60.

36 Taylor JK, Zhang QQ, Wyatt JR, Dean NM. Induction of endogenous BCL-XS through the control of BCL-X pre-mRNA splicing by antisense oligonucleotides. *Nat Biotechnol* 1999; 17: 1097–100.

37 Gautschi O, Tschopp S, Olie RA, et al. Activity of a novel BCL-2/BCL-XL-bispecific antisense oligonucleotide against tumors of diverse histologic origins. *J Natl Cancer Inst* 2001; 93: 463–71.

38 Yuspa SH, Dlugosz AA, Cheng CK, et al. Role of oncogenes and tumor suppressor genes in multistage carcinogenesis. *J Invest Dermatol* 1994; 103: 90S–5S.

39 Yazaki T, Ahmad S, Chahlavi A, et al. Treatment of glioblastoma U-87 by systemic administration of an antisense protein kinase C-alpha phosphorothioate oligodeoxynucleotide. *Mol Pharmacol* 1996; 50: 236–42.

40 Geiger T, Muller M, Dean NM, Fabbro D. Antitumor activity of a PKC-alpha antisense oligonucleotide in combination with standard chemotherapeutic agents against various human tumors transplanted into nude mice. *Anticancer Drug Des* 1998; 13: 35–45.

41 Cotter FE. Antisense oligonucleotides for haematological malignancies. *Haematologica* 1999; 84: 19–22.

42 Alavi JB, Grossman SA, Supko J, et al. Efficacy, toxicity, and pharmacology of an antisense oligonucleotide directed against protein kinase C-alpha (ISIS 3521) delivered as a 21 day continous intravenous infusion in patients with recurrent high grade astrocytomas (HGA). *Proc Am Soc Clin Oncol* 2000; 19: 167.

43 Yuen A, Advani R, Fisher G, et al. A phase I/II trial of ISIS 3521, an antisense inhibitor of protein kinase C alpha, combined with carboplatin and paclitaxel in patients with non-small-cell lung cancer. *Am Soc Clin Oncol* 2000; 19: 459a.

44 Yuen A, Halsey J, Lum B, et al. Phase I/II trial of ISIS 3521, an antisense inhibitor of PKC, with carboplatin and paclitaxel in non-small cell lung cancer. *Clin Cancer Res* 2000; 6 (suppl): 4572s.

45 Tamm I, Dorken B, Hartmann G. Antisense therapy in oncology: new hope for an old idea? *Lancet* 2001; 358: 489–97.

46 Howe LR, Leevers SJ, Gomez N, et al. Activation of the MAP kinase pathway by the protein kinase raf. *Cell* 1992; 71: 335–42.

47 Kasid U, Pfeifer A, Brennan T, et al. Effect of antisense c-RAF-1 on tumorigenicity and radiation sensitivity of a human squamous carcinoma. *Science* 1989; 243: 1354–56.

48 Stevenson JP, Yao KS, Gallagher M, et al. Phase I clinical/pharmacokinetic and pharmacodynamic trial of the c-RAF-1 antisense oligonucleotide ISIS 5132 (CGP 69846A) *J Clin Oncol* 1999; 17: 2227–36.

49 Cunningham CC, Holmlund JT, Schiller JH, et al. A phase I trial of c-RAF kinase antisense oligonucleotide ISIS 5132 administered as a continuous intravenous infusion in patients with advanced cancer. *Clin Cancer Res* 2000; 6: 1626–31.

50 Oza AM, Eisenhauer E, Swenerton K, et al. Phase II study of c-RAF kinase antisense oligonucleotide ISIS 5132 in patients with recurrent ovarian cancer. *Clin Canc Res* 2000; 6 (suppl): 4572.

51 Bradbury AW, Carter DC, Miller WR, et al. Protein kinase A (PKA) regulatory subunit expression in colorectal cancer and related mucosa. *Br J Cancer* 1994; 69: 738–42.

52 Ciardiello F, Caputo R, Bianco R, et al. Cooperative inhibition of renal cancer growth by anti-epidermal growth factor receptor antibody and protein kinase A antisense oligonucleotide. *J Natl Cancer Inst* 1998; 90: 1087–94.

53 Tortora G, Bianco R, Damiano V, et al. Oral antisense that targets protein kinase A cooperates with taxol and inhibits tumor growth, angiogenesis, and growth factor production. *Clin Cancer Res* 2000; 6: 2506–12.

54 Bishop MR, Jackson JD, Tarantolo SR, et al. Ex vivo treatment of bone marrow with phosphorothioate oligonucleotide OL(1)p53 for autologous transplantation in acute myelogenous leukemia and myelodysplastic syndrome. *J Hematother* 1997; 6: 441–46.

55 Tortora G, Caputo R, Damiano V, et al. A novel MDM2 anti-sense oligonucleotide has anti-tumor activity and potentiates cytotoxic drugs acting by different mechanisms in human colon cancer. *Int J Cancer* 2000; 88: 804–09.

56 Biedenkapp H, Borgmeyer U, Sippel AE, Klempnauer KH. Viral myb oncogene encodes a sequence-specific DNA-binding activity. *Nature* 1988; 335: 835–37.

57 Barletta C, Pelicci PG, Kenyon LC, et al. Relationship between the c-MYB locus and the 6q-chromosomal aberration in leukemias and lymphomas. *Science* 1987; 235: 1064–67.

58 Ratajczak MZ, Hijiya N, Catani L, et al. Acute- and chronic-phase chronic myelogenous leukemia colony-forming units are highly sensitive to the growth inhibitory effects of c-MYB antisense oligodeoxynucleotides. *Blood* 1992; 79: 1956–61.

59 MacLeod AR, Rouleau J, Szyf M. Regulation of DNA methylation by the RAS signaling pathway. *J Biol Chem* 1995; 270: 11327–37.

60 Ramchandani S, MacLeod AR, Pinard M, et al. Inhibition of tumorigenesis by a cytosine-DNA, methyltransferase, antisense oligodeoxynucleotide. *Proc Natl Acad Sci USA* 1997; 94: 684–89.

61 Siu LL, Gelmon KA, Moore MJ, et al. A phase I and pharmacokinetik (PK) study of the human DNA methyltransferase (Metase) antisense oligodeoxynucleotide MG98 given as a 21-day continous infusion every 4 weeks. *Proc Am Soc Clin Oncol* 2000l; 19: 250.

62 Skorski T, Nieborowska-Skorska M, Nicolaides NC, et al. Suppression of Philadelphia1 leukemia cell growth in mice by BCR-ABL antisense oligodeoxynucleotide. *Proc Natl Acad Sci USA* 1994; **91**: 4504–08.

63 de Fabritiis P, Petti MC, Montefusco E, et al. BCR-ABL antisense oligodeoxynucleotide in vitro purging and autologous bone marrow transplantation for patients with chronic myelogenous leukemia in advanced phase. *Blood* 1998; **91**: 3156–62.

64 Humphreys DT, Carver JA, Easterbrook-Smith SB, Wilson MR. Clusterin has chaperone-like activity similar to that of small heat shock proteins. *J Biol Chem* 1999; 274: 6875–81.

65 Miyake H, Chi KN, Gleave ME. Antisense TRPM-2 oligodeoxynucleotides chemosensitize human androgen-independent PC-3 prostate cancer cells both in vitro and in vivo. *Clin Cancer Res* 2000; **6**: 1655–63.

66 Li F, Ambrosini G, Chu EY, et al. Control of apoptosis and mitotic spindle checkpoint by survivin. *Nature* 396, 580-583. 1998.

67 Olie RA, Simoes-Wust AP, Baumann B, et al. A novel antisense oligonucleotide targeting survivin expression induces apoptosis and sensitizes lung cancer cells to chemotherapy. *Cancer Res* 2000; **60**: 2805–09.

68 Saleh M, Posey J, Pleasani L, et al. A phase II trial of ISIS 2503, an antisense inhibitor of h-RAS, as first line therapy for advanced colorectal carcinoma. *Proc Am Soc Clin Oncol* 2000; **19**: 320.

69 Bos JL. RAS oncogenes in human cancer: a review. *Cancer Res* 1989; **49**: 4682–89.

70 Miyake H, Pollak M, Gleave ME. Castration-induced up-regulation of insulin-like growth factor binding protein-5 potentiates insulin-like growth factor-I activity and accelerates progression to androgen independence in prostate cancer models. *Cancer Res* 2000; **60**: 3058–64.

71 Nickerson T, Miyake H, Gleave ME, Pollak M. Castration-induced apoptosis of androgen-dependent shionogi carcinoma is associated with increased expression of genes encoding insulin-like growth factor-binding proteins. *Cancer Res* 1999; **59**: 3392–95.

72 Kinoshita H, Yoshikawa H, Shiiki K, et al. Cisplatin (CDDP) sensitizes human osteosarcoma cell to Fas/CD95- mediated apoptosis by down-regulating FLIP-L expression. *Int J Cancer* 2000; **88**: 986–91.

73 Nylandsted J, Rohde M, Brand K, et al. Selective depletion of heat shock protein 70 (Hsp70) activates a tumor-specific death program that is independent of caspases and bypasses BCL-2. *Proc Natl Acad Sci USA* 2000; **97**: 7871–76.

74 Davies H, Bignell GR, Cox C, et al. Mutations of the BRAF gene in human cancer. *Nature* 2002; **417**: 949–54.

75 McGill GG, Horstmann M, Widlund HR, et al. BCL-2 regulation by the melanocyte master regulator Mitf modulates lineage survival and melanoma cell viability. *Cell* 2002; **109**: 707–18.

Clinical picture

Subcutaneous seeding of pancreatic carcinoma along a VP shunt catheter

Hiroshi Nawashiro, Naoki Otani, Hiroshi Katoh, Akira Ohnuki, Sho Ogata, and Katsuji Shima

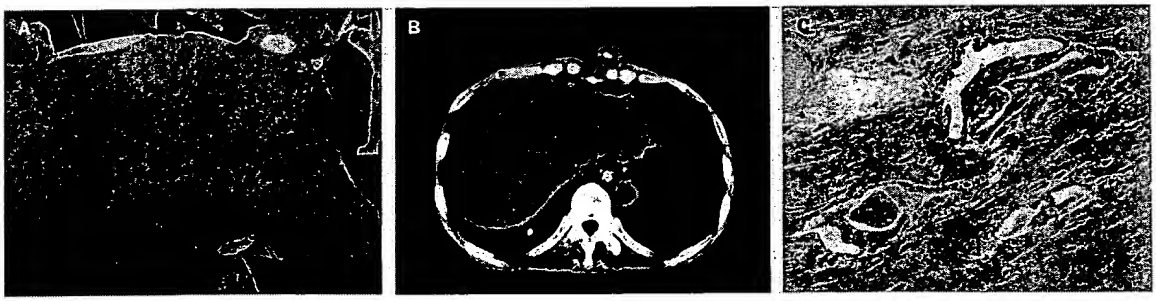

A 61-year-old woman presented with subarachnoid haemorrhage 3 years ago and had a ventriculoperitoneal (VP) shunt inserted to treat normal-pressure hydrocephalus, after which she regained normal daily activity. She later presented with a subcutaneous painless mass along a VP-shunt catheter (figure a). A computed tomography scan of her abdomen showed ascites, free air, and an isodensity mass around the catheter on the anterior abdominal wall (figure b). She underwent an emergency exploratory laparotomy and was subsequently diagnosed with a pancreatic carcinoma. Histopathological examination of the skin around the catheter showed a small number of neoplastic glands in the fibrotic background (figure c). These features are consistent with metastatic adenocarcinoma of pancreatic origin. It is well known that a VP shunt as an artificial link between vessels can facilitate the spread of brain tumour cells in the cerebrospinal fluid. Similarly, iatrogenic spread of malignancy may occur along a VP shunt catheter. This is the first case of VP-shunt-related skin metastasis of aggressive pancreatic carcinoma.

Correspondence: Dr Hiroshi Nawashiro, Department of Neurosurgery National Defense Medical College, 3–2 Namiki, Tokorozawa, Saitama 359-8513, Japan. Tel: +81 42 995 1656. Fax: +81 42 996 5207. Email: nawa1957@me.ndmc.ac.jp

EXHIBIT G

Cytokine Review

Exhibit G

Suppression of Gene Expression by Targeted Disruption of Messenger RNA: Available Options and Current Strategies

KUANG-YU JEN,[a] ALAN M. GEWIRTZ[b]

[a]Department of Cell and Molecular Biology, University of Pennsylvania School of Medicine, the [b]Department of Medicine and the Cancer Center, University of Pennsylvania School of Medicine, Philadelphia, Pennsylvania, USA

Key Words. *RNA · DNA oligonucleotide · Hammerhead ribozymes · Hairpin ribozymes · Gene targeting · Targeted gene disruption · Antisense*

ABSTRACT

At least three different approaches may be used for gene targeting including: A) gene knockout by homologous recombination; B) employment of synthetic oligonucleotides capable of hybridizing with DNA or RNA, and C) use of polyamides and other natural DNA-bonding molecules called lexitropsins.

Targeting mRNA is attractive because mRNA is more accessible than the corresponding gene. Three basic strategies have emerged for this purpose, the most familiar being to introduce antisense nucleic acids into a cell in the hopes that they will form Watson-Crick base pairs with the targeted gene's mRNA. Duplexed mRNA cannot be translated, and almost certainly initiates processes which lead to its destruction. The antisense nucleic acid can take the form of RNA expressed from a vector which has been transfected into the cell, or take the form of a DNA or RNA oligonucleotide which can be introduced into cells through a variety of means. DNA and RNA oligonucleotides can be modified for stability as well as engineered to contain inherent cleaving activity.

It has also been hypothesized that because RNA and DNA are very similar chemical compounds, DNA molecules with enzymatic activity could also be developed. This assumption proved correct and led to the development of a "general-purpose" RNA-cleaving DNA enzyme. The attraction of DNAzymes over ribozymes is that they are very inexpensive to make and that because they are composed of DNA and not RNA, they are inherently more stable than ribozymes.

Although mRNA targeting is impeccable in theory, many additional considerations must be taken into account in applying these strategies in living cells including mRNA site selection, drug delivery and intracellular localization of the antisense agent. Nevertheless, the ongoing revolution in cell and molecular biology, combined with advances in the emerging disciplines of genomics and informatics, has made the concept of nontoxic, cancer-specific therapies more viable than ever and continues to drive interest in this field. Stem Cells *2000;18:307-319*

INTRODUCTION

The notion that gene expression could be modified through use of exogenous nucleic acids derives from studies by *Paterson et al.* who first used single-stranded DNA to inhibit translation of a complementary RNA in a cell-free system in 1977 [1]. One year later, *Zamecnik* and *Stephenson* noted that a short (13nt) DNA oligonucleotide reverse complementary in sequence (antisense) to the Rous sarcoma virus could inhibit viral replication in culture [2]. This observation is credited as being among the first to suggest the therapeutic utility of antisense nucleic acids, a concept which ultimately led to the awarding of a Lasker Prize in Medicine to *Dr. Zamecnik*. In the mid 1980s, the existence of naturally occurring antisense RNAs and their role in regulating gene expression was demonstrated [3-5]. These observations were particularly important because the

Correspondence: Alan M. Gewirtz, M.D., Rm 713 BRBII/III, University of Pennsylvania School of Medicine, 421 Curie Boulevard, Philadelphia, Pennsylvania 19104, USA. Telephone: 215-898-4490; Fax: 512-573-2078; e-mail: gewirtz@mail.med.upenn.edu
Received July 18, 2000; accepted for publication July 18, 2000. ©AlphaMed Press 1066-5099/2000/$5.00/0

fact that naturally occurring antisense nucleic acids played a role in regulating gene expression lent support to the belief that exogenously introduced reverse complementary nucleic acids might be utilized to manipulate gene expression in living cells. These seminal papers, and the literally thousands which have followed, have stimulated the development of technologies employing nucleic acids to manipulate gene expression. Virtually all available methods rely on some type of nucleotide sequence recognition for targeting specificity, but differ where and how they perturb the flow of genetic information [6]. Simply stated, strategies for modulating gene expression may be thought of as being targeted to the gene itself, or to the gene's messenger RNA (mRNA). Since this review will be focused on strategies aimed at disrupting the use of mRNA, antigene strategies will be addressed only briefly and mainly for the sake of completeness.

ANTIGENE STRATEGIES

At least three different approaches may be utilized for direct gene targeting. The "gold standard" is the gene "knock-out" achieved by homologous recombination [7, 8]. This approach results in the actual physical disruption of the targeted gene as a result of crossover events which occur during cell division between the targeting vector and the gene selected for destruction (Fig. 1A). Homologous recombination is extremely powerful, but the technique is hampered by the fact that it remains inherently inefficient, time-consuming, and expensive. While improvement in the efficiency of this process has been achieved [9, 10], this is a method which remains restricted to use in cell lines and animal models, if for no other reason than selection is required to find the cells in which the desired events have taken place. In clinical situations where high efficiency gene disruptions are required, it seems unlikely that this approach will serve as a useful therapeutic modality anytime in the foreseeable future.

A second option for gene targeting employs synthetic oligodeoxynucleotides (ODN) capable of hybridizing with double-stranded DNA [11-13]. Such hybrids are typically formed within the major groove of the helix, though hybridization within the minor groove has also been reported [14]. In either case, a triple-stranded molecule is produced, hence the origin of the term triple helix-forming oligodeoxynucleotide (TFO) (Fig. 1B). TFOs do not destroy a gene but prevent its transcription either by preventing unwinding of the duplex or preventing binding of transcription factors to the gene's promoter. TFO sequence requirements are based on the need for each base comprising the TFO to form two hydrogen bonds (Hoogsteen bonds) with its complementary base in the duplex. This constrains TFOs to hybridization with the purine bases composing polypurine-polypyrimidine tracks within the DNA. The targeting efficiency of TFOs is further constrained by a number of factors, including need for divalent cations, and perhaps most importantly, by access to DNA compacted within the chromosome structure. Recent experiments from *Wang et al.* and *Kochetkova et al.* have provided evidence that triple helix formation can occur in living cells, suggesting that these difficulties may ultimately be overcome [15-17]. If shown practical, it has also been postulated that TFOs may prove useful in the treatment of certain genetic disorders such as sickle cell anemia, and hemophilia B, where their ability to trigger repair mechanisms might be used to correct single base pair mutations responsible for the disease [15, 18-20].

Final approaches worth mentioning are the use of specific nucleic acid sequences to act as "decoys" for transcription factors [21, 22], and the use of polyamides and

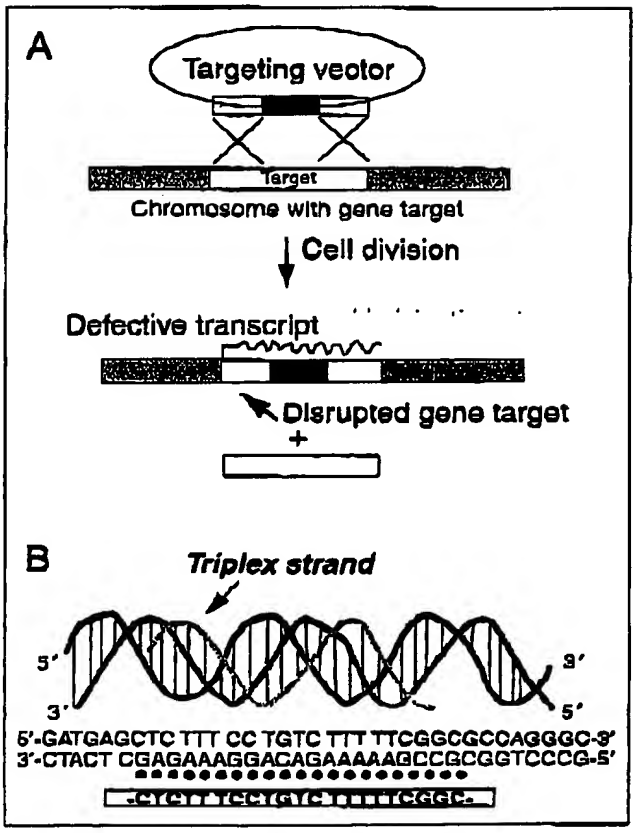

Figure 1. A) Targeting vector; B) Triplex strand. Adapted from [6].

other natural DNA-binding molecules called lexitropsins, that bind to specific bases in the minor groove of DNA [23, 24]. The use of decoy molecules evolves from the knowledge that transcription factor proteins recognize and bind specific DNA sequences. In theory then, it is possible to synthesize nucleic acids which will effectively compete with the native DNA sequences for available transcription factor proteins in vivo. If effective, the rate of transcription of the genes dependent on the particular factor involved will diminish. Unless single gene transcription factors can be identified, it is difficult to conceive how this approach, though potentially effective for controlling cell growth, can be made gene-specific. The polyamide approach may prove feasible since sequence-specific molecules can likely be designed and it appears that molecules of this type can easily access DNA within the chromosomes [23-25].

Anti-mRNA Strategies

A gene may be effectively "silenced" by destabilizing its mRNA, thereby preventing synthesis of the protein it encodes. Targeting mRNA, while less favorable than antigene strategies from a stoichiometric point of view, is nonetheless attractive because mRNA is in theory more accessible. Three basic strategies have emerged for this purpose. One employs an oligonucleotide that acts as an alternate binding site, or "decoy," for protein-stabilizing elements that normally interact with a given mRNA [26, 27]. By attracting away mRNA-stabilizing protein, the decoy induces instability, and ultimately destruction, of the mRNA. A newly developing approach is to affect RNA interference (RNAi) or post-transcriptional gene silencing [28, 29]. RNAi employs a gene-specific double-stranded RNA which, when introduced into a cell, leads to diminution of the targeted mRNA. The actual mechanism whereby this is accomplished is presently unknown but is under intense investigation with several clues being deciphered already [30, 31] including size and necessity for processing of the targeting dsRNA. In *C. elegans* and Drosophila this is a highly reproducible method for disrupting gene expression. Some reports suggest that this technique can be adapted for use in mammalian cells [32], but this remains uncertain at the moment. Finally, there is the more familiar, and more widely applied "antisense" strategy. We will focus on the latter.

Antisense (reverse complementary) nucleic acids are introduced into a cell in hopes that they will form Watson-Crick base pairs with the targeted gene's mRNA. As stated above, duplexed mRNA cannot be translated, and almost certainly initiates processes which lead to its destruction. The antisense nucleic acid can take the form of RNA expressed from a vector which has been transfected into the cell [33], or take the form of a DNA or RNA oligonucleotide which can be introduced into cells through a variety of means. DNA and RNA oligonucleotides can be modified for stability as well as engineered to contain inherent cleaving activity [34, 35]. A number of these issues will be discussed in more detail in the sections below.

Antisense Oligonucleotides (AS-ONs)

AS-ONs are short stretches of nucleotides that are complementary to a region of targeted mRNA and can specifically suppress expression of that particular transcript. The following discussion will focus on the fundamental concepts concerning AS-ONs and their mechanisms of action. Examples of AS-ON use in experimental and clinical settings have been recently reviewed [36-38].

The exact mechanism of AS-ON action remains unclear, but it is known to be different for various types of AS-ONs. Generally, these molecules block gene expression by hybridizing to the target mRNA, resulting in subsequent double-helix formation. This process can occur at any point between the conclusion of transcription and initiation of translation, or even possibly during translation. Disruption of splicing, transport, or translation of the transcripts are all possible mechanisms, as is stability of transcript. Therefore, a major question is whether AS-ONs are most effective in the cytoplasm or nucleus. In the case of antisense oligodeoxyribonucleotides (AS-ODNs), cellular RNase H is able to bind to the DNA-RNA duplex and hydrolyze the RNA, resulting in increased transcript turnover. Any modification to the deoxy moiety at the 2'-sugar position prohibits RNase H action.

Modified AS-ONs or AS-ON analogs are often employed for in vivo antisense applications due to their increased stability and nuclease resistance. A longer serum half-life ensures that the AS-ON has ample time to reach and interact with its target mRNA. Phosphorothioate AS-ODNs are most widely used due to their long serum half-life and the fact that they are a suitable RNase H substrate. However, phosphorothioates display high affinity for various cellular proteins, which can result in sequence-nonspecific effects [39, 40]. Furthermore, high concentrations of phosphorothioates inhibit DNA polymerases and RNase H, which may render them ineffective as antisense agents [41]. Interestingly, many AS-ONs with 2'-modifications with groups such as O-methyl, fluoro, O-propyl, O-allyl, or many others exhibit greater duplex stability with their target mRNA along with antisense effects independent of RNase H (Fig. 1). These modifications create bulk at the 2' position, causing steric hindrance to play a significant role in increasing nuclease resistance. Nucleotide analogs

generally are also nuclease-resistant and often demonstrate superior hybridization properties due to modified backbone charge, although they usually are not acceptable substrates for RNase H. One example is peptide nucleic acid (PNA) where the sugar-phosphate moiety has been replaced by 2-aminoethyl glycine carbonyl units [42]. To these units are attached nucleotide bases spaced equally apart to DNA nucleotide bases. Instead of phosphodiester linkages between nucleotides, peptide bonds join the monomers to create a backbone neutral in charge. Not only do PNA oligomers hybridize to complementary DNA and RNA by Watson-Crick base pairing, they do so more quickly [43] and with greater affinity [42-44] because of the neutral backbone. In addition, PNAs are better at discriminating between base pair mismatches [44] and form less nonsequence-specific associations with proteins than phosphorothioate oligonucleotides [45]. Positive charges can also be introduced to backbone structure as in the case of (2-aminoethyl)phosphonates. Increased stability of duplex formation with both RNA and DNA has been reported with hybrid stability being more pH-dependent and less salt-dependent than natural RNA or DNA duplexes [46].

Some insight into the mechanism of AS-ON action has emerged recently through the work of *Baker* and colleagues (unpublished). Differences in ability to inhibit gene expression occur when either 2'-modified AS-ONs or 2'-unmodified AS-ONs are targeted to the exon 9 region of interleukin 5 (IL-5). Two forms of IL-5 exist: a soluble IL-5 lacking the exon 9 region, and a membrane-bound form, which contains exon 9. When unmodified AS-ONs are targeted to exon 9 of the IL-5 transcript, the expression of both membrane-bound and soluble IL-5 is inhibited. However, 2'-modified AS-ONs only suppress membrane-bound IL-5 expression. These observations seem to suggest that RNase H-dependent antisense effects are a nuclear event prior to splicing, whereas RNase H-independent oligonucleotides may affect splicing in transcript processing or may suppress gene expression after splicing has taken place. Additional evidence demonstrates that in the absence of RNase H activity, antisense effects may be a result of interference with translational initiation complex formation for certain types of 2'-modified AS-ON such as 2'-O-(2-methoxy) ethyl AS-ONs [47].

Ribozymes

Naturally occurring ribozymes are catalytic RNA molecules that have the ability to cleave phosphodiester linkages without the aid of protein-based enzymes. This property has been exploited to specifically inhibit gene expression by targeting mRNA for catalytic cleavage especially in viral, cancer, and genetic disease therapeutics [48]. Similar to AS-ONs, ribozymes bind to substrate RNA through Watson-Crick base pairing, which offers sequence-specific cleavage of transcripts. Ideally, these agents should trigger enhanced transcript turnover as compared to RNase H-mediated AS-ON degradation of transcripts, considering ribozymes act through bimolecular kinetics (association of ribozyme and target transcript) whereas RNase H-dependent AS-ONs rely on trimolecular kinetics (association of AS-ON, target transcript, and RNase H). Since ribozymes are RNase H-independent, 2'-modifications to increase stability do not diminish antisense effects and experiments have shown some modifications do not attenuate catalytic ability [49]. Unlike AS-ONs, ribozymes can be expressed from a vector, which offers the advantage of continued production of these molecules intracellularly [50, 51]. However, stable transformation of cells in vivo has its own complications and will not be discussed in this review.

If ribozymes are to perform effectively as "enzymes," they must not only bind substrate RNA but also dissociate from the cleavage product in order to act on additional substrates. Studies suggest that in some cases, dissociation of cleavage product may be the rate-limiting step [52, 53]. Furthermore, some ribozymes require high divalent metal ion concentrations for efficient substrate cleavage, which may limit their use in intracellular environments [54]. All of these concerns need to be addressed and overcome in order for ribozymes to have a future in medical therapy. Two ribozymes, the hammerhead ribozyme and the hairpin ribozyme, have been extensively studied due to their small size and rapid kinetics. Their application has been recently reviewed in several publications [55-59].

Hammerhead Ribozymes

The hammerhead ribozyme consists of a highly conserved catalytic core, which will cleave substrate RNA at NUH triplets 3' to the H, where N is any nucleotide, U is uracile, and H is any nucleotide but guanidine (Fig. 2) [34]. In fact RNA cleavage may be less restricted since recent studies demonstrate exceptions to the "NUH" rule. Investigators have established that cleavage can actually occur 3' to any NHH triplet [59]. Furthermore, in vitro selection protocols have made it possible to screen for ribozymes with various cleavage specificities including one that cleaves at AUG sites [60]. Thus, the limitations for sequence specificity of triplet-cleavage sites on the target RNA are less than previously thought. In addition to the catalytic core, a particular cleavage site in a target RNA can be specifically recognized by the hammerhead ribozyme arms. By creating complementary sequences in the arms to sequences flanking the cleavage site, the ribozyme will hybridize specifically to the RNA of interest.

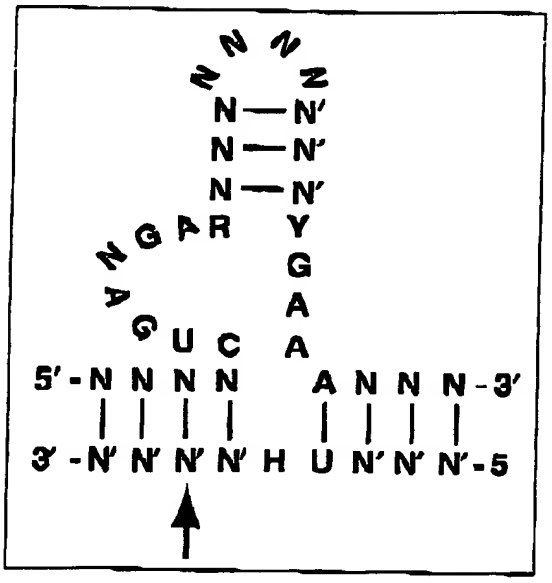

Figure 2. Hammerhead ribozyme (top strand) hybridized to target RNA. Arrow indicates position of cleavage. N = A, G, T, or C; N' = nucleotide complementary to N; H = any nucleotide but G; Y = pyrimidine nucleotide; R = purine nucleotide complementary to Y. Adapted from [56].

Subsequent cleavage will then be directed towards that particular position.

The catalytic ability of hammerhead ribozymes is dependent on the presence of divalent metal ions, of which magnesium is most often used in vitro. It is postulated that the ions not only participate in RNA folding but also in the cleavage step itself [54]. As mentioned previously, studies indicate that catalytic activity requires relatively high Mg^{2+} concentrations compared to the intracellular environment. This characteristic could be problematic in applying the hammerhead ribozyme to an in vivo setting where intracellular Mg^{2+} concentrations are 5- to 10-fold lower than optimal in vitro conditions.

Much evidence supports diminished mRNA levels and gene products directly due to hammerhead ribozyme delivery. There is also indication from reverse transcriptase-polymerase chain reaction (RT-PCR) and reverse ligation (RL)-PCR protocols of messenger RNA cleavage at the targeted position in cellular RNA extracts [61, 62]. Recently, more potent ribozyme-mediated effect on viral and cancer cell growth compared to noncatalytic RNAs was reported [63, 64]. However, in some instances, hammerhead ribozymes have not proven to be more effective than AS-ON and instead give equal degrees of gene suppression. Likewise, inactive control ribozymes where antisense binding can occur, but catalytic ability has been abolished, give similar levels of gene inhibition when compared to fully catalytic hammerhead ribozymes, suggesting that the catalytic core, in some instances, plays little role in enhancing antisense effects [65]. Only further detailed studies will reveal the true utility of hammerhead ribozymes.

Hairpin Ribozymes

The natural hairpin ribozyme is derived from a negative strand of the tobacco ringspot virus satellite RNA. Work on engineered hairpin ribozymes has resulted in a broader range of cleavage-sequence specificity. In general, a phosphodiester cleavage takes place 5' to the G in the sequence NGUC where N is any nucleotide [66], although recent studies have shown even less restriction on sequence requirements for cleavage [67].

The overall structure of the hairpin ribozyme consists of two domains connected by a hinge section (Fig. 3). One domain binds the substrate RNA to form two helical regions separated by a pair of single-stranded loops. Cleavage occurs within the single-stranded area of the substrate RNA. The other domain is similar in structure except the helixes are formed from the ribozyme folding back onto itself. The most important sequences for cleavage activity are those within the single-stranded regions where almost every nucleotide is conserved, while the helical portions can be almost any sequence as long as there is double-helix formation [58]. The hinge allows the two domains to be flexible relative to one another in space so that the two can dock together in an antiparallel orientation required for cleavage catalysis [68, 69].

Both the hairpin and hammerhead ribozymes require metal ions for cleavage catalysis. In the hammerhead ribozyme, metal ions are believed to be involved directly in the cleavage step [54, 70], whereas metal ions have not been implicated to be directly involved with cleavage for the hairpin ribozyme [71]. The metal ions in hairpin ribozymes may instead play an important role in ribozyme structure [72]. Fluorescence resonance energy transfer (FRET) studies on docking of the two domains show that docking is metal-dependent, but almost any metal will suffice even though they may not support cleavage [73]. In addition, docking is not the rate-limiting step, and since metal ions are not thought to be involved in the chemical cleavage step, it can only be assumed that there is a slower step in between docking and chemical cleavage.

One of the advantages offered by hairpin ribozymes is their unique ion-dependence for catalytic action. One group has shown that aminoglycoside antibiotics with at least four amino groups are able to both support and to

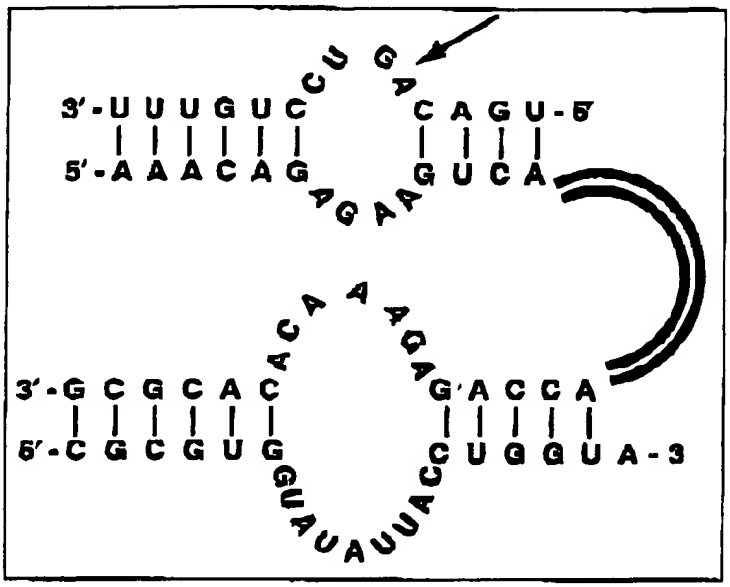

Figure 3. Hairpin ribozyme in the docked position. The two loop regions associate with each other in order to cleave the substrate RNA. Arrow indicates position of cleavage. Adapted from [58].

inhibit hairpin ribozyme cleavage depending on metal ion conditions [74]. In the presence of magnesium, aminoglycoside antibiotics inhibit ribozyme cleavage with the degree of inhibition depending on the binding affinity of the antibiotic to the ribozyme. However, in the absence of metal ions, aminoglycoside antibiotics prove to assist cleavage with an optimum reaction condition at pH 5.5 and poorer kinetics as the pH is increased, exactly opposite to trends observed for magnesium. In this case, the metal ions are most likely being replaced by the amino groups of these antibiotics.

Polyamines such as spermidine and spermine have also been reported to support hairpin ribozyme cleavage ability. In the absence of magnesium, spermidine allows the cleavage reaction to persist at very slow kinetics compared to magnesium alone [72]. However, spermine alone gives very efficient cleavage of RNA comparable to that of magnesium, and when in the presence of low magnesium concentrations similar to intracellular conditions, spermine displays considerable increase in cleavage rates [74]. The fact that spermine is the major polyamine in eukaryotic cells may explain why the hairpin ribozyme has shown remarkable intracellular cleavage activity in mammalian cells and may make future therapeutic endeavors with the hairpin ribozyme much easier [75].

DNAzymes

While investigating ways to improve the function of ribozymes, *Breaker* and *Joyce* made the assumption that because RNA and DNA are very similar chemical compounds, DNA molecules with enzymatic activity could also be developed [76]. This assumption proved correct and led to the development of a "general-purpose" RNA-cleaving DNA enzyme [77]. The molecule was identified from a library of >1,000 different DNA molecules by successive rounds of in vitro selective amplification based on the ability of individual molecules to promote Mg^{2+}-dependent, multiturnover, cleavage of an RNA target.

The selected molecule was named the "10-23 DNA enzyme," because it was derived from the 23rd clone obtained after the 10th round of selective amplification [77]. The "10-23 DNA enzyme" is composed of a catalytic domain of 15 deoxynucleotides, flanked by 2 substrate-recognition domains of ~8 nucleotides each (Fig. 4). The recognition domains provide the sequence information required for specific binding to an RNA substrate. They also supply the binding energy required to hold the RNA substrate within the active site of the enzyme. It is straightforward that by appropriately designing the flanking sequences, the DNAzyme can be made to cleave virtually any RNA that contains a purine-pyrimidine junction.

The attraction of DNAzymes over ribozymes is that they are very inexpensive to make and that because they are composed of DNA and not RNA, they are inherently more stable

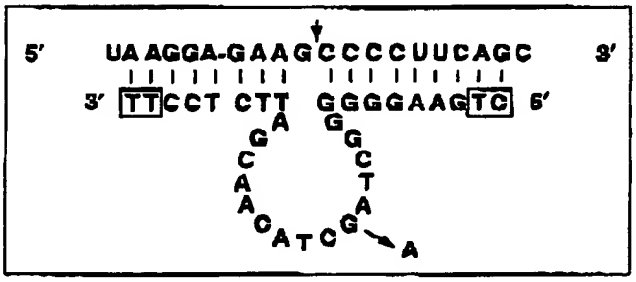

Figure 4. Complex formed by an mRNA (top strand) and a "10-23" DNAzyme (bottom strand). Vertical arrow indicates the mRNA cleavage site. Replacement of G by A within the catalytic core of the DNAzyme (diagonal arrow) will eliminate its catalytic activity. Adapted from [77].

than ribozymes. Nevertheless, DNAzymes must ultimately overcome the same problems faced by ribozymes and oligonucleotides if they are to be effective in cellular systems (see below). These are stability, ability to be targeted to the cell of interest, ability to achieve sufficient intracellular concentration to cleave to the targeted mRNA, ability to hybridize with their mRNA target, and lack of toxicity. In this regard, many of the chemical modifications employed to stabilize ODNs can be incorporated into the 10-23 DNA enzyme without loss of activity. There is a suggestion from recent reports that issues of intracellular concentration and target hybridization may also be solvable [78, 79].

Application of the "Antisense" Strategy

Although antisense interference methods appear impeccable in theory, many additional considerations must be taken into account in applying the strategy in living cells. Since both AS-ONs and ribozymes are considered oligonucleotides, quite often similar solutions can be offered to address the problems encountered. As mentioned earlier, increasing stability of antisense agents can be easily achieved through nucleotide modifications or analogs. However, additional considerations crucial to reliable experimental outcome include mRNA site selection, drug delivery, and intracellular localization of the antisense agent.

mRNA Site Selection

Within living cells, transcripts exist in low energy conformations in which secondary structures dominate in folding the linear polymer. In addition, interactions with cytoplasmic proteins produce further structural properties. The end result is that much of the mRNA sequence is hidden and only partial sequences within the total mRNA length are accessible for hybridization. RNA folding programs that generate three-dimentional folding patterns based on free energy calculations often give an unreliable depiction for in vivo relevance. Therefore, a good empirical method to probe for suitable sites is necessary.

A system to probe for suitable sites in mRNA for AS-ON or ribozyme-targeting has recently been established using RNase H cleavage as an indicator for accessibility of sequences within transcripts [80]. A mixture of ODNs that are complementary to certain regions of a transcript is added to cell extracts and exposed to RNase H. RT-PCR of the transcript can then be used to show which ODNs actually had access to the transcript and hybridized in order to create an RNase H-vulnerable site. Combining this methodology with computer-assisted sequence selection may enhance this approach as well [81].

Another technique currently being tested is the use of molecular beacons for site selection (*Gewirtz et al.*, unpublished). These molecules are ODNs with the ability to form stem-loops where the loops are targeted to regions of the transcript [82]. The stems have a fluorophore linked to either the 5′ or 3′ end and a quencher molecule is attached to the other so that in the stem-loop configuration, fluorescence is not observed due to the proximity of the quencher molecule to the fluorophore. However, when hybridization proceeds, the act of forming a double helix between the loop and the transcript causes unfolding of the stem-loop and brings the quencher and fluorophore apart in space. Thus, fluorescence should increase as a result of hybridization. Currently, these molecules are being applied to probe for accessible sites within mRNA with very encouraging results (*Jen* and *Gewirtz*, unpublished).

Delivery

One of the major limitations for the therapeutic use of AS-ONs and ribozymes is the problem of delivery. Import of these compounds into cells can be accomplished by exogenous delivery in which presynthesized oligonucleotides come in direct contact with the plasma membrane, resulting in subsequent cellular uptake [83]. Naked oligonucleotides are poorly incorporated into cells in this fashion and often require a vehicle for efficient delivery. In tissue culture, many classes of compounds have been used as delivery vehicles including cationic liposomes, cationic porphyrins, fusogenic peptides, and artificial virosomes. These compounds share the characteristic of forming complexes with oligonucleotides through electrostatic interactions between the negatively charged oligonucleotide phosphate groups and positive charges contained by the vehicles themselves. In addition, some degree of protection from nuclease degradation is conferred to the oligonucleotide when associated with such delivery vehicles. Other strategies including cell permeabilization with streptolysin-O and electroporation have been used [84] but are restricted in utility for clinical settings. Presently, some success has been achieved in tissue culture, but efficient delivery for in vivo animal studies remains questionable.

Cationic lipids form stable complexes with oligonucleotides, which exhibit improved cellular uptake [85-87]. The result is enhanced antisense activity. Further studies indicate that phosphorothioated ODNs dissociate from cationic lipids before entering the nucleus where it is free to hinder target transcript function [88]. These compounds have proven to be quite effective in cell culture and have been commercialized, but their relatively high cytotoxic properties may restrict their use.

Alternatives to cationic lipids are being explored. Recently, cationic porphyrins have proven to be effective vehicles for AS-ONs in tissue culture [89, 90]. Two cationic porphyrins used by *Bentmetskaya* and colleagues, tetra(4-methylpyridyl) porphyrin (TMP) and tetraanilinium porphyrin (TAP), demonstrate properties important for AS-ON delivery. 5'-fluorescein-labeled phosphorothioates show that both TMP and TAP more efficiently deliver AS-ONs into cells than naked AS-ONs. Nuclear fluorescence is observed after porphyrin/AS-ON complex exposure to cells while fluorescein labeled AS-ONs alone are taken up into vesicular structures. Thus, cationic porphyrins not only help AS-ON delivery into the cell, but they are also able to localize the AS-ON in the nucleus where mRNA and RNase H are present. FRET studies on the ability of cationic porphyrins to quench 5'-fluorescein-labeled phosphorothioates suggest intracellular dissociation of the oligonucleotide from the porphyrin.

Fusogenic peptides form peptide cages around oligonucleotides in order to boost oligonucleotide uptake. Many of these peptides contain polylysine residues, which cause membrane destabilization [91]. Others are derived from viral proteins such as the fusion sequence of HIV gp41 [92] and hemagglutinin envelop protein [93, 94]. Generally, these agents are less cytotoxic than lipids but are still able to achieve similar delivery efficacy. Artificial virosomes are another class of delivery vehicles which take advantage of the natural ability of a virus to gain entry into cells. Reconstituted influenza virus envelopes known as virosomes can fuse with endosomal membranes after internalization through receptor-mediated endocytosis [95]. Recently, cationic lipids have been incorporated into virosome membranes to further aid delivery [96, 97].

Finally, *Dheur* and colleagues have noted that while oligonucleotides delivered with lipofectins usually do not elicit antisense activity (likely because cationic lipid formulations do not protect unmodified oligonucleotides from nuclease degradation), a cationic polymer, polyethylenimine (PEI) [98], improves the uptake and antisense activity of antisense phosphodiester oligodeoxynucleotides (PO-ODN) [99]. Interestingly, PEI-phosphorothioate (PS) ODN particles were efficiently taken up by cells but PS-ODN did not dissociate from the carrier. These investigators suggested that the low cost of PEI compared with cytofectins, the increased affinity for target mRNA and decreased affinity for proteins of PO-ODN compared with PS-ODN might make the use of PEI-PO-ODN very attractive.

Localization

In order for AS-ONs or ribozymes to suppress gene expression, they must be colocalized to the same intracellular compartment as their target mRNA. Intracellular trafficking seems to play an important role in the fate of these molecules since their spatial distribution does not correspond to simple diffusion. Many factors determine localization patterns of AS-ON and ribozymes including the antisense agent itself, delivery vehicle, and targeted cell type. In addition, evidence for cell cycle-dependent localization patterns has been reported with nuclear localization predominantly in the G_2/M phase [100].

mRNAs can exist in several cellular compartments including the cytoplasm, nucleus, and nucleolus. It remains unclear as to where oligonucleotides should be directed for most efficient antisense activity to occur, although endosomal localization usually predicts ineffective antisense response. The optimal site for mRNA degradation may be dependent on the type of antisense agent used [47]. Recently, ribozymes attached to small nucleolar RNAs (snoRNAs) called snoribozymes exhibited nearly 100% efficiency in cleaving a target RNA also localized to the nucleolus by snoRNA attachment [101]. Even though this particular experiment is based on cleavage of an artificial substrate, the expanding roles associated with the nucleolus may prove the nucleolus to be an important site to target mRNA degradation [102]. In another study, antisense RNA inserted within a variable region of ribosomal RNA (rRNA) proved to heighten ribozyme efficiency and may be due to colocalization of rRNA with mRNA [103].

Antisense Drug Design

Certain issues to be aware of concerning antisense experimental design are quite important to the consistent and efficacious outcome of inhibiting gene expression. Even when the above considerations regarding the potential problems of antisense experiments are addressed, other factors may come into play especially involving antisense drug design. Only two will be mentioned here: formation of G quartets and chirality of modified oligonucleotides. Purine-rich oligonucleotides, especially ones containing four consecutive guinine residues, have a tendency to form stable tetrameric structures under physiologic conditions [104]. The guinosines of single-stranded oligonucleotides are not restrained in space by rigid double-helix structure and can therefore form various hydrogen bonds not observed in Watson-Crick base pairing. Tetraplexes known as G quartets arise as a result. Dissociation rates of these structures may be quite slow and may prevent hybridization of AS-ONs or ribozymes to their target transcript, rendering them ineffective as antisense agents. However, the absence of G quartet structures at 37°C under cellular salt conditions could mean that G quartet formation is irrelevant at physiologic temperatures [105].

Interestingly, nonsequence-specific gene inhibition by phosphorothioate oligonucleotides containing tetraguinosine tracts prove aptameric properties can play an important role in gene inhibition for some sequences of ONs [106].

Another important aspect to consider is the issue of chirality for certain oligonucleotides. Unmodified phosphodiester oligonucleotides do not have a chiral center at the phosphorous position. However, when a terminal oxygen of the phosphate is replaced by a sulfur, as in PS-ONs, the phosphorous gains chirality. The digestion kinetics of PS-ONs by 3'-exonucleases display bi-exponential decay with a fast and slow phase of digestion. These phases are due to stereoselectivity of the 3'-exonucleases on the chiral phosphorothioate center [107]. A 25-mer containing a 3'-terminal internucleotide linkage in the S-configuration degrades 300-fold slower than the same 25-mer with an R-configuration phosphorothioate linkage.

Conclusions

The ongoing revolution in cell and molecular biology, combined with advances in the emerging disciplines of genomics and informatics, has made the concept of non-toxic, cancer-specific therapies more viable then ever. The recent development of a relatively specific biochemical inhibitor of the bcr/abl protein tyrosine kinase in patients with chronic myelogenous leukemia is a stunning example of this principle [108]. For therapies focused on direct replacement, repair, or disabling of disease-causing genes, progress has been much slower and a successful equivalent to the biochemical bcr/abl inhibitor has yet to be achieved. In the case of anti-mRNA strategies, it is hoped that the above discussion will have made the reasons for this clearer. Given the state of the art, it is perhaps not surprising that effective and efficient clinical translation of the antisense strategy has proven elusive. While a number of phase I/II trials employing ONs have been reported [109-116], virtually all have been characterized by a lack of toxicity but only modest clinical effects. A recent paper by *Waters et al.* describing the use of a bcl-2-targeted ON in patients with non-Hodgkin's lymphoma is typical in this regard [117, 118].

The key challenges to this field have been outlined above. It is clear that they will have to be solved if this approach to specific antitumor therapy is to become a useful treatment approach. A large number of diverse and talented groups are working on this problem, and we can all hope that their efforts will help lead to establishment of this promising form of therapy.

Acknowledgment

This work was supported by grants from the NIH. *Dr. A.G.* is a distinguished Clinical Scientist of the Doris Duke Charitable Foundation.

References

1 Paterson BM, Roberts BE, Kuff EL. Structural gene identification and mapping by DNA-mRNA hybrid-arrested cell-free translation. Proc Natl Acad Sci USA 1977;74:4370-4374.

2 Stephenson ML, Zamecnik PC. Inhibition of Rous sarcoma viral RNA translation by a specific oligodeoxyribonucleotide. Proc Natl Acad Sci USA 1978;75:285-288.

3 Simons RW, Kleckner N. Translational control of IS10 transposition. Cell 1983;34:683-691.

4 Mizuno T, Chou MY, Inouye M. A unique mechanism regulating gene expression: translational inhibition by a complementary RNA transcript (micRNA). Proc Natl Acad Sci USA 1984;81:1966-1970.

5 Izant JG, Weintraub H. Inhibition of thymidine kinase gene expression by anti-sense RNA: a molecular approach to genetic analysis. Cell 1984;36:1007-1015.

6 Gewirtz AM, Sokol DL, Ratajczak MZ. Nucleic acid therapeutics: state of the art and future prospects. Blood 1998;92:712-736.

7 Bronson SK, Smithies O. Altering mice by homologous recombination using embryonic stem cells. J Biol Chem 1994;269:27155-27158.

8 Camerini-Otero RD, Hsieh P. Parallel DNA triplexes, homologous recombination, and other homology-dependent DNA interactions. Cell 1993;73:217-223.

9 Marth JD. Recent advances in gene mutagenesis by site-directed recombination. J Clin Invest 1996;97:1999-2002.

10 Haber JE. DNA recombination: the replication connection. Trends Biochem Sci 1999;24:271-275.

11 Gunther EJ, Havre PA, Gasparro FP et al. Triplex-mediated, in vitro targeting of psoralen photoadducts within the genome of a transgenic mouse. Photochem Photobiol 1996;63:207-212.

12 Maher Jr L. Prospects for the therapeutic use of antigene oligonucleotides. Cancer Invest 1996;14:66-82.

13 Raha M, Wang G, Seidman MM et al. Mutagenesis by third-strand-directed psoralen adducts in repair-deficient human cells: high frequency and altered spectrum in a xeroderma pigmentosum variant. Proc Natl Acad Sci USA 1996;93:2941-2946.

14 Afonina I, Kutyavin I, Lukhtanov E et al. Sequence-specific arrest of primer extension on single-stranded DNA by an oligonucleotide-minor groove binder conjugate. Proc Natl Acad Sci USA 1996;93:3199-3204.

15 Wang G, Seidman MM, Glazer PM. Mutagenesis in mammalian cells induced by triple helix formation and transcription-coupled repair. Science 1996;271:802-805.

16 Kochetkova M, Shannon MF. DNA triplex formation selectively inhibits granulocyte-macrophage colony-stimulating factor gene expression in human T cells. J Biol Chem 1996;271:14438-14444.

17 Kochetkova M, Iversen PO, Lopez AF et al. Deoxyribonucleic acid triplex formation inhibits granulocyte macrophage colony-stimulating factor gene expression and suppresses growth in juvenile myelomonocytic leukemic cells. J Clin Invest 1997;99:3000-3008.

18 Kmiec EB. Genomic targeting and genetic conversion in cancer therapy. Semin Oncol 1996;23:188-193.

19 Wang G, Levy DD, Seidman MM et al. Targeted mutagenesis in mammalian cells mediated by intracellular triple helix formation. Mol Cell Biol 1995;15:1759-1768.

20 Kren BT, Bandyopadhyay P, Steer CJ. In vivo site-directed mutagenesis of the factor IX gene by chimeric RNA/DNA oligonucleotides [see comments]. Nat Med 1998;4:285-290.

21 Morishita R, Gibbons GH, Horiuchi M et al. A gene therapy strategy using a transcription factor decoy of the E2F binding site inhibits smooth muscle proliferation in vivo. Proc Natl Acad Sci USA 1995;92:5855-5859.

22 Sharma HW, Perez JR, Higgins-Sochaski K et al. Transcription factor decoy approach to decipher the role of NF-kappa B in oncogenesis. Anticancer Res 1996;16:61-69.

23 Kielkopf CL, Baird EE, Dervan PB et al. Structural basis for G.C recognition in the DNA minor groove. Nat Struct Biol 1998;5:104-109.

24 Goodsell DS. The molecular perspective: DNA. STEM CELLS 2000;18:148-149.

25 Walker WL, Kopka ML, Goodsell DS. Progress in the design of DNA sequence-specific lexitropsins. Biopolymers 1997;44:323-334.

26 Beelman CA, Parker R. Degradation of mRNA in eukaryotes. Cell 1995;81:179-183.

27 Liebhaber SA. mRNA stability and the control of gene expression. Nucleic Acids Symp Ser 1997;36:29-32.

28 Sharp PA. RNAi and double-strand RNA. Genes Dev 1999;13:139-141.

29 Guru T. A silence that speaks volumes [news]. Nature 2000;404:804-808.

30 Zamore PD, Tuschl T, Sharp PA et al. RNAi: double-stranded RNA directs the ATP-dependent cleavage of mRNA at 21 to 23 nucleotide intervals. Cell 2000;101:25-33.

31 Grishok A, Tabara H, Mello CC. Genetic requirements for inheritance of RNAi in C. elegans [see comments]. Science 2000;287:2494-2497.

32 Wianny F, Zernicka-Goetz M. Specific interference with gene function by double-stranded RNA in early mouse development. Nat Cell Biol 2000;2:70-75.

33 Zhao RC, McIver RS, Griffin JD et al. Gene therapy for chronic myelogenous leukemia (CML): a retroviral vector that renders hematopoietic progenitors methotrexate-resistant and CML progenitors functionally normal and nontumorigenic in vivo. Blood 1997;90:4687-4698.

34 Eckstein F. The hammerhead ribozyme. Biochem Soc Trans 1996;24:601-604.

35 Joyce GF. Nucleic acid enzymes: playing with a fuller deck. Proc Natl Acad Sci USA 1998;95:5845-5847.

36 Agrawal S, Zhao Q. Antisense therapeutics. Curr Opin Chem Biol 1998;2:519-528.

37 Galderisi U, Cascino A, Giordano A. Antisense oligonucleotides as therapeutic agents. J Cell Physiol 1999;181:251-257.

38 Gewirtz AM. Antisense oligonucleotide therapeutics for human leukemia. Curr Opin Hematol 1998;5:39-71.

39 Shoeman RL, Hartig R, Huang Y et al. Fluorescence microscopic comparison of the binding of phosphodiester and phosphorothioate (antisense) oligodeoxyribonucleotides to subcellular structures, including intermediate filaments, the endoplasmic reticulum, and the nuclear interior. Antisense Nucleic Acid Drug Dev 1997;7:291-308.

40 Guvakova MA, Yakubov LA, Vlodavsky I et al. Phosphorothioate oligodeoxynucleotides bind to basic fibroblast growth factor, inhibit its binding to cell surface receptors, and remove it from low affinity binding sites on extracellular matrix. J Biol Chem 1995;270:2620-2627.

41 Gao WY, Han FS, Storm C et al. Phosphorothioate oligonucleotides are inhibitors of human DNA polymerases and RNase H: implications for antisense technology. Mol Pharmacol 1992;41:223-229.

42 Nielsen PE, Egholm M, Berg RH et al. Peptide nucleic acids (PNAs): potential antisense and anti-gene agents. Anticancer Drug Res 1993;8:53-63.

43 Smulevitch SV, Simmons CG, Norton JC et al. Enhancement of strand invasion by oligonucleotides through manipulation of backbone charge [see comments]. Nat Biotechnol 1996;14:1700-1704.

44 Egholm M, Buchardt O, Christensen L et al. PNA hybridizes to complementary oligonucleotides obeying the Watson-Crick hydrogen-bonding rules [see comments]. Nature 1993;365:566-568.

45 Hamilton SE, Corey DR. Telomerase: anti-cancer target or just a fascinating enzyme? Chem Biol 1996;3:863-867.

46 Fathi R, Huang Q, Coppola G et al. Oligonucleotides with novel, cationic backbone substituents: aminoethylphosphonates. Nucleic Acids Res 1994;22:5416-5424.

47 Baker BF, Lot SS, Condon TP et al. 2'-O-(2-Methoxy)ethyl-modified anti-intercellular adhesion molecule 1 (ICAM-1) oligonucleotides selectively increase the ICAM-1 mRNA level and inhibit formation of the ICAM-1 translation initiation complex in human umbilical vein endothelial cells. J Biol Chem 1997;272:11994-20000.

48 Rossi JJ. Ribozymes, genomics and therapeutics. Chem Biol 1999;6:R33-R37.

49 Pieken WA, Olsen DB, Benseler F et al. Kinetic characterization of ribonuclease-resistant 2'-modified hammerhead ribozymes. Science 1991;253:314-317.

50 Irie A, Anderegg B, Kashani-Sabet M et al. Therapeutic efficacy of an adenovirus-mediated anti-H-ras ribozyme in experimental bladder cancer. Antisense Nucleic Acid Drug Dev 1999;9:341-349.

51 Smith SM, Maldarelli F, Jeang KT. Efficient expression by an alphavirus replicon of a functional ribozyme targeted to human immunodeficiency virus type 1. J Virol 1997;71:9713-9721.

52 Herrel KJ, Herschlag D, Uhlenbeck OC. A kinetic and thermodynamic framework for the hammerhead ribozyme reaction. Biochemistry 1994;33:3374-3385.

53 Hegg LA, Fedor MJ. Kinetics and thermodynamics of intermolecular catalysis by hairpin ribozymes. Biochemistry 1995;34:15813-15828.

54 Dahm SC, Uhlenbeck OC. Role of divalent metal ions in the hammerhead RNA cleavage reaction. Biochemistry 1991;30:9464-9469.

55 Hampel A. The hairpin ribozyme: discovery, two-dimensional model, and development for gene therapy. Prog Nucleic Acid Res Mol Biol 1998;58:1-39.

56 Vaish NK, Kore AR, Eckstein F. Recent developments in the hammerhead ribozyme field. Nucleic Acids Res 1998;26:5237-5242.

57 Birikh KR, Heaton PA, Eckstein F. The structure, function and application of the hammerhead ribozyme. Eur J Biochem 1997;245:1-16.

58 Earnshaw DJ, Gait MJ. Progress toward the structure and therapeutic use of the hairpin ribozyme. Antisense Nucleic Acid Drug Dev 1997;7:403-411.

59 Kore AR, Eckstein F. Hammerhead ribozyme mechanism: a ribonucleotide 5' to the substrate cleavage site is not essential. Biochemistry 1999;38:10915-10918.

60 Vaish NK, Heaton PA, Fedorova O et al. In vitro selection of a purine nucleotide-specific hammerheadlike ribozyme. Proc Natl Acad Sci USA 1998;95:2158-2162.

61 Ferbeyre G, Bratty J, Chen H et al. A hammerhead ribozyme inhibits ADE1 gene expression in yeast. Gene 1995;155:45-50.

62 Perriman R, de Feyter R. tRNA delivery systems for ribozymes. Methods Mol Biol 1997;74:393-402.

63 Albuquerque-Silva J, Millican F, Bollen A et al. Ribozyme-mediated decrease in mumps virus nucleocapsid mRNA level and progeny in infected vero cells. Antisense Nucleic Acid Drug Dev 1999;9:279-288.

64 Giannini CD, Roth WK, Piiper A et al. Enzymatic and antisense effects of a specific anti-Ki-ras ribozyme in vitro and in cell culture. Nucleic Acids Res 1999;27:2737-2744.

65 Bramlage B, Alefelder S, Marschall P et al. Inhibition of luciferase expression by synthetic hammerhead ribozymes and their cellular uptake. Nucleic Acids Res 1999;27:3159-3167.

66 Anderson P, Monforte J, Tritz R et al. Mutagenesis of the hairpin ribozyme. Nucleic Acids Res 1994;22:1096-1100.

67 Perez-Ruiz M, Barroso-Delleaus A, Berzal-Herranz A. Specificity of the hairpin ribozyme. Sequence requirements surrounding the cleavage site. J Biol Chem 1999;274:29376-29380.

68 Feldstein PA, Bruening G. Catalytically active geometry in the reversible circularization of 'mini-monomer' RNAs derived from the complementary strand of tobacco ringspot virus satellite RNA. Nucleic Acids Res 1993;21:1991-1998.

69 Komatsu Y, Koizumi M, Sekiguchi A et al. Cross-ligation and exchange reactions catalyzed by hairpin ribozymes. Nucleic Acids Res 1993;21:185-190.

70 Dahm SC, Derrick WB, Uhlenbeck OC. Evidence for the role of solvated metal hydroxide in the hammerhead cleavage mechanism. Biochemistry 1993;32:13040-13045.

71 Young KJ, Gill F, Grasby JA. Metal ions play a passive role in the hairpin ribozyme catalysed reaction. Nucleic Acids Res 1997;25:3760-3766.

72 Chowrira BM, Berzal-Herranz A, Burke JM. Ionic requirements for RNA binding, cleavage, and ligation by the hairpin ribozyme. Biochemistry 1993;32:1088-1095.

73 Walter NG, Hampel KJ, Brown KM et al. Tertiary structure formation in the hairpin ribozyme monitored by fluorescence resonance energy transfer. EMBO J 1998;17:2378-2391.

74 Earnshaw DJ, Gait MJ. Hairpin ribozyme cleavage catalyzed by aminoglycoside antibiotics and the polyamine spermine in the absence of metal ions. Nucleic Acids Res 1998;26:5551-5561.

75 Seyhan AA, Amaral J, Burke JM. Intracellular RNA cleavage by the hairpin ribozyme. Nucleic Acids Res 1998;26:3494-3504.

76 Breaker RR, Joyce GF. A DNA enzyme that cleaves RNA. Chem Biol 1994;1:223-229.

77 Santoro SW, Joyce GF. A general purpose RNA-cleaving DNA enzyme. Proc Natl Acad Sci USA 1997;94:4262-4266.

78 Wu Y, Yu L, McMahon R et al. Inhibition of bcr-abl oncogene expression by novel deoxyribozymes (DNAzymes). Hum Gene Ther 1999;10:2847-2857.

79 Zhang X, Xu Y, Ling H et al. Inhibition of infection of incoming HIV-1 virus by RNA-cleaving DNA enzyme. FEBS Lett 1999;458:151-156.

80 Scherr M, Rossi JJ. Rapid determination and quantitation of the accessibility to native RNAs by antisense oligodeoxynucleotides in murine cell extracts. Nucleic Acids Res 1998;26:5079-5085.

81 Scherr M, Rossi JJ, Sczakiel G et al. RNA accessibility prediction: a theoretical approach is consistent with experimental studies in cell extracts. Nucleic Acids Res 2000;28:2455-2461.

82 Sokol DL, Zhang X, Lu P et al. Real time detection of DNA.RNA hybridization in living cells. Proc Natl Acad Sci USA 1998;95:11538-11543.

83 Bellinger C, Saragovi HU, Smith RM et al. Binding, uptake, and intracellular trafficking of phosphorothioate-modified oligodeoxynucleotides. J Clin Invest 1995;95:1814-1823.

84 Spiller DG, Giles RV, Orzybowski J et al. Improving the intracellular delivery and molecular efficacy of antisense oligonucleotides in chronic myeloid leukemia cells: a comparison of streptolysin-O permeabilization, electroporation, and lipophilic conjugation. Blood 1998;91:4738-4746.

85 Bennett CF, Chiang MY, Chan H et al. Cationic lipids enhance cellular uptake and activity of phosphorothioate antisense oligonucleotides. Mol Pharmacol 1992;41:1023-1033.

86 Lappalainen K, Urtti A, Soderling E et al. Cationic liposomes improve stability and intracellular delivery of antisense oligonucleotides into CaSki cells. Biochim Biophys Acta 1994;1196:201-208.

87 Capaccioli S, Di Pasquale G, Mini E et al. Cationic lipids improve antisense oligonucleotide uptake and prevent degradation in cultured cells and in human serum [published errarum appears in Biochem Biophys Res Commun 1994;200:1769]. Biochem Biophys Res Commun 1993;197:818-825.

88 Marcusson EG, Bhat B, Marcharan M et al. Phosphorothioate oligodeoxyribonucleotides dissociate from cationic lipids before entering the nucleus. Nucleic Acids Res 1998;26:2016-2023.

89 Flynn SM, George ST, White L et al. Water-soluble, meso-substituted cationic porphyrins—a family of compounds for cellular delivery of oligonucleotides. Biotechniques 1999;26:736-742, 744, 746.

90 Benimetskaya L, Takle GB, Vilenchik M et al. Cationic porphyrins: novel delivery vehicles for antisense oligodeoxynucleotides. Nucleic Acids Res 1998;26:5310-5317.

91 Citro G, Perrotti D, Cucco C et al. Inhibition of leukemia cell proliferation by receptor-mediated uptake of c-myb antisense oligodeoxynucleotides. Proc Natl Acad Sci USA 1992;89:7031-7035.

92 Morris MC, Vidal P, Chaloin L et al. A new peptide vector for efficient delivery of oligonucleotides into mammalian cells. Nucleic Acids Res 1997;25:2730-2736.

93 Wagner E, Plank C, Zatloukal K et al. Influenza virus hemagglutinin HA-2 N-terminal fusogenic peptides augment gene transfer by transferrin-polylysine-DNA complexes: toward a synthetic virus-like gene-transfer vehicle. Proc Natl Acad Sci USA 1992;89:7934-7938.

94 Bongartz JP, Aubertin AM, Milhaud PG et al. Improved biological activity of antisense oligonucleotides conjugated to a fusogenic peptide. Nucleic Acids Res 1994;22:4681-4688.

95 Bron R, Ortiz A, Wilschut J. Cellular cytoplasmic delivery of a polypeptide toxin by reconstituted influenza virus envelopes (virosomes). Biochemistry 1994;33:9110-9117.

96 Schoen P, Chonn A, Cullis PR et al. Gene transfer mediated by fusion protein hemagglutinin reconstituted in cationic lipid vesicles. Gene Ther 1999;6:823-832.

97 Waelti ER, Gluck R. Delivery to cancer cells of antisense L-myc oligonucleotides incorporated in fusogenic, cationic-lipid-reconstituted influenza-virus envelopes (cationic virosomes). Int J Cancer 1998;77:728-733.

98 Coll JL, Chollet P, Brambilla E et al. In vivo delivery to tumors of DNA complexed with linear polyethylenimine. Hum Gene Ther 1999;10:1659-1666.

99 Dheur S, Dias N, van Aerschot A et al. Polyethylenimine but not cationic lipid improves antisense activity of 3'-capped phosphodiester oligonucleotides. Antisense Nucleic Acid Drug Dev 1999;9:515-525.

100 Helin V, Gottikh M, Mishal Z et al. Cell cycle-dependent distribution and specific inhibitory effect of vectorized antisense oligonucleotides in cell culture. Biochem Pharmacol 1999;58:93-107.

101 Samarsky DA, Ferbeyre G, Bertrand E et al. A small nucleolar RNA:ribozyme hybrid cleaves a nucleolar RNA target in vivo with near-perfect efficiency. Proc Natl Acad Sci USA 1999;96:6609-6614.

102 Rossi JJ. Ribozymes in the nucleolus. Science 1999;285:1685.

103 Sweeney R, Fan Q, Yan MC. Antisense in abundance: the ribosome as a vehicle for antisense RNA. Genet Eng (NY) 1998;20:143-151.

104 Wyatt JR, Vickers TA, Roberson JL et al. Combinatorially selected guanosine-quartet structure is a potent inhibitor of human immunodeficiency virus envelope-mediated cell fusion. Proc Natl Acad Sci USA 1994;91:1356-1360.

105 Basu S, Wickstrom E. Temperature and salt dependence of higher order structure formation by antisense c-myc and c-myb phosphorothioate oligodeoxyribonucleotides containing tetraguanylate tracts. Nucleic Acids Res 1997;25:1327-1332.

106 Yaswen P, Stampfer M, Ghosh K et al. Effects of sequence of thiolated oligonucleotides on cultured human mammary epithelial cells. Antisense Res Dev 1993;3:67-77.

107 Gilar M, Belenky A, Budman Y et al. Impact of 3'-exonuclease stereoselectivity on the kinetics of phosphorothioate oligonucleotide metabolism. Antisense Nucleic Acid Drug Dev 1998;8:35-42.

108 Druker BJ, Lydon NB. Lessons learned from the development of an abl tyrosine kinase inhibitor for chronic myelogenous leukemia. J Clin Invest 2000;105:3-7.

109 Stevenson JP, DeMaria D, Reilly D et al. Phase I/pharmacokinetic trial of the novel thioxanthone SR233377 (WIN33377) on a 5-day schedule. Cancer Chemother Pharmacol 1999;44:228-234.

110 O'Dwyer PJ, Stevenson JP, Gallagher M et al. c-raf-1 depletion and tumor responses in patients treated with the c-raf-1 antisense oligodeoxynucleotide ISIS 5132 (CGP 69846A). Clin Cancer Res 1999;5:3977-3982.

111 Nemunaitis J, Holmlund JT, Kraynak M et al. Phase I evaluation of ISIS 3521, an antisense oligodeoxynucleotide to protein kinase C-alpha, in patients with advanced cancer. J Clin Oncol 1999;17:3586-3595.

112 Sereni D, Tubiana R, Lascoux C et al. Pharmacokinetics and tolerability of intravenous trecovirsen (GEM 91), an anti-

sense phosphorothioate oligonucleotide, in HIV-positive subjects. J Clin Pharmacol 1999;39:47-54.

113 Clark RE, Grzybowski J, Broughton CM et al. Clinical use of streptolysin-O to facilitate antisense oligodeoxyribonucleotide delivery for purging autografts in chronic myeloid leukaemia. Bone Marrow Transplant 1999;23:1303-1308.

114 de Fabritiis P, Petti MC, Montefusco E et al. BCR-ABL antisense oligodeoxynucleotide in vitro purging and autologous bone marrow transplantation for patients with chronic myelogenous leukemia in advanced phase. Blood 1998;91:3156-3162.

115 Bishop MR, Iversen PL, Bayever E et al. Phase I trial of an antisense oligonucleotide OL(1)p53 in hematologic malignancies. J Clin Oncol 1996;14:1320-1326.

116 Zhang R, Yan J, Shahinian H et al. Pharmacokinetics of an anti-human immunodeficiency virus antisense oligodeoxynucleotide phosphorothioate (GEM 91) in HIV-infected subjects. Clin Pharmacol Ther 1995;58:44-53.

117 Waters JS, Webb A, Cunningham D et al. Phase I clinical and pharmacokinetic study of bcl-2 antisense oligonucleotide therapy in patients with non-Hodgkin's lymphoma [see comments]. J Clin Oncol 2000;18:1812-1823.

118 Gewirtz AM. Oligonucleotide therapeutics: a step forward [editorial; comment]. J Clin Oncol 2000;18:1809-1811.

Human inhibitor of apoptosis protein (IAP) *survivin* participates in regulation of chromosome segregation and mitotic exit[1]

MARKO J. KALLIO,[2] MIKKO NIEMINEN,*,† AND JOHN E. ERIKSSON†

University of Oklahoma Health Sciences Center, Oklahoma City, Oklahoma 73104, USA; *Turku Centre for Biotechnology, University of Turku and Åbo Akademi University, FIN-20521, Turku, Finland; and †Department of Biology, University of Turku, FIN-20014 Turku, Finland

SPECIFIC AIM

The human inhibitor of apoptosis protein (IAP) *survivin* and its lower eukaryote homologues have been implicated in apoptosis and regulation of cell cycle. In this study, we have investigated mitotic role(s) of survivin by using survivin antisense oligonucleotides (FsO^-) and function blocking anti-survivin antibodies (s-Ab), followed by fluorescence microscopy and live cell cinematography; we postulate that the function of survivin in dividing cells is integrated with the spindle checkpoint mechanism composed of mitotic regulators that monitor integrity of the genome.

PRINCIPAL FINDINGS

1. Survivin antisense oligonucleotides induce abortive mitosis and polyploidy

To investigate the effects of survivin inhibition on mitotic progression, we introduced fluorescein isothiocyanate (FITC)-conjugated scrambled control (FcO^-) or survivin (FsO^-) oligonucleotides into the HeLa and PtK1 cells by either a microinjection method or liposome-mediated DNA transfer. In HeLa cells transfected with the FsO^-, the endogenous survivin protein was reduced significantly in a concentration-dependent manner by ~30-to-80% ($P<0.05$; 200 nM FsO^-, $P<0.01$; 400 nM FsO^-) whereas the FcO^- had no effect. Moreover, the percentage of abnormally large and micronucleated (MN) cells was significantly increased ($P<0.01$) in the FsO^- transfected PtK1 cell populations (polyploid 18.1±3.3, MN 11.5±3.5) compared with controls (polyploid 3.1±0.8, MN 2.5±1.5). Induction of polyploidy was confirmed with HeLa cells that were microinjected with FcO^- or FsO^-.

In the chemically M phase-arrested PtK1 cells, the percentage of FITC-positive cells with MN was significantly increased at 0, 2, 6 ($P<0.05$), and 8 h ($P<0.01$) in the FsO^- transfected cells compared with controls, indicating that the FsO^--treated cells were able to bypass the M phase block. We also determined how many nocodazole-treated, M phase-arrested cells showed signs of abortive mitosis such as decondensation of chromatin and formation of cleavage furrow at the various times. FsO^- targeted cells aborted M phase more frequently than control cells especially at 6 ($P<0.01$) and 8 h ($P<0.05$), when 19.0 ± 2.3% and 12.3 ± 3.5% of the FITC-positive cells were in the process of exiting M phase, respectively.

2. Anti-survivin antibody (s-Ab) induces premature onset of anaphase and escape from chemically induced M phase block

To investigate the effects of perturbed survivin function during different mitotic phases, we used a microinjection technique with s-Ab (**Fig. 1*A***). For control injections, we used KCl-PO_4 microinjection buffer (cBuf). The cells injected with the s-Ab between late prophase and early prometaphase showed specific cell division defects. The cells either separated their sister chromatids prematurely at late prometaphase or spent a significantly shorter period at the metaphase stage (Fig. 1*B, C*). Nine of 22 injected PtK1 cells initiated anaphase at late prometaphase before all the chromosomes had moved to the spindle equator. The remainder of the s-Ab-injected PtK1 cells ($n=13$) spend a significantly shorter time at the metaphase stage than the controls (Fig. 1*C*; 4.6±1.1 min vs. 8.6±1.9 min, $P<0.01$). Furthermore, the cells injected with s-Ab at late prophase or early prometaphase started anaphase in an average 26.8 ± 5.3 min (range 17–34 min) after the nuclear envelope breakdown (NEB), which is significantly different from the controls (Fig. 1*C*; 32.9±6.9 min, $P<0.05$). All s-Ab-injected cells, including those experiencing premature onset of anaphase, exit mitosis normally without defects in cytokinesis.

To determine whether blocking of survivin function during mitotic arrest would affect the length of the

[1] To read the full text of this article, go to http://www.fasebj.org/cgi/doi/10.1096/fj.01-0280fje; to cite this article, use *FASEB J.* (October 29, 2001) 10.1096/fj.01-0280fje

[2] Correspondence: University of Oklahoma Health Sciences Center, 975 N.E. 10th St., Biomedical Research Center, Rm. 266, Oklahoma City, OK 73104, USA. E-mail: Marko-Kallio@ouhsc.edu

0892-6638/01/0015-2721 © FASEB

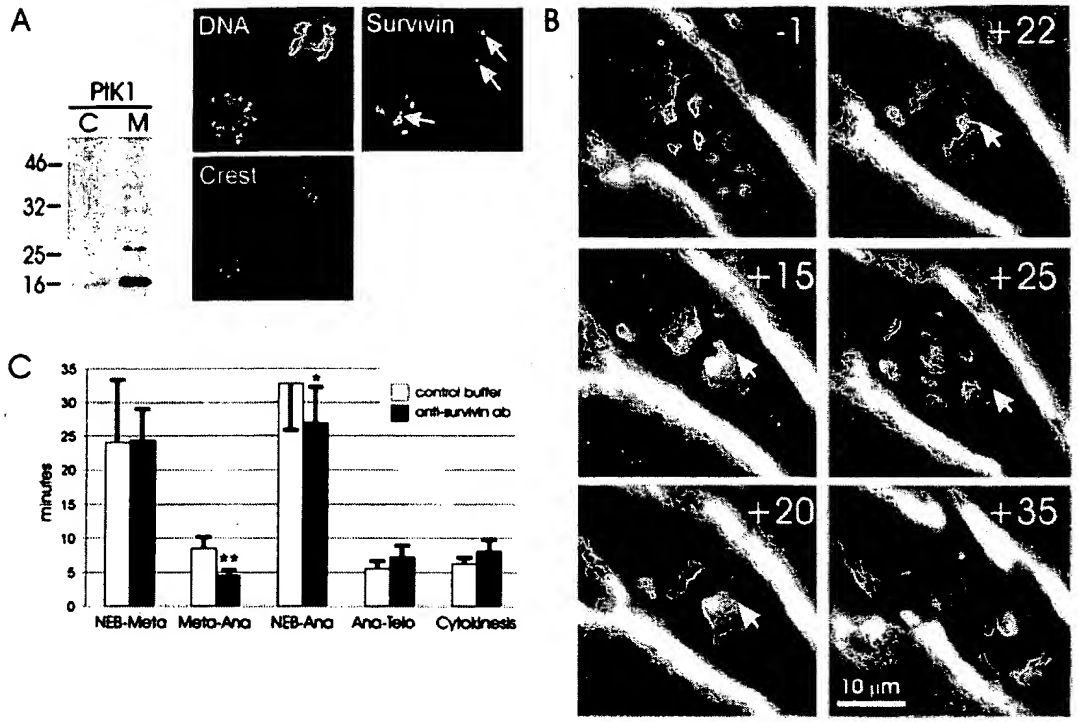

Figure 1. Effects of s-Ab microinjection on progression of cell division. *A)* In mitotic (M) PtK1 extracts, the s-Ab recognizes a major band at ~16 kDa. Microscope images show the immunofluorescent localization of survivin at the mitotic spindle poles (arrowheads). *B)* Time-lapse sequence of a PtK1 cell injected with s-Ab at early prometaphase. The chromosomes move toward the spindle equator; 15 min after the injection, all but one (arrowhead) chromosome had aligned at the equatorial plate. When the sister chromatids of the aligned chromosomes separate 22 min after the injection, the unaligned chromosome is still mal-oriented and both of its sister chromatids move to the same spindle pole. *C)* Diagram showing the duration of different mitotic phases in cBuf and s-Ab-injected PtK1 cells. The s-Ab injection did not affect the prometaphase chromosome movements, as the mean duration of the prometaphase (NEB-Meta) was the same as in the cBuf-injected cells. However, the duration of metaphase stage (Meta-Ana) and the average time from NEB to onset of anaphase were significantly shorter in the s-Ab-injected cells than controls.

metaphase delay, we injected nocodazole- or taxol-treated PtK1 cells with s-Ab. All of the s-Ab-injected cells (n=10) escaped the M phase block within 3 h of the injection (149.7±37.8 min) whereas all the control cells (n=10) remained arrested in M phase for at least 8 h. Cells treated with spindle poisons and injected with s-Ab decondensed their chromosomes and returned to interphase without completing cytokinesis, and consequently formed micronucleated giant cells.

3. The 3F3/2 phosphoepitope is lost prematurely from the mitotic kinetochores in s-Ab-injected PtK1 cells

One marker for the spindle checkpoint is the 3F3/2 phosphoepitope that responds to physical tension mediated by the opposing spindle microtubules at the sister kinetochores of a chromosome. In a normal cell, 3F3/2 epitopes are phosphorylated during prometaphase and localize to the kinetochores of chromosomes and to the spindle poles, but as the chromosomes move to the spindle equator, the 3F3/2 epitope is dephosphorylated and lost from the kinetochores (but not from the spindle poles), which marks deactivation of the spindle checkpoint. In the s-Ab-injected PtK1 cells, the 3F3/2 phosphoepitope is lost prematurely from the kinetochores of prometaphase chromosomes whereas the fluorescence of the spindle pole located 3F3/2 signals did not change over time (**Fig. 2*A***). The kinetics of the loss of fluorescent 3F3/2 signals from the kinetochores corresponds well with the timing of the precocious separation of the sister chromatids. Loss of all kinetochore-bound 3F3/2 phosphoepitope from the s-Ab-injected cells takes on average 14.0 ± 3.0 min after NEB, which is significantly shorter than 24.0 ± 4.0 min of cBuf-injected cells (Fig. 2*B*; P<0.01).

CONCLUSIONS

Here we show that perturbation of the survivin function by antisense targeting at G2 phase of the cell cycle causes cell division defects, resulting in aneuploidy and polyploidy. To investigate the possible mechanisms of the observed mitotic defects in detail, we microinjected early mitotic PtK1 cells with s-Ab and followed them through mitosis. To our surprise, the s-Ab-injected cells exhibited premature separation of sister chromatids but had no apparent difficulties in exiting mitosis. To

our knowledge this is the first data implicating survivin in the actual process of chromosome segregation. Moreover, in the s-Ab-injected cells, the kinetochore-bound 3F3/2 phosphoepitope was lost prematurely at late prometaphase, which indicates that the spindle checkpoint was affected in these cells. Finally, introduction of sO^- or s-Ab into M phase arrested cells induced abortive mitosis, yielding aneuploidy and polyploidy. Together, these results propose a link between the survivin function and control of metaphase-anaphase transition by the spindle checkpoint.

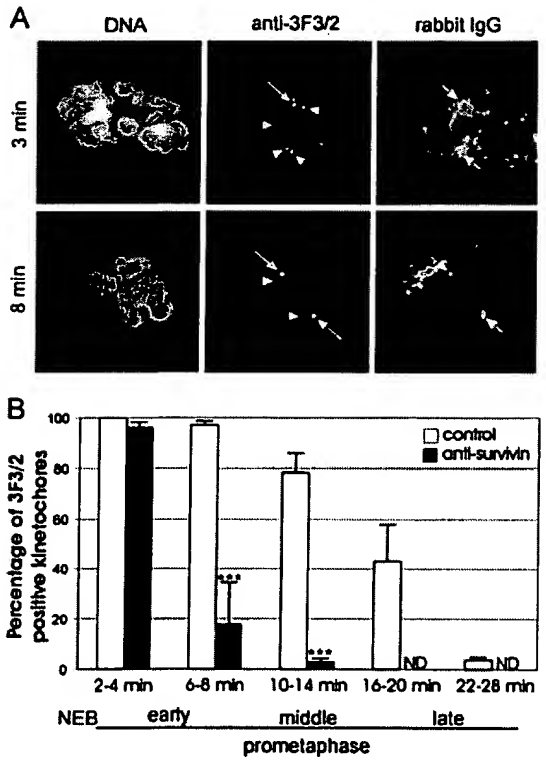

Figure 2. 3F3/2 phosphoepitope is lost precociously from the kinetochores of PtK1 cells after introduction of s-Ab. *A)* Fluorescent micrographs depicting two PtK1 cells injected with s-Ab at early prometaphase and then allowed to progress in their division for 3 and 8 min, respectively, before fixation and immunolabeling. The cell fixed 3 min after injection had a normal 3F3/2-staining pattern with bright 3F3/2 signals at the kinetochores of unaligned chromosomes (some depicted with arrowheads) and spindle poles (arrows). The cell fixed 8 min after the injection had lost most of its kinetochore-bound 3F3/2 epitope, although it was still at prometaphase stage with many unaligned chromosomes. Only two faint 3F3/2 positive kinetochores could be seen (arrowheads). The spindle poles had normal 3F3/2 signals (arrows). In both cells, the injected s-Ab accumulated at the spindle poles (arrows in the rabbit IgG panel). *B)* Percentage of 3F3/2 positive kinetochores in cell populations injected with s-Ab or cBuf. Groups of 5 to 10 PtK1 cells were injected with the antibody at late prophase/early prometaphase and allowed to progress in their division for the times indicated before fixation and immunolabeling with anti-3F3/2 ascites and Crest anti-centromere sera. The percentage of 3F3/2 spots colocalizing with Crest signals was determined for each injected cell. (ND, not detected).

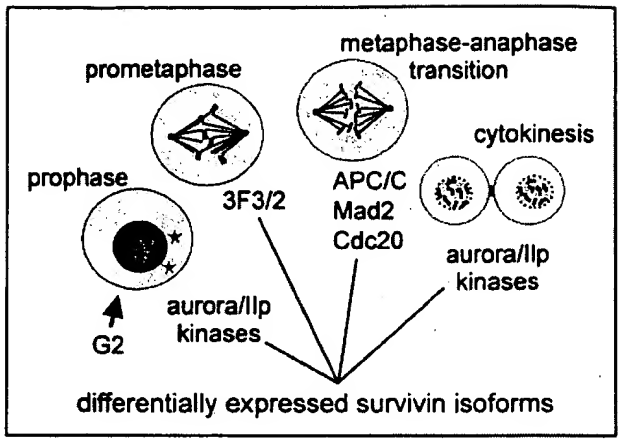

Figure 3. Possible targets of survivin isoforms during mitosis. The differentially expressed survivin isoforms may participate in regulation of various cell division events, including separation of sister chromatids and cytokinesis.

A possible explanation for the different mitotic effects induced by survivin targeting is provided by the recent discovery of three human and murine survivin isoforms. These survivin isoforms may play multiple roles in regulating apoptosis and cell division in mammals (**Fig. 3**). The present results raise questions about the possible mitotic target(s) and the mitotic signaling cascades the survivin isoforms may participate in (Fig. 3). Survivin shares some characteristics with classical M phase regulatory molecules. It transiently localizes to the kinetochores, centrosomes, and microtubules during mitosis and is destroyed by ubiquitin-mediated proteolysis in a cell cycle-dependent manner. Moreover, the survivin-like *C. elegans* BIR-1 protein interacts with aurora-like kinase AIR-2, a member of aurora/Ipl1 kinase family that has been implicated in cell division and chromosome segregation. In addition, aurora2 kinase associates with Cdc20, a regulator of anaphase-promoting complex/cyclosome (APC/C) that counteracts effects of Mad2, an inhibitor of APC/C activity. Introduction of anti-Mad2 antibodies into mitotic cells causes premature activation of APC/C and precocious onset of anaphase, an event similar to what we have observed after s-Ab injections. It is tempting to speculate that the cell division defects we detect after perturbation of survivin function could be caused by an impact on the aurora/Ipl1 kinases or on the activity of the APC/C. Finally, survivin may regulate 3F3/2 phoshoepitope phosphorylation, as the dephosphorylation and consequent loss of the 3F3/2 phosphoepitope from the metaphase kinetochores mark deactivation of the checkpoint and activation of the APC/C, an event that occurred prematurely in s-Ab-injected cells. These results suggest that survivin is a mitotic regulator and possible component of the spindle checkpoint machinery. Elucidation of the mechanisms by which survivin modulates activity of the spindle checkpoint will be valuable in understanding how aneuploidy contributes to malignant cell growth and tumorigenesis. FJ

THE JOURNAL OF BIOLOGICAL CHEMISTRY
Vol. 270, No. 14, Issue of April 7, pp. 8037–8043, 1995
Printed in U.S.A.

Expression of Antisense to DNA Methyltransferase mRNA Induces DNA Demethylation and Inhibits Tumorigenesis*

(Received for publication, October 10, 1994, and in revised form, January 24, 1995)

A. Robert MacLeod and Moshe Szyf‡

From the Department of Pharmacology and Therapeutics, McGill University, Montreal H3G 1Y6, Canada

Many tumor cell lines overexpress DNA methyltransferase (MeTase) activity; however it is still unclear whether this increase in DNA MeTase activity plays a causal role in naturally occurring tumors and cell lines, whether it is critical for the maintenance of transformed phenotypes, and whether inhibition of the DNA MeTase in tumor cells can reverse transformation. To address these basic questions, we transfected a murine adrenocortical tumor cell line Y1 with a chimeric construct expressing 600 base pairs from the 5′ of the DNA MeTase cDNA in the antisense orientation. The antisense transfectants show DNA demethylation, distinct morphological alterations, are inhibited in their ability to grow in an anchorage-independent manner, and exhibit decreased tumorigenicity in syngeneic mice. *Ex vivo*, cells expressing the antisense construct show increased serum requirements, decreased rate of growth, and induction of an apoptotic death program upon serum deprivation. 5-Azadeoxycytidine-treated cells exhibit a similar dose-dependent reversal of the transformed phenotype. These results support the hypothesis that the DNA MeTase is actively involved in oncogenic transformation.

Vertebrate DNA is methylated at the 5-position of the cytosine residues in the dinucleotide sequence CpG (1, 2). Twenty percent of the CpG sites are nonmethylated, and these sites are distributed in a nonrandom manner to generate a pattern of methylation that is site-, tissue-, and gene-specific (1–3). Methylation patterns are formed during development: establishment and maintenance of the appropriate pattern of methylation is critical for development (4) and for defining the differentiation state of a cell (5–7). The pattern of methylation is maintained by the DNA MeTase[1] at the time of replication (8), and the level of DNA MeTase activity and gene expression is regulated with the growth state of different primary (8) and immortal cell lines (9). This regulated expression of DNA MeTase has been suggested to be critical for preserving the pattern of methylation (8–10).

An activity that has a widespread impact on the genome such as DNA MeTase is a good candidate to play a critical role in cellular transformation. This hypothesis is supported by many lines of evidence that have demonstrated aberrations in the pattern of methylation in transformed cells. While many reports show hypomethylation of total genomic DNA (11) as well as individual genes in cancer cells (12), other reports have indicated that hypermethylation is an important characteristic of cancer cells (13). First, large regions of the genome such as CpG-rich islands (14) or regions in chromosomes 17p and 3p that are reduced to homozygosity in lung and colon cancer, respectively, are consistently hypermethylated (15, 16). Second, the 5′ region of the retinoblastoma (Rb) and Wilms Tumor (WT) genes are methylated in a subset of tumors, and it has been suggested that inactivation of these genes in the respective tumors resulted from methylation rather than a mutation (17). Third, the short arm of chromosome 11 is regionally hypermethylated in certain neoplastic cells (15). Several tumor suppressor genes are thought to be clustered in that area (18). If the level of DNA MeTase activity is critical for maintaining the pattern of methylation as has been suggested before (8–10), one possible explanation for this observed hypermethylation is the fact that DNA MeTase is dramatically induced in many tumor cells well beyond the change in the rate of DNA synthesis (13, 19). The observation that the DNA MeTase promoter bears AP-1 sites (20) and is activated by the Ras-AP-1 signaling pathway (21) is consistent with the hypothesis that elevation of DNA MeTase activity is an effect of activation of the Ras-Jun signaling pathway (22).

It has recently been demonstrated that forced expression of exogenous DNA MeTase cDNA causes transformation of NIH 3T3 cells supporting the hypothesis that overexpression of DNA MeTase can cause cellular transformation (23). The critical question that remains to be answered is whether indeed the level of expression of the endogenous DNA MeTase plays a causal role in tumors that are induced by naturally occurring oncogenic signal transduction pathways. To address this question, we have chosen the adrenocortical carcinoma cell line Y1 as a model system. Y1 is a cell line that is derived from a naturally occurring adrenocortical tumor in LAF1 mice (24). Y1 cells bear a 30–40-fold amplification of the *ras* proto-oncogene (25). If the level of expression of DNA MeTase activity is critical for the oncogenic state, then the transformed state of a cell should be reversed by partial inhibition of DNA methylation. We have previously demonstrated that forced expression of an "antisense" mRNA to the most 5′ 600 bp of the DNA MeTase message (pZαM) can induce limited DNA demethylation in 10T1/2 cells (7). To directly test the hypothesis that the tumorigenicity of Y1 cells is controlled by the DNA MeTase, we transfected either pZαM or a pZEM control into Y1 cells. We demonstrate that inhibition of DNA MeTase activity causes demethylation of Y1 DNA and results in reversal of the tumorigenic phenotype suggesting that DNA MeTase plays a critical role in tumorigenesis.

MATERIALS AND METHODS

Cell Culture and DNA-mediated Gene Transfer—Y1 cells were maintained as monolayers in F-10 medium which was supplemented with 7.25% heat-inactivated horse serum and 2.5% heat-inactivated fetal

* This paper was supported in part by a grant from the Cancer Research Society and the NCI (Canada). The costs of publication of this article were defrayed in part by the payment of page charges. This article must therefore be hereby marked "*advertisement*" in accordance with 18 U.S.C. Section 1734 solely to indicate this fact.

‡ Scientist of the National Cancer Institute (Canada). To whom correspondence and reprint requests should be addressed. Tel.: 514-398-7107; Fax: 514-398-6690; E-mail: mcms@musica.mcgill.ca.

[1] The abbreviations used are: MeTase, methyltransferase; 5-azaCdR, 5-azadeoxycytidine; bp, base pair(s); kb, kilobase pair(s); PCR, polymerase chain reaction.

Exhibit I

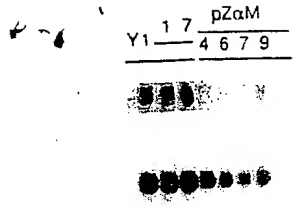

FIG. 2. **DNA MeTase expression, activity, and genomic methylation levels of pZαM transfectants.** Total cellular RNA (10 μg) prepared from pZαM lines (*4, 6, 7,* and *9*), pZEM transfectants (*1* and *7*) and from Y1 controls was subjected to Northern blot analysis and hybridization with a 1.3-kb DNA MeTase 3′-cDNA probe (encoding bases 3170–4480 from the cloned mouse cDNA (27)). The filter was stripped and rehybridized with an 18 S rRNA probe. Relative MeTase expression was determined by densitometric analysis (see text).

transfectants was subjected to a Northern blot analysis and sequentially hybridized with a probe to the putative catalytic domain of the mouse DNA MeTase mRNA (MET 3′) and an 18 S rRNA-specific ^{32}P-labeled oligonucleotide probe as described under "Materials and Methods." A result of such an analysis is presented in Fig. 2. Scanning of the autoradiogram indicates that the relative abundance of the 5-kb DNA MeTase mRNA (Fig. 2, *top panel*) relative to 18 S rRNA (Fig. 2, *bottom panel*) is reduced 2-fold in the three antisense transfectants. To quantify expression of DNA MeTase, the different RNA samples were subjected to a slot-blot analysis and sequential hybridization with the DNA MeTase and 18 S rRNA probes. The relative level of DNA MeTase mRNA in the different samples was determined by scanning densitometry. The results of such an analysis show that the pZαM transfectants exhibit an average decrease of 45% and a maximal decrease of 58% in the abundance of DNA MeTase mRNA relative to the pZEM controls ($p < 0.001$). The mean value for the control group was 0.480, S.D. = 0.104, the mean for the antisense group was 0.280, S.D. = 0.066.

We next compared the DNA MeTase enzymatic activity present in nuclear extracts prepared from antisense transfectants relative to control pZEM transfectants using *S*-[*methyl*-^{3}H]adenosyl-L-methionine as the methyl donor and a hemimethylated double-stranded oligonucleotide as a substrate. The results of two experiments with triplicate determinations each indicate that the three pZαM transfectants express a lower level of DNA MeTase activity than the control transfectants with an average inhibition of DNA MeTase activity of 42% and a maximum of 48% relative to control ($p < 0.05$).

Whereas our experiments demonstrate that the DNA MeTase antisense transfectants bear a lower level of DNA MeTase activity than the control transfectants, it is important to note that we measured only steady state levels in the transfectants. It is hard to assess the actual level of inhibition of DNA MeTase activity at the time of transfection, when a higher copy number of DNA MeTase antisense RNA might have been present in the cell. The steady state level of DNA MeTase mRNA might reflect an equilibrium of different cellular regulatory controls over the level of DNA MeTase activity in the cell. To directly demonstrate that expression of the DNA MeTase antisense leads to inhibition of DNA methylation activity in the cell, we determined whether it leads to a general reduction in the level of methylation of the genome. We performed a "nearest neighbor" analysis using [α-^{32}P]dGTP as described previously (6). This assay enables one to determine the percentage of methylated and nonmethylated cytosines residing in the dinucleotide sequence CpG (6). The results of three such experiments show that the mean value for the pZEM controls as a group was 9.7% nonmethylated cytosines, S.D. = 2.13, the mean value for the antisense lines as a group was 23.83% cytosine, S.D. = 5.88. $p < 0.001$.

In summary, our experiments demonstrate that expression of an antisense to the DNA MeTase mRNA leads to partial inhibition of DNA MeTase mRNA and DNA MeTase enzymatic activities and a significant reduction in the level of genomic cytosine methylation.

Demethylation of Specific Genes in Y1 and pZαM Transfectants—To further verify that expression of pZαM results in demethylation and to determine whether specific genes were demethylated, we resorted to a *Hpa*II/*Msp*I restriction enzyme analysis followed by Southern blotting and hybridization with specific gene probes. *Hpa*II cleaves the sequence CCGG, a subset of the CpG dinucleotide sequences, only when the site is unmethylated, while *Msp*I will cleave the same sequence irrespective of its state of methylation. By comparing the pattern of *Hpa*II cleavage of specific genes in cells expressing pZαM with that of the parental Y1 or cells harboring only the vector, we determined whether the genes are demethylated in the antisense transfectants. We first analyzed the state of methylation of the steroid 21-hydroxylase gene (C21) (29, 31). This gene is specifically expressed and hypomethylated in the adrenal cortex, but is inactivated and hypermethylated in Y1 cells (29, 31). We have previously suggested that hypermethylation of C21 in the Y1 cell is part of the transformation program that includes the shutdown of certain differentiated functions (29). DNA prepared from Y1, pZαM (4, 7, 9), and pZEM (1 and 7) transfectants was subjected to either *Msp*I or *Hpa*II digestion, Southern blot analysis, and hybridization with a 3.8-kb *Bam*HI fragment containing the body of the C21 gene and 3′ sequences (Fig. 3, *bottom panel*, for physical map). Full demethylation of this region should yield a doublet at ~1 kb, an 0.8-kb fragment, and a 0.4-kb fragment, as well as a number of low molecular weight fragments at 0.1–0.4 kb. As observed in Fig. 3, the C21 locus is heavily methylated in Y1 cells, as well as the control transfectant, as indicated by the high molecular weight fragments. Only a relatively weak digestion product is seen at 1.9 kb (Fig. 3). This pattern of hypermethylation of C21 which is observed in Y1 cells and different control transfectants, that were analyzed in our laboratory in the last 5 years, is markedly stable. On the other hand, the antisense transfectant's DNA is significantly hypomethylated at this locus as indicated by the relative diminution of the high molecular weight fragments and relative intensification of the partial fragment at 1.9 kb. The appearance of new partial fragments in the lower molecular weight range between 1 and 0.4 kb indicates partial hypomethylation at a large number of *Hpa*II sites contained in the 3′ region of the C21 gene (see physical map) (29, 31). The pattern of demethylation, indicated by the large number of partial *Hpa*II fragments, is compatible with a general partial hypomethylation rather than a specific loss of methylation in a distinct region of the C21 gene.

To determine whether demethylation is limited to genes that are potentially expressible in Y1 cells such as the adrenal cortex-specific C21 gene (29) or if the demethylation is widely spread in the genome, we tested the methylation state of the MyoD (32) and p53 5′ locus. Specific demethylation of MyoD and the p53 fragment was seen in the pZαM transfectants (data not shown).

Morphological Transformation Loss of Anchorage-independent Growth and Inhibition of Tumorigenicity of Y1 Cells Expressing Antisense to the DNA MeTase—As the level of DNA MeTase activity is regulated with the state of growth and is induced in transformed cells and in tumors *in vivo* (8, 9, 13, 19), we determined whether expression of the DNA MeTase antisense construct results in a change in the tumorigenic potential of Y1 cells. A comparison of pZαM transfectants and controls showed a small

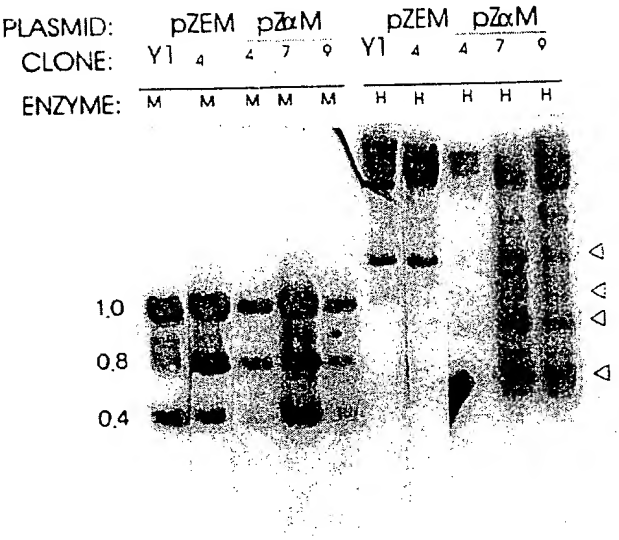

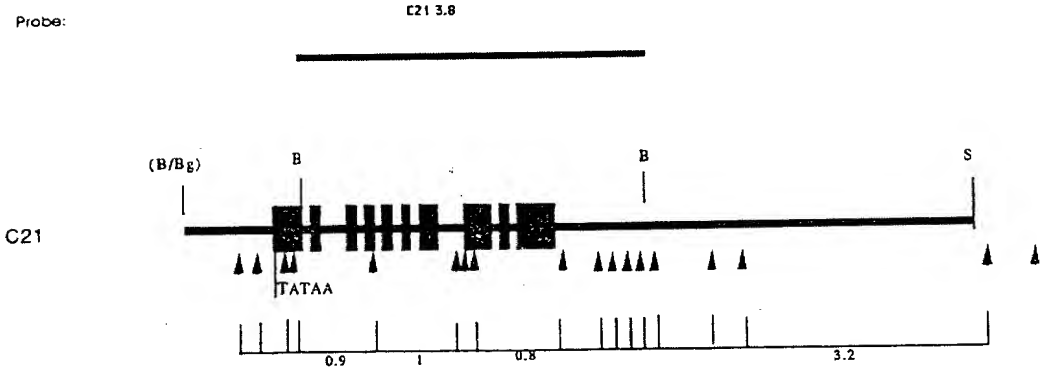

FIG. 3. **The pattern of methylation of C21 hydroxylase in pZαM transfectants and pZEM controls.** Genomic DNA (10 μg) was extracted from the transfected lines and subjected to digestion with either *Msp*I (*M*) or *Hpa*II (*H*). Southern blot transfer, and hybridization with a ^{32}P-labeled DNA probe (3.8-kb genomic fragment of the C21 gene, see *bottom panel* for physical map). The *open arrows* indicate *Hpa*II fragments resulting from demethylation of the different sites in the C21 gene in pZαM transfectants. Complete digestion of the region will yield 0.36- and 0.16-kb fragments.

but statistically significant reduction in the growth rate of antisense lines relative to the Y1 controls especially at higher densities (which is statistically significant, $p < 0.001$). This may reflect contact-inhibited growth and increased serum requirements of the antisense lines (data not shown). The morphological properties of the pZαM transfectants further support this conclusion (Fig. 4). While control Y1 and pZEM cells exhibit limited contact inhibition and form multilayer foci, pZαM transfectants exhibit a more rounded and distinct morphology and grow exclusively in monolayers, and, in many cases, pZαM cells form distinct cellular processes (Fig. 4).

The ability of cells to grow in an anchorage-independent fashion is considered to be an indicator of tumorigenicity (27). A soft agar assay performed in triplicate showed that the pZαM transfectants demonstrate a significant decrease in their ability to form colonies in soft agar: pZEM 1 and 7 form an average of 38 and 37 colonies, respectively, while pZαM transfectants 4, 7, and 9 formed an average of 12, 15, and 18 colonies, respectively. Moreover, the colonies that do form are significantly smaller and contain fewer cells.

Another indicator of the state of transformation of a cell is its

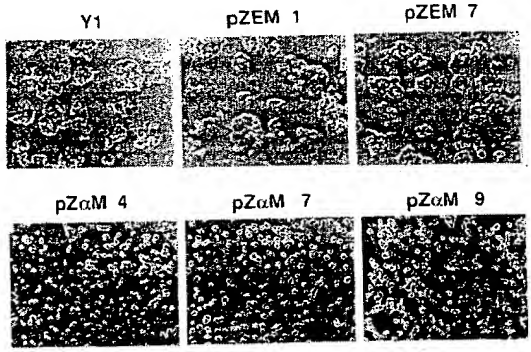

FIG. 4. **Morphological transformation of Y1 cells transfected with pZαM.** Phase contrast microscopy at × 200 magnification of living cultures of Y1 clonal transfectants with pZαM and pZEM controls. Equal numbers of cells were plated (1×10^5 cells per well in a six-well dish), and pictures were taken 72 h after seeding.

serum dependence. Tumor cells exhibit limited dependence on serum and are usually capable of serum-independent growth (33). Factors present in the serum are essential for the survival

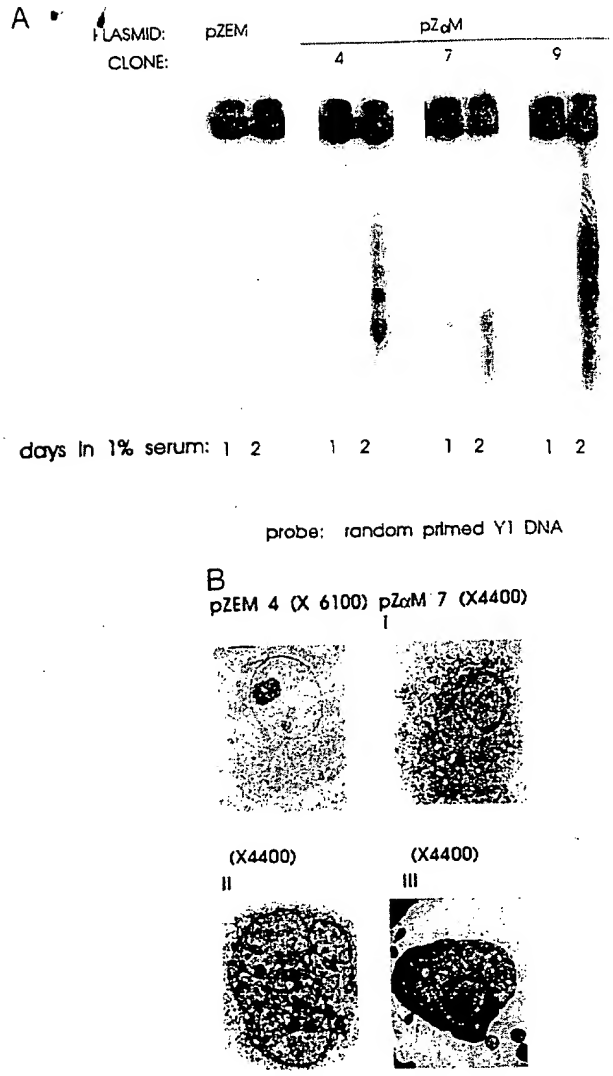

FIG. 5. **Survival and apoptosis of pZEM transfectants in serum-deprived medium.** *A*, the indicated transfectants were plated in 1% serum-containing medium and harvested after 1 and 2 days. Total cellular DNA was isolated, separated by agarose gel electrophoresis, transferred to nitrocellulose membrane, and probed with ^{32}P-labeled Y1 genomic DNA. A 180-bp internucleosomal ladder characteristic to cells dying via apoptosis can be seen in the pZαM transfectants only. *B*, Y1 transfectants were grown in 1% serum medium for 24 h, fixed, and analyzed by electron microscopy for early signs of apoptotic death; *I–III* are various sections (the magnification is indicated) of Y1 pZαM transfectants and pZEM control lines.

of many nontumorigenic cells. As observation of the pZαM transfectants indicated that they expressed enhanced dependence on serum and limited survivability under serum-deprived conditions, we determined whether this limited survivability involved an enhancement or induction of an apoptotic program. While the control cells exhibited almost 100% viability up to 72 h after transfer into serum-deprived medium, all pZαM transfectants showed up to 75% loss of viability at 48 h.

To test whether the serum-deprived pZαM cells were dying as a result of an activated apoptotic death program, cells were plated in starvation medium and harvested at 24-h intervals, and total cellular DNA was isolated from the cells and analyzed by agarose gel electrophoresis. After 48 h in serum-starved conditions, pZαM transfectants exhibit the characteristic 180-bp internucleosomal DNA ladder while the control pZEM transfectants show no apoptosis at this time point (Fig. 5*A*).

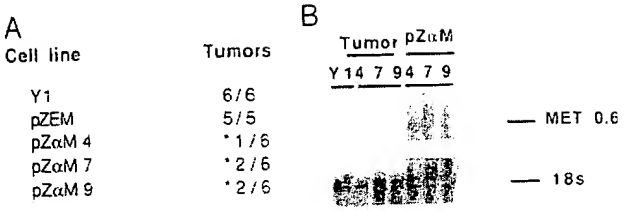

FIG. 6. ***In vivo* tumorigenicity of pZαM transfectants.** *A*, parental Y1 cells, a pZEM control line, and three pZαM transfectants (*4*, *7*, and *9*) were tested for their ability to form tumors in syngeneic LAF-1 mice. Tumor formation was assessed by palpation for 2 months after injection. The number of mice forming tumors is tabulated. The statistical significance of the difference between the control and antisense transfectants was determined using a test; $p > 0.001$. * indicates that these tumors were negative for pZαM expression. *B*, loss of antisense DNA MeTase expression in tumors derived from antisense transfectants. RNA (10 μg) isolated from the indicated tumors was subjected to Northern blot analysis and hybridization with the 0.6-kb MET cDNA probe. Expression of the 1.3-kb antisense message is seen only in the original cell lines pZαM (*4*, *7*, and *9*) and is undetectable in tumors arising from pZαM transfectants or Y1 cell lines even after long exposure. The filter was stripped of radioactivity and rehybridized with a ^{32}P-labeled oligonucleotide corresponding to 18 S rRNA (28).

To determine whether cells expressing antisense to the DNA MeTase exhibit early morphological markers of apoptosis, cells were serum-starved for 24 h, harvested, and analyzed by electron microscopy. Fig. 5*B* shows representative electron micrographs of several blocks of control pZEM and pZαM transfectants at various magnifications (*I–III*). The control cells have a fine uniform nuclear membrane whereas the pZαM cells exhibit the cardinal markers of apoptosis (34): condensation of chromatin and its margination at the nuclear periphery (*panels I* and *II*), chromatin condensation (*panel II*), nuclear fragmentation (*panel III*), formation of apoptotic bodies, and cellular fragmentation. Whereas it is still unclear whether apoptosis upon serum deprivation is directly enhanced by demethylation or is an indirect effect of the change in the transformed state of the transfectants, the serum deprivation-induced cell death is another indicator of the reversal of cellular transformation by DNA MeTase antisense.

To determine whether demethylation can result in inhibition of tumorigenesis *in vivo*, we injected 1×10^6 cells for each of the Y1, pZEM, and pZαM (4, 7, and 9) transfectants subcutaneously into the syngeneic mouse strain LAF-1. The presence of tumors was determined by palpation. While all the animals injected with Y1 or pZEM cells formed tumors, animals injected with the pZαM transfectants had very few tumors arise (Fig. 6*A*; $p > 0.005$).

One possible explanation for the fact that a small number of tumors did form in animals injected with the pZαM transfectants is that they are derived from revertants that lost expression of the antisense to the DNA MeTase under the selective pressure *in vivo*. RNA was isolated from tumors arising from the pZαM transfectants, and the level of expression of the 0.6-kb antisense message was compared with the transfectant lines *in vitro* (Fig. 6*B*). The expression of the antisense message is virtually nonexistent in the tumors derived from pZαM transfectants even after long exposure of the Northern blots, supporting the hypothesis that expression of an antisense message to the DNA MeTase is incompatible with tumor growth *in vivo*.

DNA Demethylation Induced by 5-AzaCdR Results in Reversal of Cellular Transformation ex Vivo—To further verify that inhibition of DNA methylation results in reversal of cellular transformation and to exclude the possibility that the effects observed are nonspecific results of antisense expression we used an inhibitor of DNA methylation 5-azadeoxycytidine (5-

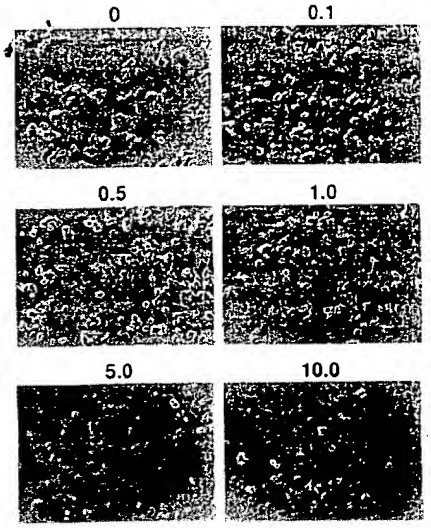

FIG. 7. **Morphological change in Y1 cells treated with 5-azaCdR.** Y1 cells were treated with concentrations of 5-azaCdR ranging from 0–10 μM every 12 h for 72 h. Phase contrast microscopy at × 200 magnification of living cultures of the treated cells is presented.

azaCdR) that acts at a different site than antisense RNA (35). 5-azaCdR is a deoxycytidine analogue that inhibits DNA methylation once it is incorporated into DNA. It has been suggested that an irreversible complex is formed between the DNA MeTase enzyme and the C-6 position of the cytosine moiety (36). We treated Y1 cells with concentrations of 5-azaCdR ranging from 0 to 10 μM every 12 h for 72 h. 5-azaCdR increases the proportion of cytosine to methylcytosine in the DNA by 1.6-fold in a dose-dependent manner (0–5.0 μM) as determined by a nearest neighbor analysis. Over the same concentration range, cell viability in low serum is reduced from 80% to ~40%, and the ability of cells to form colonies in soft agar is reduced by ~50-fold. No differences were seen in the ability of cells to form colonies on regular plastic dishes. The 5-azaCdR-treated cells exhibited dose-dependent morphological changes similar to those observed in the pZαM transfectants (Fig. 7). This experiment suggests that 5-azaCdR treatment reversed the transformed phenotype of Y1 cells but did not affect their viability.

DISCUSSION

This paper tests the hypothesis that overexpression of the DNA MeTase plays a causal role in cellular transformation by expressing an antisense message to the DNA MeTase in an adrenocortical carcinoma cell line. Expression of an antisense DNA MeTase (Fig. 1) leads to: (i) a limited reduction in DNA MeTase steady state mRNA and protein levels (Fig. 2), (ii) a general but limited reduction in the methylation content of the genome (Fig. 2), (iii) demethylation of regions aberrantly methylated in this cell line such as the adrenal specific 21-hydroxylase gene (Fig. 3), (iv) morphological changes indicative of inhibition of the transformed phenotype, (v) inhibition of anchorage-independent growth as determined by soft agar assays, (vi) inhibition of serum-independent survivability and induction of apoptosis under serum-deprived conditions, as well as (vii) inhibition of tumorigenesis in syngeneic mice (Fig. 6) and (viii) inhibition of DNA methylation by 5-azaCdR, which acts at a site completely different from antisense to the DNA MeTase, also results in reversal of transformation indicators *ex vivo*. The fact that a 2-fold inhibition in DNA MeTase expression is sufficient to induce such profound changes in the state of transformation of Y1 cells is in accordance with previously published data showing that a 2–3-fold elevation in DNA MeTase activity by forced expression of an exogenous DNA MeTase in NIH 3T3 can induce cellular transformation of these cells (23). Whereas antisense expression is considered one of the most direct means to inhibit gene expression, no experimental method is devoid of potential complications. 5-azaCdR, which is the most commonly used DNA methylation inhibitor, has side effects (36, 37). However, the fact that both inhibitors had similar effects strongly validates our conclusions. The fact that 5-azaCdR inhibited transformation indicators but not the survival of the cells and their ability to form colonies, and the fact that the reversal of transformed phenotype was expressed weeks after the inhibitor had been removed is consistent with the model that 5-azaCdR triggered a change in the cellular program rather than a cytotoxic or cytostatic effect. It stands to reason that this change in program was triggered by the initial demethylation event caused by the drug.

Our experiments support a previously proposed hypothesis that overexpression of DNA MeTase is an important component of an oncogenic pathway(s) (22). Since Y1 is a line derived from a naturally occurring tumor (24) which bears amplified copies of Ras (25), it is possible that hyperactivation of the DNA MeTase is triggered by the Ras-Jun signaling pathway (21, 22). The DNA MeTase promoter bears a number of AP-1 sites (20), and we demonstrated that the activity of the DNA MeTase promoter is dependent on binding of AP-1 (21) and that down-regulation of the the Ras-Jun pathway in Y1 cells results in inhibition of DNA MeTase activity, hypomethylation, and reversal of the transformed phenotype.[2] Our data might explain previous observations demonstrating an increase in DNA MeTase activity (13, 19) in cancer cells by suggesting that this increase is critical for the transformed state.

What is the possible mechanism by which hypermethylation can cause cellular transformation? The answer to this question is still elusive and could not be resolved by the data presented in this paper; however, several hypotheses have been previously suggested. One plausible explanation that has been previously suggested by Baylin and his colleagues (38) is that methylation may establish abnormalities of chromatin organization which in turn mediate the progressive losses of gene expression associated with tumor development. One interesting class of genes that might be affected are the tumor suppressor genes. There is evidence that ectopic inactivation of tumor suppressor genes by methylation contributes to cancer (39, 40). The promoter region of the RB-1 gene was found to be methylated in 6 of 77 retinoblastomas (17), and the 5' region of the WT-1 gene was methylated in 2 out of 29 Wilms tumors (40), while the gene methylated was otherwise grossly normal. However, there is no evidence that tumor suppressor genes are the critical targets for hypermethylation in cancer cells or that tumor suppressor genes are selectively demethylated in the DNA MeTase antisense transfectants. Also, our unpublished data do not suggest any induction in the level of expression of these genes in the pZαM transfectants.

Another interesting mechanism that has been suggested by Jones and his colleagues is that methylated CpGs are hot spots for mutations by deamination of the methylated cytosine into thymidine (41). This kind of change induced by methylation will not be reversible, the fact that we could reverse transformation by inhibiting DNA MeTase suggests that other mechanisms must be involved. While inhibition of gene expression by methylation is the best analyzed function of DNA methylation, one should bear in mind that any function of the genome might be modified by methylation. Sites that are especially sensitive to changes in methylation might be controlling DNA functions such as repair, replication, and susceptibility to

[2] A. R. MacLeod, J. Roleau, and M. Szyf, unpublished results.

death program-related endonucleases.

One question that remains to be answered is how to explain the contradiction between the fact that DNA MeTase is overexpressed in cancer cells and the observed regional hypomethylation of the genome of many cancer cells (11, 12). However, there are no data at this stage to resolve this apparent contradiction. While additional experiments will be required to address these questions, this paper demonstrates that inhibition of DNA methylation leads to a reversal of the transformed state and that DNA methylation plays a critical role in cellular transformation.

Acknowledgments—We thank Dr. Gary Tanigawa, Marc Pinard, and Shyam Ramchandani for critical reading of the manuscript and stimulating discussions, as well as Vera Bozovic for excellent technical assistance, Allan Forester for help with the photography, and Marie Ballak for her contribution to the electron microscopy analysis.

REFERENCES

1. Razin, A., and Riggs, A. D. (1980) *Science* **210**, 604–610
2. Razin, A., and Szyf, M. (1984) *Biochim. Biophys. Acta* **782**, 331–342
3. Yisraeli, J., and Szyf, M. (1985) in *DNA Methylation: Biochemistry and Biological Significance* (Razin, A., Cedar, H., and Riggs, A. D., eds) pp. 353–378, Springer-Verlag, New York
4. Li, E., Bestor, T. H., and Jaenisch, R. (1992) *Cell* **69**, 915–926
5. Jones, P. A. (1985) *Cell* **40**, 485–486
6. Razin, A., Feldmesser, E., Kafri, T., and Szyf, M. (1985) in *Biochemistry and Biology of DNA Methylation* (Razin, A., and Cantoni, G. L., eds) p. 239, Alan R. Liss, Inc., New York
7. Szyf, M., Rouleau, J., Theberge, J., and Bozovic, V. (1992) *J. Biol. Chem.* **267**, 12831–12836
8. Szyf, M., Kaplan, F., Mann, V., Giloh, H., Kedar, E., and Razin, A. (1985) *J. Biol. Chem.* **260**, 8653–8656
9. Szyf, M., Bozovic, V., and Tanigawa, G. (1991) *J. Bol. Chem.* **266**, 10027–10030
10. Szyf, M. (1991) *Biochem. Cell Biol.* **64**, 764–769
11. Feinberg, A. P., Gehrke C. W., Kuo K. C., and Ehrlich, M. (1988) *Cancer Res.* **48**, 1159–1161
12. Feinberg, A. P., and Vogelstein, B. (1983) *Nature* **301**, 89–92
13. El-Deiry, W. S., Nelkin, B. D., Celano, P., Chiu-Yen, R. W., Falco, J. P., Hamilton, S. R., and Baylin, S. B. (1990) *Proc. Natl. Acad Sci. U. S.A.* **88**, 3470–3474
14. Antequera, F., Boyes, J., and Bird, A. (1990) *Cell* **62**, 503–514
15. de Bustros, A., Nelkin, B. D., Silverman, A., Ehrlich, G., Poiesz, B., and Baylin, S. B. (1988) *Proc. Natl. Acad Sci. U. S. A.* **85**, 5693–5697
16. Makos, M., Nelkin, B. D., Lerman, M. I., Latif, F., Zbar, B., and Baylin, S. B. (1992) *Proc. Natl. Acad Sci. U. S. A.* **89**, 1929–1933
17. Ohtani-Fujita, N., Fujita, T., Aoike, A., Osifchin, N. E., Robbins, P. D., and Sakai, T. (1993) *Oncogene* **8**, 1063–1067
18. Saxon, P. J., Srivatsan, E. S., and Stanbridge, E. G. (1986) *EMBO J.* **5**, 3461–3466
19. Kautiainen, T. L., and Jones, P. (1986) *J. Biol. Chem.* **261**, 1594–1598
20. Rouleau, J., Tanigawa, G., and Szyf, M. (1992) *J. Biol. Chem.* **267**, 7368–7377
21. Rouleau, J., MacLeod, A. R., and Szyf, M. (1995) *J. Biol. Chem.* **270**, 1595–1601
22. Szyf, M. (1994) *Trends Pharmacol. Sci.* **15**, 233–238
23. Wu, J., Issa, J. P., Herman, J., Bassett, D., Nelkin, B. D., and Baylin, S. B. (1993) *Proc. Natl. Acad. Sci. U. S. A.* **90**, 8891–8895
24. Yasumura, Y., Buonassisi, V., and Sato, G. (1966) *Cancer Res.* **26**, 529–535
25. Schwab, M., Alitalo, K., Varmus, H. E., Bishop, J. M., and George, D. (1983) *Nature* **303**, 497–501
26. Ausubel, F. M., Brent, R., Kingston, R. E., Moore, D. D., Smith, J. A., Seidman, J. G., and Struhl, K. (1988) *Current Protocols in Molecular Biology*, Wiley and Sons, New York
27. Freedman, V. H., and Shin, S. (1974) *Cell* **3**, 355–359
28. Bestor, T., Laudano, A., Mattaliano, R., and Ingram, V. (1988) *J. Mol. Biol.* **203**, 971–983
29. Szyf, M., Milstone, D. S., Schimmer, B. P., Parker, K. L., and Seidman, J. G. (1990) *Mol. Endocrinol.* **4**, 1144–1152
30. Maysinger, D., Piccardo, P., Flipovic-Grcic, J., and Cuello, A. C. (1993) *Neurochem Int.* **23**, 123–129
31. Szyf, M., Schimmer, B. P., and Seidman, J. G. (1989) *Proc. Natl. Acad. Sci. U. S. A.* **86**, 6853–6857
32. Jones, P. A., Wolkowicz, M. J., Rideout, W. M., III, Gonzales, F. A., Marziasz, C. M., Coetzee, G. A., and Tapscott, S. J. (1990) *Proc. Natl. Acad Sci. U. S. A.* **87**, 6117–6121
33. Barns, D., and Sato, G. (1980) *Cell* **22**, 649–655
34. Wyllie, A. H., Beatie, G. J., and Hargreaves, A. D. (1981) *Histochem. J.* **13**, 681–692
35. Wu, J. C., and Santi, D. V. (1985) *Biochemistry and Biology of DNA Methylation* (Razin, A., and Cantoni, G. L., eds) pp. 119–129, Alan R. Liss Inc., New York
36. Jones, P. A. (1984) in *DNA Methylation: Biochemistry and Biological Significance* (Razin, A., Cedar, H., and Riggs, A. D., eds) pp. 165–187, Springer-Verlag New York Inc., New York
37. Tammame, M., Antequera, F., Villanueva, J. R., and Santos, T. (1983) *Mol. Cell. Biol.* **3**, 2287–2297
38. Baylin, S. B., Makos, M., Wu, J., Chiu Yen, R.-W., de Bustros, A., Vertino, P., and Nelkin, B. D. (1991) *Cancer Cells* **3**, 383–390
39. Bestor, T. H., and Coxon, A. (1993) *Curr. Biol.* **3**, 384–386
40. Royer-Pokora, B., and Schneider, S. (1992) *Genes Chromosomes Cancer* **5**, 132–140
41. Jones, P. A., Rideout, W. M., Shen, J., Spruck, C. H., and Tsai, Y. C. (1992) *Bioessays* **14**, 33–36

Proc. Natl. Acad. Sci. USA
Vol. 94, pp. 684–689, January 1997
Medical Sciences

Inhibition of tumorigenesis by a cytosine–DNA, methyltransferase, antisense oligodeoxynucleotide

SHYAM RAMCHANDANI*, A. ROBERT MACLEOD*, MARC PINARD*, ERIC VON HOFE†, AND MOSHE SZYF*‡

*Department of Pharmacology and Therapeutics, McGill University, Montreal, PQ, Canada H3G 1Y6; and †Hybridon, Inc., Worcester, MA 01605

Communicated by Robert L. Sinsheimer, University of California, Santa Barbara, CA, November 6, 1996 (received for review July 23, 1996)

ABSTRACT **This paper tests the hypothesis that cytosine DNA methyltransferase (DNA MeTase) is a candidate target for anticancer therapy. Several observations have suggested recently that hyperactivation of DNA MeTase plays a critical role in initiation and progression of cancer and that its up-regulation is a component of the Ras oncogenic signaling pathway. We show that a phosphorothioate-modified, antisense oligodeoxynucleotide directed against the DNA MeTase mRNA reduces the level of DNA MeTase mRNA, inhibits DNA MeTase activity, and inhibits anchorage independent growth of Y1 adrenocortical carcinoma cells *ex vivo* in a dose-dependent manner. Injection of DNA MeTase antisense oligodeoxynucleotides i.p. inhibits the growth of Y1 tumors in syngeneic LAF1 mice, reduces the level of DNA MeTase, and induces demethylation of the adrenocortical-specific gene C21 and its expression in tumors *in vivo*. These results support the hypothesis that an increase in DNA MeTase activity is critical for tumorigenesis and is reversible by pharmacological inhibition of DNA MeTase.**

Modification of DNA by methylation is now recognized as an important mechanism of epigenetic regulation of genomic functions (1–3). Methylation of DNA is a postreplication event catalyzed by the DNA methyltransferase (DNA MeTase) enzyme using *S*-adenosyl methionine as a methyl donor (4). Approximately 80% of cytosines located in the CpG dinucleotide sequence are methylated in the genome of most vertebrate cells, but the distribution of methylated sites is cell- and tissue-specific (5). Patterns of methylation are generated during development by enzymatic *de novo* methylation and demethylation processes (1–7) and are maintained in somatic cells.

A number of observations have suggested that the pattern of DNA methylation is disrupted in cancer cells (8, 9). Both hypomethylation (9) and hypermethylation (10–12) of different CpG sites in cancer cells and tissues relative to the cognate normal tissue have been documented. Some of the sites that are hypermethylated in tumors are located in tumor–suppressor loci such as p16 (13), retinoblastoma (14), von Hippel–Lindau (15), and Wilms tumor (16), and, recently, a new candidate tumor–suppressor gene was cloned by molecular analysis of the hypermethylated region in chromosome 17p13.3 (17). One possible explanation that has been proposed to explain the changes in DNA methylation observed in cancer cells is that they are the end result of a change in the enzymatic machinery controlling DNA methylation in the cell (7, 12, 18–20). In accordance with this hypothesis, cancer cell lines (21) and human tumors (22) have been shown to express elevated levels of DNA MeTase. Recently, Belinsky *et al.* (23) showed that increased DNA MeTase activity is an early event in carcinogen-initiated lung cancer in the mouse. Forced expression of DNA MeTase cDNA in murine NIH 3T3 cells leads to genomic hypermethylation and neoplastic transformation (24), and expression of an antisense mRNA to the DNA MeTase leads to loss of tumorigenicity of the adrenocortical carcinoma cell line Y1 (25).

Many stimuli may account for increased DNA MeTase activity in tumors. One possible molecular mechanism explanation of this elevation of DNA MeTase in cancer cells is that the expression of the DNA MeTase gene is regulated by oncogenic signaling pathways such as the Ras–Jun signaling pathway (18, 19). Modulation of this pathway can alter DNA MeTase expression and DNA methylation (26–28). Similarly, ectopic expression of *Ha-ras* leads to induction of demethylation activity in P19 cells (29), which can explain (18) the observed hypomethylation of some CpG sites in cancer cells (8, 9).

If hyperactivity of DNA MeTase is a critical, downstream component of oncogenic programs (25–28), it should be an excellent target for anticancer therapy (19). To test this hypothesis in an animal model, specific inhibitors of DNA MeTase are required. The only DNA MeTase inhibitor that has been available to date is the nucleoside analog 5-azadeoxycytidine (30). Although 5-azadeoxycytidine is an effective inhibitor of DNA methylation (30), it has many side effects that might compromise the interpretation of the experimental data and limit its clinical utility (19, 31, 32). The advent of antisense oligodeoxynucleotides as specific inhibitors of protein expression in whole animal systems offers new opportunities in approaching this hypothesis (33).

Y1 cells offer a model to test our hypothesis. First, this line [which was isolated from a naturally occurring adrenocortical tumor in an LAF1 mouse (34)] bears a 30- to 60-fold amplification of the cellular proto oncogene c-Ki-*ras* (35). Second, the molecular link between hyperactivation of Ras, DNA MeTase hyperactivity, and DNA methylation and the state of cellular transformation has been recently demonstrated (25, 28). Third, identification of effective antisense oligodeoxynucleotide inhibitors requires screening of a number of potential candidates. This can only be done effectively *ex vivo*. Y1 cells can be grown and tested for tumorigenic characteristics *ex vivo* as well as implanted in syngeneic LAF1 mice (25) *in vivo*, thus enabling the study of the effects of inhibition of DNA methylation in a whole animal system.

MATERIALS AND METHODS

Cell Culture, *ex Vivo* Oligodeoxynucleotide Treatment, and Tumorigenicity Assays. Y1 cells were maintained as monolayers in F-10 medium, which was supplemented with 7.25% heat-inactivated horse serum and 2.5% heat-inactivated fetal calf serum (Immunocorp, Montreal). The sequences of the oligodeoxynucleotides used in this study were as follows: antisense (HYB101584), 5′-TCT ATT TGA GTC TGC CAT TT-3′ corresponding to bases −2 to +18 in the murine DNA MeTase mRNA [relative to the putative translation initiation site (9)]; the scrambled sequence corresponding to the antisense sequence (HYB102277), 5′-TGT GAT TCT CCT TAT

The publication costs of this article were defrayed in part by page charge payment. This article must therefore be hereby marked "*advertisement*" in accordance with 18 U.S.C. §1734 solely to indicate this fact.

0027-8424/97/94684-6$2.00/0
PNAS is available online at http://www.pnas.org.

Abbreviation: DNA MeTase, DNA methyltransferase.

‡To whom reprint requests should be addressed.

TCG AT-3′; and the reverse sequence (HYB101585), 5′-TTT ACC GTC TGA GTT TAT CT-3′. Phosphorothioate oligodeoxynucleotides were synthesized using phosphoramadite chemistry on a Biosearch model 8700 automated synthesizer and were purified by HPLC using a phenyl Sepharose column followed by DEAE 5PW anion exchange chromatography. The purity of all oligonucleotides was greater than 98% as determined by ion exchange chromatography. These experiments were performed in the absence of any lipid carrier to avoid nonspecific effects of the carrier in long term treatments and to recapitulate the situation *in vivo*, in which no carrier was used. This experimental paradigm required using oligodeoxynucleotides at the micromolar concentration range, which is higher than the concentrations required when lipid carriers are used.

DNA and RNA Analyses. Genomic DNA was prepared from pelleted nuclei, and total cellular RNA was prepared from cytosolic fractions according to standard protocols (36–38).

Western Blot Analysis of DNA MeTase. Rabbit polyclonal antibodies were raised (Pocono Rabbit Farm, Canadensis, PA) against a peptide sequence consisting of amino acids 1107–1125 of the mouse DNA MeTase (1101–1119 of the human DNA MeTase). The specificity of the polyclonal serum was tested by competition with the antigen peptide. Nuclear extracts (50 μg) were resolved on a 5% SDS/PAGE, transferred onto poly(vinylidene difluoride) membrane (Amersham), and subjected to immunodetection for the DNA MeTase according to standard protocols using a 1:2000 dilution of primary antibody and an enhanced chemiluminescence detection kit (Amersham) (40).

Assay of DNA MeTase Activity. DNA MeTase activity (3 μg) was assayed by incubating 3 μg of nuclear extract with a synthetic, hemimethylated, double-stranded oligodeoxynucleotide (37) substrate and *S*-[*methyl*-^{3}H]-*S*-adenosyl-L-methionine (78.9 Ci/mmol; Amersham) as a methyl donor for 3 h at 37°C as described (36).

Assay of C21 mRNA by Reverse Transcriptase–PCR. The expression of the C21 gene was determined using our described primers and amplification conditions (41).

RESULTS

Antisense Oligodeoxynucleotides to the Translation Initiation Region of the Murine DNA MeTase Inhibit DNA MeTase mRNA, DNA MeTase Activity, and Tumorigenesis *ex Vivo*. We have shown that expression of a 600-bp fragment bearing sequences encoding the 5′ domain of the DNA MeTase mRNA in

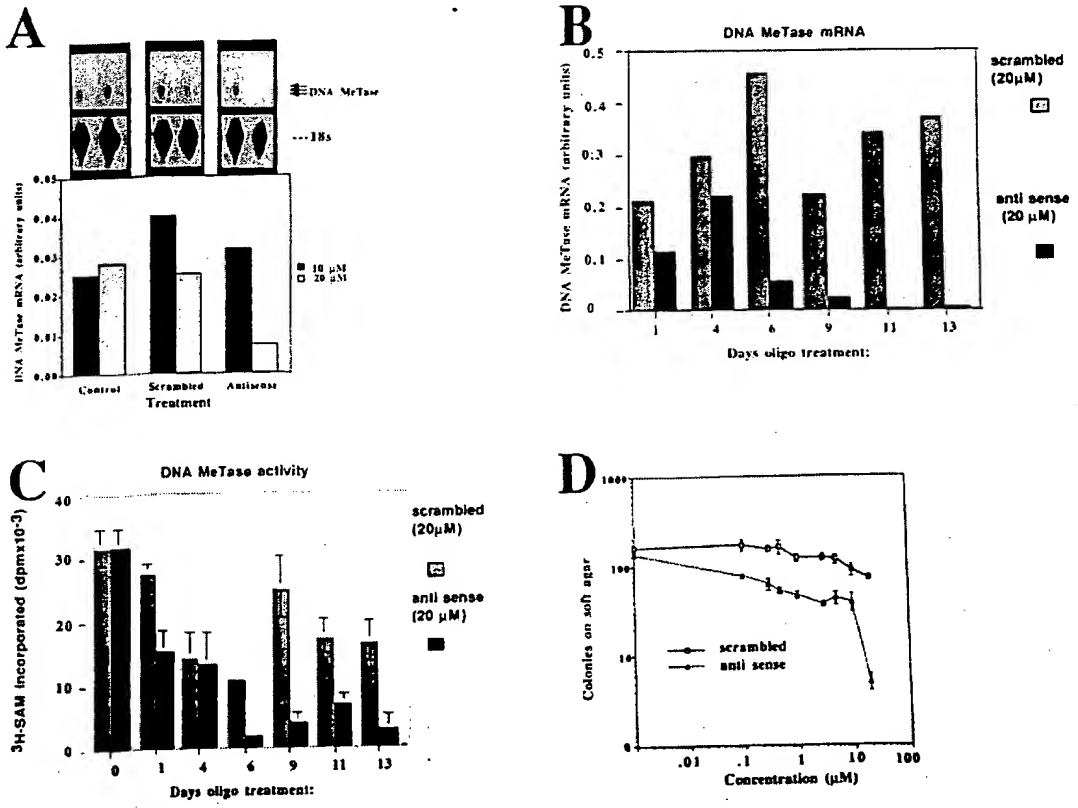

FIG. 1. DNA MeTase antisense oligodeoxynucleotides inhibit DNA MeTase mRNA, DNA MeTase activity, and anchorage independent growth *ex vivo*. (*A*) RNase protection analysis of DNA MeTase mRNA in Y1 cells treated with control scrambled and antisense oligodeoxynucleotides. Y1 cells were cultured in the presence of different concentrations of scrambled and antisense oligodeoxynucleotides (sequence shown in *Materials and Methods*) as indicated for 48 h. RNA (3 μg) extracted from the cells was subjected to an RNase protection assay as described (26) using a 700-bp riboprobe [probe A in Rouleau *et al.* (26)] encoding the DNA MeTase genomic sequence from −0.39 to +318. The major bands representing the two major initiation sites are indicated (92-, 90-bp, protected fragments) as well as the first exon, which gives a 99-bp, protected fragment. (*B*) Time course of inhibition of DNA MeTase mRNA by antisense oligodeoxynucleotides. Y1 cells were incubated in the presence of 20 μM of either antisense or scrambled oligodeoxynucleotides, and the medium was replaced with oligodeoxynucleotide-containing medium every 24 h. Cells were harvested at the indicated time points, and RNA and nuclear extracts were prepared as described. RNA was subjected to RNase protection assay as described in *A*. An autoradiogram similar to the one presented in *A* was scanned, and the amount of DNA MeTase mRNA at each point was normalized to the signal obtained for 18s ribosomal RNA. (*C*) Nuclear extracts prepared from oligodeoxynucleotide-treated Y1 cells described in *B* were assayed for DNA MeTase activity as described. The results represent an average of triplicate determination ± SD. (*D*) Y1 cells were treated with scrambled and antisense oligodeoxynucleotides as described in *B* and seeded onto soft agar for determination of anchorage-independent growth as described. The results represent an average of triplicate determinations ± SD.

the antisense orientation can inhibit DNA methylation and induce both cellular differentiation of 10T½ cells (43) and reversal of transformation of Y1 cells (25). Antisense expression vectors could not be used easily to study the function and therapeutic potential of inhibiting DNA MeTase *in vivo*. We therefore tested the possibility that shorter antisense oligodeoxynucleotides directed against the same region of the mRNA could recapitulate these effects. An antisense oligodeoxynucleotide [+18 to −2 (sequence as in *Materials and Methods*) when the translation initiation site is indicated, as in Bestor *et al.* (44)] was found to be active in a preliminary screen, and we further determined its mechanism of action.

One of the possible mechanisms of action of antisense oligodeoxynucleotides is targeting RNase H activity to the RNA–DNA duplex, resulting in degradation of the mRNA (45). We first determined the dose–response relationship of

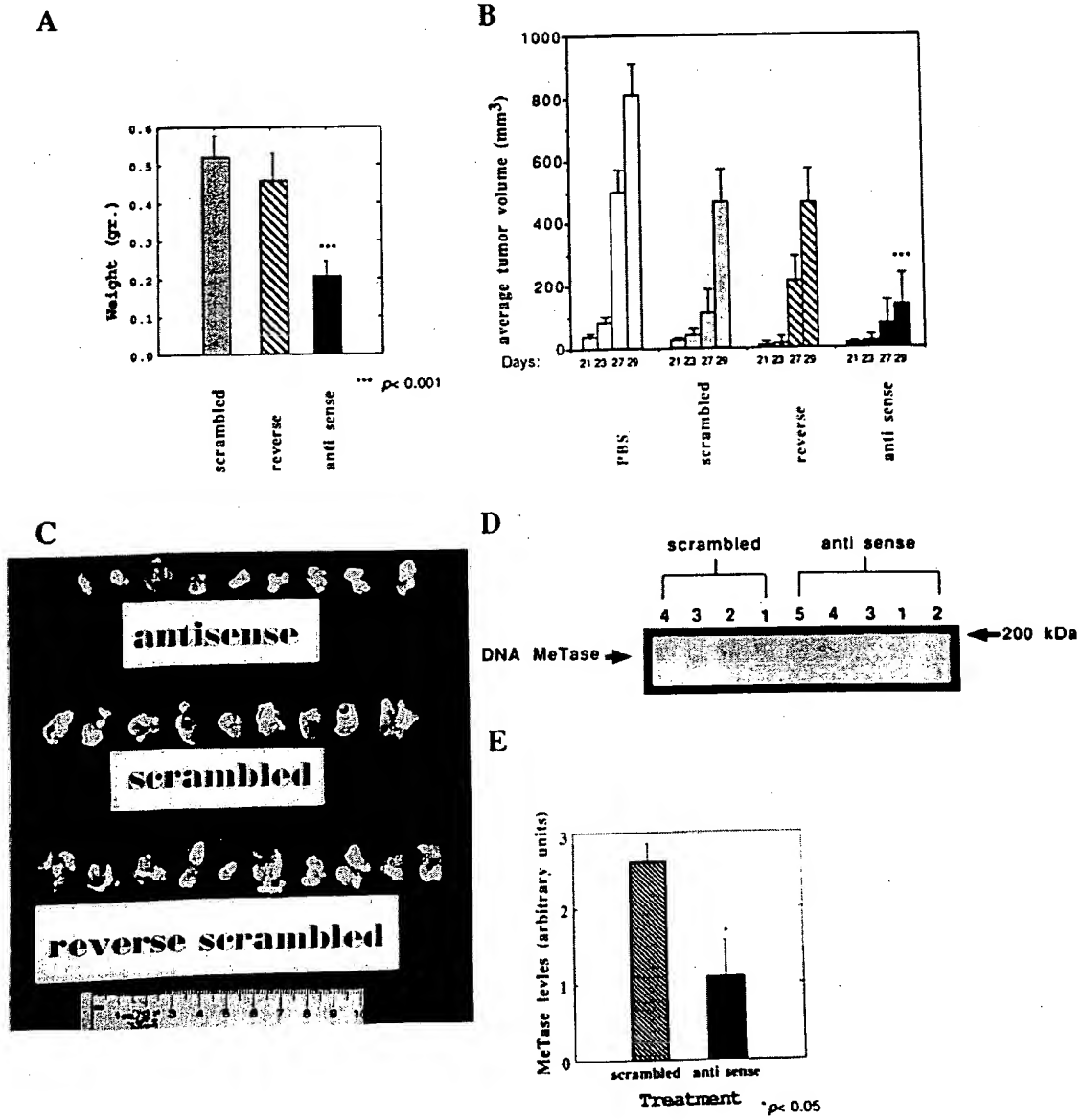

FIG. 2. DNA MeTase antisense oligodeoxynucleotide inhibits tumor growth *in vivo*. (*A*) Average weight of tumors isolated from LAF1 mice bearing Y1 tumors that were injected with antisense, scrambled, or reverse oligodeoxynucleotide (5 mg/kg) every 48 h for 29 days. The results are presented as an average ± SEM. The statistical significance of the difference between the scrambled or reverse groups and the antisense group was determined by a Student's *t* test to be $P < 0.001$. There was no statistically significant difference between the two control groups ($P > 0.5$). (*B*) Average volume of tumors determined as described at the indicated time points postimplantation [determined as described in Plumb *et al.* (42)]. (*C*) Photograph of the tumors removed from the antisense, reverse, and scrambled oligodeoxynucleotide-treated mice described above. (*D*) LAF1 mice bearing Y1 tumors were injected with 5 mg/kg scrambled ($n = 4$) or antisense ($n = 5$) oligodeoxynucleotides three times every 24 h s.c. Tumors were removed from each mouse (indicated by serial numbers 1–4 for the scrambled group and 1–5 for the antisense group), and nuclear extracts prepared from the tumors were subjected to a Western blot analysis as described. The band corresponding to the DNA MeTase is indicated by an arrow. The amount of signal corresponding to the DNA MeTase (OD arbitrary units) was normalized to the level of total protein transferred onto the membrane as determined by Amido black staining and quantified by scanning (OD arbitrary units). The values obtained (OD of DNA MeTase signal divided by OD of the total protein staining) for the tumors extracted from each of the treated mice (serial number of mice in bold) were as follows: scrambled: 1, 2.2; 2, 3.1; 3, 2.7; and 4, 2.5: antisense: 1, 0.6; 2, 0.5; 3, 0.16; 4, 1.0; and 5, 2.9. (*E*) Average DNA MeTase level per group is plotted with the SEM. The difference between the scrambled and antisense groups was determined by a Student's *t* test to be statistically significant ($P < 0.05$).

DNA MeTase mRNA abundance and DNA MeTase antisense oligodeoxynucleotide concentration at one time point. Y1 cells (10^6 cells) were treated with different concentrations (0, 10, and 20 μM) of antisense oligodeoxynucleotides and scrambled controls for 48 h. Cellular RNA was subjected to an RNase protection assay as described in *Materials and Methods*. The results presented in Fig. 1*A* demonstrate a sharp decrease in abundance of DNA MeTase mRNA after incubation of the cells with 20 μM of the DNA MeTase antisense oligodeoxynucleotides, which was not observed after treatment with scrambled oligodeoxynucleotides. We then defined the time dependence of reduction in DNA MeTase activity at the inhibitory concentration of the antisense oligodeoxynucleotide (20 μM). The results presented in Fig. 1 *B* (RNA) and *C* (MeTase activity) show that both DNA MeTase activity and mRNA are reduced by 10- to 100-fold after 6 days of treatment. Some fluctuations are observed in the levels of DNA MeTase in Y1 cells treated with control oligodeoxynucleotides (2-fold) as well as antisense oligodeoxynucleotides (such as the relatively high levels of DNA MeTase at 4 days). These oscillations in DNA MeTase mRNA expression might reflect changes in the cell cycle kinetics of the cells at different time points because DNA MeTase levels are regulated with the cell cycle (35, 37). Alternatively, they might result from nonspecific effects of oligodeoxynucleotides on different cellular parameters or reflect some inaccuracies in our measurements. However, an overall reduction in DNA MeTase activity was established after 6 to 9 days of treatment with the antisense oligodeoxynucleotides.

Can DNA MeTase antisense oligodeoxynucleotides induce a dose-dependent inhibition of tumorigenicity *ex vivo* as measured by anchorage-independent growth on soft agar? Y1 cells were treated with a range of concentrations of antisense and scrambled oligodeoxynucleotides (0–20 μM) for 13 days. The cells were harvested and plated onto soft agar as described (39). The results presented in Fig. 1*D* demonstrate a dose-dependent inhibition of colony formation on soft agar in antisense-treated cells vs. the scrambled control. The drop in the number of colonies formed on soft agar between 10 and 20 μM corresponds to the precipitous drop in DNA MeTase mRNA at this concentration of antisense oligodeoxynucleotide (Fig. 1*A*).

Inhibition of anchorage-independent growth of antisense-treated cells was observed even though the soft agar medium was not supplemented with antisense oligodeoxynucleotides, suggesting that the changes in the level of tumorigenicity of antisense-treated cells were irreversible. This is consistent with the hypothesis that, once DNA MeTase is inhibited, the cells are reprogrammed to a less transformed state (18, 25). The experiments described above demonstrated that antisense oligodeoxynucleotides could inhibit DNA MeTase activity *ex vivo* and that this inhibition corresponded to a dose-dependent inhibition of tumorigenicity.

Inhibition of Tumor Growth and DNA MeTase *in Vivo* by a DNA MeTase Antisense Oligodeoxynucleotide. To test the hypothesis that inhibition of DNA MeTase *in vivo* can result in inhibition of tumor growth and to determine the general toxic effects of DNA MeTase antisense treatment, Y1 cells (1×10^6) were implanted in the flank of the syngeneic mouse strain LAF1 and were treated by i.p. injections every 48 h with PBS, antisense oligodeoxynucleotide, or two control oligodeoxynucleotides: a scrambled version of the antisense oligodeoxynucleotide and a reverse sequence (see *Materials and Methods* for sequence). Preliminary experiments with a small number of animals per group ($n = 3$) established a dose-dependent relationship between oligodeoxynucleotide concentrations and tumor growth. No effects were observed at 0.5 mg/kg whereas inhibition of tumor appearance and growth was observed in the 1- to 5-mg/kg range. At 20 mg/kg, nonspecific effects were observed with the scrambled oligodeoxynucleotides in two out of three experiments whereas a statistically significant reduction in tumor growth with antisense oligodeoxynucleotides vs. controls was observed in one experiment (data not shown). Forty LAF1 mice were implanted with Y1 cells, randomized, and divided into color-coded groups of 10 mice each and were treated and evaluated as follows in a double-blind fashion. Three days postimplantation, the mice were injected i.p. with 100 μl of PBS or PBS containing 5 mg/kg of either antisense, scrambled, or reverse oligodeoxynucleotides. Injections were repeated every 48 h, and tumor diameter measurements were taken at each time point. Thirty days postinjection, the animals were killed, and tumors were excised and weighed. The results described in Fig. 2 show that tumor growth was inhibited by injection of DNA MeTase antisense oligodeoxynucleotides relative to control oligodeoxynucleotides as determined by the rate of increase in the average tumor volume (Fig. 2*B*) as well as by the final weight and size of the tumors (Fig. 2 *A* and *C*). The difference in the average tumor volume between the antisense-treated group and either of the different control groups (PBS, scrambled, and reverse) at 29 days was highly statistically significant, as determined by a Student's *t* test ($P < 0.005$) whereas the difference between the different control oligodeoxynucleotide-treated groups and the PBS-treated group was not statistically significant. Similarly, the difference in average final tumor weight at 30 days between the antisense- and control oligodeoxynucleotide-treated groups was highly statistically significant ($P < 0.001$). One of the antisense-treated animals did not develop tumors whereas all of the members of the control groups developed tumors (one mouse of the reverse group died with a heavy tumor load before termination of the experiment).

We determined the general toxic effects of *in vivo* DNA MeTase antisense oligodeoxynucleotide treatment vs. treatment with the control oligodeoxynucleotides. Blood parameters and weight loss of antisense-, reverse-, and scrambled-injected (20 mg/kg) tumor-bearing LAF1 mice ($n = 5$) were assayed. As shown in Table 1, there were no significant reductions in red blood cell count, hematocrit, or percentage of hemoglobin in DNA MeTase antisense-treated animals vs. controls. Similarly, platelet and white blood cell counts were not increased but rather were decreased slightly in antisense-treated animals (Table 1). There was no significant weight loss even though tumor load was decreased significantly in this experiment by DNA MeTase antisense oligodeoxynucleotides.

These experiments demonstrated that *in vivo* treatment of tumor-bearing LAF1 mice with DNA MeTase antisense oligodeoxynucleotides can inhibit tumor growth, supporting the hypothesis that DNA MeTase is a critical component in maintaining the transformed state and that *in vivo* treatment with an antisense-based inhibitor of DNA MeTase can inhibit tumor growth.

DNA MeTase Antisense Oligodeoxynucleotide Inhibits DNA MeTase Levels, Induces Limited Demethylation of the

Table 1. Hematological analysis of LAF1 mice treated with antisense or control oligodeoxynucleotides (20 mg/kg) for 30 days ($n = 5$).

Treatment	Hematocrit	% hemoglobin	WBC	RBC	Platelets
Reverse	17.2 ± 9.2	6.4 ± 3.3	59.6 ± 2.19	3.4 ± 2.19	514 ± 291
Scrambled	16.1 ± 2.5	6.16 ± 0.9	71.8 ± 21.9	2.99 ± .45	503.2 ± 104
Antisense	21.9 ± 9.5	7.44 ± 3.8	50.7 ± 33	4.4 ± 1.8	302 ± 95

WBC, RBC, and hematocrit in g/dcl. Numbers represent mean and SD.

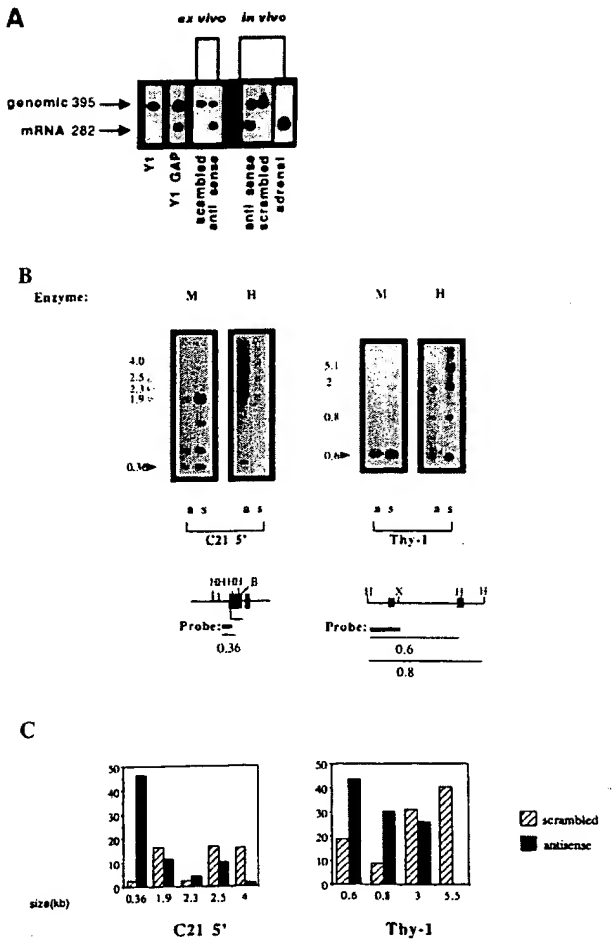

FIG. 3. Expression and demethylation of the C21 gene in Y1 tumors isolated from LAF1 mice treated with antisense oligodeoxynucleotides. (*A*) C21 expression was determined by reverse transcriptase–PCR amplification with C21-specific primers of total RNA isolated from Y1 cells, Y1GAP transfectants expressing hGAP (a GTPase- activating protein), an attenuator of Ras activity (28), Y1 cells treated with 20 μM of either scrambled oligodeoxynucleotide or DNA MeTase antisense oligodeoxynucleotides (*ex vivo* as indicated), Y1 tumors from LAF1 mice injected with either 5 mg/kg of scrambled or DNA MeTase antisense oligodeoxynucleotides (*in vivo*) as well as adrenal RNA. C21 plasmid DNA encoding the C21 gene (46) was included in the amplification reaction to control for nonspecific inhibition of amplification. The expected genomic and C21 mRNA amplification products are indicated by arrows. (*B*) DNA was extracted from Y1 tumors isolated from LAF1 mice injected with either scrambled oligodeoxynucleotides (scrambled 4, indicated as s) or antisense oligodeoxynucleotides (antisense 3, indicated as a) for 3 days as described. The DNA was subjected to *Hin*dIII digestion followed by either *Hpa*II (*H*) (which cleaves the sequence CCGG when the internal C is not3 methylated) or *Msp*I (*M*) (which cleaves the sequence CCGG even when the internal C is methylated) agarose gel fractionation (2.5%), Southern blotting analysis, and hybridization with the indicated probes. For the promoter region of the C21 gene, complete digestion of the gene should result in a 0.36-kb fragment (46), as indicated by the dark arrow. The partially methylated fragments are indicated by shaded arrows. The partial cleavage with *Msp*I is a consequence of the fact that the *Msp*I sites are nested within a *Hae*III site. These sites are highly resistant to cleavage by *Msp*I when fully or partially methylated, as described (47). For Thy-1, DNA prepared from the tumors indicated was subjected to a similar *Hpa*II–*Msp*I restriction enzyme analysis and hybridization with a 0.36 probe from the 5′ region of the *thy-1* gene (48). The expected *Hpa*II fragment is indicated by a dark arrow. Partially methylated fragments are indicated by shaded arrows. (*Lower*) Physical maps of the sequences analyzed for their methylation state. The first exons of the three genes are shown and are indicated as filled boxes, the probes used are indicated as thick lines, and the thin line indicates the expected nonmethylated and partially methylated *Hpa*II fragments. (X, *Xba*I; B, *Bam*HI). (*C*) Relative abundance of the *Hpa*II fragments was determined by densitometry as described. The size in kilobases of the scanned fragments is indicated. The results are presented as intensity of a specific fragment as a percentage of the total intensity in all scanned fragments per lane.

Adrenocortical-Specific C21 Gene, and Reactivates It. To determine whether injection of DNA MeTase antisense oligodeoxynucleotide can inhibit DNA MeTase activity, we treated tumor-bearing LAF1 mice for 3 days with either DNA MeTase antisense oligodeoxynucleotide (n = 5; 5 mg/kg) or the scrambled oligodeoxynucleotide (n = 4; 5 mg/kg) by s.c. injection near the tumor (1 cm) for 3 days. To limit (as much as possible) complicating, indirect factors that might have clouded the interpretation of data, we did not look at DNA methylation in tumors that were chronically treated. Tumors were harvested, nuclear extracts were prepared, and DNA MeTase levels in the nuclear extracts were determined by a Western blot analysis as described. The results of such an analysis are demonstrated in Fig. 2*D*, and the normalized average levels of DNA MeTase in each of the treatment groups plotted in Fig. 2*E* demonstrate a statistically significant reduction in DNA MeTase levels in antisense-treated animals ($P < 0.05$). The level of inhibition varied, however, from 90% inhibition in mouse number 3 in the group treated with antisense (Fig. 2*D*, lane 3) to no detectable inhibition in mouse number 5 (Fig. 2*D*, lane 5).

C21 is specifically expressed in the adrenal cortex, and the enzyme encoded by this gene, steroid 21 hydroxylase, is required for the synthesis of glucocorticoids, which is the main normal function of this tissue. The gene is expressed at very high levels in the adrenal cortex but is totally repressed and heavily methylated in Y1 tumor cells (41). No C21 mRNA is detected in Y1 cells even when the most sensitive assays, such as reverse transcriptase–PCR, are used (41). We have not observed any expression of C21 in Y1 cells in multiple Y1 cultures in the last decade under any conditions. We have suggested that this is a consequence of the increase in *de novo* DNA methylation activity in these cancer cells (41). Reexpression of C21 could serve as a good marker of demethylation and the reprogramming of Y1 cells to a nontransformed state.

To address this question, we performed a reverse transcriptase–PCR analysis of C21 expression on RNA prepared from the following samples: Y1 cells treated with either antisense DNA MeTase or scrambled oligodeoxynucleotides (20 μM) *ex vivo*; a tumor isolated from a mouse treated with antisense oligodeoxynucleotides *in vivo* for 3 days (antisense 3 exhibited the highest reduction in DNA MeTase activity: 90%); and Y1 cells transfected with hGAP [which attenuates the Ras signaling pathway, resulting in inhibition of DNA MeTase activity and partial demethylation of the C21 gene (28)]. C21 expression was induced under all of these conditions (Fig. 3*A*). This is the first induction of C21 reexpression in Y1 cells under any conditions observed in our laboratory. These results strongly support the hypothesis that DNA MeTase antisense oligodeoxynucleotides induce a partial demethylation and reprogramming of gene expression in Y1 cells that is similar to that observed after attenuation of the Ras signaling pathway.

To determine whether the 5′ promoter region of the C21 gene was demethylated in tumor DNA after antisense treatment, tumor DNA was subjected to *Msp*I/*Hpa*II restriction enzyme analysis, Southern blotting, and hybridization with a 5′ C21 probe [0.36-kb *Xba*I–*Bam*HI fragment encoding the promoter region of the C21 gene (41)]. Hypomethylation of the two *Hpa*II sites in the promoter region will result in a 0.36-kb fragment. As shown in Fig. 3*B*, the Y1 tumor that was extracted from a mouse (antisense 3) that was injected with antisense

oligodeoxynucleotides *in vivo* exhibits an increase in the abundance (as determined by densitometric analysis; Fig. 3*C*) of the 0.36-kb *Hpa*II fragment relative to the partially methylated fragments at 1.9, 2.5, and 4 kb compared with the control tumor. Demethylation of C21 is observed in other tumors injected with antisense (data not shown).

CpG island-containing genes are *de novo* methylated in tumor cells (13, 49–51). We therefore determined the state of methylation of a generally expressed CpG island-containing gene, *thy-1*, in mice treated with either antisense or control oligodeoxynucleotides. There was an increase in the relative abundance of the 600-bp *Hpa*II fragment contained in the 5′ *thy*-1 CpG island (48) (Fig. 3*B*) and a decrease in the relative abundance of the partial *Hpa*II fragments (≈3–5.5 kb) in tumors extracted from antisense-treated mice (labeled "a" in Fig. 3*B*) relative to the pattern observed in the control tumor (labeled "s" in Fig. 3*B*) (see Fig. 3*C* for quantification). These experiments demonstrated limited hypomethylation in tumor DNA in response to DNA MeTase antisense treatment *in vivo*.

DISCUSSION

The goal of this study was to test the hypothesis that tumorigenesis could be reversed by pharmacological inhibition of DNA MeTase activity and to suggest that DNA MeTase inhibitors could serve as potential anticancer agents. This study demonstrated that an antisense oligodeoxynucleotide directed against DNA MeTase mRNA can inhibit, in a dose-dependent manner, DNA MeTase mRNA expression, DNA MeTase activity, and tumorigenesis *ex vivo* and *in vivo*. Similar effects were not observed when a scrambled sequence was used. This is consistent with the hypothesis that the observed effects are a result of reduction in the level of DNA MeTase. The sequences used in our experiments did not bear the CG sites or G quartets that have been shown to bear nonantisense-related immunogenic and antitelomerase effects (52, 53). Although it is clear that phosphorothioate oligodeoxynucleotides might exhibit nonspecific antitumorigenic effects, our experiments revealed that the nonspecific and sequence-specific effects could be differentiated. One interesting question that was not addressed by this experiment is whether there is a critical size or level of tumor organization that is not treatable by DNA MeTase antisense inhibitors. Future studies will directly address this question.

Why are elevated levels of DNA MeTase critical for maintaining the cancer state? Three models have been suggested. (*i*) Elevated levels of DNA MeTase might result in disruption of the appropriate gene expression profile of a cell, leading to inactivation of tumor suppressor genes (17) and other genes that are characteristic of the differentiated state of the cell, such as C21 in Y1 cells (41). (*ii*) High levels of DNA MeTase might have a direct effect on origins of replication (18, 19). (*iii*) Methylated cytosines are hot spots for mutation, and deamination of methylated cytosines will result in C-T transition mutations (54).

Although more data are required to determine which of these mechanisms is involved in the genesis and maintenance of cancer, two issues are critical for the pharmacological and therapeutic application of DNA MeTase inhibitors. First, are the changes caused by aberrant methylation in carcinogenesis irreversible, as has been suggested (55), or are they reversible by pharmacological intervention? *Min* mice bearing a mutation in the homolog of the human repair-associated tumor suppressor gene *APC* were protected from formation of adenopolyps in the intestines when treated prophylactically with 5-azadeoxycytidine early after birth (55). The development of polyps could not be reversed when 5-azadeoxycytidine was applied later, suggesting an irreversible mechanism.

Second, is the aberrant methylation observed in cancer a consequence of the enhanced levels of DNA MeTase and therefore reversible by reducing the level of DNA MeTase (18, 19)? Although additional experiments will be required to demonstrate that similar results to those reported here can be obtained with cancers formed in the animal rather than in implanted tumors, our results lend support to the hypothesis that the effects of DNA MeTase induction are reversible and therefore suggest that DNA MeTase be a target for anticancer intervention.

We thank Dr. Kirk Field for critical reading of the manuscript and his thoughtful suggestions. We also thank Deanna Collier, Vera Bozovic, and Johanne Theberge for excellent technical assistance. This research was supported by the National Cancer Institute Canada, by a contract with Hybridon, Inc. (Worcester, MA), and by MethylGene, Inc. (Montreal).

1. Razin, A. & Riggs A. D. (1980) *Science* **210**, 604–610.
2. Razin, A. & Cedar, H. (1991) *Microbiol. Rev.* **55**, 451–458.
3. Tate, P. H. & Bird, A. P. (1993) *Curr. Opin. Genet. Dev.* **3**, 226–231.
4. Adams, R. L., McKay, E. L., Craig, L. M. & Burdon, R. H. (1979) *Biochim. Biophy. Acta* **561**, 345–57.
5. Yisraeli, J. & Szyf, M. (1984) in *DNA Methylation and Its Biological Significance*, eds. Razin, A. Cedar, H. & Riggs, A. D. (Springer, New York), pp. 353–378.
6. Razin, A. & Kafri, T. (1994) *Prog. Nucleic Acid Res. Mol. Biol.* **48**, 53–81.
7. Szyf, M. (1991) *Biochem. Cell Biol.* **69**, 764–767.
8. Gama-Sosa, M. A., Midgett, R. M., Slagel, V. A., Githens, S., Kuo, K. C., Gehrke, C. W. & Ehrlich, M. (1983) *Biochim. Biophys. Acta* **740**, 212–219.
9. Feinberg, A. P. & Vogelstein, B. (1983) *Nature (London)* **301**, 89–92.
10. de Bustros, A., Nelkin, B. D., Silverman, A., Ehrlich, G., Poiesz, B. & Baylin, S. B. (1988) *Proc. Natl. Acad. Sci. USA* **85**, 5693–5697.
11. Nelkin, B. D., Przepiorka, D., Burke, P. J., Thomas, E. D. & Baylin, S. B. (1991) *Blood* **77**, 2431–2434.
12. Baylin, S. B., Makos, M., Wu, J. J., Yen, R. W., de Bustros, A., Vertino, P. & Nelkin B. D. (1991) *Cancer Cells* **3**, 383–390.
13. Merlo, A., Herman, J. G., Mao, L., Lee, D. J., Gabrielson, E., Burger, P., Baylin, S. B. & Sidransky, D. (1995) *Nat. Med.* **1**, 686–692.
14. Ohtani-Fujita, N., Fujita, T., Aoike, A., Osifchin, N. E., Robbins, P. D. & Sakai, T. (1993) *Oncogene* **8**, 1063–1067.
15. Herman, J. G., Latif, F., Weng, Y., Lerman, M. I., Zbar, B., Liu, S., Samid, D., Duan, D. S., Gnarra, J. R., Linehan, W. M. & Baylin, S. M. (1994) *Proc. Natl. Acad. Sci. USA* **91**, 9700–9704.
16. Royer-Pokora, B. & Schneider, S. (1992) *Genes Chromosomes Cancer* **5**, 132–140.
17. Makos-Wales, M., Biel, M. A., El Deiry, W., Nelkin, B. D., Issa, J-P., Cavenee, W. K., Kuerbitz, S. J. & Baylin, S. B. (1995) *Nat. Med.* **1**, 570–577.
18. Szyf, M. (1994) *Trends Pharmacol. Sci.* **15**, 233–238.
19. Szyf, M. (1996) *Pharmacol. Ther.* **70**, 1–37.
20. Szyf, M., Avraham-Haetzni, K., Reifman, A., Shlomai, J., Kaplan, F., Oppenheim, A. & Razin A. (1984) *Proc. Natl. Acad. Sci. USA* **81**, 3278–3282.
21. Kautiainen, T. L. & Jones, P. A. (1986) *J. Biol. Chem.* **261**, 1594–1598.
22. el-Deiry, W. S., Nelkin, B. D., Celano, P., Yen, R. W., Falco, J. P., Hamilton, S. R. & Baylin, S. B. (1991) *Proc. Natl. Acad. Sci. USA* **88**, 3470–3474.
23. Belinsky, S. A., Nikula, K. J., Baylin, S. B. & Issa, J. P. J. (1996) *Proc. Natl. Acad. Sci. USA* **93**, 4045–4050.
24. Wu, J., Issa, J. P., Herman, J., Bassett, D. E., Jr., Nelkin, B. D. & Baylin, S. B. (1993) *Proc. Natl. Acad. Sci. USA* **90**, 8891–8895.
25. MacLeod, A. R. & Szyf, M. (1995) *J. Biol. Chem.* **270**, 8037–8043.
26. Rouleau, J., Tanigawa, G. & Szyf, M. (1992) *J. Biol. Chem.* **267**, 7368–7377.
27. Rouleau, J., MacLeod, A. R. & Szyf, M. (1995) *J. Biol. Chem.* **270**, 1595–1601.
28. MacLeod, A. R., Rouleau, J. & Szyf, M. (1995) *J. Biol. Chem.* **270**, 11327–11337.
29. Szyf, M., Theberge, J. & Bozovic, V. (1995) *J. Biol. Chem.* **270**, 12690–12696.
30. Jones, P. A. (1985) *Cell* **40**, 485–486.
31. Tamame, M., Antequera, F., Villanueva, J. R. & Santos T. (1983) *Mol. Cell. Biol.* **3**, 2287–2297.
32. Juttermann, R., Li, E. & Jaenisch, R. (1994) *Proc. Natl. Acad. Sci. USA* **91**, 11797–11801.
33. Dean, N. M. & McKay, R. (1994) *Proc. Natl. Acad. Sci. USA* **91**, 11762–11766.
34. Yasumura, Y., Buonsassisi, V. & Sato, G. (1966) *Cancer Res.* **26**, 529–535.
35. Schwab, M., Alitalo, K., Varmus, H. E. & Bishop, M. (1983) *Nature (London)* **303**, 497–501.
36. Szyf, M., Kaplan, F., Mann, V., Gilloh, H., Kedar, E. & Razin, A. (1985) *J. Biol. Chem.* **260**, 8653–8656.
37. Szyf, M., Bozovic, V. & Tanigawa, G. (1991) *J. Biol. Chem.* **266**, 10027–10030.
38. Ausubel, F. M., Kingston, R., Moore, D., Seidman, J., Smith, J. & Struhl, K., eds. (1988) *Current Protocols in Molecular Biology (Wiley, New York)*.
39. Freedman, V. H. & Shin, S. (1974) *Cell* **3**, 355–359.
40. Mayer, R. J. & Walker, J. H. (1987) *Immunochemical Methods in Cell and Molecular Biology* (Academic, London).
41. Szyf, M., Milstone, D. S., Schimmer, B. P., Parker, K. L. & Seidman, J. G. (1990) *Mol. Endocrinol.* **4**, 1144–1152.
42. Plumb, J. A., Wishart, C., Setanoians, A., Morrison, J. G., Hamilton, T., Bicknell, S. R. & Kaye, S. B. (1994) *Biochem. Pharmacol.* **47**, 257–266.
43. Szyf, M., Rouleau, J., Theberge, J. & Bozovic, V. (1992) *J. Biol. Chem.* **267**, 12831–12836.
44. Bestor, T. H., Laudano, A., Mattaliano, R. & Ingram, V. (1988) *J. Mol. Biol.* **203**, 971–983.
45. Walder, R. Y. & Walder, J. A. (1988) *Proc. Natl. Acad. Sci. USA* **85**, 5011–5015.
46. Szyf, M., Schimmer, B. P. & Seidman, J. G. (1989) *Proc. Natl. Acad. Sci. USA* **86**, 6853–6857.
47. Keshet, E. & Cedar, H. (1983) *Nucleic Acids Res.* **11**, 3571–3580.
48. Szyf, M., Tanigawa, G. & McCarthy, P. L., Jr. (1990) *Mol. Cell. Biol.* **10**, 4396–4340.
49. Jones, P. A., Wolkowicz, M. J., Rideout, W. M., III, Gonzales, F. A., Marziasz, C. M., Coetzee, G. A. & Tapscott, S. J. (1990) *Proc. Natl. Acad. Sci. USA* **87**, 6117–6121.
50. Issa, J. P., Zehnbauer, B. A., Civin, C. I., Collector, M. I., Sharkis, S. J., Davidson, N. E., Kaufmann, S. H. & Baylin, S. B. (1996) *Cancer Res.* **56**, 973–977.
51. Herman, J. G., Jen, J., Merlo, A., & Baylin, S. B. (1996) *Cancer Res.* **56**, 722–727.
52. Zahler, A. M., Williamson, J. R., Cech, T. R. & Prescott, D.M. (1991) *Nature (London)* **350**, 718–720.
53. Krieg, A. M., Yi, A. K., Matson, S., Waldschmidt, T. J., Bishop, G. A., Teasdale, R., Koretzky, G. A. & Klinman, D. M. (1995) *Nature (London)* **374**, 546–549.
54. Rideout, W. M., III, Coetzee, G. A., Olumi, A. F. & Jones, P. A. (1990) *Science* **249**, 1288–1290.
55. Laird, P. W., Jacksongrusby, L., Fazeli, A., Dickinson, S. L., Jung, W. E., Li, E., Weinberg, R. A. & Jaenisch, R. (1995) *Cell* **81**, 197–205.

Journal of Neurochemistry, 2001, 79, 426–436

Survivin inhibition induces human neural tumor cell death through caspase-independent and -dependent pathways

Sai Latha Shankar,* Sridhar Mani,† Kathleen Norman O'Guin,* Ekambar R. Kandimalla,‡ Sudhir Agrawal‡ and Bridget Shafit-Zagardo*

*Departments of *Pathology and †Oncology, Albert Einstein College of Medicine, Bronx, New York, USA*
‡Hybridon Inc., Cambridge, Massachusetts, USA

Abstract

Survivin inhibits apoptosis during development and carcinogenesis and is absent in differentiated cells. To determine whether survivin inhibition induces cell death in neural tumor cells, survivin antisense oligonucleotides (SAO) were administered to a human neuroblastoma (MSN) and an oligodendroglioma (TC620) resulting in a dose-dependent reduction in survivin protein. Although 74% of the SAO-treated MSN cells were trypan blue$^+$, PARP cleavage or activated caspase-3 was not observed. However nuclear translocation of AIF occurred and XIAP increased dramatically. Co-administration of z-Val-Ala-Asp(OMe)-fluoromethyl ketone (zVAD-fmk) with SAO did not inhibit cell death suggesting a caspase-independent mechanism of cell death. Propidium iodide (PI) staining revealed multiple large macronuclei with no apoptotic bodies supporting a role for survivin in cell division. By contrast, while 70% of the SAO-treated TC620 cells were trypan blue$^+$, PARP was cleaved, cells were TUNEL$^+$ and PI-staining revealed macronuclei and numerous apoptotic bodies. Co-treatment of the TC620 cells with SAO and zVAD-fmk blocked cell death. While no macronuclei or apoptotic bodies were observed there was a two-fold increase in metaphase cells. Our results suggest that survivin inhibition decreases the viability of human neural tumor cells and as a result of mitotic catastrophe, cell death can be initiated by either a classic apoptotic mechanism or a caspase-independent mechanism.

Keywords: antisense oligonucleotides, apoptosis, cell death, human brain tumors, survivin.
J. Neurochem. (2001) **79**, 426–436.

Members of anti-apoptotic gene families such as the bcl-2 family and the inhibitor of apoptosis (IAP) family are often up-regulated in brain tumors where their role in blocking apoptosis contributes to tumor progression (LaCasse *et al.* 1998; Leaver *et al.* 1998; Deininger *et al.* 1999). Human survivin, one of seven IAP family members, is increased in abundance in neuroblastomas and portends poor prognosis (Adida *et al.* 1998). Neuroblastomas often have a gain in the distal region of 17q suggesting that survivin expression at 17q25 may contribute to tumor pathogenesis (Islam *et al.* 2000).

Survivin is cell cycle regulated and increased during the G2/M phase of the cell cycle. During G2/M survivin associates with and is phosphorylated by cdc2/cyclin B1 and subsequently binds to tubulin on the mitotic spindle (Li *et al.* 1998; O'Connor *et al.* 2000). Survivin also associates with the midbody, kinetochore (Li *et al.* 1998; Skoufias *et al.* 2000), and binds cdk4 to aid in the G1/S transition (Suzuki *et al.* 2000) implicating survivin with normal G2/M and G1/S checkpoint transitions and mitosis.

The purpose of this study was to determine whether survivin was expressed in a variety of neural tumors and whether survivin antisense oligonucleotides (SAO) could down-regulate survivin in neural cell lines and induce tumor cell death. In lung and colon carcinomas (Chen *et al.* 2000;

Received June 26, 2001; revised manuscript received August 3, 2001; accepted August 6, 2001.

Address correspondence and reprint requests to Dr Bridget Shafit-Zagardo, Department of Pathology, Forchheimer 524, Albert Einstein College of Medicine, 1300 Morris Park Avenue, Bronx, NY 10461, USA. E-mail: zagardo@aecom.yu.edu

Abbreviations used: AIF, apoptosis-inducing factor; DAPI, 4′,6-diamidino-2-phenylindole; DTT, dithiothreitol; FCS, fetal calf serum; DMSO, dimethyl sulfoxide; IAP, inhibitor of apoptosis; PARP, poly-(ADP-ribose)-polymerase; PI, propidium iodide; SAO, survivin antisense oligonucleotides; SDS–PAGE, sodium dodecyl sulfate–polyacrylamide gel electrophoresis; TBS, Tris-buffered saline; TRITC, tetramethylrhodamine isothiocyanate; TUNEL, TdT-mediated dUTP nick-end labeling; XIAP, X-linked inhibitor of apoptosis; zVAD-fmk, z-Val-Ala-Asp(OMe)-fluoromethyl ketone.

Olie *et al.* 2000) survivin down-regulation induced apoptosis, however, survivin levels are higher in neuroblastomas (Islam *et al.* 2000). We have determined that SAO down-regulated survivin protein resulting in caspase-independent cell death in a neuroblastoma cell line, while an oligodendroglioma cell line underwent caspase-dependent apoptotic cell death.

Materials and methods

Cell culture conditions

Cells were grown in a humidified atmosphere containing 5% (HOG, TC620) or 8% (MSN, HTB 14, HTB 17) CO_2 at 37°C. MSN cells were grown in RPMI 1640 supplemented with 23.8 mM sodium bicarbonate, 10% fetal calf serum (FCS), 0.1 mM non-essential amino acids, 0.47 mM L-serine and 0.38 mM L-asparagine (Reynolds *et al.* 1986). TC620 and HOG were maintained in Iscove's medium plus 10% FCS (Dr Anthony Campagnoni; UCLA). HTB 14 and the HTB 17 were maintained in DMEM plus 10% FCS (ATCC). Jurkat cells served as a positive control for survivin immunoblotting (Conway *et al.* 2000) and were grown in RPMI 1640 plus 10% FCS.

RNA isolation and northern blot analysis

Total RNA was isolated from the cell lines using TRI-reagent (Molecular Research Center; Cincinnati, OH, USA). Northern blot analysis and primings were performed as previously described (Shafit-Zagardo *et al.* 1988). The probes were labeled using [α-^{32}P]-dCTP and the Multiprime DNA labeling system (Amersham, Arlington Heights, IL, USA).

Oligonucleotide treatments

Eleven different antisense phosphorothioate oligonucleotides to the survivin gene (Genbank accession number U75285) and two mismatched phosphorothioate oligonucleotides were designed based on the selection criteria described earlier (Agrawal and Kandimalla 2000). The antisense oligonucleotides were synthesized on solid support with an automated DNA synthesizer using β-cyanoethyl-phosphoramidite chemistry. To prevent rapid degradation of the oligonucleotides by cellular nucleases, oxidation was performed with Becauge sulfurizing agent to obtain phosphorothioate backbone modified oligonucleotides. After their synthesis, the oligonucleotides were released from the solid support, deprotected, purified by reverse-phase HPLC, desalted, filtered and lyophilized. The purity and sequence integrity of oligonucleotides was ascertained by capillary gel electrophoresis and MALDI-TOF mass spectral analysis and the concentrations measured at 260 nm. The sequences of eight oligonucleotides used in this study are shown in Table 1. Cells were grown in 100-mm dishes and oligonucleotide treatment was performed for 48 h on subconfluent cultures in the presence of lipofectin (Gibco, Rockville, MD, USA).

Protein preparation and immunoblotting

Total protein homogenates were prepared as previously described (Albala *et al.* 1995). Equal amounts of protein (100 μg; Biorad detection system, Bio-Rad Laboratories, Hercules, CA, USA) were analyzed by SDS–PAGE on 10% gels (Laemmli 1970) and electrophoretically transferred to nitrocellulose (Towbin *et al.* 1979). To demonstrate specificity during immunoblotting, human survivin GST-fusion protein (10 μg) was used to absorb the survivin polyclonal antibody overnight (1 : 500) at 4°C prior to immunoblotting. Immunoblots were blocked with 5% non-fat, dry milk in 1 × Tris-buffered saline (TBS) (0.14 M NaCl, 0.001 M Tris, pH 7.4). Blots were cut at 32.9 kDa and the bottom were incubated with the survivin antibody overnight at 4°C and visualized by enhanced chemiluminescence (ECL; Amersham). The top part of the blots was incubated with a β-tubulin antibody (TUB 2.1; Sigma, St Louis, MO, USA) overnight at 4°C. Two survivin polyclonal antibodies yielded identical results (R & D Systems, Inc., Minneapolis, MN, USA; Alpha Diagnostics International, San Antonio, TX, USA). The XIAP mAb was purchased from StressGen Biotechnologies Corp. (Victoria, BC, Canada). The poly-(ADP-ribose)-polymerase (PARP) mAb was from Pharmingen (San Diego, CA, USA).

Trypan blue exclusion assay

Cells were harvested 48 h after SAO treatment, stained with 0.04% Trypan blue (Gibco) and both non-viable (trypan blue positive) and viable (trypan blue negative) cells were counted on a hemocytometer. A minimum of 250 cells were counted for each data point. The data was expressed as a percentage of dead cells relative to the total cell number. Individual experiments were performed in triplicate. MSN studies were performed three times, while TC620 studies were performed twice.

Caspase-3 activity assay

MSN cell pellets were washed twice in cold PBS and resuspended

Table 1 Sequences of 20-mer phosphorothioate survivin antisense oligonucleotides

HYB oligonucleotide number	Sequence (5′→ 3′)	Target site
900	d(GCCAGTTCTTGAATGTAGAG)	2867–2886
901	d(CAGTGGATGAAGCCAGCCTC)	3180–3199
903	d(CCCTAGCTCACACTCTCATT)	4385–4404
904	d(TCTTGGCTCTTTCTCTGTCC)	5248–5267
905	d(GAGCCTTCCTCTTCATGTCC)	11432–11451
906	d(GCTTCCCAGTCACATCCTGT)	11897–11916
908	d(GCCACTGTTACCAGCAGCAC)	12241–12260
1132	d(GCACCTAGTCTCCCTGCACC)	Mismatched oligo

in ice-cold hypotonic cell lysis buffer (25 mM HEPES, pH 7.5, 5 mM $MgCl_2$, 5 mM EDTA, 5 mM DTT, 2 mM PMSF, 10 μg/mL pepstatin A, 10 μg/mL leupeptin), incubated on ice for 20 min, sonicated briefly and centrifuged at 11 000 *g* for 20 min at 4°C. Supernatant (50–100 μg) was incubated in caspase-3 assay buffer [100 mM HEPES, pH 7.5, 10% sucrose, 0.1% CHAPS and 10 mM dithiothreitol (DTT)], 2 μL of dimethyl sulfoxide (DMSO), 100 mM DTT in a final volume of 100 μL at 30°C for 30 min in black opaque 96-well plates (USA Scientific Inc; Orlando, FL, USA). Subsequently, 2 μL of the caspase-3 substrate Ac-DEVD-AMC (50 μM, Pharmingen) was added to each well. Plates were incubated at 30°C for 60 min in the dark. Fluorescence of the reaction was measured at an excitation of 355 nm and an emission of 460 nm with a cut-off filter of 455 nm using a SPECTRAmax GEMINI spectrofluorometer with SOFTmax® PRO software (Molecular Devices; Sunnyvale, CA, USA). Assays were performed in triplicates. The data is presented as mean relative fluorescence units/mg protein ± SD. The negative controls included the caspase-3 inhibitor Ac-DEVD-CHO that eliminated caspase-3 activation.

Propidium iodide (PI) staining

SAO-treated cells were fixed with 4% paraformaldehyde for 30 min at room temperature, washed with 1 × TBS, permeabilized with 0.1% Triton X-100 for 30 min and treated with 10 μg/mL DNase free RNase A (Sigma) for 60 min. Nuclei were stained with 200 μg/mL PI for 30 min at 4°C and washed twice with 1 × TBS. Nuclear morphology was assessed on an inverted Olympus IX70 fluorescence microscope equipped with phase and epifluorescence optics. For each treatment about 600 nuclei were scored as normal, condensed, or abnormal on 15 random, 40 × objective fields in duplicate.

TUNEL assay

The TUNEL assay was performed to assess apoptotic cell death in SAO-treated TC620 cells using the In Situ Cell Death Detection Kit, Fluorescein (Roche Molecular Biochemicals, Indianapolis, IN, USA). The TUNEL reaction preferentially labels cleaved genomic DNA generated during apoptosis, by the addition of fluorescein dUTP at strand breaks. Lipofectin, mismatch 1132 or SAO-treated TC620 cells were fixed and permeabilized as described for PI staining. Cells were washed and incubated in the TUNEL reaction mixture, prepared according to the manufacturer's recommendations, for 1 h at 37°C. Omission of the terminal deoxynucleotidyl transferase in the label solution served as a negative control for the TUNEL fluorescence staining. Cells were washed twice and counterstained with the DNA specific dye DAPI (1 : 1000 of a 1 mg/mL stock; 15 min at room temperature). Cells were examined with an Olympus IX70 inverted microscope. For each treatment 15 random, 40 × objective fields consisting of ~1000 cells were examined in duplicate chamber slides. TUNEL-positive nuclei were expressed as a percent of the total number of cells per individual field.

Apoptosis-inducing factor (AIF) immunostaining and quantitation

Lipofectin, mismatch 1132 or SAO-treated MSN cells were fixed and permeabilized as described for PI staining, and blocked for 1 h at room temperature with 10% normal goat serum in 5% non-fat, dry milk in 1 × TBS. The cells were incubated with an AIF polyclonal antibody (1 : 100; Santa Cruz Biotechnology Inc, Santa Cruz, CA, USA) overnight at 4°C, and revealed with a goat anti-rabbit IgG conjugated to TRITC (Southern Biotechnology Associates, Birmingham, AL, USA). Omission of the primary antibody confirmed that the immunostaining was specific. Cells were counterstained with the DNA-specific dye DAPI (1 : 1000 of a 1 mg/mL stock; 15 min at room temperature). Cells were examined with an Olympus IX70 inverted microscope. Fluorescent images were collected using a 12-bit Photometrics cooled CCD camera. For each treatment, 15 random, 40 × objective fields consisting of ~600 cells were examined. TRITC (red) and DAPI (blue) stained cells were scored as having AIF staining either in the mitochondria or the nucleus relative to the total cell number examined. In parallel, the DAPI stained nuclei were also scored as normal, condensed, or abnormal nuclei. Experiments were performed in duplicate.

Results

Expression of survivin in human neural tumor cell lines

Northern and western blot analysis were performed to verify survivin expression in human neural tumor cell lines derived from a human neuroblastoma (MSN), two oligodendrogliomas (HOG and TC620), an astrocytoma (HTB17) and a glioblastoma (HTB14). Northern blot analysis revealed the expression of the 1.9 kb survivin transcript in the five neural tumor lines examined (Fig. 1a). When normalized to 18S RNA, higher expression of survivin was found in the two oligodendroglioma cell lines, while the neuroblastoma, glioblastoma and the astrocytoma showed comparable survivin expression. Immunoblotting confirmed the presence of the 16.5-kDa survivin protein in all neural tumor lines (Fig. 1B). When normalized to β-tubulin, survivin protein levels were three-fold higher in the HTB-14, MSN and the HTB-17 homogenates relative to the HOG cell homogenate. Examination of two additional neuroblastomas (IMR32 and SK-N-SH; data not shown) and the oligodendroglioma (TC620; Fig. 2b) also confirmed the presence of survivin. To verify the specificity of the survivin antibody, identical protein blots were incubated with the survivin antibody preincubated with the GST–survivin fusion protein. Absorption of the antibody eliminated survivin immunoreactivity (Fig. 1B).

Regulation of survivin expression at G2/M cell cycle checkpoints

As shown in Fig. 2(a), a 1.7–2.6-fold increase in survivin protein was observed in total cell lysates from MSN cells treated with three G2/M checkpoint blockers relative to the DMSO control. A similar 1.6-fold increase in survivin protein was observed in the nocodazole-treated TC620 cells (Fig. 2b) demonstrating that in neural tumor cell lines survivin expression is increased in a G2/M cell cycle phase-dependent manner. In contrast, cells treated with agents such as flavopiridol that typically block cells in G1/S (Carlson

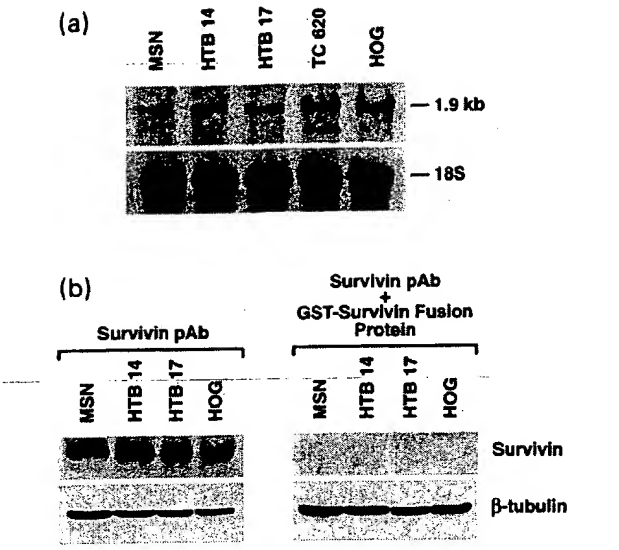

Fig. 1 Survivin is expressed in human brain tumors. (a) Total RNA (30 μg) were run on a 1% agarose–formaldehyde gel and transferred to nitrocellulose. The blot was first hybridized with a cDNA probe to the entire coding region of the survivin gene and subsequently hybridized with a cDNA to 18S. The survivin RNA expression was normalized to the expression of 18S RNA. The relative amounts were MSN, 0.075; HTB-14, 0.11; HTB-17, 0.065; TC620, 0.25; HOG, 0.25. (b) Total protein was isolated from MSN, HTB 14, HTB 17 and HOG cells. The blots were cut at 32.9 kDa and was incubated with a β-tubulin mAb (1 : 1000) to confirm equal loading. The lower halves were incubated with a survivin polyclonal antibody (1 : 500) or with the survivin polyclonal antibody (1 : 500) pretreated with 10 μg of GST-survivin fusion protein. Blots were scanned in the linear range and data was presented as a ratio of survivin over tubulin in each cell type. The relative quantities were MSN, 0.35; HTB-14, 0.45; HTB-17, 0.39; HOG, 0.13. Two independent experiments were performed and consistent results were obtained.

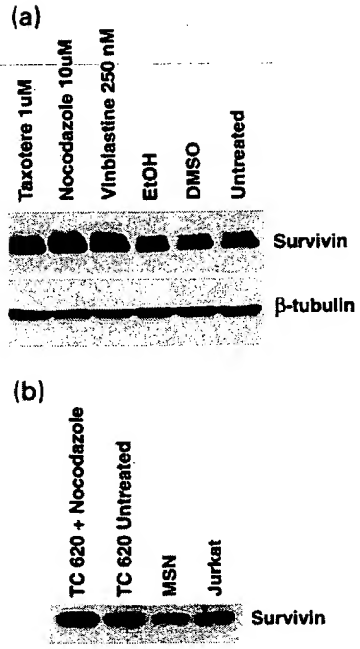

Fig. 2 Survivin protein increases following treatment with G_2/M checkpoint blockers. (a) G_2/M cell cycle checkpoint blockers elevate survivin protein expression. Total protein was isolated from MSN cells either untreated or treated with vinblastine (250 nM), nocodazole (10 μM) or taxotere (1 μM) for 16 h. DMSO and ethanol (EtOH) were added as carriers. In each of the treatments, the increase of survivin protein relative to DMSO or EtOH was vinblastine, 1.9-fold; nocodazole, 2.6-fold; taxotere, 1.7-fold. (b) Total protein was isolated from nocodazole-treated (10 μM, 24 h) and untreated TC620 cells, MSN cells and Jurkat cells. A 1.6-fold increase in survivin protein was observed on the nocodazole-treated TC620 cells. Three independent experiments were performed and consistent results were obtained.

et al. 1996; our data) did not alter survivin protein abundance (data not shown).

In MSN cells, SAO decrease survivin protein abundance, do not activate caspase-3 and undergo caspase-independent cell death

To determine whether the inhibition of survivin was sufficient to induce cell death in nervous system tumors, 11 SAO spanning the survivin gene were analyzed in MSN and TC620 cell lines. Seven SAO and the mismatch oligonucleotide used in this study are shown in Table 1. As shown in Fig. 3(a), SAO 904 treatment decreased survivin protein levels in MSN cells in a dose-dependent manner. At 400 and 600 nM, SAO 904 decreased survivin protein levels by 46% and 60% while survivin levels were unchanged in cells incubated with the mismatched oligonucleotide 1132. By contrast, treatment with SAO 908 that binds within the 3′-untranslated region of the survivin mRNA did not result in a significant decrease in survivin protein. Examination of other SAO in the MSN cells showed that 901, 903, 904 and 906 (400 nM) were most effective in decreasing survivin protein levels (Fig. 3b). Further, mismatched oligonucleotides had no effect on the relative abundance of survivin.

Survivin's role as an IAP and a survival protein for neuroblastomas was investigated by examining whether the down-regulation of survivin was sufficient to induce cell death in MSN cells. Following transfection with lipofectin, mismatched oligonucleotide 1132 (600 nM) or SAO 904 and 906 (600 nM), the numbers of trypan blue positive cells, indicative of dead cells, were counted 48 h post-treatment. In the presence of 600 nM SAO 904 and 906, the percentage of cells that were trypan blue positive were 73% and 81% (Fig. 3c). Upon treatment with lipofectin or the mismatched oligonucleotide 1132, only 7–11% of the cells were trypan blue-positive. These data therefore demonstrate that the inhibition of survivin following SAO treatment is sufficient to induce cell death in MSN cells.

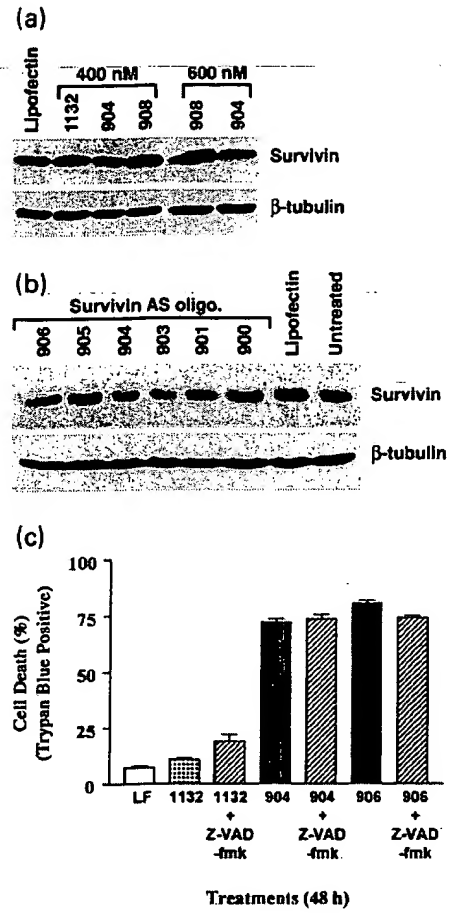

Fig. 3 SAO treatment of MSN cells results in reduced survivin protein levels and increased cell death. (a) MSN cells were treated with lipofectin, SAO 904 and 908 at 400 and 600 nM or mismatched oligonucleotide 1132 at 400 nM. With SAO treatment, the percentage of survivin protein over β-tubulin relative to lipofectin was 904 (400 nM), 54%; 904 (600 nM), 40%; 908 (400 nM), 129%; 908 (600 nM), 91%; 1132 (400 nM), 109%. (b) Six SAOs (900–906) were administered at 400 nM. The percentage of survivin protein over β-tubulin relative to lipofectin was: 900, 77.7%; 901, 38.3%; 903, 24.3%; 904, 35.7%; 905, 55.6%; 906, 26.9%. Three independent experiments were performed. (c) MSN cells treated with lipofectin, 600 nM SAO 904, 906, mismatch oligonucleotide 1132, or co-treated with SAO or 1132 and 20 μM zVAD-fmk for 48 h, were stained with 0.04% trypan blue. The data are expressed as the percentage of dead cells relative to the total cell number ± SEM. Three independent experiments were performed in duplicate.

To determine whether MSN cell death by SAO was mediated by caspase-3 activation, we examined whether PARP was cleaved. Immunoblotting of MSN protein homogenates with a PARP antibody failed to detect PARP cleavage and a single 116-kDa PARP protein band that was not cleaved was observed in MSN cells following SAO treatment for either 24 h or 48 h (data not shown). Also, higher concentrations of SAO failed to cleave PARP. As a result of the PARP data, we examined whether SAO-treated cells have active caspase-3. Previous studies from our laboratory demonstrated that MSN cells activate caspase-3 following staurosporine treatment, and when caspase-3 is activated PARP is cleaved. As shown in Table 2, over a seven-fold increase in caspase-3 activity was observed upon staurosporine treatment of MSN cells, however, no significant increase in caspase-3 activity was observed following SAO treatment. This data was consistent with our PARP immunoblotting data.

We then examined if SAO-induced cell death could be blocked by the broad-spectrum caspase inhibitor z-Val-Ala-Asp(OMe)-fluoromethyl ketone (zVAD-fmk). As shown in Fig. 3(c), SAO 904 and 906 treatment resulted in 73% and 80% trypan blue positive cells and upon incubation of SAO 904 and 906 with zVAD-fmk, 73% and 74% of the cells remained trypan blue positive indicating that inhibiting caspases did not affect cell death. Taken together, the caspase-3, PARP and the zVAD-fmk experimental data suggest that in MSN cells SAO treatment induced cell death in a caspase-independent manner.

Induction of nuclear abnormalities in SAO-treated MSN cells

PI staining and phase microscopy were used to assess the nuclear morphology of the SAO-treated MSN cells. Lipofectin-treated or mismatch oligonucleotide 1132 treated cells showed normal nuclear morphology (Figs 4a and b) consistent with our previous observation that at any given time approximately 5% of MSN cells exhibited abnormal nuclei. By contrast, PI staining of SAO-treated cells revealed a dramatic increase in abnormal appearing nuclei that included multiple, multilobulated nuclei (Figs 4c and e,

Table 2 Caspase 3 is inactive in survivin antisense oligonucleotide-treated MSN cells

Treatment	Time	Relative units/ mg protein ± SD
Lipofectin	48 h	30 556 ± 899
903 (400 nM)	48 h	27 850 ± 2311
904 (400 nM)	48 h	33 532 ± 3732
1132 (400 nM)	48 h	30 961 ± 1681
Staurosporine (1 μM)	6 h	264 281 ± 8130
DMSO control for staurosporine	6 h	34 770 ± 900

Determination of caspase-3 activity in lipofectin, mismatch 1132 or SAO 903-, 904-treated MSN neuroblastoma cells. Staurosporine treatment served as positive control for caspase-3 activity in MSN cells. Caspase activity was determined by measuring the cleavage of the caspase-3 fluorescence substrate Ac-DEVD-AMC. Caspase-3 activity was expressed as mean relative fluorescence units/mg protein ± SD. All values were assayed in triplicate.

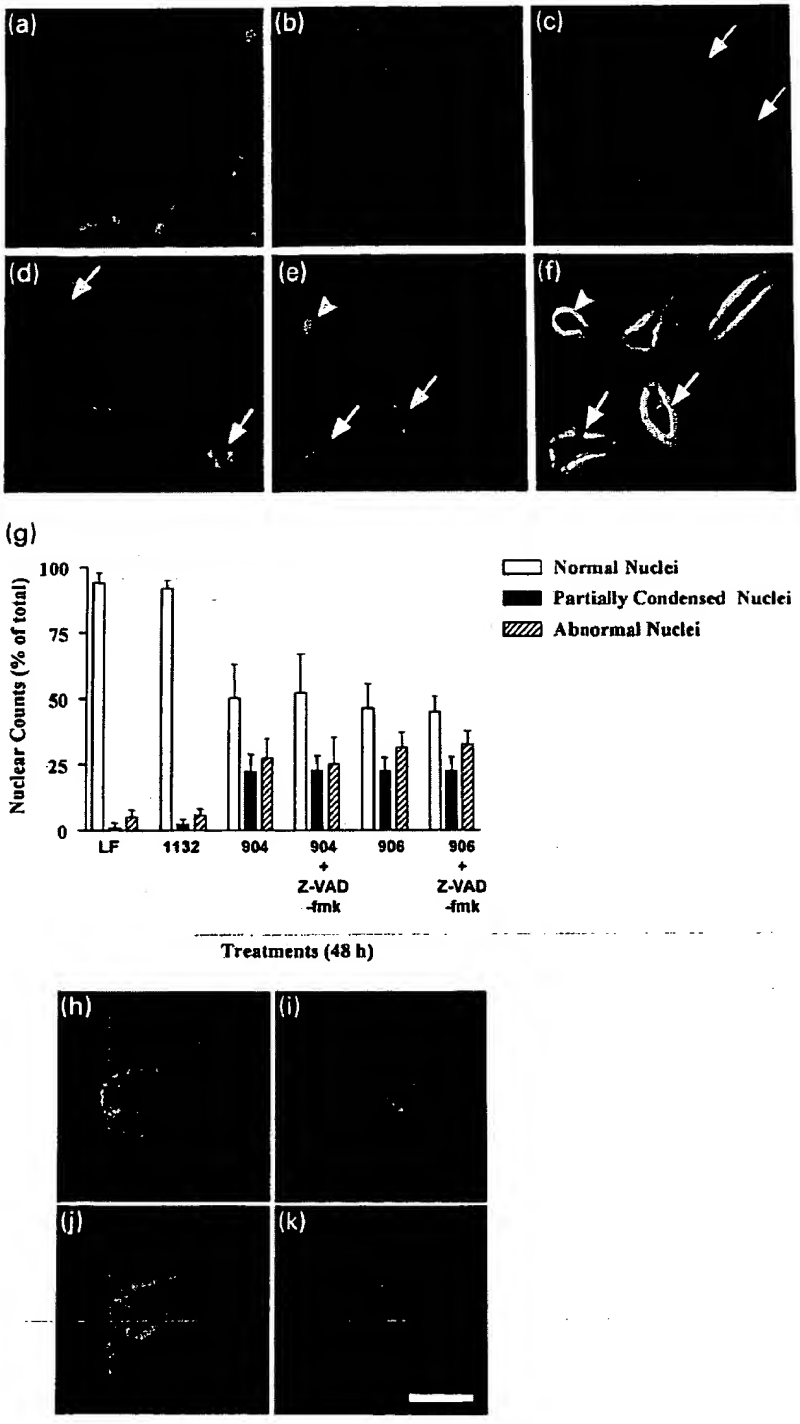

Fig. 4 SAO-treated MSN cells undergo caspase-independent nuclear morphologic changes. MSN cells were treated with lipofectin (a), 600 nM of mismatch 1132 (b), or SAO 904 (c and e), 906 (d) and stained with PI. Arrows in panels (c), (d), (e) and (f) point to abnormal multiple multilobed nuclei. Panel (f) shows the phase of panel (e) demonstrating that the abnormal multilobed nuclei are present within individual cells. The arrowhead in panel (e) shows a partially condensed nuclei. Two independent experiments were performed in duplicate. (g) Co-administration of SAO and zVAD-fmk does not alter the nuclear morphology in SAO-treated MSN cells. MSN cells were treated with 600 nM SAO 904, 906 or mismatch 1132 alone, or in the presence of 20 μM of zVAD-fmk and stained with PI. Approximately 500–600 nuclei were scored on 15 random 40 × objective fields in duplicate as described. The experiment was performed twice and the results are mean ± SEM obtained from the two independent experiments. (h–k) SAO-treated MSN cells show nuclear translocation of AIF. Lipofectin-treated MSN cells (h), MSN cells treated with 600 nM SAO 904 (i), mismatch 1132 (j) or SAO 906 (k) were double-labeled with AIF and DAPI. Note that in the SAO–treated cells the nuclei are pink when the AIF (red) and the DAPI (blue) colocalize. Photomicrographs are from a representative experiment performed in duplicate and similar results were obtained in an additional experiment. Scale bar = 20 μm.

arrows) and abnormally large nuclei (Fig. 4d) consistent with cells blocked in cell division when the nuclear membrane reassociated. Quantitation of the SAO 904 and 906 determined that the percentage of cells with this abnormal nuclear morphology were 27% and 31%, respectively, and this percentage was unaltered in cells co-treated with SAO and zVAD-fmk (Fig. 4g). While no apoptotic bodies or chromatin fragmentation were observed in the SAO-treated cells, 22% of the SAO-treated cells contained nuclei with partially condensed chromatin (Fig. 4e, arrowhead; Fig. 4g) and the percentage did not differ with zVAD-fmk treatment. Thus, approximately 50% of the SAO-treated cells contained

abnormal nuclei and condensed chromatin. The partially condensed chromatin is inconsistent with necrotic cell death and is suggestive of cells undergoing but not completing apoptotic cell death.

Apoptotic cell bodies and further condensation of the cell requires activated caspases and our data indicates that the existing phenotypes are caspase-independent even upon prolonged (≥ 72 h) SAO exposure. In cells undergoing death by a caspase-independent mechanism apoptosis-inducing factor (AIF) is translocated from the mitochondria to the nucleus prior to cytochrome *c* release from the mitochondria and concomitant partial chromatin condensation is observed (Daugas *et al.* 2000). To examine whether down-regulation of survivin induces AIF nuclear translocation, AIF and DAPI double-labeling was performed on SAO-treated MSN cells. As shown in Fig. 4(h and j), both lipofectin-treated and mismatch oligonucleotide 1132 treated cells show robust AIF staining in the cytosol. Only 4–8% of the cells contained nuclear localization of AIF, and DAPI staining showed that 95% of the cells had normal appearing nuclei. By contrast, 45–51% of SAO 904- and 906-treated cells showed AIF nuclear translocation (Figs 4i and k). DAPI staining indicated that 37% of these SAO-treated cells contained partially condensed chromatin, and 25% had abnormal nuclei similar to the PI staining in Fig. 4(g). The lack of highly condensed apoptotic bodies, the nuclear translocation of AIF, and the morphologic appearance of the nuclei by PI and DAPI are consistent with cells undergoing cell death by a caspase-independent mechanism. Thus, the combined PI, DAPI and AIF data is consistent with a disruption in the cell cycle, likely mitotic catastrophe, resulting in cell death.

Increase in XIAP levels following SAO treatment of MSN cells

We considered why caspase-3 was inactive and PARP was not cleaved following SAO treatment of the MSN cells. We speculated that during the SAO treatment another IAP family member might be activated and effectively blocking caspase activation and subsequently PARP cleavage. Therefore, following SAO treatment, XIAP, another member of the IAP family was examined by immunoblotting. As shown in Fig. 5, an eight-fold increase in XIAP was observed in MSN cells 48 h following treatment with SAO 904 while the lipofectin-treated MSN cells had low XIAP levels. This suggests that a dramatic increase of XIAP observed in MSN cells may account for possible inhibition of caspase activation.

Apoptotic cell death in the TC620 oligodendroglioma following SAO treatment

Transfection of TC620 cells with SAO 904 induced a concentration-dependent reduction in survivin protein levels and at 400 nM, a 54% decrease relative to lipofectin-treated cells was observed (Fig. 6a). To determine whether the decrease in survivin was associated with an apoptotic mode of cell death, PARP cleavage was examined by immunoblotting. SAO treatment induced PARP cleavage and generated the 85-kDa fragment characteristic of caspase induction during apoptosis. At concentrations of 100–400 nM SAO 904, a dramatic decrease of the 116-kDa PARP protein and an increase of the 85-kDa cleaved fragment was seen relative to the cleaved fragment seen in the lipofectin-treated cells and untreated cells. PARP cleavage in the lipofectin-treated (Fig. 6b) and untreated cells reflects the basal level of spontaneous apoptosis (Yang *et al.* 2000) in the TC620 cells prior to survivin antisense treatment. These experiments demonstrated that inhibition of survivin expression with SAO treatment is sufficient to induce apoptotic cell death in the TC620 cells.

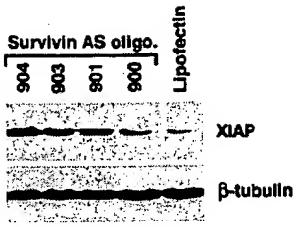

Fig. 5 XIAP was increased in MSN cells following SAO treatment. Cells were treated with lipofectin or 400 nM of SAO 900, 901, 903 and 904 for 48 h. The blot was sequentially incubated with a XIAP monoclonal antibody (1 : 1000; IgG_1) and β-tubulin (1 : 1000). Experiment was performed twice. With SAO treatment, the change of XIAP protein over β-tubulin relative to lipofectin was: 900, 2.3-fold; 901, 3.9-fold; 903, 5.2-fold; 904, 8.0-fold. The result is representative of a single experiment. Similar results were obtained in an additional experiment.

Trypan blue cell viability assays confirmed that SAO 904 induced a concentration-dependent increase in trypan blue-positive cells after 48 h treatment (Fig. 6c). At 100 nM, 200 nM and 400 nM the percentage of dead cells was 28%, 36%, and 62%, respectively. The percentage of trypan blue-positive cells treated with 600 nM mismatched oligonucleotide 1132 (8%) was similar to the lipofectin control (6%). As shown in Fig. 6(d), the percentages of trypan blue positive cells with SAO 904 and 906 at 600 nM concentration was 70% and 67%, respectively, and zVAD-fmk effectively decreased the numbers of trypan blue positive cells induced by SAO treatment to 11% and 15% further supporting a caspase-dependent mechanism of apoptotic cell death in the SAO-treated TC620 cells.

To confirm the results of the PARP data that survivin down-regulation induced apoptosis, a TUNEL assay was performed on lipofectin, mismatch oligonucleotide 1132 and SAO-treated TC620 cells. The percentages of TUNEL positive cells with SAO 904 and 906 at 400 nM concentration was 52% and 54%, respectively. At 600 nM, 63% of

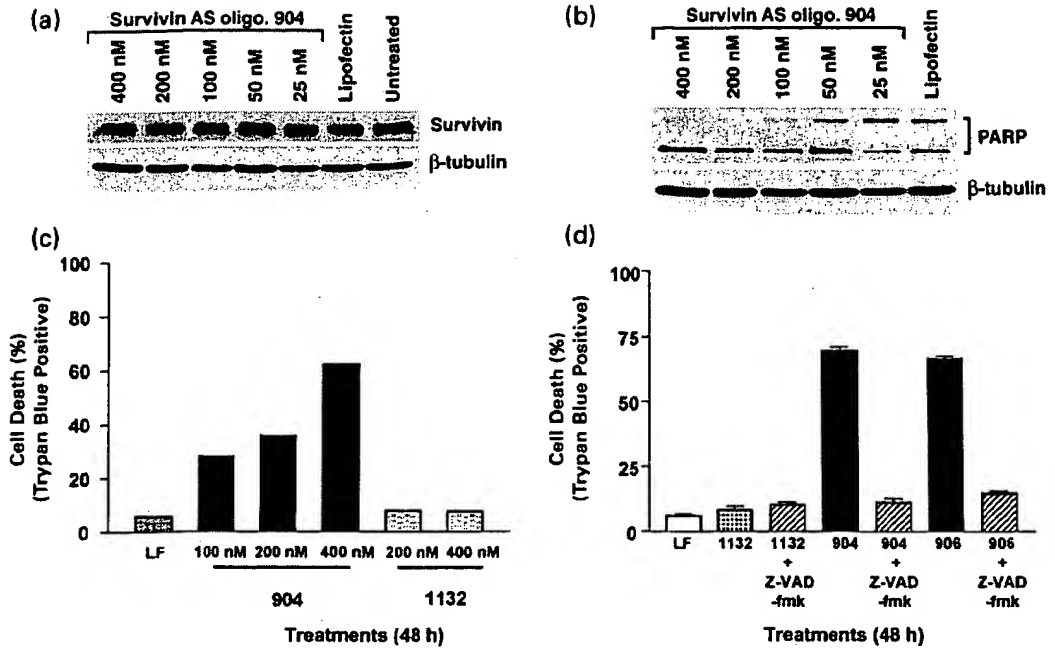

Fig. 6 SAO reduced survivin protein levels and induced apoptosis in TC620 cells. All experiments were performed at least twice. (a) TC620 cells were treated with lipofectin or increasing concentrations of SAO 904 (25–400 nM) for 48 h. The percentage of survivin protein over β-tubulin relative to lipofectin upon treatment with SAO 904 was: 25 nM, 109.1%; 50 nM, 97.4%; 100 nM, 67.6%; 200 nM, 45.2%; 400 nM, 45.7%. (b) PARP is cleaved in TC620 cells following SAO treatment. The blot was incubated with a PARP monoclonal antibody (1 : 500) and visualized by ECL. (c) TC620 cells were treated with lipofectin, SAO 904 at 100, 200 and 400 nM or mismatched oligonucleotide 1132 at 200 nM and 400 nM concentrations, and stained with trypan blue. All time points were calculated in triplicate. (d) TC620 cells were treated with lipofectin, 600 nM SAO 904, 906 or mismatch oligonucleotide 1132 alone, or co-treated with 20 μM of zVAD-fmk as above. Data represent mean ± SEM obtained from two independent experiments performed in duplicate.

SAO 904- and 906-treated TC620 cells were TUNEL positive. Only 4% of the cells were TUNEL positive in the presence of lipofectin or mismatch oligonucleotide 1132.

PI staining of lipofectin or mismatch oligonucleotide 1132 treated TC620 cells showed normal nuclear morphology (Figs 7a and b) with very few apoptotic cells (2%) or cells with abnormal nuclei (1%; Fig. 8a). By contrast, 40–43% of the SAO-treated TC620 cells revealed nuclei with chromatin fragmentation and apoptotic bodies characteristic of an apoptotic mode of cell death (Fig. 7c, arrows; Fig. 8a). In addition, 9% of the SAO-treated cells exhibited multiple multilobed nuclei (Figs 7d and e, arrows; Fig. 8a). Thus,

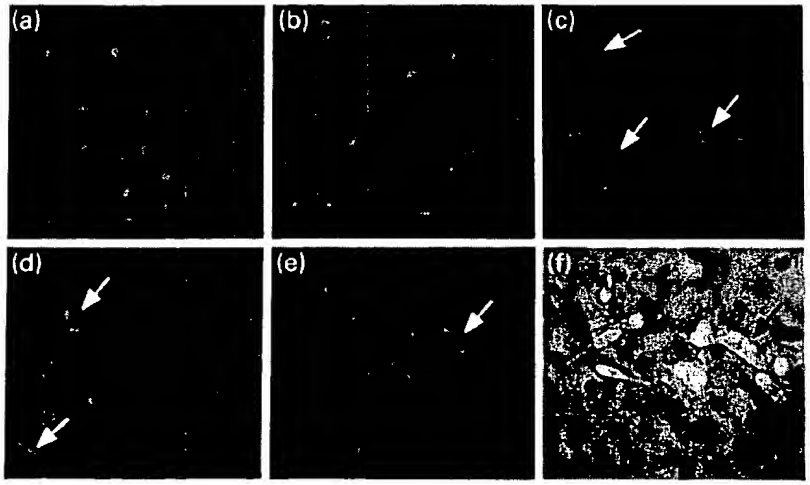

Fig. 7 PI staining demonstrates abnormal nuclear morphology of TC620 cells following SAO treatment. TC620 cells were treated with lipofectin (a), 600 nM of mismatch 1132 (b) or SAO 904 (c and e), 906 (d) and stained with PI. Arrows in panel (c) point to apoptotic nuclei, and in panels (d), (e) and (f) point to abnormal macronuclei that are multi-lobed. Panel (f) shows phase micrograph of panel (e) demonstrating that the abnormal multilobed nuclei are within individual cells. Two independent experiments were performed in duplicate.

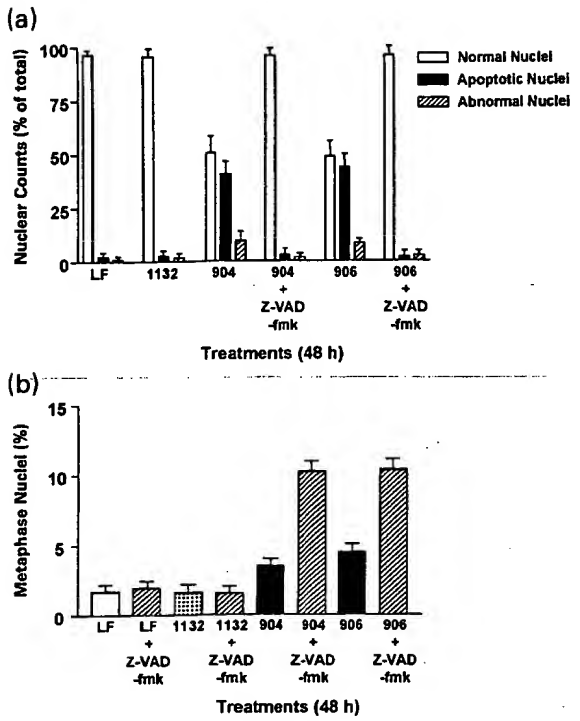

Fig. 8 Analysis of SAO-treated TC620 cells following PI treatment. (a) TC620 cells were treated with 600 nM SAO 904, 906, mismatch 1132, or in the presence of zVAD-fmk. Approximately, 500–600 nuclei were scored as normal, apoptotic or abnormal (macronuclei, multilobed) on 15 random 40 × objective fields in duplicate following PI staining. (b) TC620 cells were treated as described in (a) were stained with PI. Cells in metaphase were identified as those with chromosomes aligned on the metaphase plate; 15 random 40 × objective fields were counted. Results are mean ± SEM obtained from two independent experiments performed in duplicate.

49–52% of the SAO-treated TC620 cells had abnormal nuclei. Co-treatment with SAO and zVAD-fmk dramatically inhibited apoptosis and the abnormal nuclear morphology (Fig. 8a) indicating that down-regulation of survivin results in caspase activation and apoptosis. Taken together, the 85-kDa PARP cleavage product, PI staining of apoptotic bodies, zVAD-fmk inhibition of cell death and TUNEL staining of apoptotic cells definitively established apoptotic cell death in the survivin down-regulated TC620 cells.

Co-administration of SAO and the caspase inhibitor zVAD-fmk decreased the numbers of abnormal nuclei from >40% to 2% (Fig. 8a). Microscopic assessment of the SAO plus zVAD-fmk-treated cells demonstrated an approximate two-fold increase in the number of cells in metaphase compared with cells treated with SAO 904 or 906 alone (Fig. 8b). zVAD-fmk in the presence of lipofectin and mismatch 1132 did not affect the number of cells in metaphase. This suggests that in the absence of survivin, SAO-treated TC620 cells cannot complete the normal mitotic cycle, arrest in metaphase and subsequently undergo apoptosis as a result of mitotic catastrophe. Our results support an interplay between mitotic regulation, tumor survival and cell death.

Discussion

In this study, we have shown that all of the brain tumor cell lines examined in our laboratory expressed survivin. While the neuroblastoma, glioblastoma and the astrocytoma cells showed comparable survivin expression, the presence and abundance of survivin is indicative of a role for survivin as a regulator of neural tumor survival and pathogenesis. Precisely, how survivin regulates tumor progression is not completely understood, however it is clear from both the MSN and TC620 cell lines that survivin plays a major role in progression through mitosis.

Our results show that inhibition of survivin resulted in a dramatic increase in macronuclei and multinucleated cells in the SAO-treated MSN cells relative to the scrambled oligonucleotide-treated cells or the untreated cells consistent with failed cytokinesis. PI staining and flow cytometry could not definitively demonstrate changes in ploidy due to the existing aneuploidy of MSN cells (54–96 chromosomes; Shafit-Zagardo, unpublished observation). Our studies are consistent with other reports that showed that SAO treatment results in cell death (Li *et al.* 1999; Chen *et al.* 2000; Olie *et al.* 2000), however, in the MSN cells SAO treatment did not activate caspase-3 or cleave PARP, and zVAD-fmk did not alter cell death suggesting that MSN cells die by a caspase-independent pathway. Our observation that the percentage of cell death in the SAO-treated MSN cells was unaltered in the presence of zVAD-fmk (Figs 3c and 4g) further supports our finding that caspase-3 was not activated upon SAO treatment. This result led us to speculate that MSN cells suppress caspase activation by the activation of another caspase binding protein. XIAP, c-IAP-1, c-IAP-2 and livin have the ability to interact directly with caspases and inhibit their ability to cleave substrates (Deveraux *et al.* 1997; Roy *et al.* 1997; Kasof and Gomes 2000). XIAP is considered to be the strongest inhibitor of caspase-3 activation (Datta *et al.* 2000). Therefore, we examined XIAP and determined that SAO treatment resulted in a dramatic increase in XIAP. This demonstrates that MSN cells and likely other tumor types can compensate for the loss of survivin function by up-regulating other IAP family members. Since these cells still underwent cell death indicates that survivin's main role in MSN cells is in cell cycle progression, and the possible inhibition of caspases cannot block cell death.

While we did not observe caspase activation or PARP cleavage in MSN cells following SAO treatment, we did observe abnormal nuclei and partial chromatin condensation even in the presence of zVAD-fmk. Partial chromatin

condensation suggests that an early stage of nuclear apoptosis was initiated in the absence of caspase activation (Daugas *et al.* 2000; Susin *et al.* 1999, 2000). Partial chromatin condensation can occur in cells that undergo caspase-independent atypical apoptosis and involves the nuclear translocation of apoptosis-inducing factor (AIF), a mitochondrial intermembrane flavoprotein, resulting in DNA fragmentation (> 50 kb) and partial chromatin condensation similar to the first stage of nuclear apoptosis in intact cells (Susin *et al.* 2000; Joza *et al.* 2001). AIF has been shown to be translocated to the nucleus prior to the release of cytochrome *c* from the mitochondria (Daugas *et al.* 2000). By immunofluorescence, we observed a consistent AIF and cytochrome *c* redistribution pattern in the SAO-treated MSN cells (data not shown). Our data clearly demonstrate that AIF nuclear translocation and ensuing partial chromatin condensation occurs following SAO treatment consistent with caspase-independent cell death.

In contrast to MSN cells, SAO-treated TC620 cells did not up-regulate XIAP and underwent caspase-dependent apoptotic cell death that was blocked when SAO and zVAD-fmk were co-administered. SAO and zVAD-fmk co-treated cells had two-fold more metaphase cells than untreated cells suggesting that the down-regulation of survivin inhibited cell cycle progression and mitotic catastrophe contributed to apoptosis.

Based on our studies, it appears that survivin functions predominantly in cell division. Since cell cycle progression is universal it is not surprising that we observe survivin expression in all neural tumor cells examined. Survivin null mice die in embryogenesis, are polyploid and have disrupted microtubules consistent with a role in cell division (Uren *et al.* 2000). Proteins involved in control of chromosome number or ploidy have been implicated in regulating programmed cell death and survivin may have developed IAP function via its BIR domain to aid in normal cell division and survival. In tumor cells, the death program is often compromised and regulated abnormally by a process of random mutation and selection, becoming progressively more malignant as they accumulate mutations that improve their ability to survive and proliferate. Thus, survivin's role in cell division has been co-opted by the tumor cell to aid in its survival.

Our results indicate that inhibition of survivin expression unequivocally induced cell death in both the neuroblastoma and oligodendroglioma cell lines by a caspase-independent and caspase-dependent mechanism. Following survivin down-regulation, caspase activation appears to be contingent upon the ability of the cell to regulate and alter the levels of other IAP family members, particularly XIAP. This in part also supports the observation that survivin binds quantitatively *in vitro* to an IAP-inhibiting protein Smac/DIABLO (Du *et al.* 2000), raising the possibility that it might suppress caspases indirectly by freeing other IAP family proteins from the constraints of this protein.

Acknowledgements

We thank Ms. M. Heather Knowles for performing the caspase-3 assays. We thank Dr Anthony Sandler, University of Iowa and Dr Dario C. Altieri, Yale University for the pCMV-survivin cDNA construct. This work was supported by the National Institutes of Health Grant R01NS38102 (BS-Z) and by the Albert Einstein College of Medicine Department of Pathology Pilot Project Grant for Postdoctoral Fellows (SLS).

References

Adida C., Berrebi D., Peuchmaur M., Reyes-Mugica M. and Altieri D. C. (1998) Anti-apoptosis gene, survivin, and prognosis of neuroblastoma. *Lancet* **351**, 882–883.

Agrawal S. and Kandimalla E. R. (2000) Antisense therapeutics: is it as simple as complementary base recognition? *Mol. Med. Today* **6**, 72–81.

Albala J. S., Kress Y., Liu W.-K., Weidenheim K., Yen S.-H.C. and Shafit-Zagardo B. (1995) Human microtubule-associated protein-2c localizes to dendrites and axons in fetal spinal motor neurons. *J. Neurochem.* **64**, 2480–2490.

Carlson B. A., Dubay M. M., Sausville E. A., Brizuela L. and Worland P. J. (1996) Flavopiridol induces G1 arrest with inhibition of cyclin-dependent kinase (CDK) 2 and CDK4 in human breast carcinoma cells. *Cancer Res.* **56**, 2973–2978.

Chen J., Wu W., Tahir S. K., Kroeger P. E., Rosenberg S. H., Cowsert L. M., Bennett F., Krajewski S., Krajewska M., Welsh K., Reed J. C. and Ng S. C. (2000) Down-regulation of survivin by antisense oligonucleotides increases apoptosis, inhibits cytokinesis and anchorage-independent growth. *Neoplasia* **2**, 235–241.

Conway E. M., Pollefeyt S., Cornelissen J., DeBaere I., Steiner-Mosonyi M., Ong K., Baens M., Collen D. and Schuh A. C. (2000) Three differentially expressed survivin cDNA variants encode proteins with distinct antiapoptotic functions. *Blood* **95**, 1435–1442.

Datta R., Oki E., Endo K., Biedermann V., Ren J. and Kufe D. (2000) XIAP regulates DNA damage-induced apoptosis downstream of caspase-9 cleavage. *J. Biol. Chem.* **275**, 31733–31738.

Daugas E., Susin S. A., Zamzami N., Ferri K. F., Irinopoulou T., Larochette N., Prevost M. C., Leber B., Andrews D., Penninger J. and Kroemer G. (2000) Mitochondrio-nuclear translocation of AIF in apoptosis and necrosis. *FASEB J.* **14**, 729–739.

Deininger M. H., Weller M., Streffer J. and Meyermann R. (1999) Antiapoptotic Bcl-2 family protein expression increases with progression of oligodendroglioma. *Cancer* **86**, 1832–1839.

Deveraux Q. L., Takahashi R., Salvesen G. S. and Reed J. C. (1997) X-linked IAP is a direct inhibitor of cell-death proteases. *Nature* **388**, 300–304.

Du C., Fang M., Li Y., Li L. and Wang X. (2000) Smac, a mitochondrial protein that promotes cytochrome c-dependent caspase activation by eliminating IAP inhibition. *Cell* **102**, 33–42.

Islam A., Kageyama H., Takada N., Kawamoto T., Takayasu H., Isogai E., Ohira M., Hashizume K., Kobayashi H., Kaneko Y. and Nakagawara A. (2000) High expression of survivin, mapped to 17q25, is significantly associated with poor prognostic factors and promotes cell survival in human neuroblastoma. *Oncogene* **19**, 617–623.

Joza N., Susin S. A., Daugas E., Stanford W. L., Cho S. K., Li C. Y., Sasaki T., Elia A. J., Cheng H. Y., Ravagnan L., Ferri K. F.,

Zamzami N., Wakeham A., Hakem R., Yoshida H., Kong Y. Y., Mak T.W., Zuniga-Pflucker J. C., Kroemer G. and Penninger J. M. (2001) Essential role of the mitochondrial-apoptosis-inducing factor in programmed cell death. *Nature* **410**, 549–554.

Kasof G. M. and Gomes B. C. (2000) Livin, a novel inhibitor of apoptosis protein family member. *J. Biol. Chem.* **276**, 3238–3246.

LaCasse E. C., Baird S., Korneluk R. G. and MacKenzie A. E. (1998) The inhibitors of apoptosis (IAPs) and their emerging role in cancer. *Oncogene* **17**, 3247–3259.

Laemmli U. K. (1970) Cleavage of structural proteins during the assembly of the head of the bacteriophage T4. *Nature* **227**, 680–685.

Leaver H. A., Whittle I. R., Wharton S. B. and Ironside J. W. (1998) Apoptosis in human primary brain tumours. *Br. J. Neurosurg.* **12**, 539–546.

Li F., Ambrosini G., Chu E. Y., Plescia J., Tognin S., Marchisio P. C. and Altieri D. C. (1998) Control of apoptosis and mitotic spindle checkpoint by survivin. *Nature* **396**, 580–584.

Li F., Ackermann E. J., Bennett C. F., Rothermel A. L., Plescia J., Tognin S., Villa A., Marchisio P. C. and Altieri D. C. (1999) Pleiotropic cell-division defects and apoptosis induced by interference with survivin function. *Nat. Cell. Biol.* **1**, 461–466.

O'Connor D. S., Grossman D., Plescia J., Li F., Zhang H., Villa A., Tognin S., Marchisio S. and Altieri D. C. (2000) Regulation of apoptosis at cell division by p34cdc2 phosphorylation of survivin. *Proc. Natl Acad. Sci. USA* **97**, 13103–13107.

Olie R. A., Simoes-Wust A. P., Baumann B., Leech S. H., Fabbro D., Stahel R. A. and Zangemeister-Wittke U. (2000) A novel antisense oligonucleotide targeting survivin expression induces apoptosis and sensitizes lung cancer cells to chemotherapy. *Cancer Res.* **60**, 2805–2809.

Reynolds C. P., Biedler J. L., Spengler B. A., Reynolds D. A., Ross R. A., Frenkel E. P. and Smith R. G. (1986) Characterization of human neuroblastoma cell lines established before and after therapy. *J. Natl Cancer Inst.* **76**, 375–387.

Roy N., Deveraux Q. L., Takahashi R., Salvesen G. S. and Reed J. C. (1997) The c-IAP-1 and c-IAP-2 proteins are direct inhibitors of specific caspases. *EMBO J.* **16**, 6914–6925.

Shafit-Zagardo B., Peterson C. and Goldman J. E. (1988) Rapid increases in glial fibrillary acidic protein mRNA and protein levels in the copper-deficient, brindled mouse. *J. Neurochem.* **51**, 1258–1266.

Skoufias D. A., Mollinari C., Lacroix F. B. and Margolis R. L. (2000) Human survivin is a kinetochore-associated passenger protein. *J. Cell. Biol.* **151**, 1575–1581.

Susin S. A., Lorenzo H. K., Zamzami N., Marzo I., Snow B. E., Brothers G. M., Mangion J., Jacotot E., Costantini P., Loeffler M., Larochette N., Goodlett D. R., Aebersold R., Siderovski D. P., Penninger J. M. and Kroemer G. (1999) Molecular characterization of mitochondrial apoptosis-inducing factor. *Nature* **397**, 441–446.

Susin S. A., Daugas E., Ravagnan E., Samejima K., Zamzami N., Loeffler M., Costantini P., Ferri K. F., Irinopoulou T., Prevost M. C., Brothers G., Mak T. W., Penninger J., Earnshaw W. C. and Kroemer G. (2000) Two distinct pathways leading to nuclear apoptosis. *J. Exp. Med.* **192**, 571–579.

Suzuki A., Hayashida M., Ito T., Kawano H., Nakano T., Miura M., Akahane K. and Shiraki K. (2000) Survivin initiates cell cycle entry by the competitive interaction with Cdk4/p16 (INK4a) and Cdk2/cyclin E complex activation. *Oncogene* **19**, 3225–3234.

Towbin H., Staehelin T. and Gordon J. (1979) Electrophoretic transfer of proteins from polyacrylamide gels to nitrocellulose sheets: procedure and some applications. *Proc. Natl Acad. Sci. USA* **76**, 4350–4354.

Uren A. G., Wong L., Pakusch M., Fowler K. J., Burrows F. J., Vaux D. L. and Choo K. H. A. (2000) Survivin and the inner centromere protein INCENP show similar cell-cycle localization and gene knockout phenotype. *Curr. Biol.* **10**, 1319–1328.

Yang Y., Fang S., Jensen J. P., Weismann A. M. and Ashwell J. D. (2000) Ubiquitin protein ligase activity of IAPs and their degradation in proteasomes in response to apoptotic stimuli. *Science* **288**, 874–877.

ELSEVIER

Pharmacology & Therapeutics 85 (2000) 231–236

Pharmacology & Therapeutics

Associate editor: D. Shugar

Is irrelevant cleavage the price of antisense efficacy?

C.A. Stein*

Departments of Medicine and Pharmacology, Columbia University, College of Physicians and Surgeons, 630 W. 168 Street, New York, NY 10032, USA

Abstract

Antisense oligonucleotides are useful reagents for the suppression of gene expression. Their mechanism of action in eukaryotic cells appears to depend heavily on the activity of RNase H, a ubiquitous enzyme that cleaves the mRNA strand of an RNA-DNA duplex. However, the stringency requirements of RNase H are very low, and as little as a 5-base complementary region of oligomer to target may be sufficient to elicit RNase H activity. This would result in scission of nontargeted mRNAs, or what is known as "irrelevant cleavage." One strategy to reduce RNase H competency that has been employed is modification of the oligonucleotide backbone, replacing phosphodiester linkages with uncharged methylphosphonates, which are not RNase H competent. Another strategy involves replacement of deoxyribonucleic acid with 2′-O-alkylribonucleic acid. A third strategy, eliminating RNase H dependency entirely, requires activation of RNase P. The relative merits of these strategies will be discussed in the context of selective inhibition of gene function.

Keywords: Antisense oligonucleotides; RNase H; Irrelevant cleavage; Backbone modifications

Abbreviations: EGS, external guide sequence; PKC, protein kinase C; T_m, melting temperature; tRNA, transfer RNA.

Contents

1. Introduction

Over the past decade, the antisense biotechnology has been employed many times to reproducibly demonstrate truly stunning down-regulation of protein expression in a variety of systems. For example, leaving aside conflicting data concerning antitumor effects in animals, targets, such as protein kinase C (PKC)-α (Shen et al., 1999; Dean & McKay, 1994; Dean et al., 1996), c-raf kinase (Monia, 1998), intercellular adhesion molecule-1 (Bennett et al., 1997), and bcl-2 (Jansen & Brown, 1998), have been examined by several laboratories, producing a consensus that in these examples, down-regulation of translation is indeed due to a Watson-Crick hybridization-dependent mechanism of action. Indeed, evidence exists that such a mechanism may have clinical applicability. In an intriguing set of preliminary data (Yacyshyn et al., 1998), 7 of 15 patients (47%) with active, steroid-treated Crohn's disease treated with a phosphorothioate antisense oligonucleotide targeted to the intercellular adhesion molecule-1 mRNA were in remission at the end of treatment, as compared with 1 of 5 (20%) of the placebo control. Some patients remained in remission for as long as 6 months, and steroid doses were significantly lower in the antisense-treated patient cohort. Needless to say, follow-up of these data is eagerly anticipated.

In addition, the United States Food and Drug Administration recently has approved the marketing of Fomivirsen, a phosphorothioate oligodeoxynucleotide targeted to the cytomegalovirus immediate early (1E55) mRNA, as treatment for cytomegalovirus retinitis (Anderson et al., 1996). In this particular case, however, while Fomivirsen is undeniably active clinically, some doubts remain as to its mechanism of

* Tel.: 212-305-3606; fax: 212-305-7348.
E-mail address: stein@cuccfa.ccc.columbia.edu (C.A. Stein)

0163-7258/00/$ – see front matter
PII: S0163-7258(99)00053-4

action. These doubts relate to the nonspecificity of phosphorothioates, engendered by their ability to nonsequence-specifically bind heparin-binding proteins (Guvakova et al., 1995; Fennewald & Rando, 1995). In addition, this oligonucleotide can be immunostimulatory, due to the presence of the CpsG motif. The immunostimulation may take the form of a systemic release of potentially virucidal cytokines (i.e., interleukin-6, interleukin-12) and other soluble pro-inflammatory mediators, such as the chemokines macrophage inflammatory protein-1β and monocyte chemoattractant protein-1, at least in mice (Zhao et al., 1997). These nonsequence-specific effects of phosphorothioate oligonucleotides themselves may be therapeutic. Sorting out specific and nonspecific mechanisms of action may often be extremely difficult, if not well nigh impossible. Fortunately, this matters neither to the physical health of a patient being treated with an antisense oligonucleotide nor to the financial health of the treating entity.

On the other hand, if an antisense strategy is employed to determine gene function rather than in the design of a potential drug, the degree of specificity may be extremely important. Clearly, the ability of phosphorothioates to nonsequence-specifically bind (often with nanomolar affinity) to proteins, such as basic and acidic fibroblast growth factors, epidermal growth factor receptor (Rockwell et al., 1997), platelet-derived growth factor, and vascular endothelial growth factor, among many others (Neckers & Iyer, 1998), confounds the connection between a molecular event and a biological readout. Many successful attempts have been made to reduce the phosphorothioate content of antisense oligomers, and to this end, a set of molecules called "gap-mers" have been developed (Agrawal et al., 1997; Dagle et al., 1990; Quartin & Wetmur, 1989). Gap-mers are chimeric oligonucleotides in which the 5′ and 3′ regions of the molecule have had the phosphorothioate linkages replaced with phosphodiesters, which, in turn, requires substitution of 2′-*O*-methylribose for deoxyribose to preserve nuclease resistance. A region of contiguous phosphorothioates, often greater than 6 and less than 10 in length, is allowed to remain for reasons that will be described below. Because it appears that the K_d of binding of a phosphorothioate to a heparin-binding protein is highly dependent on chain length (Stein et al., 1993), such molecules probably have far fewer nonsequence-specific properties than the all-phosphorothioate congeners. However, there is an additional specificity problem that must be considered, one that is intrinsic to one of the fundamental mechanisms of action of antisense oligonucleotides.

2. RNase H can mediate the antisense effect

It has long been known (Walder & Walder, 1988; Minshull & Hunt, 1986) that RNase H, an enzyme that cleaves the mRNA strand at the site of hybridization of a complementary strand of DNA, can mediate the antisense effect in a variety of systems, including wheat germ extract (Cazenave et al., 1987) and *Xenopus* oocytes (Shuttleworth & Coleman, 1988). While not rigorously proven to be so, RNase H activity probably is a major mediator of the antisense effect in intact mammalian cells also. Giles et al. (1995) have detected RNase H-generated 3′-fragments of the p53 mRNA after microinjection of an antisense p53 oligonucleotide. The critical role of RNase H is also inferred by the fact that identical antisense sequences will either be effective or not, depending on whether the oligonucleotide backbone is competent to elicit RNase H activity. Competent backbones include phosphodiester and phosphorothioate linkages (Stein et al., 1988), as long as the sugar moiety is deoxyribose. Molecules containing uncharged backbones, composed exclusively of methylphosphonate (Furdon et al., 1989) or peptide nucleic acid linkages, and molecules that exclusively contain either N3′-P5′ phosphoramidate linkages or 2′-*O*-methylribose (or any substitution at the 2′ position) are not competent.

Cazenave et al. (1987) first noted that in wheat germ extract, RNase H could cleave the β-globin mRNA at a site that was only a 13-bp complement to a 17-mer antisense oligonucleotide. In fact, it has long been recognized (Monia et al., 1993) that a 5 (and perhaps even as low as 4) contiguous base region of homology, under some circumstances, may be sufficient to elicit RNase H activity. Observations of this type led Giles and Tidd (1992a, 1992b) to propose the hitherto unthinkable notion that the longer the length of an RNase-H competent oligonucleotide, the less specific it would become. This follows directly from the fact that only a small number of contiguous bases are required for competency; as the length of the oligomer increases, the number of nested short sequences also increases. Thus, as described by Giles and Tidd (1992a, 1992b), any 15-mer can be viewed as containing 8 overlapping 8-mers. However, every 8-mer, each representing a potential RNase H cleavage site, would be expected to occur approximately once in every 6.55×10^4 bases of random sequence, or once in every 8192 bases, for the sum of the 8. This is far greater than the 1 in 10^9 predicted purely on the basis of sequence homology alone. (Nevertheless, it is also probably true that very few of these 1 in 8192 sites are accessible, either for hybridization or to RNase H. In fact, recent data [Mir & Sothern, 1999] suggest that nucleation and zippering, initial events in duplex formation, can only occur in select regions of defined mRNA structure.)

This cleavage of nontargeted mRNAs by RNase H has been informally termed "irrelevant cleavage," and the extent to which it may create problems in the interpretation of results probably is dependent not only on oligomer length, but on backbone and concentration. Intracellular concentration, in turn, may depend on the nature of the agent used to deliver the oligonucleotide.

Suppression of irrelevant cleavage potentially can be accomplished in a number of ways, the most common one in-

volving backbone modification to prevent RNase H competency (Larrouy et al., 1992; Giles & Tidd, 1992a, 1992b; Giles et al., 1993). Larrouy et al. (1992) examined inhibition of globin mRNA translation in cell-free wheat germ extract by a 15-mer phosphodiester oligonucleotide targeted to nucleotides 37-51 on the α-globin mRNA. This oligomer, however, was also partially complementary to the β-globin sequence, and included runs of 7 and 10 base contiguous homology. Fifty percent inhibition was observed of both α- and β-globin protein production at ~0.3–0.5 μM. In congruence, β-globin mRNA was also rapidly cleaved to fragments corresponding to the regions of maximum complementarity (13 bases total out of 15; 12 contiguous) between oligomer and message. When the concentration of oligomer was increased, an additional mRNA cleavage fragment was observed that corresponded to a region of somewhat lesser complementarity (7 bases out of 15).

The authors then synthesized two oligonucleotides that substituted six and four non-RNase H competent methylphosphonate linkages for phosphodiester at the 3′ molecular terminus. Stereo-random methylphosphonates also have lower affinity for their complementary mRNA targets, and thus, tend to destabilize duplexes, a property that, in theory, would also contribute to diminished RNase H sensitivity. Two additional methylphosphonate substitutions were made near the 5′ terminus, leaving phosphodiester gaps (which retain RNase H competency), comprising the remaining five [A] and seven [B] linkages, respectively. For both [A] and [B], the IC_{50} increased by approximately 5-fold, although many factors may account for this. However, [B] (but not [A]) increased specificity, as at a concentration of 1 μM [B], α-globin synthesis was inhibited by about 50%, while inhibition of β-globin synthesis was minimal. Northern blotting for β-globin mRNA fragments revealed no cleavage, even at a concentration of 5 μM oligomer.

A similar set of results was obtained by Giles and Tidd (1992a). A 1700 nucleotide in-vitro transcribed c-myc mRNA fragment was the target, and a 14-mer phosphodiester oligomer was employed to elicit RNase H activity and mRNA cleavage. In theory, two fragments of 270 and 1430 nucleotides were expected, but in fact, the 1430 nt fragment was also rapidly cleaved. However, 6 regions of contiguous homology to the oligomer, of at least 6 bases in length, were identified within the c-myc mRNA. Interestingly, regions of complementarity (6 bases) were also observed, even with sense and nonsense oligonucleotides, which were also shown to cleave the c-myc mRNA. Strikingly, in this system, the activity of RNase H is so high that even a p53 control, mRNA was cleaved under the influence of the c-myc oligonucleotide, which, at least in theory, should not have promoted any cleavage. However, a region of 11-base complementarity to this oligomer was found in the p53 mRNA. No region of 6 base or greater complementarity was present in the nonsense sequence, which did not elicit cleavage. Similar results were obtained for an all-phosphorothioate oligomer (Giles et al., 1993).

Progressive substitution of methylphosphonate linkages for phosphodiester significantly decreased the number of additional RNase H cleavage sites, while retaining cleavage at the target site. The most effective oligomer tested contained 5 methylphosphonates at each molecular terminus separated by 4 contiguous phosphodiester linkages. This substitution pattern also greatly reduced (but did not eliminate) the irrelevant cleavage of the p53 mRNA control.

Subsequently, Giles et al. (1993) determined that an antisense c-myc oligomer containing only a 2-base phosphodiester segment (the remainder of the backbone being methylphosphonate) was sufficient to elicit appropriate cleavage of the target mRNA, while cleavage at other sites was almost entirely suppressed, save for low activity at a single additional site. A single phosphodiester residue was not sufficient for RNase H competency. Similarly, control p53 mRNA cleavage was directed only to a trivial extent by the oligomer containing 2 phosphodiester linkages. However, it should be noted that such extremely low RNase H stringency has not been commonly observed, at least to the best information of this author.

Gap-mer oligonucleotides were also shown to efficiently discriminate between its target and a single base-mismatched target (Giles et al., 1995). Two 1270 nt p53 mRNA transcripts were employed: the wild-type and one with a G-A mutation at position 1032 (the so-called Harlow sequence). A gap-mer (oligomer [C]) was also created with 3 methylphosphonate linkages at the 3′ and 5′ termini and 7 central phosphodiesters. In in vitro experiments in which the wild-type and Harlow targets were combined, the all-phosphodiester wild-type oligomer induced cleavage of about 80% of the wild-type target, but also about 45% of the Harlow target. Conversely, the all-phosphodiester oligomer targeted to the Harlow sequence induced cleavage of >80% of the Harlow mRNA, but also 70% of the wild-type mRNA. Remarkably, however, wild-type antisense oligomer [C], while inducing cleavage of about 60% of the wild-type p53 sequence, did not induce any scission of the Harlow sequence. Similarly, Harlow antisense oligomer [C] induced cleavage of its appropriate mRNA target, but little or no cleavage of the wild-type target.

Similar findings were obtained in living MOLT4 leukemia cells (Giles et al., 1995) that had been permeabilized with streptolysin O to promote cytoplasmic and nuclear delivery of the antisense p53 oligonucleotides. Oligomer [C], the gap-mer, caused a 78% reduction in levels of p53 mRNA, while the Harlow oligomer [C] was inactive. This compares to a reduction of wild-type p53 mRNA expression of about 30% by the all-phosphodiester anti-Harlow sequence oligomer.

However, this improvement in discrimination on reduction of phosphodiester (or phosphorothioate) content and its replacement by methylphosphonate can be reversed if the backbone is modified to increase the affinity of the oligomer for its mRNA target. This occurs (Larrouy et al., 1995)

when several 2′-*O*-alkylribonucleotides (alkyl = methyl, allyl, butyl) replace deoxyribonucleotides at the 3′ and 5′ molecular termini. These molecules are nuclease resistant, but they are not RNase H competent, requiring the gap to be filled with deoxyribonucleotides. However, the presence of the 2′-*O*-alkylribonucleotide residues dramatically increases the value of the melting temperature (T_m) of the duplex. For example, for the antisense α-globin (100% complementary at positions 37–51) oligomer, the T_m for the gap-mer retaining just 5 central deoxyribonucleotide phosphodiesters (oligomer [D]) is 72°C, compared with 59.5°C for the all-deoxyribonucleotide congener and 36.5°C for the methylphosphonate gap-mer described in Section 2 (e.g., oligomer [C]). Presumably due to this increased affinity, oligomer [D] decreased translation of both α- and β-globin to approximately the same extent, in contrast to what was observed for the methylphosphonate gap-mer, which, as described in Section 2, was far more discriminating. These in vitro results underscore the difficulty inherent in obtaining a "pure" antisense effect: If the oligomer sequence is sufficiently short, perfect complementarity to nontargeted sequences can be approached. If the sequence is too long, partial, but RNase H-competent, complementarity can result. A duplex of low T_m may not be antisense active, but if modifications to the oligomer are made to increase T_m, RNase H competency may also increase. Furthermore, as described in the next section, it is probably true that these types of problems also occur with some regularity in intact cells, as well as in cell-free systems.

3. Potential irrelevant cleavage in intact cells

Recently, Benimetskaya et al. (1998) were evaluating cationic porphyrins as a novel delivery reagent for oligonucleotides. The target was the 3′ untranslated region of the PKC-α mRNA and the antisense species was a 20-mer all-phosphorothioate (Dean & McKay, 1994; Dean et al., 1996) oligodeoxyribonucleotide, also known as Isis 3521. In initial reports, Isis 3521, when delivered in complex with Lipofectin, was highly effective in T24 bladder carcinoma cells at down-regulating the expression of PKC-α protein and mRNA, as assessed by Western and Northern blotting, respectively. The authors examined levels of other isoforms of PKC (β1 and ζ), but did not find inhibition of either by Isis 3521.

However, when we delivered Isis 3521 in complex with the cationic porphyrin meso tetra(methylpyridyl) porphine, inhibition was observed not only of PKC-α protein and mRNA expression, but of PKC-ζ (although not of PKC-β1, δ, or ϵ) protein and mRNA expression also. Indeed, the expression of the 4.0 and 2.2 kb PKC-ζ transcripts was reduced by >95%, while levels of control PKC-λ/ι mRNA were essentially unchanged.

It is a strong possibility that the co-down-regulation of PKC-ζ expression by an antisense PKC-α oligonucleotide is due to irrelevant cleavage. There is a contiguous 11-base match between Isis 3521 and the PKC-ζ mRNA, which, in theory, and certainly in cell-free systems, is more than sufficient for RNase H competency. Another antisense oligomer, Isis 3522, which is targeted to the 5′ region of the PKC-α mRNA, inhibits PKC-α protein and mRNA expression, but does not inhibit PKC-ζ expression. In this case, however, only a 4-base region of complementarity exists between the oligonucleotide and the PKC-ζ target, which probably is not sufficient in this system for RNase H competency. (This experiment rules out the possibility that down-regulation of PKC-α expression is directly responsible for down-regulation of PKC-ζ expression.) Irrelevant cleavage was not seen when the delivery vehicle was the cationic lipid Lipofectin, probably because the IC_{50} was somewhat lower when the oligomer was delivered by Lipofectin than when delivered by porphyrin delivery vehicle. However, this does not imply that cationic lipids are always superior delivery vehicles, as they may display significant cellular toxicity and produce confusion in the interpretation of results (Maus et al., 1999). In fact, in our hands, cationic lipids probably are too toxic to be used in human prostate cancer cell lines.

4. Potential elimination of irrelevant cleavage

The data in cell-free systems discussed in Section 2, in combination with that obtained by Benimetskaya et al. (1998), underscore the necessity of examining the levels of proteins and mRNAs that are related to any given target. Furthermore, in these experiments, there is no reason to believe that PKC-ζ is the only gene affected by irrelevant cleavage; there are undoubtedly many more; however, at the present time, they are difficult to identify, although this may change when microarray technology is applied to this problem. These experiments also highlight the difficulties in extrapolating a biologic or physiologic readout from antisense inhibition of a single gene, simply because due to the low stringency requirements of RNase H, it is not likely that a single gene is being inhibited when commercially available backbones (e.g., phosphorothioates) are employed. Even when "designer" oligomers are employed, irrelevant cleavage still occurs, albeit possibly to a lesser extent, depending on the modification.

Put more simply, the catchphrase "one oligo, one gene" at this time, does not represent experimental reality. However, since the development of much antisense technology is predicated on that very idea, it becomes necessary to devise strategies to approach the ephemeral goal. Conceptually, this is not difficult; simply eliminate any RNase H activity. In practice, however, this is difficult because the elimination of RNase H competency creates one or more additional problems. Partial diminution in RNase H competency can be accomplished by charge reduction, as we have seen, but excessive charge reduction can lead to insolubility and formulation difficulties, and drastically diminished deliverability by cationic (e.g., lipid, porphyrin, Starburst dendrimer) carriers. In addition, uncharged molecules usually

are not very active antisense effectors, not only because RNase H competency has been eliminated. To produce activity, these molecules must depend on steric blockade of translation. However, 80S elongating ribosomes have intrinsic unwinding ability (Liebhaber et al., 1984; Shakin & Liebhaber, 1986), and probably can be read through the steric block. The retention of charge by substitution of nuclease-resistant, but non-RNase H competent, 2′-*O*-alkyloligoribonucleotides throughout the length of the backbone retains the property of aqueous solubility, but also diminishes efficacy, probably also because of ribosome-promoted unwinding.

Altman and colleagues (Altman, 1993; Forster & Altman, 1990) over the past decade have initiated and developed the idea of eliminating RNase H-dependent mRNA cleavage and instead, inducing cleavage by RNase P. RNase P, like RNase H, is also a ubiquitous cellular enzyme, but its function is to cleave the 5′ terminus of precursor transfer RNAs (tRNAs) to generate the mature tRNA. If a 32-mer synthetic complementary oligonucleotide (called an external guide sequence [EGS]) is designed to mimic certain structural features of precursor tRNA (i.e., to incorporate a stem with a 7 residue loop, in addition to the 2 hybridizing arms), then it can be been shown in cell-free systems that RNase P will cleave the target RNA at the junction between the single-stranded leader sequence and the duplex formed with the EGS (Ma et al., 1998).

RNAse P cleavage of chloramphenicol acetyltransferase mRNA has also been demonstrated in HeLa cells (Yuan et al., 1992), but this EGS was a 68-mer derived from a transfected construct driven by a mouse U6 polIII promoter. This molecule is too long for scale-up synthesis, and because it is RNA, it is easily hydrolyzable. Ma et al. (1998) recently have developed a series of nuclease-resistant, serum-stable EGSs that efficiently induce RNase P cleavage in vitro of a 29-mer derived from the hepatitis B virus genome. Ma et al. (2000) employed the antisense PKC-α model in T24 bladder carcinoma cells and demonstrated that EGS targeted to the same site as the all-phosphorothioate Isis 3521 indeed can perform this function in living cells, and that moreover, problems of irrelevant cleavage of the PKC-ζ mRNA that we observed with the antisense oligonucleotide did not occur with EGS. This suggests that if a way can be found to synthesize these molecules in bulk and at less expense, the EGS approach potentially may have value in experiments designed to evaluate specific gene function. A note of caution must still be raised, however, as EGS, like all other charged species, needs to be delivered by cationic carriers; the effects of these materials on gene expression, however, have not been well studied.

5. Concluding remarks

Antisense oligonucleotide biotechnology has entered a phase of its development in which many problems engendered by nonsequence specificity are being recognized and actively addressed. However, in order to improve the specificity of the methodology, attention must now also be paid to co-suppression of gene activity due to irrelevant cleavage. To the extent that this issue also is addressed, correlations between the down-regulation of a defined target and an observed biological outcome (e.g., growth suppression) eventually may be possible. The removal of RNase H-associated in favor of RNase P-associated mechanisms may represent an advance towards this end.

Acknowledgments

Generous NIH support to the author is appreciated. I would also like to acknowledge the advice and insights of Paul Miller and Wojciech Stec, and the dedication of members of my laboratory, including Lyuba Benimetskaya, Irina Lebedeva, Li-Ming Zhang, and Maria Vilenchik.

References

Agrawal, S. A., Jiang, Z., Zhao, Q., Shaw, D., Cai, Q., Roskey, A., Channavajjala, L., Saxinger, C., & Zhang, R. (1997). Mixed-backbone oligonucleotides as second generation antisense oligonucleotides: in vitro and in vivo studies. *Proc Natl Acad Sci USA 94*, 2620–2625.

Altman, S. (1993). RNA enzyme-directed gene therapy. *Proc Natl Acad Sci USA 90*, 10898–10900.

Anderson, K. P., Fox, M. C., Brown-Driver, V., Martin, M. J., & Azad, R. F. (1996). Inhibition of human cytomegalovirus immediate-early gene expression by an antisense oligonucleotide complementary to immediate-early RNA. *Antimicrob Agents Chemother 40*, 2004–2011.

Benimetskaya, L., Takle, G., Vilenchik, M., Lebedeva, I., Miller, P., & Stein, C. A. (1998). Cationic porphyrins: novel delivery vehicles for antisense oligodeoxynucleotides. *Nucleic Acids Res 26*, 5310–5317.

Bennett, C. A., Kornbrust, D., Henry, S., Stecker, K., Howard, R., Cooper, S., Dutson, S., Hall, W., & Jacoby, H. I. (1997). An ICAM-1 antisense oligonucleotide, ISIS 3082, prevents and reverses dextran sulfate sodium-induced colitis in mice. *J Pharmacol Exp Ther 280*, 988–1000.

Cazenave, C., Loreau, N., Thuong, N. T., ToulmÈ, J.-J., & Helene, C. (1987). Enzymatic amplification of translation inhibition of rabbit β-globin mRNA medicated by anti-messenger oligodeoxynucleotides covalently linked to intercalating agents. *Nucleic Acids Res 15*, 4717–4736.

Dagle, J. M., Walder, J. A., and Weeks, D. L. (1990). Targeted degradation of mRNA in *Xenopus* oocytes and embryos directed by modified oligonucleotides: studies of An2 and cyclin in embryogenesis. *Nucleic Acids. Res 18*, 4751–4757.

Dean, N., & McKay, R. (1994). Inhibition of protein kinase C-α expression in mice after systemic administration of phosphorothioate antisense oligodeoxynucleotides. *Proc Natl Acad Sci USA 91*, 11762–11766.

Dean, N., McKay, R., Condon, T., & Bennett, C. F. (1996). Inhibition of protein kinase C-α expression in human A549 cells by antisense oligonucleotides inhibits induction of intercellular adhesion molecule 1 (ICAM-1) mRNA by phorbol esters. *J Biol Chem 269*, 16416–16424.

Fennewald, S., & Rando, R. (1995). Inhibition of high affinity basic fibroblast growth factor binding by oligonucleotides. *J Biol Chem 270*, 21718–21721.

Forster, A., & Altman, S. (1990). External guide sequences for an RNA enzyme. *Science 249*, 783–786.

Furdon, P. J., Dominski, Z., & Kole, R. (1989). RNase-H cleavage of RNA hybridized to oligonucleotides containing methylphosphonate, phosphorothioate and phosphodiester bonds. *Nucleic Acids Res 17*, 9193–9204.

Giles, R. V., & Tidd, D. M. (1992a). Increased specificity for antisense oligodeoxynucleotide targeting of RNA cleavage by RNase H using chimeric methylphosphonodiester/phosphodiester structures. *Nucleic Acids Res 20*, 763–770.

Giles, R. V., & Tidd, D. M. (1992b). Enhanced RNase H activity with methylphosphonodiester/phosphodiester chimeric antisense oligodeoxynucleotides. *Anticancer Drug Des 7*, 37–48.

Giles, R. V., Spiller, D. G., & Tidd, D. M. (1993). Chimeric oligodeoxynucleotide analogues: enhanced cell uptake of structures which direct ribonuclease H with high specificity. *Anticancer Drug Des 8*, 33–51.

Giles, R. V., Ruddell, C. J., Spiller, D. G., Green, J. A., & Tidd, D. M. (1995). Single base discrimination for ribonuclease H-dependent antisense effect within intact human leukaemia cells. *Nucleic Acids Res 23*, 954–961.

Guvakova, M. A., Yakubov, L. A., Vlodavsky, I., Tonkinson, J. L., & Stein, C. A. (1995). Phosphorothioate oligodeoxynucleotides bind to basic fibroblast growth factor, inhibit its binding to cell surface receptors, and remove it from low affinity binding sites on extracellular matrix. *J Biol Chem 270*, 2620–2627.

Jansen, B., & Brown, B. D. (1998). Bcl-2. In C. A. Stein and A. Krieg (Eds.), *Applied Antisense Oligonucleotide Technology* (pp. 317–334). New York: Wiley-Liss.

Larrouy, B., Blonski, C., Boiziau, C., Stuer, M., Moreau, S., Shire, D., & Toulme, J.-J. (1992). RNase H-mediated inhibition of translation by antisense oligodeoxyribonucleotides: use of backbone modification to improve specificity. *Gene 121*, 189–194.

Larrouy, B., Boiziau, C., Sproat, B., & Toulme, J.-J. (1995). RNase H is responsible for the non-specific inhibition of in vitro translation by 2′-*O*-alkyl chimeric oligonucleotides: high affinity or selectivity, a dilemma to design antisense oligomers. *Nucleic Acids Res 23*, 3434–3440.

Liebhaber, S. A., Cash, F. E., & Shakin, S. H. (1984). Translationally associated helix-destabilizing activity in rabbit reticulocyte lysate. *J Biol Chem 259*, 15597–15602.

Ma, M., Jacob-Samuel, B., Dignam, J., Pace, U., Goldberg, A., & George, S. (1998). Nuclease-resistant external guide sequence-induced cleavage of target RNA by human ribonuclease P. *Antisense Nucleic Acid Drug Dev 8*, 415–426.

Ma, M., Benimetskaya, L., Lebedeva, I., Dignam, J., Takle, G., & Stein, C. A. (2000). Intracellular mRNA cleavage induction via activation of RNase P by nuclease-resistant external guide sequences (EGS). *Nat Biotechnol 18*, 58–61.

Maus, U., Rosseau, S., Mandrakas, N., Schlingensiepen, R., Maus, R., Muth, H., Grimminger, F., Seeger, W., & Lohmeyer, J. (1999). Cationic lipids employed for antisense oligodeoxynucleotide transport may inhibit vascular cell adhesion molecule-1 expression in human endothelial cells: a word of caution. *Antisense Nucleic Acid Drug Dev 9*, 71–80.

Minshull, J., & Hunt, T. (1986). The use of single-stranded DNA and RNase-H to promote quantitative hybrid arrest of translation of mRNA/DNA hybrids in reticulocyte lysate cell-free translations. *Nucleic Acids Res 14*, 6433–6451.

Mir, K. U., & Sothern, E. M. (1999). Determining the influence of structure on hybridization using oligonucleotide arrays. *Nat Biotechnol 17*, 788–792.

Monia, B. (1998). Disruption of the map kinase signaling pathway using antisense oligonucleotide inhibitors targeted to Ras and Raf kinase. In C. A. Stein & A. Krieg (Eds.), *Applied Antisense Oligonucleotide Technology* (pp. 245–261). New York: Wiley-Liss.

Monia, B. P., Lesnik, E. A., Gonzalez, C., Lima, W. F., Mcgee, D., Guinosso, C. J., Kawasaki, A. M., Cook, P. D., & Freier, S. M. (1993). Evaluation of 2′-modified oligonucleotides containing 2′-deoxy gaps as antisense inhibitors of gene expression. *J Biol Chem 268*, 14514–14522.

Neckers, L., & Iyer, K. (1998). Nonantisense effects of antisense oligonucleotides. In C. A. Stein & A. Krieg (Eds.), *Applied Antisense Oligonucleotide Technology* (pp. 147–160). New York: Wiley-Liss.

Quartin, R. S., & Wetmur, J. G. (1989). Effect of ionic strength on the hybridization of oligodeoxynucleotides with reduced charge due to methylphosphonate linkages to unmodified oligodeoxynucleotides containing the complementary sequence. *Biochemistry 28*, 1040–1047.

Rockwell, P., O'Connor, W., King, K., Goldstein, N., Zhang, L. M., and Stein, C. A. (1997). Cell surface perturbations of the EGF and VEGF receptors by phosphorothioate oligodeoxynucleotides. *Proc Natl Acad Sci USA 94*, 6523–6528.

Shakin, S. H., & Liebhaber, S. A. (1986). Destabilization of messenger RNA/complementary DNA duplexes by the elongating 80 S ribosome. *J Biol Chem 261*, 16018–16025.

Shen, L., Dean, N. M., & Glazer, R. I. (1999). Induction of p53-dependent, insulin-like growth factor-binding protein-3 mediated apoptosis in glioblastoma multiforne cells by a protein kinase C-alpha antisense oligonucleotide. *Mol Pharmacol 55*, 396–402.

Shuttleworth, J., & Coleman, A. (1988). Antisense oligonucleotide-directed cleavage of mRNA in *Xenopus* oocytes and eggs. *EMBO J 7*, 427–434.

Stein, C. A., Subasinghe, C., Shinozuka, K., & Cohen, J. (1988). Physicochemical properties of phosphorothioate oligodeoxynucleotides. *Nucleic Acids Res 16*, 3209–3221.

Stein, C. A., Tonkinson, J. L., Zhang, L.-M., Yakubov, L. Gervasoni, J., Taub, R., & Rotenberg, S. A. (1993). Dynamics of the internalization of phosphodiester oligodeoxynucleotides in HL60 cells. *Biochemistry 32*, 4855–4861.

Walder, R. Y., & Walder, J. A. (1988). Role of RNase-H in hybrid-arrested translation by antisense oligonucleotides. *Proc Natl Acad Sci USA 85*, 5011–5015.

Yacyshyn, B. R., Bowen-Yacyshyn, M. D., Jewell, L., Tami, J. A., Bennett, C. F., Kisner, D. L., & Shanahan, W. R. (1998). A placebo-controlled trial of ICAM-1 antisense oligonucleotide in the treatment of Crohn's disease. *Gastroenterology 114*, 1133–1142.

Yuan, Y., Hwang, E., & Altman, S. (1992). Targeted cleavage of mRNA by human RNase P. *Proc Natl Acad Sci USA 89*, 8006–8010.

Zhao, Q., Temasamani, J., Zhou, R.-Z., & Agrawal, S. (1997). Pattern and kinetics of cytokine production following administration of phosphorothioate oligonucleotides in mice. *Antisense Nucleic Acid Drug Dev 7*, 495–502.

THE JOURNAL OF BIOLOGICAL CHEMISTRY
Vol. 271, No. 32, Issue of August 9, pp. 19080–19083, 1996
Printed in U.S.A.

Changes in Plasma Lipoprotein Cholesterol Levels by Antisense Oligodeoxynucleotides against Cholesteryl Ester Transfer Protein in Cholesterol-fed Rabbits*

(Received for publication, March 14, 1996, and in revised form, May 14, 1996)

Masahiro Sugano‡ and Naoki Makino

From the Department of Bioclimatology and Medicine, Medical Institute of Bioregulation, Kyushu University, 4546 Tsurumihara, Beppu, Oita 874, Japan

Cholesteryl ester transfer protein (CETP) is the enzyme that facilitates the transfer of cholesteryl ester from high density lipoprotein (HDL) to apoB-containing lipoproteins and also affects the low density lipoprotein metabolism. On the other hand, the liver is the major tissue responsible for the production of CETP (CETP mRNA) in rabbits. To test the hypothesis that a reduction of CETP mRNA in the liver by antisense oligodeoxynucleotides (ODNs) may affect the plasma lipoprotein cholesterol levels, we intravenously injected antisense ODNs against rabbit CETP coupled with asialoglycoprotein carrier molecules, which serve as an important method to regulate liver gene expression, to cholesterol-fed rabbits via their ear veins. All rabbits were fed a standard rabbit chow supplement with 0.1% cholesterol for 10 weeks before and throughout the experiment. After injecting rabbits with antisense ODNs, the plasma total cholesterol concentrations and plasma CETP activities all decreased at 24, 48, and 96 h, whereas the plasma HDL cholesterol concentrations increased at 48 h. A reduction in the hepatic CETP mRNA was also observed at 6, 24, and 48 h after the injection with antisense ODNs. However, in the rabbits injected with sense ODNs, the plasma total and HDL cholesterol concentrations and the plasma CETP activities did not significantly change, and the hepatic CETP mRNA did not change either throughout the experimental period. Although the exact role of CETP in the development of atherosclerosis remains to be clarified, these findings showed for the first time that the intravenous injection with antisense ODNs against CETP coupled to asialoglycoprotein carrier molecules targeted to the liver could thus inhibit plasma CETP activity and, as a result, could induce a decrease in the plasma low density lipoprotein and very low density lipoprotein cholesterol and an increase in the plasma HDL cholesterol in cholesterol-fed rabbits.

Cholesteryl ester transfer protein (CETP)[1] is a plasma glycoprotein that catalyzes the transfer of cholesteryl ester and triglyceride among lipoproteins (1, 2). CETP deficiency in humans (3–5) has been proposed to be associated with longevity (3). The homozygotes for CETP deficiency demonstrated markedly elevated HDL-C and plasma apoA-I levels as well as decreased LDL cholesterol and plasma apoB levels (4, 6). CETP-deficient subjects have also been found to have a substantially increased catabolic rate of apoB as the primary metabolic basis for the low plasma levels of LDL apo B (7). This finding indicates that the LDL receptor pathway may thus be up-regulated during CETP deficiency. It has also been proposed that a CETP deficiency may be associated with protection against ischemic heart disease, based on the observed longevity in one kindred (3), as well as the lack of any evidence of coronary heart disease (6) in other kindreds with CETP deficiency; however, these findings remain controversial. Several other lines of evidence also support the hypothesis. The plasma level of CETP is directly correlated with the extent of coronary atherosclerosis in monkeys fed a cholesterol diet (8). A transgenic mouse overexpressing simian CETP developed accelerated atherosclerosis (9). Thus, the inhibition of plasma CETP activity may potentially be a novel method of reducing the plasma levels of LDL cholesterol by enhancing LDL catabolism (7) and decreasing the transfer of cholesteryl ester from HDL to apoB-containing lipoproteins (1, 2). Since the liver is the major tissue responsible for the production of CETP (CETP mRNA) in rabbits (10, 11) (even though adipose tissue may also be the major tissue responsible for the production of CETP in monkeys (12)), a reduction of CETP in the liver by antisense oligodeoxynucleotides (ODNs) may thus cause a reduction in the plasma LDL and/or VLDL cholesterol concentrations. The present study was therefore undertaken to determine the effect of an intravenous injection with antisense ODNs to the liver on the CETP mRNA expression, plasma CETP activity and plasma cholesterol concentrations in rabbits fed a low cholesterol diet. These antisense ODNs were originally designed to be coupled with asialoglycoprotein carrier molecules, and this coupling serves as an important method to regulate liver gene expression (13).

MATERIALS AND METHODS

Construction of ODNs—The sequences of ODNs against rabbit CETP used in this study were as follows: antisense, 5′-CTTGACCCGGCCGAGGAGCAT-3′; sense, 5′-ATGCTCCTCGGCCGGGTCAAG-3′, positions +148 to +168 of the rabbit sequence (11). These selected target sequences have relatively low homology with any of the other known cDNA sequences found in the GenBank data base. The synthetic ODNs were purified on the column, dried down, resuspended in Tris-EDTA (10 mM Tris, pH 7.4, and 1 mM EDTA), and then quantitated by spectrophotometry. Asialoglycoprotein-poly-L-lysine (M_r approximately 71,400), which was prepared according to the method of Wu and Wu (14) and Wu *et al.* (15), was added to the ODNs (at a molar ratio of 25:1) with vigorous mixing. The solution was incubated at 4 °C overnight and dialyzed (two times) against 0.15 M saline (1500:1; membrane M_r cutoff, 3500). The samples were electrophoresed through a 2% agarose gel using Tris/borate/EDTA buffer and then stained with ethidium bromide to visualize DNA. The samples were filtered through a 0.2-μm mem-

* The costs of publication of this article were defrayed in part by the payment of page charges. This article must therefore be hereby marked "*advertisement*" in accordance with 18 U.S.C. Section 1734 solely to indicate this fact.

‡ To whom correspondence should be addressed. Tel.: 81-977-24-5301; Fax: 81-977-24-8945.

[1] The abbreviations used are: CETP, cholesteryl ester transfer protein; HDL, high density lipoprotein; LDL, low density lipoprotein; ODN, oligodeoxynucleotide; VLDL, very low density lipoprotein; PCR, polymerase chain reaction.

Exhibit M

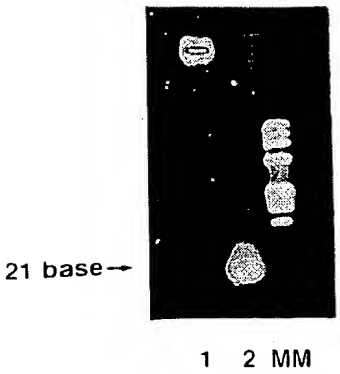

FIG. 1. **Asialoglycoprotein-poly-L-lysine-ODN complex and ODNs alone were electophoresed through 2% agarose gel using a Tris/borate/EDTA buffer and then were stained with ethidium bromide to visualize DNA.** *Lane 1*, asialoglycoprotein-poly-L-lysine-ODN-complex; *lane 2*, ODNs alone; *MM*, *Hae*III molecular marker.

brane (Millipore Corp., Bedford, MA) before injection.

Experimental Protocol—Twenty-six male Japanese white rabbits weighing 2.0–2.5 kg were used in the experiment. All animals were housed individually, had free access to water, and were fed a standard rabbit chow supplement with 0.1% cholesterol for 10 weeks before and throughout the experiment. The plasma total and HDL cholesterol concentrations, which did not significantly change between the period after 9 and 10 weeks of feeding, were determined. Thirteen animals were injected with asialoglycoprotein-poly-L-lysine-antisense ODN complex, whereas the remaining 13 animals were injected with asialoglycoprotein-poly-L-lysine-sense ODN complex via the ear veins. The amount of ODNs injected was 30 μg/kg for each rabbit. At 6, 24, 48, and 96 h after injection, two rabbits in each group were killed, and liver specimens were taken. At the same time, about 1 ml of the blood was drawn from the remaining animals via their ear veins.

Measurement of CETP mRNA—Total RNA was isolated from the liver with a RNAzolB solution (Biotex, Friendswood, TX) according to the the manufacturer's procedure with slight modifications (12). The abundance of CETP mRNA was determined by quantitative dot blotting (16). The rabbit cRNA probe labeled with fluorescein-dUTP was produced by the nonradiolabeled, reverse transcription polymerase chain reaction (PCR) (Amersham Corp.), according to the rabbit sequence (11). The sense and antisense primers used for PCR, the sizes of the PCR products, and the PCR cycles in each cRNA probe were: CETP, sense, 5'-CTTTCCATAAACTGCTCCTG-3'; antisense, 5'-CCTGGGTCTCCGCACTTTCT-3'; size, 482 base pairs; 30 cycles; and glyceraldehyde-3-phosphate dehydrogenase, sense, 5'-ATGGTCTACATGTTCCAGTA-3'; antisense, 5'-TAAGCAGTTGGTGGTGCAGG-3'; size, 343 base pairs; 30 cycles.

Biochemical Analysis—The plasma cholesterol concentrations were measured in whole plasma and in the HDL-containing supernatant after the precipitation of VLDL and LDL with dextran-Mg^{2+} using the Wako total and HDL cholesterol measuring kit (Wako Ltd., Osaka, Japan). The plasma constituents related to liver function were analyzed using an automatic analyzer (Hitachi Ltd., Tokyo, Japan). The CETP activity in the plasma was determined by a radioassay according to the modified method of Yen *et al.* (17). A volume of 20 μl of plasma was incubated for 30 min at 37 °C in the presence of [^{3}H]cholesteryl oleate-labeled HDL (3–10 nmol CE) and an excessive amount of VLDL and LDL (0.2 μmol of CE). The volume was adjusted to 200 μl with Tris-saline (pH 7.4) before incubation. After the precipitation of VLDL and LDL by heparin and $MnCl_2$ (18), half of the supernatant volume was then removed and counted in a liquid scintillation counter.

Statistical Analysis—All values are presented as the mean ± standard error of the mean. The statistical analysis was performed by a paired *t* test for comparisons in the intragroup and by Student's *t* test for comparisons between the groups. Differences were considered statistically significant at a value of $p < 0.05$.

RESULTS

We characterized the asialoglycoprotein-ODN complex by gel electrophoresis. The samples were electrophoresed through a 2% agarose gel using Tris/borate/EDTA buffer and then were stained with ethidium bromide to visualize DNA (Fig. 1). The

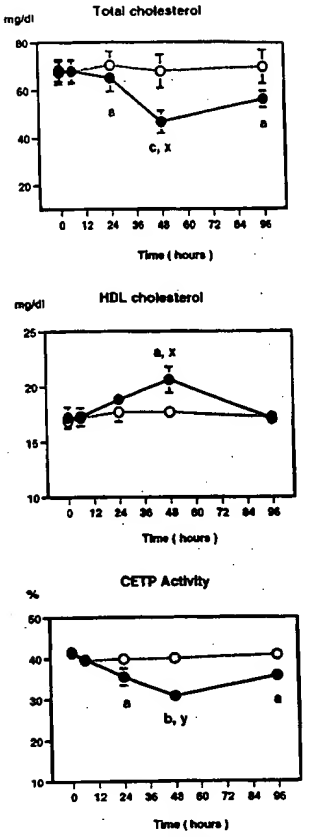

FIG. 2. **Changes in the plasma cholesterol concentrations and plasma CETP activities.** Concentrations were measured at 0 (n = 13), 6 (n = 11), 24 (n = 9), 48 (n = 7), and 96 (n = 5) h for each group. ●, rabbits injected with antisense ODNs; ○, rabbits injected with sense ODNs. Values are mean ± S.E. *a*, $p < 0.05$; *b*, $p < 0.01$; *c*, $p < 0.001$ compared with 0 h, as determined by a paired *t* test. *X*, $p < 0.05$; *y*, $p < 0.01$ compared with rabbits injected with sense ODNs, as determined by Student's *t* test.

ODNs were retained by the asialoglycoprotein-poly-L-lysine conjugate in the well, whereas ODNs alone entered the gel. In the rabbits injected with antisense ODNs, the total cholesterol concentrations and the CETP activities were all significantly decreased at 24, 48, and 96 h compared with those at 0 h. At 48 h, the total cholesterol concentrations and the CETP activities were also significantly lower in the rabbits injected with antisense ODNs than in those injected with sense ODNs (Fig. 2). The HDL cholesterol concentrations significantly increased at 48 h compared with those at 0 h and the rabbits injected with sense ODNs (Fig. 2). In the rabbits injected with sense ODNs, the total and HDL cholesterol concentrations and the CETP activities did not significantly change throughout the experiment (Fig. 2). Fig. 3 shows a typical example of the dot blot analyses of hepatic CETP mRNA treated with antisense ODNs. A reduction of hepatic CETP mRNA was observed at 6, 24, and 48 h after injection with antisense ODNs. When the amount of hepatic CETP mRNA was measured by scanning and expressed as a ratio to glyceraldehyde-3-phosphate dehydrogenase mRNA, the mean values were 0.83 (100%) at 0 h, 0.43 (51.8%) at 6 h, 0.40 (48.2%) at 24 h, 0.65 (78.3%) at 48 h, and 0.87 (104.8%) at 96 h (the parentheses express the percentages against the value at 0 h). Hepatic CETP mRNA treated with sense ODNs did not change throughout the experimental period (data not shown). We measured the plasma constituents related to liver function (aspartate aminotransferase, alanine aminotransferase γ-GTP, alkaline phosphatase, and total bilirubin), including triglyceride in the rabbits (data not shown). These levels did not significantly change throughout the exper-

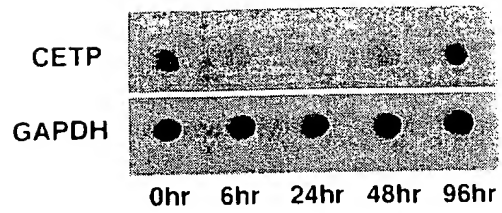

FIG. 3. **Dot blot analyses of hepatic CETP mRNA treated with antisense ODNs.** Glyceraldehyde-3-phosphate dehydrogenase mRNA (*GAPDH*) is indicated as the control.

imental period and were also not significantly different between the animals injected with sense and antisense ODNs.

DISCUSSION

In the present study, an injection of asialoglycoprotein-poly-L-lysine-antisense complex reduced the hepatic CETP mRNA, plasma CETP activities, and plasma total cholesterol, whereas it increased HDL cholesterol concentrations. The antisense ODNs used in the present study demonstrated no side effects within 4 days after injection. The antisense ODNs are widely used as inhibitors of specific gene expression because they offer the possibility of blocking the expression of a particular gene without any changes in the functions of other genes (19). However, for successful antisense delivery, some criteria must be fulfilled (19–21). Recently, an efficient gene transfer method mediated by a viral liposome complex has been used as a delivery system of antisense ODNs *in vivo* (22–24). However, to use the methods mentioned above, many technical and methodological difficulties still need to be overcome in comparison with those in our study, and such gene targeting is also troublesome to use in chronic clinical situations, such as in the treatment of atherosclerosis. Regarding lipoprotein metabolism, almost all enzymes and apolipoproteins are produced in the liver; therefore, the efficient receptor-mediated delivery of antisense ODNs to the liver *in vivo* used in our study may be useful for both diagnostic and therapeutic applications for lipoprotein metabolism. In our study, the total cholesterol concentrations and the CETP activities were all significantly decreased at 24, 48, and 96 h, whereas the HDL cholesterol concentrations significantly increased only at 48 h compared with those at 0 h. At 48 h, the total cholesterol decreased substantially more than the HDL cholesterol increased (Fig. 2). Although we could not conclusively clarify the exact reason for these results, the following factors are considered to play a role. The assay used for the CETP activity in this study cannot always show the true CE mass transfer *in vivo*, because the assay uses exogenous lipoprotein substrates added in the assay, whereas *in vivo* the CE is transferred among the endogenous lipoproteins of plasma (25). This may partly explain why the CETP activity is still significantly reduced at 96 h, whereas the HDL cholesterol levels returned to normal. It has been reported that there is an inverse relationship between the plasma CETP and liver LDL receptor mRNA in CETP transgenic mice (26). The induced LDL receptor expression in LDL receptor transgenic mice leads to a marked reduction in plasma VLDL and LDL (27), possibly because approximately 50–80% of VLDL and/or LDL is cleared by hepatocytes, due to LDL receptor-mediated endocytosis (28, 29). LDL receptor protein and activity are generally parallel to LDL receptor mRNA levels (27). It is also indicated that the reduction of plasma CETP reduces the plasma levels of LDL and VLDL cholesterol possibly by enhancing LDL catabolism (7) and possibly by decreasing the transfer of cholesteryl ester from HDL to apoB-containing lipoproteins (1, 2), and it also increases the plasma level of HDL cholesterol, possibly due to the latter reason. Since normal rabbits have a large degree of CETP activity (30), and the LDL receptor is down-regulated, and CETP mRNA in the liver and plasma CETP increase especially in the rabbits fed an atherogenic diet more than in those fed a standard diet (10), the inhibition of CETP by antisense ODNs in our study may thus affect not only the decrease in CETP but also the increase in the LDL receptor much more than other models. Thus, as a result, the VLDL and LDL cholesterol levels might be reduced more than the HDL level was increased. Our antisense injection was considered successful for the following reasons: (*a*) the asialoglycoprotein-poly-L-lysine-antisense complex is rapidly and preferentially taken up by the liver (13) and has enhanced resistance to nuclease degradation in plasma (31); (*b*) the amount of CETP mRNA in the liver is thought to be relatively low compared with other lipoprotein mRNAs in the liver; however, these findings have only been previously seen in the cynomolgus monkey (12); and (*c*) the liver is the major tissue responsible for the production of CETP (CETP mRNA) in rabbits (10, 11) (although adipose tissue may also be found in monkeys (12)). The exact role of CETP in the development of atherosclerosis has yet to be clarified. Marotti *et al.* (9) demonstrated that transgenic mice expressing cynomolgus monkey CETP had significantly more early atherosclerotic lesions in the proximal aorta than controls when fed a high cholesterol diet. On the other hand, more recently Hayek *et al.* (32) concluded that CETP expression inhibited the development of early atherosclerotic lesions in hypertriglyceridemic mice. The CETP expression in hypertriglyceridemic animals produced a much greater reduction in the HDL size (33). These small particles, which can be produced by CETP (34), may thus be an optimal mediator of cellular cholesterol efflux (35).

In conclusion, in this study we have shown that the intravenous administration of the asialoglycoprotein-poly-L-lysine-antisense complex is a beneficial method for reducing the plasma levels of LDL and VLDL cholesterol and increasing the plasma level of HDL cholesterol, possibly by enhancing LDL catabolism (7) and decreasing the transfer of cholesteryl ester from HDL to apoB-containing lipoproteins (1, 2). However, it must be mentioned that our results were limited to the period comprising only several days after the injection. Therefore, to elucidate the exact effect of CETP on atherosclerosis development, further longer term studies are called for.

Acknowledgments—We thank Sachiyo Taguchi and Miha Watanabe for their expert technical assistance.

REFERENCES

1. Tall, A. R. (1986) *J. Lipid Res.* **27**, 361–367
2. Hesler, C. B., Swenson, T. L., and Tall, A. R. (1987) *J. Biol. Chem.* **262**, 2275–2282
3. Saito, F. (1984) *Metab. Clin. Exp.* **33**, 629–633
4. Koizumi, J., Mabuchi, H., Yoshimura, A., Michishita, I., Takeda, M., Itoh, H., Sakai, Y., Sakai, T., Ueda, K., and Takeda R. (1985) *Atherosclerosis* **58**, 175–186
5. Brown, M. L., Inazu, A., Hesler, C. B., Agellon, L. B., Mann, C., Whitlock, M. E., Marcel, Y. L., Milne, R. W., Koizumi, J., Mabuchi, H., and Tall, A. R. (1989) *Nature* **342**, 448–451
6. Inazu, A., Brown, M. L., Hesler, C. B., Agellon, L. B., Koizumi, J., Tanaka, K., Maruhama, Y., Mabuchi, H., and Tall, A. R. (1990) *N. Engl. J. Med.* **323**, 1234–1238
7. Ikewaki, K., Nishiwaki, M., Sakamoto, T., Ishikawa, T., Fairwell, T., Zech, L. A., Nagano, M., Nakamura, H., Brewer, H. B., Jr., and Rader, D. J. (1995) *J. Clin. Invest.* **96**, 1573–1581
8. Quinet, E., Tall, A. R., Ramakrishnan, R., and Rudel, L. (1992) *J. Clin. Invest.* **87**, 1559–1566
9. Marotti, K. R., Castle, C. K., Boyle, T. P., Lin, A. H., Murray, R. W., and Melchior, G. W. (1993) *Nature* **364**, 73–75
10. Quinet, E. M., Agellon, L. B., Kroon, P. A., Marcel, Y. L., Lee, Y. C., Whitlock, M. E., and Tall, A. R. (1990) *J. Clin. Invest.* **85**, 357–363
11. Nagashima, M., McLean, J. W., and Lawn, R. M. (1988) *J. Lipid Res.* **29**, 1643–1649
12. Pape, M. E., Rehberg, E. F., Marotti, K. R., and Melchior, G. W. (1992) *Arterioscler. Thromb.* **11**, 1759–1771
13. Lu, X. M., Fischman, A. J., Jyawook, S. L., Hendricks, K., Tompkins, R. G., and Yarmush, M. L. (1994) *J. Nucl. Med.* **35**, 269–275
14. Wu, G. Y., and Wu, C. H. (1987) *J. Biol. Chem.* **262**, 4429–4432
15. Wu, G. Y., Wilson, J. M., Shalaby, F., Grossman, M., Shafritz, D. A., and Wu,

C. H. (1991) *J. Biol. Chem.* **266**, 14338–14342
16. Lin-Lee, Y. C., Kao, F. T., Cheung, P., and Chan, L. (1985) *Biochemistry* **24**, 3751–3756
17. Yen, F. T., Deckelbaum, R. J., Mann, C. J., Marcel, Y. L., Milne, R. W., and Tall, A. R. (1989) *J. Clin. Invest.* **83**, 2018–2024
18. Warnick, G. R., and Albers, J. J. (1978) *J. Lipid Res.* **19**, 65–76
19. Helene, C., and Toulme, J. J. (1990) *Biochim. Biophys. Acta* **1049**, 99–125
20. Stein, C. A., and Cheng, Y.-C. (1993) *Science* **261**, 1004–1012
21. Piwnica-Worms, D. (1994) *J. Nucl. Med.* **35**, 1064–1066
22. Morishita, R., Gibbons, G. H., Ellison, K. E., Nakajima, M., Zang, L., Kaneda, Y., Ogihara, T., and Dzau, V. J. (1993) *Proc. Natl. Acad. Sci. U. S. A.* **90**, 8474–8478
23. Morishita, R., Gibbons, G. H., Ellison, K. E., Nakajima, M., Leyen, H. V. L., Zang, L., Kaneda, Y., Ogihara, T., and Dzau, V. J. (1994) *J. Clin. Invest.* **93**, 1458–1464
24. Tomita, N., Morishita, N., Higaki, J., Aoki, M., Nakamura, Y., Mikami, H., Fukamizu, A., Murakami, K., Kaneda, Y., and Ogihara, T. (1995) *Hypertension* **26**, 131–136
25. Mann, C. J., Yen, F. T., Grant, A. M., and Bihain, B. E. (1991) *J. Clin. Invest.* **88**, 2059–2066
26. Jiang, X. C., Masucci-Magoulas, L., Mar, J., Lin, M., Walsh, A., Breslow, J. L., and Tall, A. (1993) *J. Biol. Chem.* **268**, 27406–27412
27. Yokode, M., Hammer, R. E., Ishibashi, S., Brown, M. S., and Goldstein, J. L. (1990) *Science* **250**, 1273–1275
28. Spady, D. K., Bilheimer, D. W., and Dietschy, J. M. (1983) *Proc. Natl. Acad. Sci. U. S. A.* **80**, 3499–3503
29. Spady, D. K., and Dietschy, J. M. (1985) *J. Lipid Res.* **26**, 465–472
30. Ha, Y. C., and Barter, P. J. (1982) *Comp. Biochem. Physiol.* **71B**, 265–269
31. Chiou, H. C., Tangco, M. V., Levine, S. M., Robertson, D., Kormis, K., Wu, C. H., and Wu, G. Y. (1994) *Nucleic Acids Res.* **22**, 5439–5446
32. Hayek, T., Masucci-Magoulas, L., Jiang, X., Walsh, A., Rubin, E., Breslow, J. L., and Tall, A. R. (1995) *J. Clin. Invest.* **96**, 2071–2074
33. Hayek, T., Chajek-Shaul, T., Walsh, A., Agellon, L. B., Moulin, P., Tall, A. R., and Breslow, J. L. (1992) *J. Clin. Invest.* **90**, 505–510
34. Sugano, M., Shah, R., and Rudel, L. L. (1991) *Circulation* **84**, 378a (abstr.)
35. Fielding, C. J., and Fielding, P. E. (1995) *J. Lipid. Res.* **36**, 211–228